THE UNIVERSITY
of LIVERPOOL

Evaluation of Acid Ceramidase as Response Predictor and Therapeutic Target in Neoadjuvant Chemoradiotherapy for Rectal Cancer

Thesis submitted in accordance with the requirements of the University of Liverpool for the degree of Doctor of Medicine

by

David Lewis Bowden

November 2018

Dedication

To my family – you are my inspiration and motivation, thank you for all your love and support.

x R A E J x

Declaration

The work presented in this thesis was carried out in the Institute of Translational Medicine at the University of Liverpool and facilitated by the Madel research fellowship, supported by Health Education North West. The material contained within this thesis has not been, nor is currently being presented wholly, or in part, for any other degree or qualification.

I declare that all the work presented in this thesis has been carried out by me except where indicated below:

- Histopathological assessment of tumour regression grading and immunohistochemical expression of acid ceramidase was performed by Dr Michael Wall (FRCPath, Countess of Chester Hospital)
- Tissue microarray construction and sectioning was performed by Mr Michael Neill (Liverpool Bio-Innovation Hub Biobank)

David Bowden

Acknowledgements

I am indebted to everyone who has helped me with this research. Thank you.

I would firstly like to thank my supervisors: Mr Dale Vimalachandran, Dr Neil Kitteringham, Dr Jason Parsons and Mr Paul Sutton. Your doors have always been open and your guidance and advice invaluable. Thank you particularly for your patience.

One of the more laborious aspects of the work undertaken was in the assessment of histopathological tumour response and immunohistochemical expression of acid ceramidase on the tissue microarrays. I will be eternally grateful for the time and expertise provided by Dr Michael Wall.

I am also grateful for the resourcefulness and assistance of Mrs Angela Kalaher and Mrs Julie Scanlon in identifying and retrieving the paraffin tissue blocks pertaining to the rectal cancer cases.

Thank you to Mr Michael Neill for your effort in creating the tissue microarrays and thank you to Dr Helen Kalirai and Dr Theun van Veen for your expert assistance with the immunohistochemical staining.

I would also like to thank Dr Katie Nickson for your welcoming approach and assistance with my weekly trip over the road for cell irradiation.

I am indebted to the many other people in the Medical Research Council Centre for Drug Safety Science who have informally helped me acquire the necessary laboratory technique to produce this research, in particular Mr Jonathan Evans and Dr Charles Winiarski.

I would finally like to thank the Bowel Disease Research Foundation for funding this project, and Health Education North West for the privileged opportunity to undertake this research with the Madel research fellowship.

Contents

Abstract

Evaluation of acid ceramidase as response predictor and therapeutic target in neoadjuvant chemoradiotherapy for rectal cancer.

Bowden D, Sutton P, Wall M, Parsons J, Kitteringham N, Vimalachandran D

Introduction

Colorectal cancer represents the second commonest cause of cancer-related mortality in the UK, with one-third of cases involving the rectum. Response to chemoradiotherapy (CRT) in rectal cancer varies from pathological complete response (pCR, with associated survival benefit) to disease progression. Predicting response is not currently possible but biomarkers to do this would facilitate personalised treatment, minimise morbidity from CRT and prevent delays in the systemic and local management of the disease in non-responders. Therapeutic targets may also be revealed to improve the efficacy of CRT, and further facilitate non-operative or rectal-preservation strategies. Initial proteomic profiling of rectal cancer has revealed differential expression of acid ceramidase (AC) between relative responders and non-responders to CRT.

Aims

1) Validation of initial proteomic findings.
2) Confirmation of biological manipulation of AC *in vitro*.
3) Subsequent assessment of cell survivability post-irradiation.

Methods

Tissue microarrays (TMAs) were constructed, comprising pre-CRT biopsies and post-CRT resection specimens from 111 rectal cancer patients, and used to correlate immunohistochemical expression of AC with pathological response to CRT (χ^2).

Genetic (siRNA) and pharmacological (carmofur) manipulation were used independently to inhibit AC expression and activity in a colorectal cancer cell line. Cells were subsequently irradiated, and survival measured by clonogenic assay.

Results

TMA analysis demonstrated low AC expression in tumour stroma to correlate with pCR ($p=0.003$) and relative responders to CRT ($p=0.048$), whereas high AC expression in normal colonic epithelium correlated with a non-response ($p=0.012$). High AC expression in residual cancer epithelium post-CRT also correlated with an increased risk of local disease recurrence ($p=0.031$).

Preliminary *in vitro* modelling demonstrated no irradiation specific benefit to pharmacological or genetic inhibition of AC activity. Genetic manipulation of AC resulted in reduced cell viability and higher caspase activity, suggesting an apoptotic mechanism.

Conclusions

This study supports a role for AC in the response to CRT, implicating tumour-stromal interaction and apoptosis as potential mechanisms of action. Inhibition of AC, by drugs such as carmofur, may yet provide a promising therapeutic strategy as an adjunct to CRT in patients with rectal cancer. Further prospective analysis of AC in a wider clinical dataset and further evaluation of the potential mechanism of AC-dependent radio-resistance in rectal cancer and apoptosis is required.

List of Figures

	white-bottomed 96-well plates at 2,500 cells per well. Luminescence (as a surrogate for cell proliferation) was observed at time points over the subsequent 72 hours following the application of VivoGlo™ Luciferin. Triplicate wells were seeded for each time point for each population, with three independent experiments performed. Mean fluorescence values observed are plotted with error bars representing one SD.	
4.23	Luminescence observed in HCT116 cells subsequent to undertaking the Caspase-Glo® 3/7 assay (Promega) in ASAH1 siRNA transfected (siRNA3), non-coding siRNA transfected (siRNA-NC) and non-transfected (Media) cell populations. Transfection or control treatment was undertaken prior to re-seeding the cells in white-bottomed 96-well plates at 10,000 cells per well. Luminescence (as a marker of caspase 3/7 activity) was observed at 0, 2.5, 7 and 24 hours following the application of Caspase-Glo® reagent. Triplicate wells were seeded for each time point for each population, with three independent experiments performed. Mean fluorescence values observed are plotted, with error bars representing one SD.	188

List of Tables

Abbreviations

3D	three-dimensional
5'DFCR	5'deoxy-5-fluorocytidine
5'DFUR	5'deoxy-5-fluorouridine
5-FU	5-fluorouracil
5-FUR	5-fluorouridine

AC	acid ceramidase
ACPGBI	Association of Coloproctology of Great Britain and Ireland
ACTB	β-actin
AIF	apoptosis inducing factor
AKT	protein kinase B
AML	acute myeloid leukaemia
ANOVA	analysis of variance
AP	apurinic/apyrimidinic
APC	adenomatous polyposis coli
APE	abdomino-perineal excision
AREG	amphiregulin
ARN14988	$C_{16}H_{24}ClN_3O_5$
ASAH1	N-acylsphingosine amidohydrolase 1
Bax	bcl-2-like protein 4
Bcl-2	B-cell lymphoma 2
Bcl-xl	B-cell lymphoma-extra large
BSA	bovine serum albumin
BSCP	bowel cancer screening programme
BMI	body mass index
BMPR1a	bone morphogenetic protein receptor, type 1a
BRAF	v-Raf murine sarcoma viral oncogene homolog B
C57BL/6	C57 black 6
C6-ceramide	N-Hexanoyl-D-erythro-sphingosine
CAPOX	capecitabine and oxaliplatin
cCR	complete clinical response
CD95	cluster of differentiation 95
CDD	cytosine deaminase
cDNA	complementary deoxyribonucleic acid
CENPE	centromere-associated protein E
CES	carboxylesterase
CHARM™	Compact Hough and Radial Map

ChoKα	choline kinase α
CI	confidence interval
CIMP	CpG island methylator phenotype
CIN	chromosomal instability
CO_2	carbon dioxide
CONTRE	COmplete Neoadjuvant Treatment for REctal cancer
Cox-2	cyclooxygenase-2
CpG	C-phosphate-G
CRC	colorectal cancer
CRCSC	colorectal cancer subtyping consortium
CMS	consensus molecular subtype
CRM	circumferential resection margin
CRT	chemoradiotherapy
CT	computed tomography
Ct	cycle threshold
CTC	CT colonography
CYP2A6	cytochrome p450 2A6
DAB	diaminobenzidine tetrahydrochloride
DCBE	double contrast barium enema
DCC	deleted in colorectal cancer
DCIS	ductal carcinoma in situ
dH_2O	distilled water
DHP	dihydropyrimidinase
DM102	[2R, 3Z]-N-(1-hydroxyoctadec-3-en-2-yl)pivaloylamine
DMEM	Dulbecco's modified Eagle's medium
DMSO	dimethyl sulphoxide
DNA	deoxyribonucleic acid
DOK3	docking protein 3
DPC4	deleted in pancreatic carcinoma, locus 4
DPD	dihydropyrimidine dehydrogenase
DPX	distyrene, plasticiser and xylene

DRE	digital rectal examination
dTMP	thymidine monophosphate
dUMP	deoxyuridine monophosphate
dUTP	deoxyuridine triphosphate
DWI	diffusion weighted images
ECL	electrochemiluminescence
EDTA	ethylenediaminetetraacetic acid
EGFR	endothelial growth factor receptor
ELAPE	extra-levator abdomino-perineal excision
EMT	epithelial mesenchymal transition
EMVI	extramural vascular invasion
ERCC1	excision repair cross-complementation group 1
ERK	extracellular signal-regulated kinases
EUROCARE	EUropean CAncer Registry
FAK	focal adhesion kinase
FAP	familial adenomatous polyposis
Fas	first apoptosis signal
FasL	Fas ligand
FBAL	fluoro-b-alanine
FDG	18-fluorodeoxyglucose
FdUDP	fluorodeoxyuridine diphosphate
FdUMP	fluorodeoxyuridine monophosphate
FdUTP	fluorodeoxyuridine triphosphate
FFPE	formalin-fixed and paraffin-embedded
FIT	faecal immunohistochemical test
FOBT	faecal occult blood test
FOxTROT	Fluoropyrimidine, Oxaliplatin and Targeted Receptor pre-Operative Therapy
FRMD3	FERM domain containing 3
FUH2	dihydro-5-fluorouracil
FUDP	fluorouridine diphosphate
FUdR	fluorodeoxyuridine

FUMP	fluorouridine monophosphate
FUTP	fluorouridine triphosphate
GAPDH	glyceraldehyde 3-phosphate dehydrogenase
GI	gastrointestinal
GoI	gene of interest
GRECCAR	French Research Group of Rectal Cancer Surgery
Gt	goat
GTBP	G/T binding protein
H&E	haematoxylin and eosin
HER2	human epidermal growth factor receptor 2
HIF-1α	hypoxia-inducible factor 1-alpha
HK	housekeeper
HNC	head and neck cancer
HNPCC	hereditary non-polyposis colon cancer
HRAS	transforming protein p21
HRP	horseradish-peroxidase
IAP	inhibitors of apoptosis
IC_{50}	half maximal inhibitory concentration
IGFR	insulin-like growth factor receptor
IgG	immunoglobulin G
IHC	immunohistochemistry
IMRT	intensity-modulated radiation therapy
IPA	Ingenuity Pathway Analysis
IQR	interquartile range
IRF8	interferon regulatory factor 8
IRS-1	insulin-receptor substrate-1
KIF5B	kinesin-1 heavy chain
KRAS	Kirsten RAt Sarcoma
LARS	low anterior resection syndrome
LCL204	(1R,2R)-1-(4-nitrophenyl)-2-(tetradecylamino)propane-1,3-diol
LCL385	(1R, 2R)-2-N-(tetradecylamino)-1-phenyl-1, 3-propandiol hydrochloride

LCL521	(1R,2R)-1-(4'-nitrophenyl)-2-N-(tetradecanoylamino)propyl-1,3-O-di-(N,N-dimethylamino)acetate dihydrochloride
lincRNA	long non-coding ribonucleic acid
LKB1	liver kinase B1
LOREC	low rectal cancer development programme
LRRIQ3	leucine-rich repeat and IQ domain-containing protein 3
LVI	lympho-vascular invasion
Mad2	mitotic arrest deficient 2
MAPK	mitogen-activated protein kinase
Mcl-1	myeloid cell leukaemia 1
MEK	serine/tyrosine/threonine kinase
MERCURY	Magnetic rEsonance imaging and Rectal Cancer eURopean equivalence study
miRNA	micro ribonucleic acid
MLH1	mutL homolog 1
MMR	mismatch repair
MRI	magnetic resonance imaging
mRNA	messenger ribonucleic acid
Ms	mouse
MSH2	mutS protein homolog 2
MSH6	mutS homolog 6
MSI	microsatellite instability
MTS	3-(4,5-dimethylthiazol-2-yl)-5-(3-carboxymethoxyphenyl)-2-(4-sulfophenyl)-2H-tetrazolium
MTT	3-(4,5-dimethylthiazol-2-yl)-2,5-diphenyltetrazolium bromide
MW	Dr Michael Wall, FRCPath
MYH	mutY homolog
MTHFR	methylenetetrahydrofolate reductase
MTOR	mammalian target of rapamycin
NAD(P)H	nicotinamide adenine dinucleotide
NC	non-coding
NCIN	national cancer intelligence network

NHS	National Health Service
NICE	National Institute for Health and Clinical Excellence
NRAS	neuroblastoma RAS viral oncogene homolog
NSG	NOD scid gamma
OnCoRe	rectal cancer complete response audit project
OPRT	uridine monophosphate synthetase
OR	odds ratio
p21	cyclin-dependent kinase inhibitor 1
p27	cyclin-dependent kinase inhibitor 1B
PARP	poly-ADP-ribose-polymerase
PBS	phosphate buffered saline
pCR	pathological complete response
PET	positron emission topography
PF	protein fragment
PI3K	phosphatidylinositol-4,5-bisphosphate 3-kinase
PKcs	protein kinase catalytic subunit
PRIDE	PRoteomics IDEntifications
PT	pre-treatment
PTEN	phosphatase and tensin homolog
RabMAb®	rabbit monoclonal antibody
RAF	serine/threonine protein kinase
RAS	rat sarcoma
Rb	rabbit
RECIST	response evaluation criteria in solid tumours
REG4	regenerating islet-derived protein 4
RIPA	radio-immunoprecipitation assay
RLU	relative light units
RNA	ribonucleic acid
RNR	ribonucleotide reductase
RT-PCR	reverse transcription polymerase chain reaction
S1P	sphingosine-1-phosphate

SAMD5	sterile alpha motif domain containing 5
SATB1	special AT-rich sequence-binding protein-1
SCNA	somatic copy number alteration
SCPRT	short course pre-operative radiotherapy
SD	standard deviation
SDS-PAGE	sodium dodecyl sulphate-polyacrylamide gel electrophoresis
SIGGAR	special interest group in gastrointestinal and abdominal radiology
siRNA	small interfering ribonucleic acid
SK	sphingosine kinase
sm	submucosa
smac	second mitochondria-derived activator of caspases
SMAD	mothers against decapentaplegic
Smase	sphingomyelinease
SNP	single nucleotide polymorphism
SPH	sphingosine
SPSS	statistical package for the social sciences
STAR-TREC	can we Save the rectum by watchful waiting or TransAnal microsurgery following (chemo) Radiotherapy versus Total mesorectal excision for early REctal Cancer
STK11	serine/threonine kinase 11
TBST	tris-buffered saline and tween
TCF4	transcription factor 4
TGFβ	transforming growth factor beta
TK	thymidine kinase
TMA	tissue microarray
TMC7	transmembrane channel like 7
TME	total mesorectal excision
TNM	tumour node metastasis
TP	thymidine phosphorylase
TP53	tumour protein p53
TREC	Transanal endoscopic microsurgery (TEM) and Radiotherapy in Early rectal Cancer

TRG	tumour regression grade
Tris	trisaminomethane
TS	thymidylate synthetase
UICC/AJCC	Union for International Cancer Control / American Joint Committee for Cancer
UK	United Kingdom
UKCCCR	United Kingdom Coordinating Committee of Cancer Research
UK2	uridine-cytidine kinase 2
UP1	uridine phosphorylase 1
VEGF	vascular endothelial growth factor
WNT	int/Wingless
χ^2	chi-squared
XIAP	X-linked inhibitor of apoptosis protein
XRCC1	x-ray repair cross-complementing protein 1
λem	emission wavelength
λex	excitation wavelength

Chapter 1

General Introduction

1.1 Colorectal Cancer

1.1.1 Epidemiology of Colorectal Cancer

Colorectal cancer (CRC) represents the second commonest cause of cancer related mortality in the United Kingdom, according to the Cancer Research (UK) dataset from 2011, despite crude 5-year survival more than doubling from 24.4% to 58.7% over the last 40 years. It is the fourth most commonly diagnosed malignancy in the country overall, with 41,581 new cases reported in 2011 but is the third commonest malignancy in men and women individually (behind prostate and lung cancer, and breast and lung cancer respectively). The national incidence of the disease has increased by 6% over the last decade, likely with the introduction and gradual roll out of the UK bowel cancer screening programme since 2006, and 95% of cases occur in those over the age of 50. Males are more frequently affected (55.7% vs. 44.3%), and approximately one third of cases involve the rectum or recto-sigmoid junction. These figures are representative of global disease burden, with 447,000 and 1,360,000 new cases diagnosed in Europe and worldwide respectively in 2012. (http://www.cancerresearchuk.org/health-professional/cancer-statistics/statistics-by-cancer-type/bowel-cancer)

The overall five-year relative survival of CRC patients in England is 50.7% but there is significant variation according to disease stage at diagnosis. According to National Cancer Intelligence Network (NCIN) data published in 2009, 93.2% of patients with Dukes A disease at diagnosis survive at least five years, in comparison with only 6.6% of those with Dukes D disease (table 1.1). (http://www.ncin.org.uk/cancer_type_and_topic_specific_work/cancer_type_specific_work/colorectal_cancer)

Survival between patients with colon cancer and those with rectal cancer is comparable, as is longer-term survival between sexes. The latest data from EUROCARE-5 (De Angelis et al, 2014) demonstrates that five-year age-standardised relative survivals for colon and rectal cancer in England are 51.3% and 53.7% respectively. Whilst most recent data from Cancer Research (UK) demonstrates better one-year age-standardised survival in the UK for men with colorectal cancer (77.4% vs. 73.9%), survival at five years is equivalent (59.2% vs. 58.2%) for men and women respectively.

Dukes Stage	Cases (%)	Five-year survival (%)
A	8.7	93.2
B	24.2	77.0
C	23.6	47.7
D	9.2	6.6
Unknown	34.3	35.4

Table 1.1 – Percentage of cases and five-year relative survival by Dukes stage at diagnosis for CRC patients diagnosed 1996-2002 in England. (Adapted from NCIN data briefing – CRC Survival by Stage, June 2009)

1.1.2 Risk Factors for Colorectal Cancer

It is considered that lifestyle and environmental risk factors are associated with 54% of CRC (Parkin *et al*, 2011). A meta-analysis of prospective studies assessing meat consumption and CRC risk demonstrated the relative risks of cancer development to be 1.28 (95% confidence interval (CI) 1.15-1.42) and 1.20 (95% CI 1.11-1.31) for those with the highest intake of red meat and processed meat respectively against those with the lowest intake (Larsson and Wolk, 2006). An increased intake of dietary fibre and whole grains reduces the risk of CRC (Aune *et al*, 2011).

Colonic cancer risk was observed to be 18% and 48% higher in men who are overweight or obese respectively, compared with men of a normal weight on meta-analysis (Xue *et* al, 2017). The same study demonstrated a 12% higher risk of colonic cancer in obese women but did not demonstrate any association with rectal cancer with a raised BMI in women. The rectal cancer risk was 6% and 25% higher in overweight and obese men respectively compared with men of a normal weight. Another meta-analysis observed the risk of colorectal adenoma to be 47% higher in an obese population compared to those of a normal weight (Omata *et al*, 2013). Complimentary to this is the association of a sedentary lifestyle to colon (but not rectal) cancer risk in a meta-analysis of observational studies (Cong *et al*, 2014).

Alcohol has also been associated with CRC on meta-analysis (Bagnardi *et al*, 2015), with a relative risk of 1.44 in those who drink more than 6 units of alcohol per day, and a 17% higher incidence in those who consume 1.5-6 units daily, compared to non- or occasional drinkers. A daily consumption of 3 units of alcohol also contributes to a 27% higher incidence of colonic (but not rectal) adenoma (Ben *et al*, 2015). Smoking confers a 20% increased risk of CRC compared to non-smokers (Huxley *et al*, 2009), with twice the risk of adenomatous polyp in smokers against non-smokers (Botteri *et al*, 2009).

There is an increase in the relative risk (1.28, 95% CI 1.19-1.39) of developing CRC in people with diabetes mellitus compared to those without (Luo *et al*, 2011). A diagnosis of inflammatory bowel disease also predisposes to CRC, with increased disease extent and duration contributing to a 5% risk after 20 years (Lutgens *et al*, 2013).

The risk of CRC is more than doubled with a first degree relative affected by the disease and increases in those with more than one affected relative or a relative diagnosed at a younger age (Butterworth *et al*, 2006). Having an adoptive parent with a CRC does not increase an individual's risk, suggesting genetic rather than environmental factors underpin the familial risk (Zöller *et al*, 2014). The genetics of CRC and associated familial syndromes is therefore discussed.

1.1.3 Genetics of Colorectal Cancer

There are known genetic defects which predispose to CRC with known somatic mutations that present in sporadic tumours. These alterations are considered to initiate novel or improved function in oncogenes and/or loss of function of tumour suppressor genes, with subsequent malignant development. It is estimated that approximately 15-30% of CRC has a significant hereditary component (Lynch and de la Chapelle, 2003), of which 5% have a Mendelian cancer syndrome which predisposes to CRC (Rustgi, 2007). The majority of these are attributable to hereditary non-polyposis colorectal cancer (HNPCC) and familial adenomatous polyposis (FAP), where the lifetime risk of cancer development is 80% by age 70 in HNPCC and 100% by age 40 in FAP (Fearnhead *et al*, 2002). These conditions and other less common CRC syndromes with their associated genetic defects are summarised in table 1.2 below.

Syndrome	Common Features	Gene Defect(s)
Familial Adenomatous Polyposis (FAP)	Multiple adenomatous polyps (>100) and carcinomas of the colon and rectum; duodenal polyps and carcinomas, fundic gland polyps in the stomach, congenital hypertrophy of the retinal pigment epithelium	APC (>90%)
Gardner syndrome	Same as FAP; also, desmoid tumours and mandibular osteomas	APC
Turcot's syndrome	Polyposis and colorectal cancer with brain tumours (medulloblastomas); colorectal cancer and brain tumours (glioblastoma)	APC
		MLH1
Attenuated ademomatous polyposis coli	Fewer than 100 polyps, although marked variation in polyp number (from ~5 to >1,000) observed in mutation carriers within a single family	APC (predominantly 5' mutations)
Hereditary non-polyposis colorectal cancer	Colorectal cancer without extensive polyposis; other cancers include endometrial, ovarian and stomach cancer, and occasionally urothelial, hepatobiliary and brain tumours	MSH2
		MLH1
		PMS2
		GTBP, MSH6
Peutz-Jeghers syndrome	Hamartomatous polyps throughout the GI tract; mucocutaneous pigmentation; increased risk of GI and non-GI cancers	LKB1, STK11 (30-70%)
Cowden disease	Multiple hamartomas involving breast, thyroid, skin, central nervous system and GI tract; increased risk of breast, uterus and thyroid cancers; risk of GI cancer unclear	PTEN (85%)
Juvenile polyposis syndrome	Multiple hamartomatous / juvenile polyps with predominance in colon and stomach; variable increase in colorectal and stomach cancer risk; facial changes	DPC4 (15%)
		BMPR1a (25%)
		PTEN (5%)
MYH-associated polyposis	Multiple adenomatous GI polyps, autosomal recessive basis; colon polyps often have somatic *KRAS* mutations	MYH

Table 1.2 – Genetics of inherited CRC syndromes. (Adapted from Fearon, 2011).

CRC arises most frequently from dysplastic polyps, and therefore an understanding of adenoma to carcinoma transformation is essential. Most polyps are hyperplastic in nature and less than 5mm in diameter, however it is the larger adenomas which harbour malignant potential (Jass, 2007). An adenoma is a benign lesion of glandular epithelium, and has prevalence of approximately 25% and 50% by ages 50 and 70 respectively (Rex *et al*, 1993). A small number of polyps will progress to malignancy, often over a period of years to decades, with polyp surveillance studies demonstrating that a 1cm polyp has a 10-15% chance of becoming malignant within 10 years (Stryker *et al*, 1987). Adenoma-carcinoma progression was first described as a series of genetic alterations responsible for sporadic colorectal cancer (Fearon and Vogelstein, 1990), beginning with mutation in the adenomatous polyposis coli (*APC*) gene, and followed by mutations in *KRAS* and *TP53* genes. These mutations are positively selected for during colorectal carcinogenesis and are intrinsically involved in DNA repair, cell adhesion and proliferation (Wood *et al*, 2007).

1.1.3.1 *Adenomatous polyposis coli*

The *APC* tumour suppressor gene encodes for a protein known to regulate cell-adhesion, migration and apoptosis (Fearon and Vogelstein, 1990), and is the genetically defective gene in FAP as well as some of the less common inherited cancer syndromes. The defect is present in over 75% of colorectal cancers, and is widely believed to be an early step in sporadic carcinogenesis due to its reported presence across the adenoma-carcinoma sequence, including microscopic adenomas with a small number of dysplastic glands (Kinzler and Vogelstein, 1996).

The most well understood downstream effect of *APC* mutation is disruption of the WNT pathway. *APC* targets β-catenin for proteasomal degradation, and therefore mutation results in the nuclear accumulation of β-catenin, increased WNT activity and cellular proliferation (Polakis, 2007). WNT signalling is also significantly implicated in cell migration via epithelial-mesenchymal transition.

1.1.3.2 *KRAS / BRAF*

The RAS family of proteins (KRAS, HRAS and NRAS) are G-proteins which predominantly undertake the role of molecular switches. *KRAS* is a proto-oncogene which, following activation through the endothelial growth factor receptor (EGFR) pathway, triggers downstream signalling through the PI3K/AKT/MTOR and RAF/MEK/ERK pathways resulting

in cellular proliferation (Fearon, 2011). Up to 40% of colorectal tumours have a mutated version of the *KRAS* gene, most commonly in codon 12, with smaller subsets affecting codon 13 and rarely codon 61 (Downward, 2003). The mutation is found in a number of flat colonic epithelial lesions without dysplasia, questioning its role in early carcinogenesis (Pretlow and Pretlow, 2005), however disruption of mutant *KRAS* in advanced CRC demonstrates that inactivation inhibits tumour growth both *in vitro* and in animal studies, highlighting its role in disease progression (Shirasawa *et al*, 1993).

BRAF is a downstream target of KRAS and exhibits its effect through the MEK/ERK pathways. *BRAF* mutation occurs in approximately 5-10% of CRC and appears to be independent of *KRAS* mutation, however mutation in either gene can result in pathway upregulation, and activation of relevant downstream transcription factors such as myc (Rajagopalan *et al*, 2002).

1.1.3.3 *TP53*

TP53 (p53) is a tumour suppressor gene implicated in a wide range of malignancies, most likely due to its significant role as a regulator of cell-cycle checkpoints, genomic stability, apoptosis and angiogenesis (Vousden and Prives, 2009). Under conditions of DNA damage resulting from cellular stress, p53 activates DNA repair proteins, arrests growth by holding the cell cycle at the G1/S regulation point and initiates apoptosis. Over 50% of all tumours have ineffective p53 (Hollstein *et al*, 1991), thought to be a combination of loss of heterogeneity of one allele of 17p and somatic mutation in the other (Fearon and Vogelstein, 1990). This pattern is not observed in most adenomas, highlighting these mutations as significant events in the transition from adenoma to carcinoma (Baker *et al*, 1990).

1.1.3.4 Mismatch repair and microsatellite instability

Whilst germline mutations account for a relatively small proportion of tumours they offer a unique opportunity to understand the genetic instability which contributes to the development of CRC. Mismatch repair (MMR) genes such as *MLH1, MSH2, MSH6* and *PMS2*, are responsible for correcting base mismatches and short insertions or deletions which normally occur during DNA replication (Grady and Carethers, 2008). Where these genes are defective, DNA sequences are not faithfully replicated and microsatellites are created; short sections of repeating DNA, 1-6 base pairs long.

Germ-line mutations in MMR genes are present in only 2-4% of CRC patients, however 15% of sporadic CRC exhibit microsatellite instability (MSI). A key mechanism for this is thought to be hypermethylation of the promoter of *MLH1*, resulting in a loss of function (Aaltonen *et al*, 1993). Microsatellite unstable tumours exhibit a specific phenotype; they tend to be poorly differentiated right colonic tumours with high mucinogen and tumour related lymphyocytes and are less likely to metastasise than microsatellite stable tumours (Buecher *et al*, 2013). These pathological features confer a survival advantage, despite a reported resistance to fluorouracil based chemotherapeutic regimens (Ribic *et al*, 2003). Tumours with MSI can be sub-classified as MSI-low or MSI-high by the presence of fewer or greater than 30% unstable loci in a panel of 5-10 points respectively (Boland *et al*, 1998). The distinction of MSI-high and MSI-low is associated with further variations in tumour phenotype and disease characteristics.

1.1.3.5 Chromosomal instability

The chromosomal instability (CIN) phenotype is observed in approximately 70%–85% of CRC. It is widely accepted that most microsatellite stable tumours follow the CIN mechanism of carcinogenesis, however the MSI and CIN phenotypes are not mutually exclusive (Lengauer *et al*, 1997).

The cause of CIN is not clearly understood, although it is believed to be due to defects in genes which regulate formation of the mitotic spindle, and alignment and segregation of chromosomes at mitosis (Grady, 2004). A small number of specific defects have been suggested, including alterations in Mad2, BubR1, Bub3 and CENPE proteins as well as loss of heterogenicity in chromosome 18q, containing the tumour suppressor genes *SMAD2*, *SMAD4,* and *DCC* (Barber *et al*, 2008). *APC* mutation is also thought to play a role but its presence in many other chromosomal stable tumour phenotypes suggests that the molecular basis for CIN is more heterogenous than the relationship between MMR genes and MSI (Alberici and Fodde, 2006).

1.1.3.6 CpG island methylator phenotype

DNA methylation is thought to serve the biological function of silencing repetitive elements of the genome (Yoder *et al*, 1997). The significance of hypermethylation resulting in loss of function of *MLH1* has already been discussed. The majority of C-phosphate-G (CpG) sites have been lost from the human genome during evolution, however hypermethylation of

residual sites, defined as methylation of at least 3 loci from a panel of 5 gene-associated CpG islands, results in the silencing of tumour suppressor or other tumour related genes, and ultimately carcinogenesis (Carragher *et al*, 2010). The CpG island methylator phenotype (CIMP) represents a further subset of colorectal cancers with a particular molecular and biological profile. Specifically, these tumours have a higher incidence of concurrent mutations in *KRAS/BRAF* but wild type *TP53* and are more frequently proximal tumours with mucinous and poorly differentiated histopathological features, most often presenting in older female patients (Issa, 2004). CIMP tumour status has been used to infer potential response to irinotecan-based chemotherapy (Shiovitz *et al*, 2014).

1.1.3.7 Summary of colorectal cancer genetics

The majority of colorectal tumours reflect a series of hereditary and somatic mutations in key genes such as APC, KRAS, BRAF and TP53. These mutations are most frequently associated with a chromosomal instability phenotype. The acquisition of these mutations frequently occurs in differing orders, although the sequence of events may be relevant to tumour development. A subset of tumours initiaite through inactivation of MMR function, which may be through inherited, or less commonly, somatic mutation. Epigenetic inactivation of CpG islands through hypermethylation can alternatively lead to high MSI, with cumulative mutations in the APC/KRAS/BRAF/TP53 genes ultimately leading to carcinogenesis.

The understanding of colorectal carcinogenesis has developed significantly since the model first proposed by Vogelstein in 1990 and is summarised in figure 1.1.

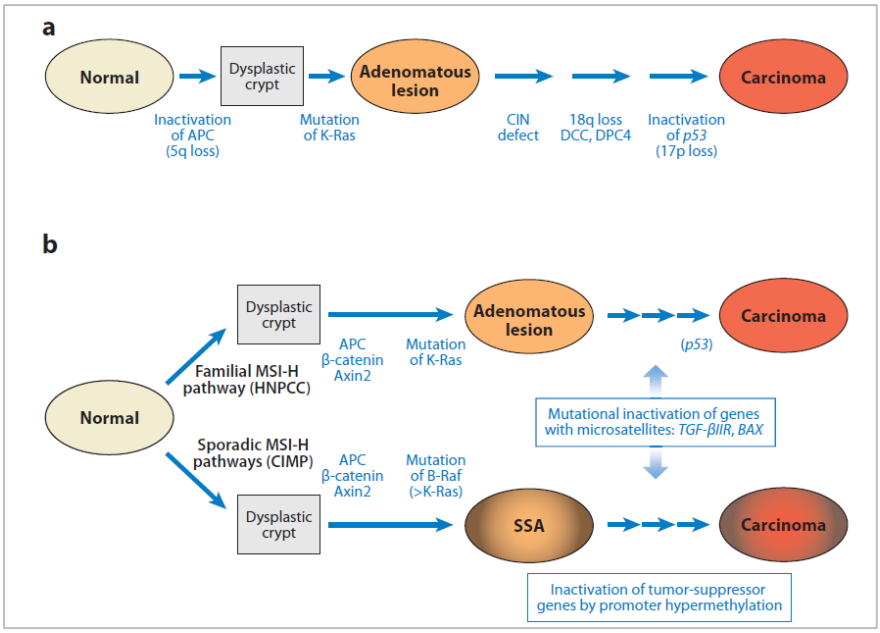

Figure 1.1 – The suggested genetic model for CRC. (a) A number of hereditary and sporadic mutations drive the transformation of normal epithelium to adenomatous lesion and subsequently carcinoma. (b) An inherited or acquired defect in DNA MMR function is the initiator for carcinogenesis. (Taken from Fearon, 2011)

1.1.4 Consensus Molecular Subtypes of Colorectal Cancer

An international expert collaboration recently defined colorectal cancer into four clear consensus molecular subtypes (CMS). The colorectal cancer subtyping consortium (CRCSC) was formed to assess the presence or absence of core subtype patterns among existing gene expression-based CRC subtyping algorithms. They characterised the key biological features of the core subtypes, integrating other data regarding mutations, copy number, methylation status, microRNA, and proteomics, and correlated the subtype assignment with patient outcome. The intention was for the subtypes to have a clear biological interpretation, in order to form the basis for future stratification and subtype-based targeted interventions (Guinney *et al*, 2015), and are detailed below.

CMS1 (MSI immune, 14%) tumours are frequently right sided, diagnosed in females, and present with higher histopathological grade. This subtype is hypermutated, has a low

prevalence of somatic copy number alterations (SCNA), and accounts for the majority of MSI tumours. These tumours over-expressed DNA repair proteins and display a high CIMP. *BRAF* mutations commonly seen in MSI frequently occur in this subtype, and genes associated with immune infiltration and activation are increasingly expressed.

CMS2 (canonical, 37%) tumours are predominantly left sided, and display high CIN demonstrated by high SCNA, with more frequent copy number gains in oncogenes and losses in tumour suppressor genes than other subtypes. These tumours display epithelial differentiation and strong upregulation of WNT and MYC downstream targets, both of which are classically implicated in CRC carcinogenesis. There is a superior survival after relapse in this patient group.

CMS3 (metabolic, 13%) tumours are characterised by *KRAS* mutations and the associated metabolic deregulation. These tumours display high CIN but with fewer SCNA, a mixed MSI status, and low CIMP.

CMS4 (mesenchymal, 23%) tumours demonstrate high CIN with high SCNA. There is clear upregulation of genes implicated in epithelial mesenchymal transition and gene signatures associated with TGFβ signalling, angiogenesis and stromal infiltration, with over-expression of extra-cellular matrix proteins and those associated with stromal invasion, mesenchymal activation and complement pathways. These tumours are diagnosed at a more advanced stage, with associated poorer overall and relapse-free survival.

CMS1 MSI Immune	CMS2 Canonical	CMS3 Metabolic	CMS4 Mesenchymal
14%	37%	13%	23%
MSI, CIMP high, hypermutation	SCNA high	Mixed MSI status, SCNA low, CIMP low	SCNA high
BRAF mutations		*KRAS* mutations	
Immune infiltration and activation	WNT and MYC activation	Metabolic deregulation	Stromal infiltration, TGFβ activation, angiogenesis
Worse survival after relapse			Worse relapse-free and overall survival

Figure 1.2 – Summary of CMS of CRC according to the CRCSC international collaboration. (Taken from Guinney *et al,* 2015)

The remaining 13% of samples are considered to represent a transition sub-type or intra-tumour heterogeneity.

1.1.5 NHS Bowel Cancer Screening Program (BCSP)

The NHS BCSP offers biennial population screening to those aged 60-74, as over 80% of bowel cancers occur at and after this age. Screening with the guaiac faecal occult blood test (FOBT) has been demonstrated to reduce CRC mortality in four large population based randomised controlled trials, each with more than 10 years follow up (Hewitson *et al*, 2008). The UK data demonstrated a relative mortality risk of 0.87 (95% CI 0.78-0.97) with a follow up period of 11.7 years. People with positive FOBT tests are offered a screening colonoscopy, with earlier detection of CRC facilitating the increased use of minimally invasive treatment techniques, with subsequent improvement in 30-day post-operative mortality and overall survival.

The guaiac FOBT is being replaced with the faecal immunohistochemical test (FIT), which has been demonstrated to be both more accurate in detecting CRC and advanced adenomas, and with improved uptake (Moss *et al*, 2017). The FIT eliminates potential dietary interference and can measure very low concentrations of human-specific haem in stool from bleeding cancers and pre-cancerous lesions. It only requires one stool sample, whereas three are required for the current guaiac FOBT, and also uses a simple and cleaner sampling technique with an easy-return postal package. The uptake with the FIT increased to 63.9% in all those at age 60 invited to undertake screening for the first time, compared to 54.4% with the guaiac FOBT.

A one-off flexible sigmoidoscopy is also being rolled out as part of the BCSP under the 'Bowel Scope' program for those age 55 with the option to opt-in until age 60. This is based on a randomised controlled trial from the UK demonstrating a 23% reduced incidence of CRC, and a 31% reduced CRC mortality following a screening flexible sigmoidoscopy, after a median follow up of 11 years (Atkin *et al*, 2010).

1.1.6 Diagnosis of Colorectal Cancer

Despite the NHS BCSP, the majority of patients with CRC continue to present symptomatically. Typical symptoms of left sided lesions include alteration in bowel habit, rectal bleeding, and tenesmus with rectal lesions, whereas right sided lesions more commonly present with anaemia, abdominal pain or mass, and systemic symptoms of malignancy such as anorexia or weight loss (Majumdar *et* al, 1999). The National Institute for Health and Clinical Excellence (NICE) define criteria for urgent assessment under two-week wait referral guidelines based upon these features (NG12, updated 2017), where duration of bowel habit and/or rectal bleeding (in the absence of anal symptoms) for more than 6 weeks based on a patient's age, and abdominal or rectal mass and/or anaemia at any age, are considered for straight to test assessment. Patients over 75 years should be reviewed within two weeks in an outpatient clinic to determine appropriate investigation potentially based upon co-morbidity (NICE, 2015).

1.1.6.1 Choice of investigation

The UK Special Interest Group in Gastrointestinal and Abdominal Radiology (SIGGAR) trials provided level I evidence on the choice for whole colon imaging in patients with symptoms suggestive of CRC. The two arms of the trial compared CT colonography (CTC) with double contrast barium enema (DCBE) to assess cancer and large polyp detection rate, and compared CTC with colonoscopy in assessing the requirement for further colonic assessment following CTC. CTC was superior to DCBE in detecting cancers and large polyps (7.3% vs 5.6% p=0.039), and patients randomised to CTC were diagnosed with fewer cancers during the three-year follow up (Halligan *et al*, 2013). No significant differences were observed in detection rate, or sensitivity based on post-test cancer diagnoses during follow up, between CTC and colonoscopy. CTC did generate an increased number of further colonic investigation with a relative risk of 3.75 (Atkin *et al*, 2013), although either CTC or colonoscopy is recommended for investigation by the Association of Coloproctology of Great Britain and Ireland (ACPGBI) (Cunningham *et al*, 2017).

1.1.6.2 Colonoscopy

Colonoscopy allows the visualisation of the entire colonic and rectal mucosa whilst facilitating biopsy of any suspicious lesion, and the procedure can be considered therapeutic in the context of undertaking polypectomy. Full assessment of the colon is important given

the incidence of synchronous cancers (2-3%), or significant other benign disease (20%), which may influence subsequent management (Langevin and Nivatvongs, 1984). The procedure also facilitates the marking of the most significant distal colonic lesion with a tattoo on the anal side (but not in the rectum), particularly for subsequent localisation during laparoscopic surgery (Williams *et al*, 2013).

1.1.6.3 CT Colonography

This investigation combines the use of oral faecal tagging agents with mechanical rectal insufflation with CO_2 to produce detailed mucosal images of the colon and rectum. It can be performed following full purgative bowel preparation, although some faecal tagging agents (such as Gastrograffin) have a laxative effect and can be used as a combined cleansing/tagging agent. In the context of frail patients where only exclusion of clinically relevant malignancy is required, dietary modification with non-laxative faecal tagging may be appropriate. The investigation can also be combined with intravenous contrast to assess for the presence of extra-colonic disease (Neri *et al*, 2013).

1.1.6.4 Diagnosis of colorectal cancer

Tissue obtained at endoscopy is assessed by histopathological examination. This involves formalin-fixing and paraffin-embedding (FFPE) the tissue, before cut sections are stained with haematoxylin and eosin (H&E) and assessed under microscopy. The histological diagnosis of CRC is based on tumour invasion through the muscularis mucosae into the submucosa, as depicted in figure 1.3. The digestive tract can be considered as a continuum which, from mouth to anus, is outside the body - biopsies can therefore be taken without fear of seeding tumour into adjacent tumour free tissue.

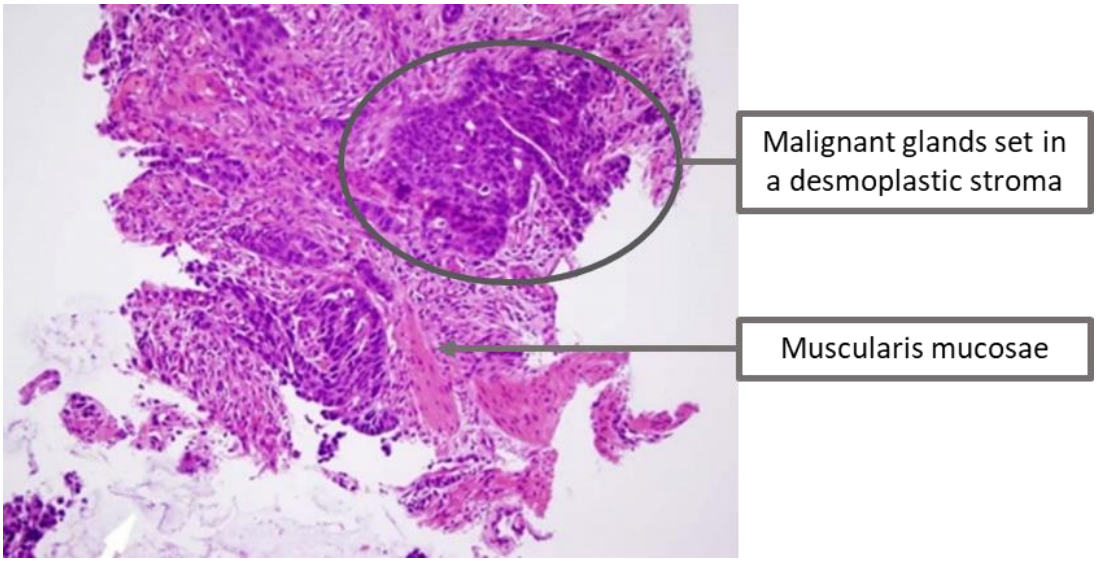

Figure 1.3 – Invasive colonic adenocarcinoma stained with H&E, demonstrated by penetration of the muscularis mucosa. Photomicrograph taken at x200 magnification. (Adapted from Rose and Wu, 2010)

Virtually all CRC is adenocarcinoma, with other rare types being mucinous carcinoma (a variant of adenocarcinoma with >50% composed of extracellular mucin), signet ring cell carcinoma (another variant of adenocarcinoma with >50% signet ring cells), adenosquamous carcinoma, primary squamous carcinoma, goblet cell carcinoids and other mixed adenocarcinoma-neuroendocrine carcinoma, medullary carcinoma, and undifferentiated carcinoma (Hamilton et al, 2010).

An important element of the histopathological assessment of colorectal adenocarcinoma is an interpretation of the degree of differentiation from the morphology of the original tissue. This considers features such as nuclear pleomorphism, cellular architecture and mitotic count to determine poorly differentiated tumours from moderately or well differentiated tumours for prognostic purposes.

1.1.7 Radiological Assessment of Colorectal Cancer

Radiological assessment of CRC should assess and stage local disease as well as assessing for the presence of metastases or synchronous disease.

1.1.7.1 Computed tomography

Computed tomography (CT) is used for colonic tumours to assess the extent of disease relative to the bowel wall and local organs, in order to plan anatomical or non-anatomical resection, and to determine the requirement for neo-adjuvant or systemic treatment in the case of unresectable disease. It is considered that CT has sensitivities of 86% and 70% on meta-analysis for the prediction of T3 disease and lymph node status respectively (Dighe *et al*, 2010), and further reliable prognostic information to separate low from high risk groups based on extent of trans-mural spread and local lymph node status can be determined (Smith *et al*, 2007). This information may well be used in the future to select higher risk patients for neo-adjuvant chemotherapy; a question that will be determined by the FOxTROT trial (FOxTROT Collaborative Group, 2012), which finished recruiting in 2016. Modern techniques of dual-phase helical scanning have significantly improved lesion characterisation in the liver (Scott et al, 2001), and it is used for the detection and characterisation of both hepatic and extra-hepatic metastases in all CRC, where it has a sensitivity of 60-90% (Ong and Leen, 2007).

1.1.7.2 Magnetic resonance imaging

Magnetic resonance imaging (MRI) is used in the local staging of rectal cancer, where pre-operative high-resolution imaging provides information not previously known until the surgical specimen had undergone histopathological assessment. Knowledge of this in advance of surgery affords the opportunity to deliver neo-adjuvant therapy in attempt to influence outcome. On T2-weighted images obtained with a 1.5T system with phased array coils, information regarding tumour morphology and stage, lymph node status and extramural vascular invasion (EMVI) can be obtained (Taylor *et al*, 2011). The greatest significance of MRI is in the reliable identification of a 'threatened' or involved circumferential resection margin (CRM), where tumour is within 1mm of (or involving) the mesorectal fascia. This is a very sensitive predictor of a positive CRM following surgery (with associated poorer outcome), with a non-threatened CRM on MRI pre-operatively demonstrating a 92% specificity for a clear surgical CRM (MERCURY Study Group, 2006). MRI can also determine the higher risk low rectal cancers, defined by a tumour with its lower edge at or below the level of origin of the levator muscle on the pelvic side-wall. Specific management issues for this patient group have been identified and addressed by the Low Rectal Cancer (LOREC) development programme (Moran *et al*, 2014).

MRI is also used to further assess indeterminate lesions in the liver, where gadolinium contrast enhanced imaging is considered the most effective modality for accurate characterisation (Kamel and Bluemke, 2003).

1.1.7.3 Positron emission tomography

Positron emission tomography (PET) utilises the increased glucose metabolism in tumour cells to distinguish them by uptake of the radiotracer 18-fluorodeoxyglucose (FDG). FDG is phosphorylated and becomes metabolically inactive upon uptake and thus accumulates. When combined with CT scanning, PET imaging allows for the accurate localisation of small disease deposits, for example extra-hepatic abdominal metastases or local disease recurrence. The principle for use of this modality is that metabolic changes in cells can be detected, and this precedes any anatomical variance that would be detected on contrast enhanced CT imaging (Arulampalam *et al*, 2004). The additional information from PET-CT imaging has been shown to alter disease management in 29% of patients with colorectal liver metastases (Huebner *et al*, 2000), and prevents futile surgery in those being considered for non-anatomical resection (Adams *et al*, 2013).

1.1.8 Staging of Colorectal Cancer

The first staging system described was devised for rectal cancer by Dr Cuthbert Dukes in 1932. Initially this classification assigned a Dukes' stage from A-C, where stage A represented a malignant invasion into but not through the bowel wall, stage B represented malignant growth through the bowel wall, and stage C represented lymph node involvement (Dukes, 1932). The system was refined to correlate pathological grade with prognosis (Dukes and Bussey, 1958), at which time the subdivision of stages C1 (regional lymph node involvement) and C2 (apical node involvement) were made. Stage D representing distant or metastatic disease was later added (Turnbull *et al*, 1967), and the scoring system was informally applied to carcinomas arising in the colon.

Advancements in both our understanding of disease biology and in radiological techniques, have led to the current gold standard staging system of the Union for International Cancer Control / American Joint Committee for Cancer (UICC/AJCC) TNM classification. This classification is a disease specific extension of the original TNM system devised by Denoix *et*

al in 1946, whereby the degree of invasion and tumour spread is characterised by a T stage referring to the primary tumour, N stage recording the presence and extent of local lymph node involvement, and M stage describing the presence or absence of metastatic disease. The current version in widespread clinical use is the 7th edition published in 2010 (table 1.3).

TNM Stage	Description
TX	Primary tumour cannot be assessed
T0	No evidence of primary tumour
Tis	Carcinoma in situ: intra-mucosal carcinoma
T1	Tumour invades submucosa
T2	Tumour invades muscularis propria
T3	Tumour invades through muscularis propria into peri-colorectal tissues
T4a	Tumour invades through visceral peritoneum
T4b	Tumour directly invades or is adherent to adjacent organs or structures
NX	Regional lymph nodes cannot be assessed
N0	No regional lymph node metastasis
N1	Metastasis in 1-3 regional lymph nodes
N1a	Metastasis in 1 regional lymph node
N1b	Metastasis in 2-3 regional lymph nodes
N1c	Tumour deposits in sub-serosa, mesentery, or non-peritonealised pericolic or perirectal tissues without regional nodal metastasis
N2	Metastasis in 4 or more regional lymph nodes
N2a	Metastasis in 4-6 regional lymph nodes
N2b	Metastasis in 7 or more regional lymph nodes
M0	No distant metastasis by imaging, no evidence
M1	Distant metastasis
M1a	Metastasis confined to 1 organ or site without peritoneal metastasis
M1b	Metastases in 2 or more organs or sites without peritoneal metastasis
M1c	Metastasis to the peritoneal surface alone or with other site or organ metastases

Table 1.3 – UICC/AJCC TNM staging of CRC, 8th edition (2017). (Adapted from http://pathologyoutlines.com/topic/colontumourstaging8ed.html)

It is possible to stage a patient's disease for some parameters at different points in their treatment pathway. Supplementary prefixes to the TNM system have been developed to highlight the origin of the information used for staging; c indicates the stage is given by

clinical examination of the patient, p indicates the stage is given by histopathological examination of a surgical specimen, y indicates the stage is assessed after chemotherapy and/or radiation therapy (i.e. the patient received neoadjuvant treatment), r indicates staging of a recurrent tumour following a substantial disease-free period, a indicates staging determined at post mortem examination, and u is for staging determined by ultrasonography.

Stage	Description	TNM Stages
0	No tumour	Tis, N0, M0
I	Primary tumour into but not through muscularis propria, and no metastases	T1-2, N0, M0
IIa	Primary tumour grown through to serosa and peritoneal surface but no metastases	T3, N0, M0
IIb		T4a, N0, M0
IIc		T4b, N0, M0
IIIa	Any size of primary tumour with lymph node metastases	T1-2, N1-N1c, M0 *or* T1, N2a, M0
IIIb		T3-T4a, N1-N1c, M0 *or* T2-T3, N2a, M0 *or* T1-T2, N2b, M0
IIIc		T4a, N2a, M0 *or* T3-T4a, N2b, M0 *or* T4b, N1-2, M0
IVa	Presence of distant metastatic disease	Any T, Any N, M1a
IVb		Any T, Any N, M1b
IVc		Any T, Any N, M1c

Table 1.4 - UICC/AJCC stage groupings for CRC, 8th edition (2017). (Adapted from http://pathologyoutlines.com/topic/colontumourstaging8ed.html)

There are numerous potential combinations of TNM criteria, which are grouped together into stages 0-IV (table 1.4) by UICC/AJCC for the benefit of simplifying treatment decisions (Carrato, 2008). Alternative staging systems have been established to further guide treatment or gain prognostic information. The most commonly used of these is the Jass classification (figure 1.4), which combines some of the common genetic aberrations identified, with a number of macroscopic and microscopic pathological correlates, and patient features (Jass, 2007).

Feature	Group 1	Group 2	Group 3	Group 4	Group 5
MSI status	H	S/L	S/L	S	H
Methylation	+++	+++	++	+/−	+/−
Ploidy	Dip > An	Dip > An	An > Dip	An > Dip	Dip > An
APC	+/−	+/−	+	+++	++
KRAS	−	+	+++	++	++
BRAF	+++	++	−	−	−
TP53	−	+	++	+++	+
Location	R > L	R > L	L > R	L > R	R > L
Gender	F > M	F > M	M > F	M > F	M > F
Precursor	SP	SP	SP/AD	AD	AD
Serration	+++	+++	+	+/−	+/−
Mucinous	+++	+++	+	+	++
Dirty necrosis	+	+	?	+++	+
Poor differentiation	+++	+++	+	+	++
Circumscribed	+++	+	?	++	++
Tumour budding	+/−	+	?	+++	+
Lymphocytes	+++	+	?	+	+++

MSI, microsatellite instability; H, high; S, stable; L, low; Dip, diploid; An, aneuploid; Serration, serrated morphology; SP, serrated polyp; AD, adenoma; Circumscribed, circumscribed invasive margin.

Figure 1.4 – The Jass classification combines a number of patient, histopathological and genetic factors to allocate a patient to a group (1-5). (Taken from Jass, 2007)

The Jass classification is often used as a decision-making tool for those patients with Dukes' B (or Stage II) disease. A study of 183 patients with Dukes' B disease who were also Jass grouped, identified that cancer specific mortality was considerably higher in those with Jass group III than in those groups I or II. The additional prognostic information from Jass grouping may facilitate the selection of patients who are most likely to benefit from adjuvant chemotherapy (Mander *et al*, 2006), although the classification highlights the complexity of CRC.

1.2 The Curative Management of Rectal Cancer

The rectum is distal to the sigmoid colon, with its upper limit at the termination of the sigmoid mesocolon, although the common surgical definition is that the rectum starts at the sacral promontory, and generally a rectal cancer is defined as being at or below 15cm from the anal verge as measured by rigid sigmoidoscopy (UKCCCR, 1989).

1.2.1 Early Rectal Cancer

Small tumours contained within polyps are often removed by polypectomy at the time of colonoscopy, and rectal tumours may be amenable to local or trans-anal excision (Atallah and Albert, 2013) preserving the rectum and its function, and avoiding the morbidity and mortality of radical surgery. Full thickness excision offers accurate pathological assessment, and potential cure for many pT1 and pT2 cancers, which can be prior selected by accurate staging with MRI and endorectal ultrasound (Ashraf *et al,* 2012).

The presence of untreated involved mesorectal lymph nodes is a cause of local disease failure following local excision, with 2%, 8% and 23% risks of lymph node involvement for Kikuchi sm1, sm2 and sm3 penetration respectively in pT1 tumours (Tytherleigh *et al*, 2008). Tumour implantation is a potential source for luminal recurrence with depth of invasion, maximum tumour diameter and the presence of lympho-vascular invasion (LVI) as independent predictors (Bach *et al*, 2009). The ACPGBI introduced guidance for the use of local excision in early rectal cancer, advising that an acceptable <10% risk of local disease failure can be expected in T1 tumours with a maximum diameter of 3cm, and in those that are well or moderately differentiated, and without LVI (Williams *et al*, 2013). Regular surveillance and early detection of local recurrence to facilitate salvage surgery can mitigate the consequences (De Graaf *et al*, 2009).

Whilst short course pre-operative radiotherapy (SCPRT) before trans-anal excision has shown promising results in a retrospective analysis of patients unfit for total mesorectal excision (TME) (Smart *et al*, 2016), pre-operative chemoradiotherapy (CRT) has demonstrated unacceptable toxicity in the context of an organ sparing approach (Verseveld *et al*, 2015). The role of radiotherapy and local excision in early rectal cancer remains to be defined in

those fit for major resection, with outcomes from the TREC trial awaited and recruitment to STAR-TREC (Rombouts *et* al, 2017) underway. It can be considered currently in those who refuse or are unfit for major resection.

1.2.2 Resectable Rectal Cancer

Surgical resection remains the mainstay of treatment for rectal cancer, with tumours in the middle and lower thirds of the rectum resected using the technique of TME. This was popularised by Professor Bill Heald in 1982, recognising that the lateral, deep or circumferential margins were much better predictors of local disease recurrence than the distal margin (Heald *et al*, 1982), and later published (Heald, 1988). The follow up data reported local recurrences of 3-6%, which were significantly reduced from the historical 30% (Heald *et al*, 1998). Tumours in the upper third of the rectum can be adequately resected with a mesorectal transection 5cm beyond the distal margin of the tumour. It is widely accepted that involvement of the CRM predicts local disease recurrence, distant metastasis and survival (Nagtegaal and Quirke, 2008).

The risk of pelvic local recurrence remains the basis for the stratification of rectal cancers in considering treatment strategies according to NICE (CG 131, 2011) and is presented in table 1.5.

Low and moderate risk groups are considered resectable, whereas the high local recurrence risk group is at significant risk of a positive surgical CRM, unless pre-operative downstaging can be achieved. The aims of radiotherapy in the intended curative management of rectal cancer are therefore to reduce the risk of local disease recurrence, and to downstage high-risk tumours to achieve successful surgical resection. Moderate- and high-risk groups remain at significant risk of distant metastases, which overall is the main cause of mortality (Gollins et al, 2017).

Risk of pelvic local recurrence	Characteristics of rectal tumours predicted by MRI
Low (resectable)	cT1 or cT2 or cT3a **and** no lymph node involvement
Moderate (resectable)	any cT3b or greater, in which the potential surgical margin is not threatened **or** any suspicious lymph node not threatening the surgical resection margin **or** the presence of extramural vascular invasion
High (borderline resectable or unresectable i.e. threatened or involved CRM)	a threatened (<1 mm) or breached resection margin **or** low tumours encroaching onto the inter-sphincteric plane or with levator involvement

Table 1.5 - Risk assessment for pelvic local recurrence according to MRI findings. (Adapted from NICE, CG131, 2011)

1.2.3 Radiotherapy in Rectal Cancer

The addition of pre- or post-operative radiotherapy to surgery originally demonstrated a reduction of local disease recurrence risk (Colorectal Cancer Collaborative Group, 2001) but without an improvement in overall survival where historical radiotherapy techniques (large parallel-opposed fields), were associated with non-cancer deaths.

Epithelium within the small bowel are rapidly dividing, and are therefore prone to the risks of radiation, with resultant radiation enteritis. This feature, in combination with the relative mobility of the colon within the abdomen, limits the use of radiotherapy to rectal cancer exclusively. In the context of resectable disease, radiotherapy can be administered either pre- or post-operatively. The main advantage of pre-operative treatment is that pelvic anatomy is undisturbed and toxic doses of radiation to the small bowel are reduced. Post-operative radiotherapy however allows for potentially better treatment personalisation by targeting those patients with adverse pathological features.

Pre-operative radiotherapy has been commonly delivered as short or long course treatment, consisting of 25Gy in 5 fractions over one week, or 45-50.4Gy in 25-28 fractions over 5 weeks respectively. Short course treatment (SCPRT) is followed by immediate surgery one week later, whereas long course treatment (commonly combined with chemotherapy, CRT), is followed by a 'downstaging' period to allow for maximal response to occur, prior to surgery 6-12 weeks after CRT completion (Gollins *et al*, 2017).

1.2.4 Biological Effects of Radiation

Radiotherapy is administered by an external beam, delivered via a linear accelerator, and works by inducing DNA damage, either by direct or indirect ionisation from photons or charged particles. The indirect effects occur as a consequence of radiation interaction with intra-cellular water, where free radicals (notably hydroxyl radicals) are formed and interact with DNA. This indirect ionisation comprises the majority of the effect of radiation therapy. Cells have mechanisms for repairing both single-stranded and double-stranded DNA damage but double-stranded breaks increase the probability that a cell will undergo cell death. The sensitivity of cells to radiotherapy is proportional to their rate of replication, and the accumulation of single stranded breaks is exploited by radiotherapy in cancer cells which are less well differentiated than normal cells and reproduce more frequently but have a reduced ability to repair sub-lethal damage. This results in the accumulation of single-stranded breaks and increases the likelihood of creating stalled replication forks, leading to replication fork collapse and the generation of double-stranded breaks, which ultimately leads to cell death (Bauer *et al,* 2015).

The ability of tumour cells to repair DNA damage from radiotherapy may determine the response or resistance to treatment, and base excision repair is the process by which single-stranded DNA damage repair is undertaken. This process is initiated by DNA glycosylases which recognise and remove damaged or inappropriate bases, forming AP sites, which are then cleaved by an AP endonuclease. The resulting DNA break is then repaired by replacement of a single nucleotide in short-patch base excision repair, or by 2-10 nucleotides in long-patch base excision repair (Liu *et al*, 2007). In humans, the main proteins involved in this process are AP endonuclease 1, DNA polymerase β (which catalyses short-patch repair), and DNA ligase III along with its cofactor XRCC1 (which catalyse the nick-sealing step in short-

patch repair) (Carter & Parsons, 2016). The expression of these proteins has been investigated for their potential as biomarkers and therapeutic targets but are not in routine clinical use (Vens & Begg, 2010).

Double-stranded DNA breaks are ultimately the most likely contributor to ionising radiation-induced cell death. Whilst these breaks are frequently lethal to a cell, repair either by homologous recombination requiring a homologous DNA sequence, or non-homologous end joining involving ligation of the DNA ends of a double-stranded break in the absence of a homologous sequence, can be attempted (Le Guen *et al,* 2015).

1.2.5 Radiotherapy in Resectable Rectal Cancer

The Swedish Rectal Cancer Trial popularised the use of SCPRT, where in n=1168 patients, an improved overall survival at five years (58% vs. 48%, p=0.004) and reduced local recurrence (11% vs. 27%, p<0.001) was demonstrated in patients undergoing SCPRT then surgery compared to surgery alone (Swedish Rectal Cancer Trial, 1997), albeit with non-TME surgery. In the context of standardised TME surgery, the Dutch Colorectal Cancer Study Group trial compared SCPRT and TME surgery with TME surgery alone in n=1861 patients. A reduced risk of 2.4% vs. 8.2% (p<0.001) was observed in those receiving SCPRT before surgery (Kapiteijn *et al*, 2001). The UK Medical Research Council CR07/NCIC-CTG C016 trial, compared SCPRT and surgery to surgery with selective post-operative CRT (in those with a positive CRM) in n=1350 patients, demonstrating a relative risk reduction of 61% at 3 years in n=1350 patients (4.4% vs. 10.6% respectively, p<0.0001), although without an improvement in overall survival (Sebag-Montefiore *et al*, 2009).

Comparison of pre-operative long course radiotherapy with pre-operative CRT was studied in the EORTC 22921 (n = 1011) (Bosset *et al*, 2006) and FFCD 9203 (n = 733) (Gérard *et al*, 2006) trials, where local disease recurrence was significantly reduced (8-9% vs. 17%) with the addition of synchronous intravenous 5-fluorouracil (5-FU) to radiotherapy. The oral fluoropyrimidine capecitabine has also been demonstrated to be non-inferior to intravenous 5-FU in pre-operative CRT regimens for rectal cancer (Hofheinz *et al*, 2012).

A comparison of the efficacy of SCPRT against long course CRT was studied in two randomised controlled trials. The Polish trial (n-316) compared SCPRT against CRT followed by TME at 4-6 weeks in patients with palpable (low) rectal cancer (Bujko *et al*, 2006). There was no difference in the primary end-point of sphincter preservation rate, and despite a higher pathological complete response (pCR) observed with CRT, there were no differences in local recurrence rate, disease-free or overall survival. The Trans-Tasman Radiation Oncology Group 01.04 trial (n = 326), made a similar comparison in T3 N0-2 M0 rectal cancers (Ngan *et al*, 2012) but with no difference in rates of 3-year local recurrence, 5-year distant metastases or overall survival.

The optimum timing for long course CRT was determined by the German CAO/ARO/AI0-94 trial (n=823), where pre- and post-operative treatment in the context of standardised TME surgery and adjuvant chemotherapy was compared (Sauer et al, 2003). Pre-operative CRT resulted in a reduced local recurrence rate (6% vs. 12%, p=0.006), and was associated with lower acute and late toxicity (12% vs. 24%, p=0.01) but with no difference in distant metastases, disease-free or overall survival (Sauer *et al*, 2012).

1.2.6 High Local Recurrence Risk Rectal Cancer

SCPRT and long course radiotherapy have both been evaluated in locally advanced disease whereby the tumour is threatening or involving the mesorectal fascia. Prior to routine MRI assessment, patients with clinically fixed or tethered tumours underwent surgery with or without SCPRT in a prospective randomised trial (Marsh *et al*, 1994). A significantly reduced local recurrence rate was observed in the SCPRT group (12.8% vs. 37.5%, p<0.0001), although there was no difference in survival benefit. The Second MRC Rectal Cancer trial (n = 279) randomised the same category of rectal cancer patients to long course radiotherapy prior to surgery or to surgery alone (Medical Research Council Rectal Cancer Working Party, 1996). Local recurrence and disease-free survival were improved in the radiotherapy group but again with no overall survival benefit.

The ability of MRI to identify patients with a threatened or involved mesorectal fascia from the primary tumour, tumour deposits or EMVI enables the selection of those appropriate for downstaging CRT. In 80 patients with tumour identified within 1mm of the mesorectal fascia

on MRI, a positive histological CRM was observed in only 13 (16%) after surgery following CRT (Kulkarni *et al*, 2008). The presence and depth of EMVI away from the CRM as identified using diffusion weighted MRI, have also both been correlated with recurrence risk and prognosis (Smith et al, 2008).

The presence of suspicious lymph nodes on MRI less than 1mm from the mesorectal fascia does not itself predict for a positive CRM. In a study of 396 patients where 31 had this finding, none had a positive CRM following resection (Shihab *et al*, 2010). The presence of tumour in mesorectal lymph nodes at histopathological assessment is associated with a higher risk of local disease recurrence independent of a positive CRM however. In a subgroup analysis of patients with stage III disease, the Dutch Colorectal Cancer Study Group and UK Medical Research Council CR07/NCIC-CTG C016 trials demonstrated reductions in local recurrence of 19% to 9% ($p<0.001$) and 15.4% to 7.4% ($p<0.001$) respectively with SCPRT, and with a resultant improvement in 10-year overall survival (50% vs 40%, $p=0.032$) in the Dutch trial.

MRI remains poor at predicting mesorectal lymph node involvement though, despite diffusion weighted sequences and accurate characterisation of involved nodes as those with an irregular border and heterogenous signal intensity (Heijnen et al, 2013).

1.2.7 Low Rectal Cancer

It is widely accepted that low rectal cancers have historically had poorer oncological outcome, due in part to the tapering of the mesorectum and compromise of the resection margin, with higher risk of tumour perforation at surgery, CRM positivity, local recurrence and poorer survival (Nagtegaal *et al*, 2005). Whilst an attempt at sphincter preservation can be made, this should not be at the expense of oncological clearance, and in the context of neoadjuvant treatment and a very low anastomosis, functional outcome and quality of life can often be reduced (How *et al*, 2012). Involvement of the external sphincter / levator or where this margin is threatened requires an abdomino-perineal excision (APE), with curative management of these tumours requiring a permanent stoma.

Adoption of extra-levator (ELAPE) or ischio-anal approaches in APE to compliment conventional or inter-sphincteric approaches, alongside appropriate patient selection based upon accurate MRI staging can facilitate optimal personalised management of these cases (Holm, 2014). The use of neoadjuvant CRT can be further refined to optimise sphincter function, whilst reducing local recurrence rates with tailored approaches to surgery (Moran *et al*, 2014). There is no strong evidence however to support the use of CRT for the purposes of sphincter salvage (Bujko *et al*, 2006a), and perineal wound healing (particularly following ELAPE) can be problematic (Gollins *et al*, 2017).

In patients undergoing low anterior resection there is a risk of poor functional outcome. Low anterior resection syndrome (LARS) includes symptoms of stool urgency, stool clustering, evacuation difficulty and incontinence. The risk of this increases most with tumours <6cm from the anal verge and where pre-operative radiotherapy has been delivered, with up to 60% of these patients experiencing significant symptoms affecting quality of life (Battersby *et al*, 2016).

1.2.8 Pelvic Radiotherapy Toxicity

Further consequences of pelvic radiotherapy include both short- and long-term toxicities. There does not appear to be an increased risk of post-operative mortality or anastomotic leak rate (in those undergoing anterior resection) with SCPRT, although a delay to surgery beyond 11 days increases mortality, particularly in older patients (van den Broek *et al*, 2013). Perineal wound healing can also be impaired after APE following SCPRT (Sebag-Montefiore *et al*, 2009). The risk of post-operative mortality and morbidity does not seem to be increased by the use of neo-adjuvant CRT (Sauer *et al*, 2004), although the risk of acute grade 3 or 4 toxicity is significantly higher with CRT (18.2%) than with SCPRT (3.2%) (Bujko *et al*, 2004). An infrequent incidence of acute lumbosacral plexopathy (gluteal / radicular leg pain) has been associated with SCPRT (Marijnen *et al*, 2002).

Recognised late toxicities of pelvic radiotherapy include bowel obstruction, bowel / urinary / sexual dysfunction, pelvis and femoral neck fractures and second malignancies (Gilbert et al, 2015), although the incidence of these complications appears to be reducing, likely with improvements in radiotherapy techniques including reduced irradiated volumes. Along with

the significant risk of LARS as discussed, SCPRT has been observed to increase sexual dysfunction particularly in men (Stephens *et al*, 2010). No difference in quality of life scores relating to sexual function for men or women have been observed between irradiated or non-irradiated patients however (Marijnen *et al*, 2005). There appears to be no difference between SCPRT and CRT in reported bowel or sexual dysfunction (Pietrzak *et al*, 2007), or with long term quality of life (Ngan *et al*, 2012a).

The current use of neo-adjuvant radiotherapy is therefore determined by the potential risk of local recurrence from an involved or threatened CRM, by the presence of EMVI, which can be accurately predicted by pre-operative MRI, or by the presence of suspicious mesorectal lymph nodes. Tumours staged as mrT2-3 N0 have a very low (<3%) risk of local recurrence with surgery alone if a good quality TME is performed with a negative CRM (Taylor *et* al, 2011). Determining the presence of involved mesorectal lymph nodes pre-operatively remains inaccurate. In the absence of an involved or threatened CRM, the use of neo-adjuvant radiotherapy (either SCPRT or CRT) does approximately halve the local recurrence risk but the number need to treat is 17-20 (Gollins *et al*, 2017), with no impact on the risk of distant metastases or overall survival and with potentially significant morbidity. It should therefore be undertaken in carefully selected patients after MDT evaluation.

1.2.9 Pharmacology of 5-fluorouracil

Historically the only available chemotherapeutic agent for the treatment of metastatic and advanced colorectal cancer was 5-flourouracil (5-FU), which remains as the cornerstone of treatment. It is an oral pro-drug of 5-FU (capecitabine), that is conventionally used alongside radiotherapy (as CRT) in the neo-adjuvant treatment of locally advanced rectal cancer.

1.2.9.1 5-fluorouracil

5-fluorouracil (5-FU) is a fluoropyrimidine anti-metabolite. The drug was designed, synthesised and patented in 1957 as an analogue of uracil, a normal component of RNA. The analogue substitutes a hydrogen atom for fluorine at the C5 position and is a specific competitive antagonist for uracil. Its mis-incorporation into RNA and DNA arrests RNA synthesis, with resultant cytotoxicity, and therefore halts tumour growth (Longley *et al,*

2003), although an intact MMR system may be required to detect this mis-incorporation (Jo and Carethers, 2006).

As well as being incorporated into macromolecules, 5-FU is converted inside cells into a number of active metabolites which disrupt biological function: fluorodeoxyuridine monophosphate (FdUMP), fluorodeoxyuridine triphosphate (FdUTP) and fluorouridine triphosphate (FUTP). It is FdUMP which inhibits thymidylate synthetase (TS), a nucleotide synthetic enzyme which is thought to be the main target for 5-FU. TS methylates deoxyuridine monophosphate (dUMP) to form thymidine monophosphate (dTMP), therefore administration of 5-FU causes a scarcity in dTMP, with rapidly dividing cancerous cells undergo cell death via thymineless death (Longley *et al*, 2003). It is also thought to result in dinucleotide pool imbalances and increased levels of deoxyuridine triphosphate (dUTP), both of which can cause DNA damage (Yoshioka *et al*, 1987).

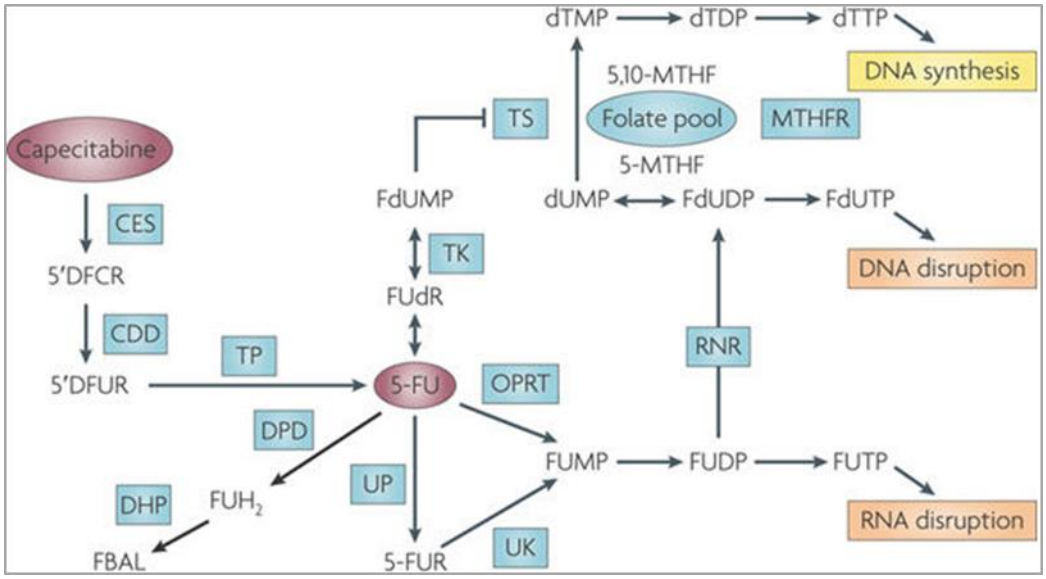

Figure 1.5 – The metabolism of 5-FU and its oral prodrug capecitabine. (Taken from Walther et al, 2009)

5'DFCR, 5'deoxy-5-fluorocytidine; 5-FUR, 5-fluorouridine; DHP, dihydropyrimidinase; FBAL, fluoro-b-alanine; MTHFR, methylenetetrahydrofolate reductase; RNR, ribonucleotide reductase; UK2, uridine-cytidine kinase 2.

The mechanism of 5-FU activation is by conversion to fluorouridine monophosphate (FUMP) by uridine monophosphate synthetase (OPRT). FUMP is then phosphorylated first to fluorouridine diphosphate (FUDP) and then to FUTP. Alternatively, thymidine phosphorylase (TP) can activate 5-FU by catalysing the conversion of 5-FU to fluorodeoxyuridine (FUdR) which is then phosphorylated by thymidine kinase (TK) to FdUMP. FdUMP can be phosphorylated to fluorodeoxyuridine diphosphate (FdUDP), and again to FdUTP. The metabolism of 5-FU is summarised in figure 1.5.

Variation in the enzymes that mediate the incorporation into RNA and DNA, the conversion of the oral prodrug capecitabine to 5-FU, or metabolism to inactive breakdown products can alter the intracellular 5-FU concentrations and cytotoxicity, leading to altered anti-tumour activity or systemic toxicity. CRC patients with higher tumour levels of TS for example, seem to have a poorer overall survival than those with lower expression (Popat et al, 2004).

The drug is predominantly catabolised by dihydropyrimidine dehydrogenase (DPD), which converts 5-FU to dihydrofluorouracil (FUH_2), with around 80% of this occurring in the liver (Diasio and Harris, 1989). It is estimated that 0.2% of individuals have a complete DPD deficiency - those with a partial or complete DPD deficiency have a significantly increased risk of severe or even fatal drug toxicities when treated with fluoropyrimidines (Caudle *et al*, 2013).

Common side-effects of 5-FU based therapy include nausea, vomiting, diarrhoea, mucositis, headache, myelosuppression, alopecia and photosensitivity.

1.2.9.2 Leucovorin

High intra-cellular concentration of the reduced folate leucovorin (folinic acid), are required for optimal binding of FdUMP to TS. Leucovorin is transported into cells via the reduced folate transporter, anabolised and polyglutamated. This not only increases intra-cellular retention of FdUMP but further stabilises the complex formed between FdUMP and TS. It is widely accepted that co-administration of leucovorin with 5-FU, increases 5-FU toxicity both *in vitro* and *in vivo* (Wright *et al*, 1989).

1.2.9.3 Capecitabine

An alternative approach to the delivery of 5-FU has originated from the design of oral pro-drugs which avoid DPD mediated catabolism in the liver. Capecitabine is an oral fluoropyrimidine absorbed via the GI tract and converted in the liver to 5'deoxy-5-fluorouridine (5'DFUR) by the enzymatic action of carboxylesterase (CES) and cytidine deaminase (CDD) (Johnston and Kaye, 2001). 5-dFUR is ultimately converted to 5-FU by thymidine phosphorylase (TP) and uridine phosphorylase (UP1). The higher abundance of these enzymes in tumour tissue is thought to account for the more tumour-specific conversion of capecitabine to 5-FU (Schüller *et al*, 2000).

1.2.9.4 Tegafur

Another alternative oral 5-FU prodrug is tegafur, although not routinely used in the UK. It is commonly administered with agents such as gimeracil, oteracil or uracil that inhibit the action of DPD to increase its bioavailability in tumour cells and therefore toxicity. It is metabolised to 5-FU by cytochrome P450 2A6 (CYP2A6), which is predominantly localised in the liver (Chionh *et al*, 2017).

1.2.10 Evaluation of Response to Chemoradiotherapy

Repeated radiological evaluation of a rectal cancer with MRI and CT after CRT ensures that appropriate subsequent treatment is undertaken. The timing of this further evaluation is performed so that the inflammation produced as a consequence of radiotherapy does not under-estimate tumour response, and also allows for the ongoing effects of radiotherapy on tumour cells undergoing attempted cell division to be realised. Following early studies whereby better clinical tumour response and pathological downstaging was observed with surgery at 6 weeks (vs. 2 weeks) following completion of radiotherapy (Francois *et al*, 1999), it has been commonplace to operate 6-8 weeks following CRT.

Whilst there is evidence to suggest that ongoing radiological downstaging occurs up to 12 weeks following cessation of treatment (Johnston *et al*, 2009), the phase 3, multi-centre, GRECCAR-6 randomised-controlled trial demonstrated no increase in pathological complete response with resection 11 weeks post-CRT (compared to 7 weeks) but with significantly

greater morbidity and with a poorer quality mesorectal specimen at the later time (Lefevre *et al*, 2016).

1.2.10.1 Radiological response to treatment

The standard evaluation of radiological response to treatment is usually performed in accordance with the international consensus guidelines defined in 1994 and referred to as the Response Evaluation Criteria in Solid Tumours (RECIST) guidelines (Therasse *et al*, 2000). These were updated to RECIST 1.1 in 2008 (Eisenhauer *et al*, 2009), where pathological lymph nodes were included as target lesions. In the context of rectal cancer and evaluating response to CRT, MRI is the optimal imaging modality for local re-staging. The challenge for radiologists is to distinguish between normal mucosa, oedema, fibrosis and residual tumour, to determine the suitability for surgical resection with respect to the CRM, or for appropriate selection for non-operative management. A specific MRI regression grading system is used (Battersby *et al*, 2014) and presented in table 1.6. The system is based upon established histopathological regression grading systems and has been validated as an independent predictor of overall- and disease-free survival (Patel *et al*, 2011).

MRI Tumour Regression Grade	**Description**
mrTRG1	Complete radiological response (linear scar only)
mrTRG2	Good response (dense fibrosis, no obvious tumour signal)
mrTRG3	Moderate response (>50% fibrosis and visible intermediate signal)
mrTRG4	Slight response (mostly tumour)
mrTRG5	No response/regrowth of tumour

Table 1.6 – MRI assessment of regression grading in rectal cancer. (Adapted from Battersby *et al*, 2014)

T2 weighted sequences in expert hands can determine residual intermediate intensity signal representing tumour from hypointense signal representing fibrosis, although the routine use of functional diffusion weighted images (DWI) has confirmed the greater bio-specificity of

this signal in the tumour bed (Lambregts *et al*, 2011). DWI is considered particularly useful for highlighting residual tumour in incomplete responders but has a limited positive-predictive value in confidently identifying complete responders (Blazic *et al*, 2017). Dynamic contrast-enhanced MR imaging is another functional MRI sequence, which evaluates tumour vessel permeability and blood flow. K^{trans} as a measure of capillary permeability, has so far been identified as the most useful potential parameter, with pre-CRT K^{trans} significantly differentiating responders from non-responders (Gollub *et al*, 2012).

The evaluation of the mrTRG system to define treatment stratification to according to response is proposed as a phase III study in the TRIGGER trial (Battersby *et al*, 2017). The assessment of safety of non-operative management in those patients achieving mrTRG 1 or 2, and the evaluation of systemic therapy after CRT (and prior to resection) in those patients with mrTRG 3-5 is planned.

1.2.10.2 Pathological response to treatment

The current definitive assessment of response to CRT is made upon histopathological assessment following surgical resection.

The earliest histopathological tumour regression grade (TRG) system originated from correlation of pathological response with outcome in oesophageal cancer (Mandard *et al*, 1994). In this system, TRG was quantified as one of five grades; TRG1 (complete regression) showed an absence of residual cancer with fibrosis extending through the oesophageal wall, TRG 2 was characterised by the presence of rare residual cancer cells scattered through the fibrosis, TRG 3 was characterised by an increase in the number of residual cancer cells but fibrosis still predominated, TRG 4 showed residual cancer outgrowing fibrosis, and TRG 5 was characterised by an absence of regressive changes. On univariate analysis, tumour size, lymph node status, TRG and oesophageal wall involvement correlated with disease free survival, however after multivariate analysis only TRG (at this point dichotomised as 1-3 vs. 4-5) remained a significant predictor of disease free survival.

A specific grading system was subsequently published for the regression of rectal tumours after neoadjuvant CRT (Dworak *et al*, 1997), including assessment of tumour mass, fibrotic change, irradiation vasculopathy and peri-tumour inflammatory reaction. The system

graded regression from TRG 0-4, as demonstrated in figure 1.6, and was later demonstrated to have prognostic value in predicting outcomes in rectal cancer (Losi *et al*, 2006).

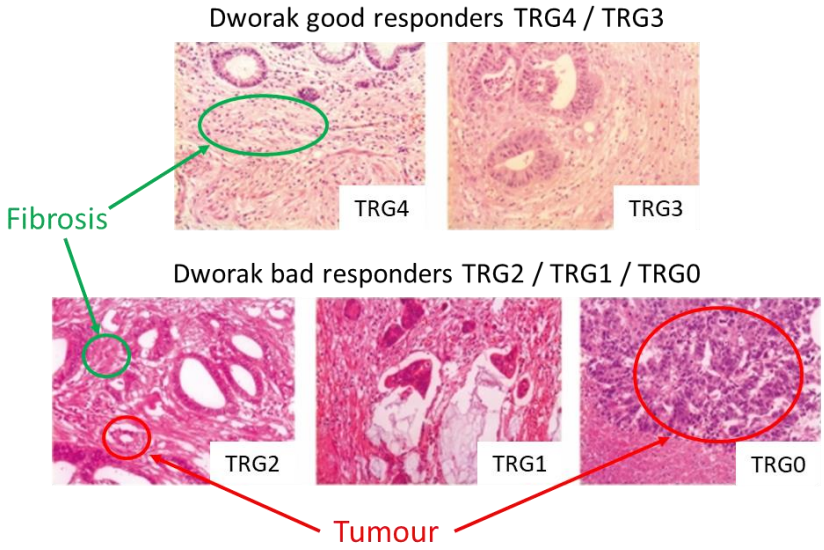

Figure 1.6 - The tumour regression grading system proposed by Dworak *et al* (1997). TRG4 – no tumour cells, only fibrotic mass (total regression); TRG3 – very few (difficult to find microscopically) tumour cells in fibrotic tissue with or without mucous substance; TRG2 – dominant fibrotic changes with few tumour cells or groups (easy to find); TRG1 – dominant tumour mass with obvious fibrosis and/or vasculopathy; TRG0 – no regression. (Adapted from Santos *et al*, 2014). Areas of fibrosis and tumour are depicted in the figure.

The Royal College of Pathologists have more recently produced a minimum dataset for reporting in CRC, where a 4-tier system based on the classification by Ryan *et al* (2005) is now endorsed. The system classifies tumour regression as: TRG 4 - no viable tumour cells (fibrosis or mucus lakes only), TRG 3 - single cells or scattered small groups of cancer cells, TRG 2 - residual cancer outgrown by fibrosis, and TRG 1 - minimal or no regression (extensive residual tumour). This system has also been accepted as the best methodology in the 7th edition of the TNM staging system and has been adopted by the currently recruiting FOxTROT trial (FOxTROT Collaborative Group, 2012).

Any tumour regression grading system needs to be cross-validated for its predictive and prognostic value and reproducibility in both clinical and research settings. At the current time there is no system that accounts for the presence of (or response in) nodal disease, which has been demonstrated to be as significant a prognostic factor as regression grading following CRT (Huebner *et al*, 2012).

1.2.11 Complete Response to Chemoradiotherapy

1.2.11.1 Pathological complete response

The reported incidence of pathological complete response (pCR) following CRT varies dependent on study populations, disease staging and neoadjuvant CRT regimens. pCR detection is also dependent upon pathological assessment which is currently non-standardised. These factors potentially account for the variability in the reported rates and makes the interpretation of studies more difficult. An overall pCR rate of 13.5% was identified in a review of phase II and III studies, where a single fluoropyrimidine based radio-sensitiser was used (Hartley *et al*, 2005). Equally of significance is that approximately 50% of patients receiving CRT will achieve a minimal or no response to treatment or will develop disease progression. Even a near-complete response does not produce a statistically significant prognostic benefit compared to those with a minimal or no response (Bujko *et al*, 2010).

There is a clear oncological benefit for patients achieving a pCR. In a meta-analysis of long-term outcomes involving 3363 patients in 16 studies (of which 1263 (37.6%) had achieved a pCR), local recurrence rate, and overall- and disease-free survival was evaluated between those with a pCR against those without, with a mean follow-up of 55.5 (40-87) months (Martin et al, 2012). The mean local recurrence rate was significantly lower (0.7%) in patients with a pCR (odds ratio (OR) 0.25, p=0.002), as well as the rate of distant failure (8.7%, OR 0.23, p<0.001). The 5-year overall survival in patients with a pCR was 90.2%, with a 5-year disease-free survival of 87.0%, significantly better than those without (OR 3.28, p=0.001 and 4.33, p<0.001 respectively).

In pursuit of increasing the rate of pCR following CRT and potential associated favourable outcome, several studies have examined the role of novel chemotherapy regimens prior to CRT or as radio-sensitisation. The EXPERT (Chau *et al*, 2006) and Spanish GCR-3 (Fernández-Martos *et al*, 2010) studies utilised capecitabine and oxaliplatin (CAPOX) as chemotherapy prior to CRT and observed pCR rates of 20% and 14% respectively. The CONTRE trial utilised longer cycles of CAPOX in 39 patients and observed a pCR rate of 33%, however also observed greater rates of grade 3/4 toxicities (Perez *et al*, 2017). The French ACCORD 12 trial (n=598) examined intensified radiotherapy with the addition of oxaliplatin to capecitabine against standard CRT but found no difference in pCR rate or disease-free or overall survival at 3 years

(Gerard *et al*, 2012). The addition of irinotecan to capecitabine with radiotherapy at 45Gy yielded a promising pCR rate of 22% in 110 patients in a phase II trial (Gollins *et al*, 2011) but was not powered to detect survival outcomes. This regimen is being further assessed in the ongoing UK phase III ARISTOTLE trial, in MRI-defined unresectable or borderline resectable rectal cancer.

A dose-response relationship has been demonstrated for tumour regression after CRT with higher than normal radiation doses between 50.4 and 70Gy and incorporating brachytherapy (Appelt *et al*, 2013), although the effect on toxicity was not assessed. It may be that this technique has greatest potential benefit for those with distal lesions with a desire to achieve sphincter preservation.

In a Danish study utilising 60Gy in 30 fractions to the tumour, 50Gy in 30 fractions to elective lymph node volumes and 5Gy endorectal brachytherapy boost, with concomitant oral tegafur-uracil, 40 of 51 patients with T2/3 N0-1 low rectal cancer were considered to have achieved a clinical complete response (cCR) and managed without surgery (Appelt *et al*, 2015). Follow up data regarding functional outcome at 2 years was only reported for 16 (40%) of these patients however.

Intensity-modulated radiation therapy (IMRT) is being used increasingly over traditional 3D conformal treatment due to the perceived benefit of delivering higher radiation doses to the tumour whilst minimising delivery to surrounding tissues. Its use is technically challenging and costly however. In a retrospective study of 7386 patients in the United States undergoing CRT between 2006 and 2013, adjusted multivariable regression modelling was used to isolate the impact of IMRT (n=3330) against 3D conformal treatment (n=4056). A higher risk of a positive margin was identified in the IMRT group (OR 1.57, $p < 0.001$) and with no difference in pathological downstaging (OR 0.89, $p = 0.051$) but with no difference in overall survival at 8 years (64% vs. 64 %, OR 1.06, $p = 0.47$) (Sun *et al*, 2017). In a recent phase II trial with 20 patients where IMRT was used with capecitabine for radio-sensitisation in stage II / III rectal cancer, 7 patients (35%) were determined to have achieved a pCR and with only 1 patient experiencing grade III radiation proctitis (Tey *et al*, 2017).

A summary of these trials is presented in table 1.7 below.

Study	Design	Tumour Characteristics	Neoadjuvant Treatment	pCR Rate	Limitations
Chau *et al,* 2006 EXPERT	Observational study n=77	CRM threatened	CAPOX prior to CRT	20%	n=4 deaths during neoadjuvant chemotherapy
Fernandez-Martos *et al,* 2010 GCR-3	Phase II randomised trial n=108	CRM threatened	A: CAPOX with CRT and adjuvant CAPOX vs. B: CAPOX then CRT	14% in each arm	Increased rate of grade 3/4 toxicities in arm A
Perez *et al,* 2017 CONTRE	Observational study n=39	Stage II / III	CAPOX then CRT	33%	n=3 did not complete CAPOX
Gerard *et al,* 2012 ACCORD 12	Phase II randomised trial n=598	T3-4 Nx M0 resectable cancer	A: CRT (45Gy) vs. B: Intensified CRT (50Gy) with CAPOX	13.9% vs. 19.2%, p=0.09	No significant difference in overall or disease-free survival after 3 years between groups
Gollins *et al,* 2012	Phase II trial n=110	CRM threatened or involved	CRT with capecitabine and irinotecan	22%	Not powered to detect survival outcomes
Appelt *et al,* 2015	Observational study n=51	T2-3 N0-1 low cancer	60Gy to tumour, 50Gy to lymph nodes, 5Gy brachytherapy boost	Clinical complete response in 78%	Local recurrence in 16%, with functional outcome at 2 years only reported in 40%
Sun *et al,* 2017	Retrospective study n=7386	Stage II / III	A: Intensity modulated vs. B: 3D conformal radiotherapy	11% vs. 13%, p=0.012	No difference in overall survival at 8 years
Tey *et al,* 2017	Phase II trial n=22	Stage II / III	Intensity modulated radiotherapy with capecitabine	35%	Limited sample size and dropout n=3

Table 1.7 – Summary of selected trials investigating novel neoadjuvant CRT regimens and the associated pCR rate.

1.2.11.2 Clinical complete response

The identification of a pCR following surgical resection has naturally raised the possibility that selected patients may not benefit from surgery after CRT. In particular, the avoidance of the morbidity and mortality associated with a pelvic operation / anastomosis, as well as the avoidance of a permanent stoma in those that would otherwise require APE, is an attractive potential. Accurate identification of those with a cCR and correlation of this with a pCR would be necessary to potentially manage patients non-operatively following CRT.

A standardised definition of cCR was proposed by Professor Habr-Gama, incorporating assessment at or after 8 weeks following completion of CRT, with the requirement for a normal digital rectal examination (DRE), normal MRI imaging and a normal endoscopic mucosal appearance (Habr-Gama *et al*, 2010). The mucosa in these cases should be intact, with only superficial whitening and the presence of telangectasia. Any residual ulceration, nodularity or irregularity should raise concern of an incomplete response. The addition of DWI with MRI increases the sensitivity of detection of pCR (Lambregts *et al*, 2011), with distinction of fibrosis from residual tumour.

A retrospective assessment of the correlation of mucosal response with histopathological findings following CRT and proctectomy was undertaken in 238 consecutive patients (Smith *et al*, 2014). 61 patients (26%) were categorised with a pCR but 45 (74%) of these were determined to have a residual mucosal abnormality (ulceration / nodularity). The remaining 16 patients with a pCR had no residual mucosal abnormality but 6/22 patients overall with a mucosal cCR still had residual disease, rendering the finding of mucosal cCR in isolation poorly sensitive (26%) but highly specific (97%).

A prospective study combining assessment modalities was undertaken in 50 patients, of whom 17 (34%) were determined to have achieved a complete response (Maas *et al*, 2015). Areas under receiver operator characteristics curves were 0.88 (0.78-1.00) for clinical assessment (comprising DRE, endoscopy +/- biopsy) and 0.79 (0.66-0.92) for MRI imaging with DWI. Combining all modalities resulted in a 98% probability of predicting a complete response, and negative likelihood ratio conversely indicated a 15% chance of a complete response even when combined modality assessment had predicted residual tumour. These statistics would suggest that combined modality assessment is a potentially safe and accurate method for selecting patients with a cCR for a watch and wait approach with

frequent surveillance, although no data from randomised-controlled trials exists (Glynne-Jones & Hughes, 2012).

The initial data to advocate a watch and wait approach in cases of suspected cCR following CRT for resectable distal rectal cancer originated from Brazil (Habr-Gama *et al*, 1998), where 30 patients (of 36/118 (31%) defined as achieving cCR) were managed non-operatively with no reported disease recurrence in the median 36-month follow-up. This approach was considered non-inferior to surgical resection on long-term follow-up for those patients downstaged to stage 0 disease (those determined to have achieved a cCR and managed with watch and wait (n=71), and those achieving a pCR after surgical resection (n=22)) in a further cohort of 265 distal rectal cancer patients (Habr-Gama *et al*, 2004). Five-year overall and disease-free survivals were 100% vs 88% and 92% vs 83% for patients managed by watch and wait compared against those with a pCR after resection respectively.

More recent data from Habr-Gama's group report a cCR rate of 68% following CRT for distal rectal cancer, with half of those in the study (35/70) avoiding surgery in the 12-month follow up period and considered to have maintained a long-term response (Habr-Gama *et al*, 2013). These studies include patients with earlier stage disease than those normally considered for CRT in the UK, and in distal (palpable) rectal cancers. The translation of these results into potentially more advanced mid- and upper-rectal cancers (and with a greater likelihood of nodal disease) remains uncertain.

The UK experience of 129 patients from the North West considered to have achieved a cCR following CRT was reported in a propensity score-matched cohort analysis (OnCoRe). During the median 33-month follow-up period, 44 (34%) of those patients managed by watch and wait developed local regrowth, and 36/41 patients (88%) of those with non-metastatic recurrence underwent salvage surgery. There was no difference in non-regrowth disease free or overall survival at 3 years comparing those in the watch and wait group with those undergoing initial surgical resection (non-cCR), indicating oncological safety, but a significantly better colostomy free survival at 3 years (74% vs 47%, $p<0.0001$) was observed in those managed by watch and wait (Renehan *et al*, 2015).

A potential alternative to radical resection in the presence of a near-cCR following CRT, is for trans-anal excision of small (<3cm) residual ulcers in those with an objective clinical response (Creavin *et al*, 2017). The aim of organ preservation in this context is to deliver equivalent

oncological outcome, with reduced surgical risk and improved functional outcome, and consequent improved quality of life. In this observational study of 785 rectal cancer patients, 60/362 (16.5%) receiving CRT were managed with an organ preservation strategy. 10 of these patients were managed entirely by a watch and wait approach; 50 patients underwent trans-anal excision of the scar/ulcer (with a desired 1cm margin), with a further 15 of these 50 patients requiring salvage TME surgery due to adverse histological findings. There was no significant difference in overall survival (85.6% vs 93.3%, p=0.414) or disease-free survival (78.3% vs 80%, p=0.846) comparing those undergoing radical surgery (n=317) against those managed with an organ preservation strategy (active surveillance and local excision, n=45). 48/302 patients (15.9%) were observed to have achieved a pCR after initial resection, with local recurrence occurring in 4 (9%) of those managed with organ preservation.

In cases of an apparent cCR, a risk of lymph node metastases remains. In one study, 17% of patients with a pCR in the primary tumour (ypT0) following resection were identified to have lymph node metastases (Hughes *et al*, 2006). These patients would be at higher risk of local or distant failure in the context of a watch and wait or local excision approach.

The phase III prospective randomised-controlled GRECCAR 2 trial was powered to evaluate outcome comparing local excision or TME following CRT in T2/3 low rectal cancer. At 2-year follow up and with analysis on an intention to treat basis, there was no difference in survival, local recurrence or significant after effects (considered as colostomy rate or the incidence of faecal incontinence or sexual dysfunction), however morbidity (48% vs 22%, p=0.001) and severe after effects (62% vs 29%, p<0.001) were significantly increased in the sub-group requiring TME after local excision (Rullier *et al*, 2017).

A summary of the trials evaluating cCR and the reported outcomes is presented in table 1.8 below.

Study	Design	Tumour Characteristics	Neoadjuvant Treatment	cCR Rate	Comments
Habr-Gama *et al,* 1998	Observational study n=118	Low and resectable	50.4Gy radiotherapy with leucovorin / 5FU	31%	Includes n=6 patients with pCR identified post-resection
Habr-Gama *et al,* 2004	Observational study n=265	Low and resectable	50.4Gy radiotherapy with leucovorin / 5FU	26.8%	No difference in survival with cCR compared to ypT0N0 post-resection
Habr-Gama *et al,* 2013	Observational study n=70	T2-4, N0-2 low cancer	54Gy radiotherapy with leucovorin / 5FU	68% (initial)	Sustained complete response (57%) at 12 months, limited follow up
Renehan *et al*, 2015 OnCoRe	Propensity-score matched cohort analysis n=259 (+98 cCR)	CRM threatened	45Gy radiotherapy with 5FU	12%	No difference in 3-year overall survival with cCR compared to resection. Improved colostomy-free survival with cCR managed by watch and wait.
Creavin *et al,* 2017	Observational study n=362	≥T3, N0-2	50-54Gy radiotherapy with 5FU	16.5% managed with organ preservation strategy	Trans-anal excision in n=50. Salvage TME in 30% of these. Tumour regrowth in 9% who had organ preservation.
Rullier *et al,* 2017 GRECCAR 2	Randomised open-label phase III trial n=186	T2-3 low cancer <4cm	50Gy radiotherapy with CAPOX	n=148 with good response and residual tumour randomised to local excision or TME	No difference in survival or significant after-effects between groups on intention to treat analysis. Increased morbidity and after-effects in n=26 (35%) requiring TME after local excision.

Table 1.8 – Summary of selected trials evaluating cCR and subsequent outcome with rectal-preservation strategies.

1.3 Biomarkers of Response to Chemoradiotherapy in Rectal Cancer

The current pCR rate with CRT remains low, with some patients experiencing disease progression despite treatment, and there are currently no biomarkers in routine clinical use to reliably predict response or guide decision making regarding the use of CRT (Ryan *et al*, 2016). The ability to predict response would positively select those patients who will derive benefit, whilst sparing others the morbidity associated with CRT and a potential delay in the local and systemic management of their disease. The necessity for further research in this area has recently been highlighted by the ACPGBI, who have advocated the need for reliably predicting the response of rectal cancer to CRT, and for novel strategies for improving the sensitivity of rectal cancer to radiation therapy (Tiernan *et al*, 2014).

Historical studies of the sensitivity of rectal cancer to CRT have been based around the core of sensitivity to 5-FU based protocols and have focussed on individual or a few markers based on immunohistochemical (IHC) expression. The profiling of rectal cancer sensitivity to CRT has been facilitated by the evolution of high-throughput analyses to produce expression profiles or signatures, particularly at genomic level, and the developing knowledge of involved pathways has further refined the focus of potential biomarkers. In the clinical setting 5-FU is being complimented by other chemotherapeutic agents such as oxaliplatin and irinotecan, and modern studies need to reflect this change in practice.

1.3.1 Gene Expression Analysis

Gantt *et al* (2014) correlated mRNA profiling of pre-treatment rectal adenocarcinoma biopsies with TRG at resection in 33 patients, subsequent to standard 5-FU based CRT. They derived 812-gene and 183-gene differentially expressed signatures (at $p<0.05$ and $p<0.01$ respectively) that separated 'non-responders' from 'responders'. Sensitivity and specificity in a small verification set was 100% for the 812-gene signature but sensitivity dropped to 33% with the 183-gene signature. Ingenuity Pathway Analysis (IPA) software was used to derive significant biological functions and canonical pathways associated with 666 of the 812 genes (78 genes with indeterminable fold change, and a further 68 unmapped genes were

eliminated from this analysis). The 'DNA double-strand break repair by homologous recombination' pathway was considered to contain amongst the highest ratio of significantly differentially expressed genes but the authors acknowledged their small sample size, and the intrinsic limitations of multiple testing / false positives associated with the evaluation of tens of thousands of genes with microarray analysis – none of their candidate genes passed a Bonferroni correction.

Watanabe *et al* (2014) constructed a predictive model comprising a 4-gene signature derived from microarray analysis of 46 pre-CRT biopsy samples. Twenty-four probes were identified as differentially expressed between responders and non-responders (*t* test with false discovery rate $p<0.046$, fold change >2.0). Eighteen genes (representing 22 probes) were identifiable, and significantly validation of the microarray data was performed on parallel samples by quantitative RT-PCR, with good correlation. Predictive modelling utilising ≤4 out of the 18 genes found the highest accuracy (89.1%) with *LRRIQ3, FRMD3, SAMD5* and *TMC7*, and further validation was performed in an independent sample (n=16) with a predictive accuracy of 81.3%.

None of these 4 genes (*LRRIQ3, FRMD3, SAMD5* and *TMC7*) has been previously associated with rectal cancer, although one of the other 18 differentially expressed genes (*REG4*) was identified as significantly over-expressed by Kobunai *et al* (2011) in relatively radio-resistant CRC cell lines. Up-regulation of *REG4* in the radio-sensitive cell lines HCT116 and Colo320 produced a significantly increased survival fraction on clonogenic assay following irradiation, and significantly inhibited radiation-induced DNA fragmentation. *REG4* expression in a limited validatory clinical sample (n=22) was also significantly 8.3 times higher in 'non-responders' to pre-operative radiotherapy.

Whilst *REG4* may play a role in radiotherapy resistance, an *in vitro* gene expression signature for sensitivity to CRT was derived from 12 CRC cell lines by Spitzner *et al* (2010). In this study, treatment response to 3μM 5-FU and 2Gy radiation was observed by clonogenic assay and correlated with pre-treatment gene expression profiles of the cell lines. 2770 genes were correlated with sensitivity to CRT at a significance level of $Q<0.05$. IPA software determined canonical pathways to include RAS-MAPK, with *DOK3* as an upstream regulator of RAS signalling and deregulation conferring resistance; insulin signalling, where insulin binding activates *PI3K-AKT;* and Wnt/β-catenin signalling. These pathways will be further considered.

When compared with other microarray gene expression studies (Ghadimi *et al*, 2005; Kim *et al*, 2007; Rimkus *et al*, 2008; Brettingham-Moore *et al*, 2011; Nishioka *et al*, 2011; Watanabe *et al*, 2006), there does not appear to be concordance of candidate genetic markers for response to CRT, as different gene expression signatures are reported between studies. This may be likely to be due to genetic differences between populations but is also confounded by variations in sample collection and preparation, by a lack of conformity to one particular CRT regimen, a varying definition of 'responder' and 'non-responder', and with the intrinsic limitations of multiple testing / false positives associated with the evaluation of tens of thousands of genes with microarray analysis. Gene expression analysis however offers the identification of a wide range of potential markers of sensitivity/resistance to CRT, as well as potential therapeutic targets but requires wider validation in larger samples and across populations.

A more focussed approach was adopted by Sebio *et al* (2014), with analysis of polymorphisms in EGFR (whose activation by radiation induces cell proliferation / radio-resistance) and its ligands, DNA repair genes and TS. Genomic DNA was extracted from blood samples in 84 patients undergoing capecitabine-based CRT. A pCR was observed in 17 patients (20.2%). Correlation with the studied polymorphisms demonstrated significant association with pCR following multivariate analysis for rs11615 in the *ERCC1* gene (DNA repair), and rs11942466 in the *AREG* gene region (EGFR ligand), which may have implications for biological therapy with cetuximab.

A summary of the discussed gene expression studies investigating the association with response to CRT is presented in table 1.9 below.

Study	Design	Evaluation	Outcome	Comments
Gant *et al,* 2014	mRNA profiling in n=33 pre-CRT biopsies	Correlation with TRG	812-gene signature separating responders and non-responders, highest ratio of differentially expressed genes implicated in 'DNA double-strand break repair by homologous recombination'	Small sample size, limitations of multiple testing / false positives with microarray analysis
Watanabe *et al,* 2014	Microarray analysis in n=46 pre-CRT biopsies, predictive modelling	Differential expression between responders and non-responders	18 genes identifiable, validated with parallel quantitative RT-PCR, predictive modelling utilising ≤4 genes demonstrated highest accuracy (89.1%) with *LRRIQ3, FRMD3, SAMD5 and TMC7*	Small sample size, limitations of microarray analysis
Kobunai *et al,* 2011	Microarray analysis in n=8 CRC cell lines pre-irradiation	Differential expression between radio-sensitive and radio-resistant	*REG4* expression 12-fold higher in radio-resistant cells, increased surviving fraction on clonogenic assay post-irradiation with *REG4* up-regulation in (radio-sensitive) HCT116 and Colo320 cell lines	*REG4* expression x8.3 higher in non-responders to CRT in a validatory clinical dataset (n=22)
Spitzner *et al*, 2010	Microarray analysis in n=12 CRC cell lines pre-CRT	Correlation of gene expression profile with sensitivity to CRT	2770 genes correlated with sensitivity to CRT at a significance level of Q<0.05, IPA software determined canonical pathways to include RAS-MAPK and insulin signalling	*In vitro* data, limitations of microarray analysis
Sebio *et al,* 2014	Genomic DNA extracted from blood samples in n=84 patients pre-CRT	Correlation of polymorphisms in EGFR, TS and DNA repair genes with pCR	Significant association with pCR following multivariate analysis for rs11615 in the *ERCC1* gene (DNA repair), and rs11942466 in the *AREG* gene region (EGFR ligand)	Liquid biopsy, stage II and III disease

Table 1.9 – Summary of gene expression studies investigating response to CRT in rectal cancer.

1.3.2 miRNA Profiling

MicroRNAs (miRNAs) are small non-coding RNAs with regulatory function at a post-transcriptional level. Each miRNA can regulate the expression of hundreds of target genes, and many proteins involved in signalling pathways in CRC have been identified to be modulated by miRNAs (Calin and Croce, 2006). miR-143 is downregulated in CRC, normally functioning as a tumour suppressor through inhibition of the KRAS oncogene. miR-145 is equally a tumour suppressor and downregulated in CRC, with its action in regulating insulin-

receptor substrate-1 (IRS-1) and control of cell growth and proliferation. miR-21 is conversely upregulated in CRC, and demonstrates inhibition of the tumour suppressor gene PTEN, which has a significant role in the regulation of the PI3-K pathway (Slaby *et al*, 2007). Drebber *et al* (2011) characterised the expression of these miRNAs pre- and post-CRT in 40 patients, identifying significant changes in expression of miR-143 and miR-145 following CRT but non-significant changes in the association with tumour regression or in predictive pre-treatment levels.

miR-21 in its mature form (miR-21-5p) was the most sensitive and specific miRNA (78% and 86% respectively) predicting pCR and cCR from fresh frozen, pre-treatment biopsies (n=43), out of 4 differentially expressed miRNAs in the study by Lopes-Ramos *et al* (2014). Further analysis of putative target genes identified using TargetScan software, found a significant negative correlation with the SATB1 gene alone but not others including PTEN. SATB1 has been associated with a poorer prognosis in rectal cancer (Meng *et al*, 2012). The group established the inverse relationship between miR-21-5p and SATB1 mRNA expression, by manipulating miR-21-5p expression in HCT116 and SW480 colorectal cancer cells. Clonogenic assay following exposure to CRT (5μM 5-FU and GammaCell 3000 irradiation) resulted in significantly increased radio-sensitivity with increased miR-21-5p expression, and significantly decreased radio-sensitivity with inhibition of miR-21-5p.

Scarpati *et al* (2011) evaluated miRNA expression in pre-treatment fresh frozen biopsies, comparing complete responders (n=9) against all others (n=29). Standard neoadjuvant CRT in this study also included oxaliplatin. 53 differentially expressed miRNAs were further analysed and 14 with the highest-fold change were selected for RT-PCR analysis. Their data revealed two miRNAs (622 and 630) with 100% sensitivity and specificity for pCR in the study, alongside a panel that could be validated further in a larger cohort. Bioinformatic prediction of the evaluated miRNAs in the study targeted EGFR pathways, IGFR pathways and DNA repair pathways, with miR-630 specifically being considered to invoke tumour inability to repair DNA damage induced by combined radiotherapy and oxaliplatin.

Another small study of miRNA expression in pre-CRT specimens (n=12) by Kheirelsied *et al* (2013) used FFPE tissue, identifying a different miRNA signature of complete vs incomplete response (miR-16, miR-590-5p and miR-153) to neoadjuvant CRT. Svoboda *et al* (2012) identified another different panel of 8 significantly differentially expressed miRNAs from fresh frozen pre-treatment biopsies, separating responders (TRG1/2) from non-responders

(TRG3/4). Putative pathways for this panel of miRNAs related to TS inhibition, highlighting the significance of 5-FU sensitivity to treatment outcomes.

An in vitro expression signature of miRNAs in 12 colorectal cancer cell lines, was studied by Salendo *et al* (2013), following on from their work establishing a cell line-based model of CRT sensitivity, where gene expression level of the miRNAs correlated significantly with sensitivity. Significant putative pathways in this model involved MAPK, Wnt signalling pathways and cell cycle genes. The functional significance of selected significant miRNAs was confirmed in vitro in SW480 and SW837 cell lines, with miRNA-mimic transfections conferring either radio-sensitivity (miR-320a, miR-132 and let7g) or radio-resistance (miR-224) to irradiation or CRT but not 5-FU in isolation. The clinical significance of these miRNAs was assessed in 128 pre-CRT biopsies but no significant correlation with TRG was found. A significant association with disease free survival was seen with high expression of let-7g, which could be further prospectively investigated for its value as a prognostic marker.

Overall, a number of miRNAs have been identified in different studies as potential predictors of response to neoadjuvant CRT, or as having prognostic value, and a summary of these studies is presented in table 1.10 below. The functional relevance of single miRNA does not currently seem to offer a robust therapeutic target but further understanding their interactions and pathways can only help to understand their role. It may be that an expression profile of miRNAs is able to predict response, and that this can be established with further validation.

Study	Design	Evaluation	Outcome	Comments
Drebber *et al,* 2011	FFPE biopsies pre- and post-CRT, n=40	Expression of miR-21, -143 and -145	Significant up-regulation of miR-143 and -145 post-CRT	Non-significant association with TRG
Lopes-Ramos *et al,* 2014	Fresh frozen biopsies pre-CRT, n=43	miRNA expression profiling	n=4 differentially expressed miRNAs between complete and incomplete responders, miR-21 most sensitive and specific (78% and 88% respectively)	*In vitro* validation of manipulation of miR-21 expression correlating with radio-sensitivity
Scarpati *et al,* 2011	Fresh frozen biopsies pre-CRT, n=38	miRNA expression profiling	n=53 differentially expressed miRNAs between pCR and others, miR-622 and -630 demonstrated 100% sensitivity and specificity for pCR	Standard CRT included oxaliplatin
Kheirelsied *et al*, 2013	FFPE biopsies pre-CRT, n=12	miRNA expression profiling	miRNA signature for complete response (miR-16, miR-590-5p and miR-153)	Limited sample size
Svoboda *et al,* 2012	FFPE biopsies pre-CRT, n=8	miRNA expression profiling	n=8 differentially expressed miRNAs between responders and non-responders, putative pathways for this panel related to TS inhibition	Limited sample size
Salendo *et al,* 2013	*In vitro* evaluation of n=12 CRC cell lines	miRNA expression profiling	n=36 miRNAs correlated with sensitivity to CRT, miRNA-mimic transfections in SW480 and SW837 CRC cells conferred radio-sensitivity (miR-320a, miR-132 and let7g) or radio-resistance (miR-224)	No correlation with TRG for these miRNAs in n=128 clinical pre-CRT biopsies

Table 1.10 – Summary of studies investigating miRNA expression and correlation to response to CRT in rectal cancer

1.3.3 Protein Biomarkers

The literature contains numerous IHC-based studies of individual or a few markers, with conclusions from previous comprehensive reviews (Grade *et* al, 2012; Kuremsky *et al*, 2009; Kapur, 2011; Aklilu and Eng, 2011; Torino *et al*, 2013) being that these studies provide conflicting evidence for many markers, without universal acceptance of any one marker individually or in combination. The most significantly studied markers include p53, p21, p27, Ki-67, Bax, Bcl-2, XIAP, survivin, VEGF, HIF-1α, EGFR, TS, and TCF4. The review by Kuremsky *et al* (2009) concluded that of the six markers cited more than five times (p53, EGFR, TS, Ki-67, p21, and Bax/Bcl-2), EGFR and TS held promise as predictive biomarkers particularly with focus on genetic polymorphisms, and further investigation of p21 and Bax was justified. These markers correlate strongly with cell pathways previously identified by gene expression studies, including apoptosis and WNT pathway signalling.

1.3.3.1 Apoptosis

Survivin and XIAP are members of the inhibitors of apoptosis (IAP) protein family. High survivin expression has been associated with reduced apoptosis in pre-treatment biopsies of rectal cancer patients, and conferred an increased risk of local disease recurrence (26% vs. 6%, p=0.05) in the study by Rödel *et al* (2005). In the study by Kim *et al* (2011) where imunohistochemical staining on tissue microarray (TMA) of seven markers (Cox-2, TS, VEGF, EGFR, Ki-67, p21 and survivin) from a pre-CRT biopsy, was correlated with Dworak tumour regression grading in a cohort of 54 patients, only survivin expression was significantly related to tumour downstaging, with higher expression observed with a poorer response.

Expression of XIAP was demonstrated to be the only significantly differentially expressed apoptotic protein in a tumour:normal mucosa ratio in biopsies of 38 rectal cancer patients (Moussata *et al*, 2012). *In vitro* analayis of XIAP expression in a radio-resistant CRC cell line (SW480) increased following irradiation, with subsequent siRNA knockdown of the protein conferring significantly increased radio-sensitivity on the basis of clonogenic assay and apoptotic index. Hehlgans *et al* (2013) further demonstrated that single or double targeting of survivin and XIAP with siRNA in 4 CRC cell lines grown in 3D culture (as a potentially closer model of *in vivo* behaviour) conferred significantly increased radio-sensitivity, and that double knockdown of these proteins significantly decreased phosphorylation of the markers FAK Y397 and Akt1 S473, which are associated with cellular survival, deregulated migration and cancer invasion.

A therapeutic model of the action of the smac mimetic JP-1201, as an inhibitor of IAPs was developed by Huerta *et al* (2010). In HT-29 CRC cells, significantly increased radio-sensitivity was observed following irradiation on clonogenic assay with JP-1201 pre-incubation, which was translated into an immunodeficient mouse xenograft model, where a 46% reduction in tumour load was observed in an irradiation + JP-1201 group against irradiation alone (and with no reduction against JP-1201 treatment in isolation). The mechanism of action for increased radio-sensitivity with JP-1201 was proposed to be evidenced by a marked reduction in XIAP expression in pre-treated cells following irradiation associated with more double-stranded DNA breaks.

Further studies in HCT116 cells and xenografts undertaken by Huerta *et al* (2013) demonstrated a radio-sensitive phenotype in DNA-PKcs, p21, and Bax deficient cell lines, and

a radioresistant phenotype in a p53 deficient cell line. In vivo work demonstrated Bax deficiency resulted in increased tumour necrosis and decreased microvessel density, with complementary *in vitro* data demonstrating decreased levels of VEGF. siRNA inhibition of apoptosis inducing factor (AIF) in Bax deficient HCT116 cells conferred a significant survival advantage following ionising radiation compared with AIF inhibition in wild type controls, implicating AIF in the radio-sensitivity of Bax deficient cells.

The effect of Bax was evaluated in a clinical dataset by Fucini *et al* (2012). IHC Bax positivity on FFPE pre-CRT biopsies was significantly associated with downstaging in a group of 34 patients (p=0.001) but not p53, Bcl-2 or Bcl-xl.

1.3.3.2 WNT pathway

Epithelial mesenchymal transition (EMT) as a marker of response to neoadjuvant CRT was evaluated by Bhangu *et al* (2014). The process represents the conversion of epithelial cells into motile mesenchymal cells under the major influence of transforming growth factor-β1, and is seen mainly at the invasive edge of the tumour. Nuclear β-catenin accumulation occurs following downregulation of E-cadherin, with activation of downstream EMT pathways (Kalluri and Weinberg, 2009). The study was performed as a proof-of-principle, using FFPE resection specimens, and equally representing post-CRT tissue. Reduced E-cadherin expression, nucleic β-catenin expression and tumour budding were significantly associated with EMVI, and miRNA 200c loss (as an upstream regulator of EMT) in addition to the other markers were strongly associated with non-response to CRT, defined by Mandard tumour regression grade 3-5.

Wang *et al* (2013) corroborate the association of nuclear β-catenin overexpression with radio-resistance. 68 patients (57.6%) who exhibited radio-resistance, as defined by Dworak TRG 0-2 had high nuclear β-catenin expression, compared with 3 radio-sensitive cases (16.7%) with low nuclear expression. It is not clear in the paper that the evaluated tissue is a pre-treatment biopsy in isolation. Equally treatment was with SCPRT and not CRT, therefore β-catenin may reflect radio-sensitivity not sensitivity to CRT.

The expression of β-catenin was also demonstrated to be influenced by lincRNA-p21 by Wang *et al* (2014). LincRNAs have been shown to be novel regulators of transcription and post-transcriptional translation, and are regulated by p53 (Huarte *et al*, 2010). Reduced lincRNA-p21 expression in CRC cells was associated with elevated β-catenin expression, and

its expression was induced by irradiation. Overexpression of lincRNA-p21 in SW1116 cells increased their radio-sensitivity by inducing apoptosis. In 30 clinical samples its expression was elevated in rectal adenocarcinoma compared to normal adjacent mucosa. Whilst the authors propose lincRNA-p21 as a novel therapeutic target, it would certainly seem appropriate to further target Wnt/β-catenin signalling.

1.3.4 Conclusions and Future Direction

A wide range of potential markers for sensitivity to CRT have been evaluated, however there remains no current universal acceptance for either a single biomarker or panel of biomarkers, in predicting outcome to neoadjuvant CRT in locally advanced rectal cancer. Variations in tissue collection and processing, different stratifications of pathological response, varying interpretations of 'responder' vs. 'non-responder', the divergent chemotherapy and radiotherapy regimens employed even within 5-FU based therapy, as well as more novel radio-sensitisers used in addition/combination, have muddied the waters in the search for predictive markers, whilst simultaneously broadening the scope for further research and redefining targets.

The future direction for further work encompasses further genome wide expression analyses, further focussed SNP analysis of key genetic markers, and further validation of key or novel protein biomarkers, in wider and co-ordinated studies, to establish markers for the range of potential CRT regimens, either within and/or across populations. This would lead to the personalisation of CRT regimens, and/or the selection of patients most appropriate for CRT, with hopefully improved cancer specific outcomes, whilst limiting off target effects, morbidity and improving functional outcome.

Modification of treatment response is equally a therapeutic goal and following the validation of robust prognostic markers at the genetic or post-transcriptional level, novel therapies may emerge. The growing development of organ preserving surgical techniques in rectal cancer mean that radiotherapy will have an even greater role to play in the future, and therefore further improvement in the efficacy and prediction of response is critical in the ongoing management of rectal cancer.

1.4 Acid Ceramidase

1.4.1 Precipitating Research

The research underpinning the experimental work presented in this thesis was performed at The University of Liverpool as one aspect of PhD studies undertaken by Mr Paul Sutton. A novel temporal proteomic profiling in patients receiving CRT for locally advanced rectal cancer was performed, in attempt to identify differentially expressed proteins that may be implicated in CRT response. Cancer tissue was obtained at the time of diagnosis before CRT, at the completion of CRT, and after the downstaging period at the time of surgical resection, then subjected to mass spectrometry analysis (with isobaric tagging for relative and absolute quantification) to determine protein expression. Differential protein expression between the respective samples was assessed to identify temporal changes with CRT and during subsequent downstaging, and a comparison of protein expression between patients dichotomised to have responded or not to CRT was performed from the potentially predictive pre-CRT samples. This data has been deposited to the ProteomeXchange Consortium via the PRIDE (Vizcaíno *et al*, 2016) partner repository with the dataset identifier PXD008436.

The abundance of contributing peptide ions for 18 proteins were significantly different between pre- and post-CRT samples, of which 16 were upregulated and 2 downregulated. There were 19 upregulated and 10 downregulated proteins when comparing pre-CRT and resection samples, and 9 upregulated and 30 downregulated between post-CRT and resection samples. When comparing tumours between those patients subsequently dichotomised as relative responders or non-responders to CRT, the abundance of contributing peptide ions for 8 proteins were significantly different, 5 of which were upregulated in responders and 3 downregulated. Tables detailing these results are included in appendix A.

Those proteins identified as statistically significantly different were subjected to analysis with IPA (Redwood City, USA). The ceramide degradation pathway was identified as the most significantly downregulated pathway in those tumours responding to CRT (p=9.92E-04) based on the significantly lower abundance of contributing peptide ions for acid ceramidase

(AC) (log fold change -1.526, p=1.17E-02). AC was also significantly differentially expressed in the tumours between the point of CRT completion and at the time of surgical resection, with downregulation (log fold change -1.568, p=1.35E-02) during this downstaging period.

1.4.2 Biology and Pathophysiology of Acid Ceramidase

AC is a hydrolase important in the regulation of sphingolipids – a group of biomolecules known to be responsible for structural components of biological membranes (particularly ceramide) but with increasing evidence to implicate them as bioactive molecules involved in the modulation of cell growth, differentiation, cell migration and apoptosis.

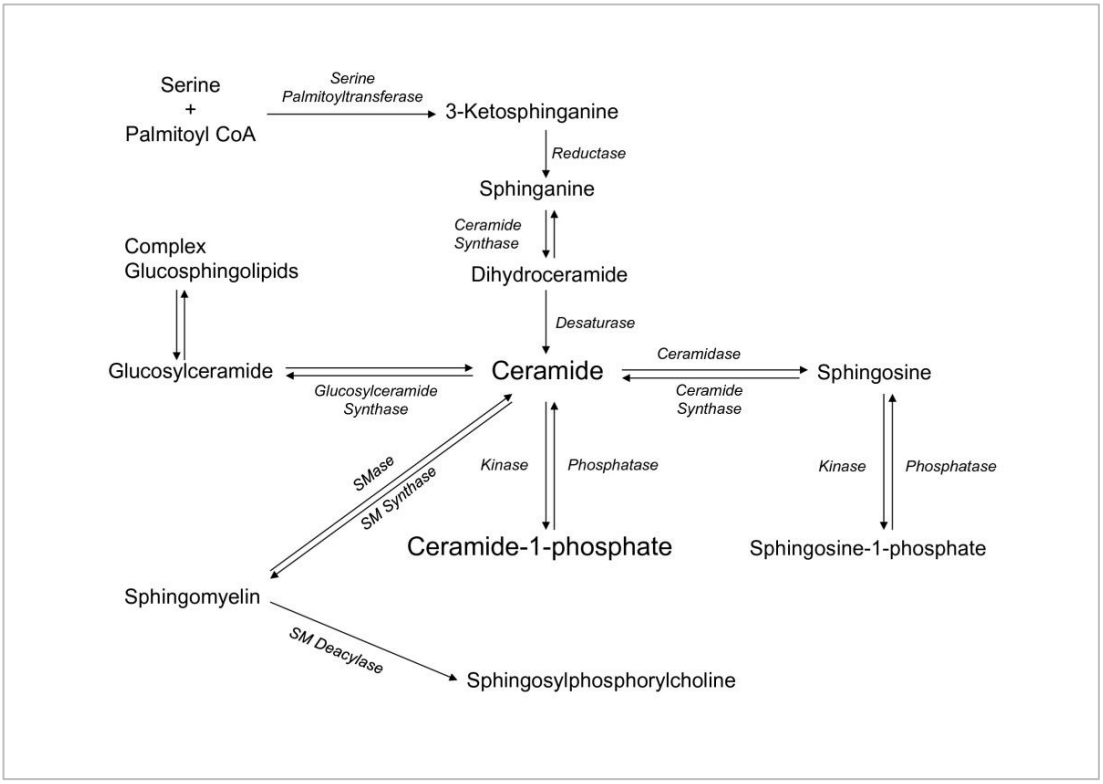

Figure 1.7 – Sphingolipid metabolism. (Taken from Arana *et al*, 2010)

Ceramide is produced by degradation of sphingomyelin by sphingomyelinase (SMase), by *de novo* synthesis through the action of serine palmitoyltransferase and dihydroceramide synthase and is generated through metabolism of more complex sphingolipids. It is metabolised to ceramide-1-phosphate by ceramide kinase, or to glucosylceramide by glucosylceramide synthase. Ceramide can be degraded by ceramidases to form sphingosine

(SPH), which can then be phosphorylated to sphingosine-1-phosphate (S1P) by sphingosine kinase (SK). SPH can be produced from S1P under the action of phosphatases, and ceramide generated from SPH under the action of ceramide synthase.

SPH, ceramide and S1P are the main bioactive molecules, with ceramide and S1P exerting opposing influences on the cell – ceramide has been demonstrated to mediate cell cycle arrest and apoptosis in response to cell stress, and S1P demonstrated to promote cell survival and proliferation (Garcia-Barros *et al*, 2014). The regulation of these molecules is controlled by enzymes such as AC, and sphingolipid metabolism is depicted in figure 1.7 above.

The degradation of ceramide to SPH occurs by hydrolysis and is catalysed by ceramidases. These are characterised by the pH required for their optimal activity (acid, neutral or alkaline).

AC is a lysosomal cysteine amidase that catalyses the breakdown of ceramide into SPH and free fatty acid. It was first discovered in rat brain homogenates and was further characterised and purified from human urine in 1995 (Bernado *et al*, 1995). AC has a molecular weight of 53-55kDa depending on the degree of glycosylation and is composed of α and β sub-units which are 13 and 40kDa in weight respectively. The sub-units are joined by a disulphide bond, with glycosylation only occurring on the β sub-unit. AC is synthesised as a pro-enzyme, undergoing autoproteolytic cleavage into its constituent sub-units post-translationally within lysosomes, and has an optimal enzymatic pH range of 4-5 (He *et al*, 2003).

The ASAH1 gene is located on chromosome 8 and encodes for AC (Li *et al*, 1999). Mis-sense mutations in this gene have been associated with an extremely rare autosomal recessive condition called Farber's disease / lipogranulomatosis. This is a lysosomal storage disease, characterised by ceramidase deficiency and resulting in ceramide accumulation in tissues. Symptoms usually present within the first few weeks of life, with impaired mental ability and dysphagia. Other symptoms include arthritis, lymphadenopathy, contractures, hoarseness and xanthomas, and hepatic, cardiac and renal impairment can occur. Most children with the condition usually die as a consequence of respiratory disease by the age of 2 (Farber, 1952). More recently another mutation in the ASAH1 gene has been associated with spinal muscular atrophy associated with progressive myoclonic epilepsy, characterised by damage to lower motor neurons. The reduced expression of AC in this condition (but not <10% as in Farber disease) is thought to allow for near-normalised ceramide levels but results in a later onset phenotype restricted to the central nervous system (Zhou *et al*, 2012).

1.4.3 Acid Ceramidase in Apoptosis

Apoptosis refers to an inducible and pre-programmed cell pathway resulting in the activation of calcium- and magnesium-dependent endonucleases that fragment nuclear chromatin. The involvement of ceramide in apoptosis was demonstrated by the induction of apoptosis with exogenously added ceramide to bovine aortic endothelial cells. In addition, radiation induced sphingomyelin hydrolysis and apoptosis, that had been blocked by protein kinase C activation, was reversed with the addition of ceramide (Haimovitz-Friedman *et al*, 1994).

The mechanism of ceramide-induced apoptosis has been considered to be both via the extrinsic pathway as a consequence of enhanced signalling from pro-apoptotic membrane molecules such as CD95 (Miyaji *et al*, 2005), or via the intrinsic pathway by the formation of trans-membrane mitochondrial channels that allow the release of apoptosis inducing proteins such as caspase-3 and cytochrome c (Siskind *et al*, 2002). Ceramide has also been associated with reduced telomerase activity and with the acceleration of telomere shortening, thus increasing the likelihood of cell senescence or apoptosis once the telomere reaches a critical length (Ogretmen *et al*, 2001).

It is proposed that many cancer cells are able to resist apoptosis as a consequence of limiting ceramide generation, or by its rapid removal (Truman *et al*, 2014). One such mechanism is via the de-acetylation of ceramide by AC to SPH, which is then modified by a SK to S1P. S1P has been demonstrated to initiate the pro-survival PI3K/AKT signalling pathway, thus opposing the effect of ceramide, with the balance between ceramide and S1P determining cell fate (Bonnaud *et al*, 2010). Co-expression of Akt2 and ASAH1 genes has been demonstrated to significantly induce cell invasion and resistance to apoptosis, with siRNA inhibition of both genes, as well as combined pharmacological inhibition, more potent than inhibiting each individually in inhibiting cell viability, proliferation and invasion (Berndt *et al*, 2013).

S1P has also been revealed to promote invasiveness in glioblastoma by upregulation of the urokinase plasminogen activator and its receptor, and the pro-invasive molecule cysteine-rich angiogenic protein 61 (Young *et al*, 2009). In the rat HTC hepatoma cell line, ceramide accumulation itself did not appear to induce apoptosis in response to tumour necrosis factor-α and cycloheximide therapy but by the lysosomal conversion to SPH by AC which causes lysosomal membrane permeability, with siRNA inhibition of AC interestingly preventing apoptosis induced by the therapy (Ullio *et al*, 2012).

AC is therefore centrally placed in the pathway of sphingolipid metabolism and may well have a key role in the fate of cells in response to stresses that induce ceramide. Over-expression seemingly catalyses the breakdown of ceramide and drives the cell away from apoptosis towards survival, with reduced expression or inhibition resulting in ceramide accumulation and apoptosis.

1.4.4 Acid Ceramidase in Malignancy

A summary of the studies implicating AC in numerous malignancies is presented in table 1.11 below with subsequent further detailed appraisal.

Study	Malignancy	Evaluation	Outcome	Comments
Roh *et al,* 2016	Head and neck cancer	AC expression, effect of genetic and pharmacological manipulation	AC over-expression in 4 of 6 primary tumours and 6 of 9 cell lines, increased cell sensitivity to cisplatin with AC inhibition	Increased ceramide and apoptotic protein levels with AC inhibition
Korbelik *et al,* 2016	Head and neck cancer	Effect of AC inhibition with LCL521 in SCCVII cells	Reduced cell survivability after photodynamic therapy	
Elojeimy *et al,* 2007	Head and neck cancer	Effect of manipulation of AC expression in SCC-1 cells	Increased resistance to Fas-induced apoptosis with over-expression of AC, and increased sensitivity with down-regulation	AC inhibition with LCL204 sensitises to Fas-induced apoptosis
Realini *et al*, 2016	Melanoma	AC expression, effect of AC inhibition with ARN14988 in proliferative melanoma cells	Melanocytes and melanoma cell lines over-express AC relative to non-melanoma skin cancer cells, synergistic action of AC inhibition with 5-FU to increase cytotoxicity	AC inhibition increases ceramide and decreases S1P levels
Bedia *et al,* 2011	Melanoma	Effect of manipulation of AC expression in A375 cells	Over-expression and down-regulation conferred resistance and sensitivity to dacarbazine respectively	
Tan *et al,* 2016	Acute myeloid leukaemia	AC expression, effect of AC inhibition with LCL204 in mouse models	Primary AML cells highly express AC, LCL204 treatment increases survival in C57BL/6 mice engrafted with C1498 leukaemia cells and reduces disease burden in NSG mice engrafted with primary human AML cells	Increased expression of anti-apoptotic Mcl-1 with AC inhibition
Hu *et al,* 2011	Acute myeloid leukaemia	AC expression relative to IRF8 expression in myeloid cells	IRF8 expression lost in AML, restoration of IRF8 reduces AC expression, increases ceramide levels and increases sensitivity to FasL-induced apoptosis	AC expression significantly increased in cells derived from IRF8 deficient mice
Ramírez de Molina *et al,* 2012	Non-small cell lung cancer	Response in primary cell culture to ChoKα inhibitors and associated AC expression	Raised AC expression in cells with acquired resistance to ChoKα inhibition	Anti-proliferative effect of ChoKα inhibition enhanced with synergistic inhibition of AC
Flowers *et al,* 2012	Breast cancer	Effect of AC inhibition with DM102 on the apoptosis inducing effects of C6-ceramide in three cell lines	AC inhibition synergistically produced a significant reduction in viability in all cell lines	AC expression related to HER2 status

Hanker *et al,* 2013	Ovarian cancer	IHC expression of AC in n=112 cancers	Low expression correlated with poorer cancer specific survival	Contrary to other data
Morales *et al,* 2007	Hepatoma	*In vitro* and *in vivo* study, effect of AC inhibition on daunorubicin treatment	Inhibition of AC with genetic (siRNA) or pharmacological (N-oleoylethanolamine) means sensitised human (HepG2) and mouse (Hepa1c17) hepatoma cell lines to treatment, *in vivo* AC inhibition with siRNA reduced growth in liver tumour xenografts of HepG2 cells	Cell death preceded by structural mitochondrial changes, stimulation of reactive oxygen species generation and cytochrome c and caspase-3 activation.
Mahdy *et al*, 2009	Prostate cancer	Effect of AC manipulation on sensitivity to radiation in PPC-1 cells	Down-regulation of AC with siRNA and inhibition with LCL385 confers radio-sensitivity	Up-regulation of AC decreased sensitivity to radiation and created cross-resistance to chemotherapy
Cheng *et al,* 2013	Prostate cancer	AC expression post-irradiation in PPC-1 cells and IHC expression in human prostate cancer	Up-regulation of AC post-irradiation, over-expression in surviving clones associated with increased radio-resistance, higher AC expression after radiotherapy failure (than in irradiation-naïve cancer, intra-epithelial neoplasia or benign tissue)	Inhibition with LCL521 in a xenograft model produced radio-sensitisation and prevented relapse
Camacho *et al*, 2013	Prostate cancer	IHC AC expression in n=33 prostate cancers and PC-3 cell line	Higher AC expression with more advanced disease stage, higher expression in tumourigenic PC-3/Mc clone than non-metastatic PC-3/S clone	siRNA inhibition of AC in PC-3/Mc clone resulted in ceramide accumulation and reduced viability
Holman *et al,* 2008	Prostate cancer	Effect of AC inhibition with LCL204 in DU 145 cells	Increased ceramide, decreased sphingosine, caspase activation and increased apoptosis with inhibition	Degradation of AC by LCL204 was cathepsin-dependent
Gouazé-Andersson *et al*, 2011	Prostate cancer	*In vitro* evaluation of AC inhibition in PC-3 and DU 145 cell lines	Synergistic cell toxicity with ceramide generation (fenretidine) and AC inhibition with DM102 (but not N-oleoylethanolamine)	Toxicity with fenretidine/DM102 treatment persisted despite blocking ceramide generation
Turner *et al,* 2011	Prostate cancer	*In vitro* evaluation of PPC1 and DU 145 cells over-expressing AC	Increased lysosomal density, high expression of lysosomal stabilising protein KIF5B, increased levels of autophagy	Possible mechanism of resistance to ceramide accumulation

Table 1.11 – Summary of studies implicating AC in malignancy and response to treatment

1.4.4.1 Head and neck cancer

AC over-expression has been observed in squamous cell head and neck cancer (HNC) in four out of six primary tumours and six out of nine HNC cell lines in a study by Roh *et al* (2016) and was correlated with resistance to cisplatin chemotherapy in the cell lines. Pharmacological (with N-oleoyl-ethanolamine) and genetic (with small hairpin RNA) inhibition of AC in the cell lines significantly increased their sensitivity to cisplatin, with increased ceramide production and activation of pro-apoptotic proteins. In another study of squamous cell cancer cells, the inhibition of AC with the small molecule inhibitor LCL521 significantly reduced the survivability of SCCVII cells on the basis of clonogenic assay after photodynamic therapy (Korbelik *et al*, 2016), with AC activity inhibition and increases in ceramide levels also having been observed after photodynamic therapy in isolation (Separovic *et al*, 2013). Over-expression of AC in the SCC-1 cancer cell line increased

resistance to Fas-induced apoptosis, with down-regulation inducing sensitivity. The AC inhibitor LCL204 was also demonstrated in this study to sensitise HNC cell lines to Fas-induced apoptosis in both *in vitro and* in a xenograft model *in vivo* (Elojeimy *et al*, 2007).

1.4.4.2 Melanoma

Melanocytes and proliferative melanoma cell lines have been demonstrated to over-express AC relative to other skin cells and non-melanoma skin cancer cells (Realini *et al*, 2016). Application of the AC inhibitor ARN14988 acted synergistically with 5-FU to increase cytotoxicity in the proliferative melanoma cell line in this study, with increased ceramide levels and reduced S1P levels noted. This may have positive implications for 5-FU based CRT in rectal cancer. In the context of the clinical management of metastatic melanoma, where dacarbazine is a chemotherapeutic option, targeting of AC may improve sensitivity to therapy. This was demonstrated by over-expression and down-regulation of AC in human A375 melanoma cells *in vitro* conferring resistance and sensitivity respectively to dacarbazine (Bedia *et al*, 2011).

1.4.4.3 Myeloid leukaemia

A comprehensive experimental assessment of the role of AC in acute myeloid leukaemia (AML) was undertaken by Tan *et al* (2016). Primary AML cells were observed to highly express AC, with AC over-expression increasing the expression of the anti-apoptotic Mcl-1, and reduced Mcl-1 expression observed with the synthetic AC inhibitor LCL204. LCL204 treatment significantly increased the overall survival of C57BL/6 mice engrafted with C1498 leukaemia cells and significantly decreased disease burden in NSG mice engrafted with primary human AML cells, implicating AC as an independent therapeutic target. IFN regulatory factor 8 (IRF8) is a key transcription factor for myeloid cell differentiation, with expression frequently lost in haematopoeitic cells in myeloid leukaemia. Hu *et al* (2011) identified AC as a general transcription target of IRF8, with expression of IRF8 regulated by promoter DNA methylation. In myeloid cells, restoration of IRF8 expression supressed AC and resulted in ceramide accumulation and increased sensitivity to FasL-induced apoptosis. In cells derived from IRF8-deficient mice AC was dramatically increased, with AC inhibition or the application of exogenous ceramide sensitising cells to FasL-induced apoptosis,

suggesting a mechanism for a pathway of resistance to Fas-mediated apoptosis and disease progression.

1.4.4.4 Non-small cell lung cancer

In non-small cell lung cancer cells with acquired resistance to the pro-apoptotic effect of choline kinase α (ChoKα) inhibitors, raised levels of AC have been demonstrated compared to non-resistant cells. The anti-proliferative effect of ChoKα therapy is enhanced with the synergistic inhibition of AC in primary cell culture, suggesting a model for combination therapy (Ramírez de Molina *et al*, 2012).

1.4.4.5 Breast cancer

High genetic expression of ASAH1 has also been observed to correlate with a better prognosis in invasive breast cancer, and with a reduced incidence of recurrence in pre-invasive DCIS (Sänger *et al*, 2015), although how this correlates with a functional post-translational expression of AC is not identified.

In three breast cancer cell lines, Flowers *et al* (2012) assessed the effect of AC inhibition (with DM102) on the apoptosis inducing effects of C6-ceramide. As single agents, C6-ceramide and DM102 were only moderately cytotoxic but co-administration produced a reduction in viability in all cell lines. This was considered to be synergistic in MDA-MB-231 and MCF-7 cells but antagonistic in BT-474 cells. Correlations of AC expression and sensitivity to C6-ceramide/DM102 were independent of oestrogen receptor status or molecular subtypes but AC expression was related to HER2 status. This potentially suggests a prognostic relevance of AC tumour expression and the sensitivity of certain breast cancer subtypes to ceramide-targeted therapy and warrants further investigation.

1.4.4.6 Ovarian cancer

On IHC analysis on n=112 ovarian cancer tumour samples, low AC expression was correlated with a poorer cancer specific survival (Hanker *et al*, 2013), although this is contradictory to the centrally described outcomes of sphingolipid metabolism as discussed. It may be that AC expression and function is not ubiquitous across all tumours, that its expression is

implicated in response to selected therapies, or that it is involved in alternative pathways in certain tumours, and further investigation in these cancers is required.

1.4.4.7 Hepatoma

AC is activated by the chemotherapeutic daunorubicin in human (HepG2) and mouse (Hepa1c17) hepatoma cell lines as well as in primary cells from murine liver tumours but not in cultured mouse hepatocytes. Inhibition of AC by siRNA or pharmacological means sensitised the cell lines to daunorubicin-induced cell death, preceded by structural mitochondrial changes, stimulation of reactive oxygen species generation and cytochrome c and caspase-3 activation. *In vivo* AC inhibition with siRNA also reduced growth in liver tumour xenografts of HepG2 cells and also enhanced daunorubicin therapy, offering a potential therapeutic target in the management of liver cancers (Morales *et al*, 2007).

1.4.4.8 Prostate cancer

The depth of literature implicating AC in tumour proliferation and resistance to treatment in greatest in relation to prostate cancer. Importantly, the study from Mahdy *et al* (2009) has convincingly demonstrated that downregulation of the corresponding gene for AC with siRNA in a prostate cancer cell line confers radio-sensitivity. This *in vitro* study in PPC-1 cells assessed radiation response by clonogenic and cytotoxic assays, demonstrating that up-regulation of AC decreased sensitivity to radiation and created cross-resistance to chemotherapy, with the small molecule AC inhibitor LCL385 also sufficient to sensitize PPC-1 cells to radiation.

In addition, the cell line is observed to preferentially upregulate AC in response to irradiation, with over-expression of AC in clones that survived an irradiation course and that were further associated with increased radio-resistance and proliferation (Cheng *et al*, 2013). This was validated with IHC analysis of human prostate cancer tissues where higher levels of AC were observed after radiotherapy failure than in irradiation-naïve cancer, intra-epithelial neoplasia or benign tissue. In addition to AC inhibition in an animal xenograft model producing radio-sensitisation, it also prevented relapse.

Higher IHC expression of AC in primary prostate cancers is associated with more advanced disease stage, and in a model derived from PC-3 prostate cancer cells, the highly

tumourigenic, metastatic and chemo-resistant PC-3/Mc clone expressed higher levels of AC than the non-metastatic PC-3/S clone, with stable knockdown of ASAH1 in PC-3/Mc cells resulting in an accumulation of ceramide, reduced clonogenic potential and inhibition of tumourigenesis and lung metastases (Camacho *et al*, 2013). The DU 145 prostate cancer cell line has also been demonstrated to be sensitive to the effect of AC inhibition following treatment with LCL204, with raised ceramide and decreased sphingosine levels, caspase activation and ultimately apoptosis observed (Holman *et al*, 2008). In this study, the degradation of AC by LCL204 was cathepsin-dependent.

The PC-3 and DU 145 prostate cancer cell lines are considered to be hormone-refractory. In a study by Gouazé-Andersson *et al* (2011), combination therapy in these cell lines with the ceramide-generating chemotherapeutic fenretinide and the synthetic AC inhibitor DM102 significantly decreased cell viability in a synergistic manner, with single-agent treatment being only weakly cytotoxic. An alternative known AC inhibitor N-oleoylethanolamine did not produce a synergistic effect with fenretinide in the cells and blocking ceramide generation (with either vitamin E or myriocin) did not prevent cytotoxicity from combined fenretinide/DM102 treatment, suggesting alternative metabolic pathways in this context.

Turner *et al* (2011) demonstrated that the PPC1 and DU 145 prostate cancer cell lines over-expressing AC relative to controls have increased lysosomal density, high expression of the lysosomal stabilising protein KIF5B and increased levels of autophagy, complimenting the enhanced stress-resistance inherent to the cells, and to potentially explain the ability of the prostate cancer cells to respond to ceramide accumulation following irradiation.

1.4.5 Summary Statement and Further Research

The above data support the findings of lower levels of AC in those rectal tumours responding to CRT, with differential expression from pre-CRT biopsies suggesting the potential for its evaluation as an up-front predictive biomarker of response. Further evaluation in a larger patient cohort, and validation *in vitro* data is clearly required.

Carmofur, in common to the widely used radio-sensitiser capecitabine, is an oral 5-FU analogue that has been used in the US and Japan in the adjuvant setting for colorectal cancer. In addition to its presumed primary mode of action as a TS inhibitor, it has also independently

been shown to potently inhibit AC in the human tumour derived cell lines SW403 (colorectal) and LNCaP (prostate), a property not shared by 5-FU or capecitabine (Realini *et al*, 2013). In light of both this and the proteomic profiling data, further investigation is required to compare the radio-sensitisation of capecitabine (TS inhibition) and carmofur (TS and AC inhibition).

1.5 Predicting and Modifying Response to Chemoradiotherapy in Rectal Cancer

It is clear from the literature that the current response to CRT in rectal cancer is poorly understood and that its efficacy needs to be improved. AC has been identified as a potential novel biomarker and therapeutic target but needs further validation. The aim of this thesis is therefore to attempt to provide this further validation with assessment in a wider clinical dataset, and by performing an *in vitro* evaluation of the effect of AC inhibition on radio-sensitivity in a CRC cell line.

1.5.1 Research Questions

The specific questions to be answered by this thesis are therefore:

- Does AC expression predict response to CRT in clinical rectal cancer samples in a larger patient cohort?
- Does the inhibition of AC in a CRC derived cell line increase radio-sensitivity?
- Does inhibition of AC increase radio-sensitivity when compared to standard 5-FU radio-sensitisation?

1.5.2 Hypotheses

These questions can be used to formulate a number of testable hypotheses to be investigated:

- Differential expression of AC is present in rectal cancer and/or normal colon
- Expression of AC in rectal cancer and/or normal colonic tissue can predict response to neoadjuvant CRT, and/or is a biomarker of response to treatment
- Expression of AC can be inhibited by siRNA transfection in the HCT116 CRC cell line, subsequently inhibiting protein activity
- AC activity +/- expression can be inhibited by the chemotherapeutic carmofur in the HCT116 CRC cell line

- HCT116 cell radio-sensitivity can be increased by the pharmacological inhibition of AC activity using the chemotherapeutic carmofur
- HCT116 cell radio-sensitivity can be increased by the genetic suppression of AC expression (and subsequent activity) using siRNA transfection
- Any increase in cell radio-sensitivity based on inhibition of AC is independent of the presence of 5-FU

Chapter 2

Validation of Acid Ceramidase as a Potential Predictive and/or Prognostic Biomarker of Response to Chemoradiotherapy in Rectal Cancer

2.1 Introduction

2.1.1 Background

In the late 1990s, TMA technology revolutionised the investigation of potential prognostic and predictive biomarkers (Kallioniemi *et al*, 2001). A TMA involves the transfer of small tissue cores, typically 0.6 mm in diameter, from FFPE tissues into an empty paraffin block, and this repeated transfer of tissue cores leads to the construction of a "tissue-archive" that can contain hundreds of tissue samples. TMAs can be used to study tissue morphology, expression of proteins or genes and chromosomal aberrations using different stains, IHC and in-situ hybridization (Voduc *et al*, 2008). The combination of TMAs and clinically annotated samples represents an elegant and cost-effective approach to study panels of biomarkers under identical experimental conditions and to develop prognostic or predictive models of patient outcomes (Horvath *et al*, 2001).

It was considered that the optimal strategy for investigation of AC expression on TMA, would include assessment of normal colon and cancer site samples, at both the point of diagnosis prior to CRT and from the resection specimen after treatment. This would mimic the tissue dataset obtained from the original proteomic profiling as closely as possible in terms of providing a temporal assessment of AC expression with treatment, as well as obtaining information from normal colon in addition as a comparison. Assessment of tissue from a diagnostic biopsy would provide information regarding the potential of AC as a predictive biomarker of response to CRT. Comparing normal and malignant tissue both before and after treatment may also yield prognostic information, or demonstrate where further studies would be needed to evaluate a potential mechanism of action.

Given that this proposed TMA study was to be performed retrospectively, it was not possible to determine the tissue collected, as it would be reliant on retrieving archived FFPE tissue blocks. The diagnostic biopsy specimens were considered to potentially harbour some normal colonic tissue within, although this was not considered to be a reliable source, as the endoscopic target biopsied is overwhelmingly likely to have been macroscopically abnormal. Even if normal tissue were to have been present, it was considered highly unlikely to be

present in sufficient volume to have technically been viable to be used to construct a meaningful TMA. The best hope for normal tissue was therefore considered to originate from the resection specimen, albeit with limitations.

2.1.2 Hypotheses

- Differential expression of AC is present in rectal cancer, and/or normal colon
- Expression of AC in rectal cancer and/or normal colonic tissue can predict response to neoadjuvant CRT, and/or is a biomarker of response to treatment

2.1.3 Aims and Study Design

- Identification of ≥100 rectal cancer cases whereby surgical resection of the primary tumour had been performed following completion of neoadjuvant CRT
- Assessment of TRG in these cases
- TMA construction comprising
    - Tissue from the diagnostic biopsy specimen
    - Normal epithelium from the resection specimen
    - Cancer site tissue from the resection specimen
- Optimisation of IHC staining of TMAs for AC
- Assessment of TMA IHC staining for AC and correlation with TRG
- Correlation of clinical and pathological data with IHC staining and TRG

2.2 Methods

2.2.1 Ethical Approval

The study was performed under existing NHS Research Ethics Committee and Research and Development approval (12/NW/0011). 111 consecutive patients were identified from histopathological records at The Countess of Chester Hospital NHS Foundation Trust to have undergone surgical resection of a primary rectal cancer at the hospital between January 2007 and July 2015, and having prior completed a course of neoadjuvant CRT. In six of the identified cases, the diagnostic biopsy specimen had been obtained and was located at Mid Cheshire Hospitals NHS Foundation Trust. A materials transfer agreement was sought and agreed to facilitate acquisition of these samples.

2.2.2 Assessment of Tumour Regression Grading

H&E stained slides for the identified cases were reviewed by consultant histopathologist (Dr Michael Wall (MW), FRCPath) to confirm the diagnosis of adenocarcinoma, and slides from the resection specimen were assessed to allocate a TRG. The four-tier system recommended by The Royal College of Pathologists, and like that described by Ryan *et al* (2005) was used (https://www.rcpath.org/resourceLibrary/dataset-for-colorectal-cancer-histopathology-reports--3rd-edition-.html).

- TRG 4: no viable tumour cells (fibrosis or mucus lakes only)
- TRG 3: single cells or scattered small groups of cancer cells
- TRG 2: residual cancer outgrown by fibrosis
- TRG 1: minimal or no regression (extensive residual tumour)

The practicable application of this system was considered to comprise; a) complete responders (TRG 4) vs. others, b) relative responders (TRG 4&3) vs relative non-responders (TRG 2&1), and c) non-responders (TRG 1) vs. others. This is in accordance with the

correlation of complete response and near-complete response with outcome, as described by Hermanek *et al* (2013).

2.2.3 Tissue Microarray Construction

Three sets of TMAs were constructed comprising; a) malignant tissue from the diagnostic biopsy specimen (n=106), b) 'normal' colonic epithelium obtained from the colonic end of the resection specimen outside the radiation field (n=111), and c) tissue from the cancer site, specifically targeting residual malignant cells where present, or areas of fibrosis consistent with radiotherapy exposure in those with a pCR (n=111). The technique for TMA construction was as described by Kononen *et al* (1998). H&E slides were reviewed by a consultant histopathologist (MW) and the best representative slide for each tissue group was marked (circled) by permanent marker to identify the area to target for obtaining donor cores. The corresponding FFPE tissue blocks were retrieved from storage. A visual comparison between the marked slides and donor blocks was made by overlying the marked slide on the tissue block, and the targeted area was subsequently marked on the donor block.

TMAs were constructed using a tissue microarrayer (Beecher Instruments Inc., Wisconsin, USA), with 0.6mm cores retrieved from donor blocks, and transferred into the recipient master paraffin blocks. Triplicate cores were randomised across three TMAs for each tissue type, with cores of kidney, lung, ovary, and thyroid tissue equally randomised into each TMA as controls. Randomisation was performed using the sequence generator facility available at https://www.random.org/sequences/. TMAs were incubated at 37°C overnight, then placed on ice prior to 5µm sections being cut on a rocking microtome. Sections were then placed onto coated glass slides, which were further incubated at 37°C prior to performing IHC staining.

H&E staining was undertaken with the initial TMA sections, which were examined to assess for adequate tissue coverage. In cases where at least one representative core of the targeted tissue wasn't observed, further TMAs were constructed to attempt to encompass as many of the cases as possible. This resulted in a further two TMAs being constructed for the normal colon blocks – triplicate cores from 29 cases randomised into one block, with further triplicate cores randomised into a subsequent block for 8 cases where the targeted tissue

had still not been represented. A single additional TMA was constructed for 42 of the cancer site blocks, where a single 2mm core from each donor block was randomised into the further recipient block, to allow for a slightly wider margin of error with these blocks to achieve the specifically targeted tissue. There was insufficient tissue in the diagnostic biopsy specimen blocks to consider it worthwhile attempting to obtain further cores if the initial cores had not yielded adequate tissue on sectioning. A subsequent TMA was constructed comprising the diagnostic biopsy blocks (n=6) that originated from Mid Cheshire Hospitals NHS Foundation Trust (Crewe), as these were acquired later. The tissue blocks for n=5 diagnostic biopsy samples were unable to be located.

The key for the respective TMAs is detailed in table 2.1 below.

Tissue Microarray	Tissue Type	Description
A	Diagnostic Biopsy	Single core from all diagnostic biopsy blocks retrieved from Chester n=100
B		As A
C		As A & B
D		Triplicate cores from diagnostic biopsy blocks retrieved from Crewe n=6
E	Cancer Site	Single core from all cancer site blocks n=111
F		As E
G		As E & F
H		Single 2mm core from cancer site blocks not adequately represented on initial H&E examination of E, F & G n=42
I	Normal Colon	Single core from all normal colon blocks n=111
J		As I
K		As I & J
L		Triplicate cores from normal colon blocks not adequately represented on initial H&E examination of I, J & K n=29
M		Triplicate cores from normal colon blocks not adequately represented on initial H&E examination of L (or I, J & K) n=8

Table 2.1 – A description of the tissue cores incorporated into the constructed TMAs.

2.2.4 Immunohistochemical Staining

Sections were de-waxed and antigen retrieval performed using the PT Link (Dako UK Ltd, Ely, UK), with slides placed in EnVision™ FLEX target retrieval solution pH 9 (K8004, Dako) diluted to the manufacturer's instruction and at 65°C, heated to 96°C for 20 minutes, then returning to 65°C prior to the slides being washed in EnVision™ FLEX wash buffer (K8007, Dako) diluted to the manufacturer's specification for 10 minutes. The tissues sections were ringed at the edge of the slides with a hydrophobic pen to prevent stain run-off. After blocking for 5 minutes at room temperature with 100µL EnVision™ FLEX peroxidase blocking reagent (S2023, Dako), further washing was performed prior to application of 100µL of the primary antibody at the required concentration in EnVision™ FLEX antibody diluent (K8006, Dako). Negative controls consisted of antibody diluent only and a mouse IgG1 isotype control (ab91353, Abcam, Cambridge, UK) to assess for background staining. The primary antibody was incubated at room temperature for 30 minutes, before being washed, and the slides then further incubated with 100µL of an appropriate linker (mouse or rabbit, K8002 and K8009 respectively, Dako) for 15 minutes at room temperature.

The slides were then washed again prior to use of the EnVision detection system (K4065, Dako) incorporating incubation with 100µL horseradish-peroxidase (HRP) conjugated secondary antibody solution (against rabbit and mouse immunoglobulins) applied for 20 minutes at room temperature, before being developed with fresh diaminobenzidine tetrahydrochloride (DAB) solution (made according to manufacturer's instruction) which was again incubated for 20 minutes at room temperature.

Further washing was performed, before the slides were dipped in distilled water prior to counter-staining with haematoxylin for 1 minute. Excess haematoxylin was removed in a running water bath until clear, the slides were then dipped momentarily in acid alcohol before being dipped in ammonia water for 30 seconds. The slides were placed back in a running water bath for one minute, before being dehydrated through an ethanol series in a fume hood. This involved vigorous agitation for 10 seconds in x5 industrial methylated spirits and x2 xylene baths. A coverslip was then applied to each slide using DPX mountant (Sigma-Aldrich, Dorset, UK).

2.2.5 Acid Ceramidase Antibody Optimisation for Immunohistochemistry

Antibody optimisation for IHC analysis of AC was undertaken subsequent to initial attempts to optimise a primary antibody for use in Western blotting, as described in chapter 3. A different primary antibody to those used in Western blotting was demonstrated to identify AC on IHC on Protein Atlas (www.proteinatlas.org) – a rabbit polyclonal anti-ASAH1 antibody (HPA005468, Sigma-Aldrich). Given the initial difficulties in achieving antibody specificity for Western blotting, it was considered appropriate that this antibody should be attempted to be optimised for IHC, alongside the others used in Western blotting, to provide verification of antibody specificity for the IHC work, and in attempt to provide cross validation between IHC and Western blotting. The anti-ASAH1 antibodies already assessed in Western blotting were a rabbit monoclonal (ab174828, Abcam), a rabbit polyclonal (ab74469, Abcam), and a mouse monoclonal (BD612302, BD Transduction Laboratories).

Protein Atlas identified kidney and lung as positive control tissues for AC expression, therefore these were sourced from The Liverpool Tissue Bank and sections cut. Each antibody was assessed at the upper and lower concentrations as recommended by manufacturer datasheets – 1/50 and 1/100 for ab174828, 1/400 and 1/1000 for ab74469, and 1/200 and 1/500 for HPA005468. Whilst BD612302 had only a recommendation for its use in Western blotting from the manufacturer's datasheet, it had been the only antibody observed to demonstrate specificity for AC on Western blotting, therefore was assessed for use in IHC. Extrapolating data observed with all antibodies on Western blotting, this mouse monoclonal antibody was initially assessed for IHC at concentrations of 1/100 and 1/250. IHC staining of the tissue sections was performed, incorporating negative control reactions using antibody diluent only and a mouse IgG1 isotype control, as described in section 2.2.4.

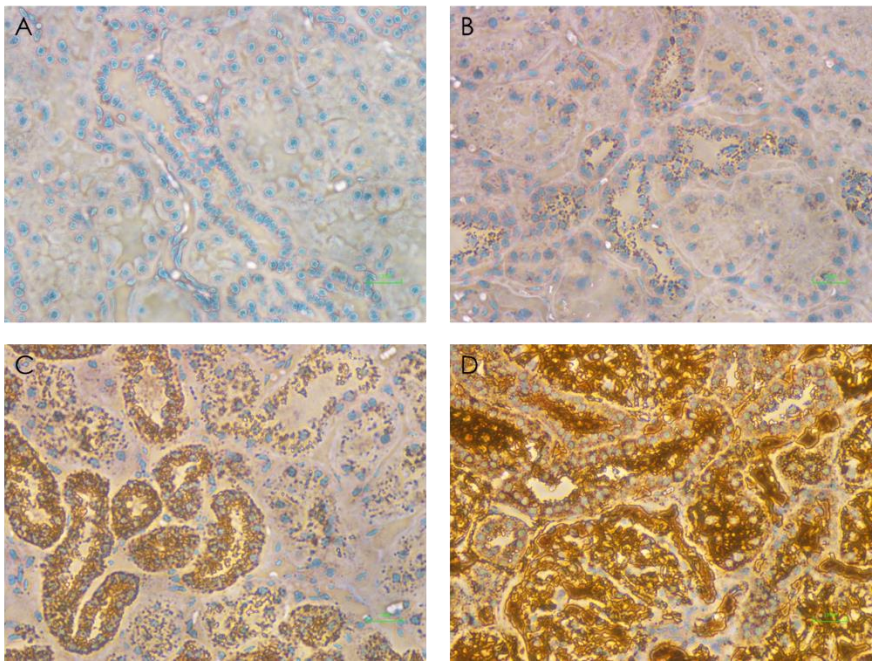

Figure 2.1 – Light microscope images of kidney sections stained for AC on IHC to facilitate antibody selection and optimisation. Images taken at x400 magnification. The brown staining in the images represents antibody binding and oxidation of DAB by HRP. The four images demonstrate the optimal results for the four anti-ASAH1 antibodies initially assessed; A) HPA005468 (Sigma-Aldrich) at 1/500, B) BD612302 (BD Transduction Laboratories) at 1/250, C) ab174828 (Abcam) at 1/100, and D) ab74469 (Abcam) at 1/1000.

Stained slides were reviewed by a consultant histopathologist (MW), where non-specific binding, as well as binding to a structural component of the cell wall was observed with ab174828 and ab74469, as can be seen in images C and D in figure 2.1. Appropriate granular cytosolic staining of the renal epithelium was observed with both HPA005468 and BD612302, which also matched the staining pattern represented on Protein Atlas. The staining pattern was equivalent to that observed in kidney across the four antibodies in the lung sections. ab174828 and ab74469 were therefore considered inappropriate to pursue for further optimisation due to their inappropriate and non-specific binding.

Further optimisation was subsequently performed with HPA005468 and BD612302 on normal colon and malignant rectal cancer tissue sections, to determine the optimal conditions with which to perform IHC staining of the TMAs. These optimisation slides and corresponding positive and negative controls were again reviewed by a consultant histopathologist (MW), who confirmed the appropriateness of the staining and advised that the optimum antibody to be used was BD612302 at a concentration of 1/500, and without

the use of a mouse linker. Images of the pertinent slides assessed in this process are demonstrated in figure 2.2 below.

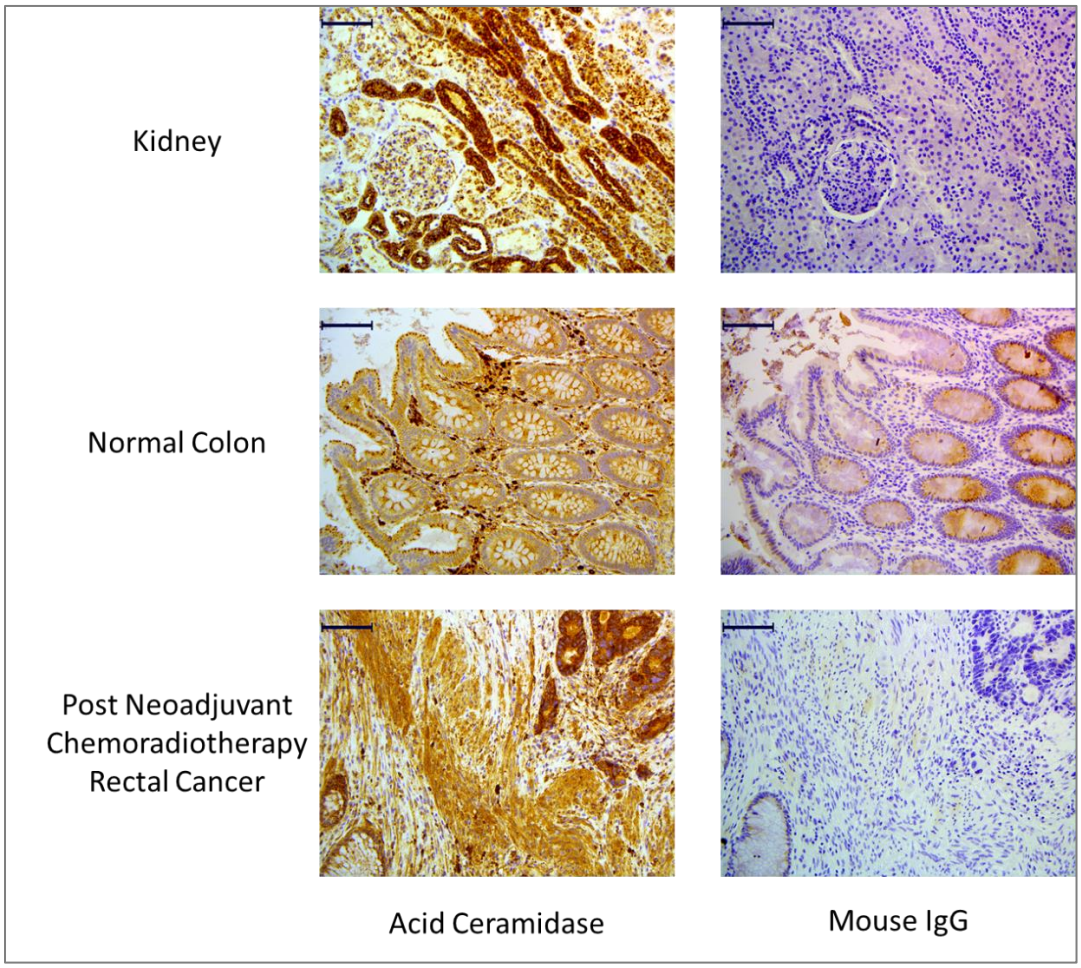

Figure 2.2 – Images of sections taken from kidney, normal colon, and rectal cancer (post-CRT) specimens, for AC antibody optimisation. The sections in the left column have been stained for AC using BD612302 mouse monoclonal antibody at a concentration of 1/500, with corresponding sections in the right column stained as a negative control. Images taken at x200 magnification, with the bar in each image representing 100µm.

Upon determination of the optimal IHC conditions for AC staining with BD612302, sections of the TMAs were cut and stained using the previously described methodology. All TMAs assessed for AC expression were stained simultaneously, alongside their respective negative controls. This staining was undertaken using the Dako Autostainer (Dako, Colorado, USA) to facilitate optimal control over the application and timing of reagent incubation on the slides.

2.2.6 Immunohistochemical Staining Analysis

Stained sections of the TMAs were assessed under light microscopy and semi-quantitative analysis for each tissue core using a simplified H-score (Allred) undertaken. The system applies a score to the percentage of positive staining cells (0-5) added to a score for the intensity of that positivity (0-3), giving a total score of 0, 2, 3, 4, 5, 6, 7 or 8 (Mohsin *et al*, 2004). The breakdown of scoring for the percentage of positive staining cells is defined as 0% = 0, <1% = 1, 1-10% = 2, 10-33% = 3, 33-66% = 4, and >66% = 5, with the intensity score defined as none = 0, weak = 1, intermediate = 2, strong = 3.

The images in figure 2.3 below demonstrate differential staining for AC and are depicted to demonstrate the H-score as was applied at each end of the scale.

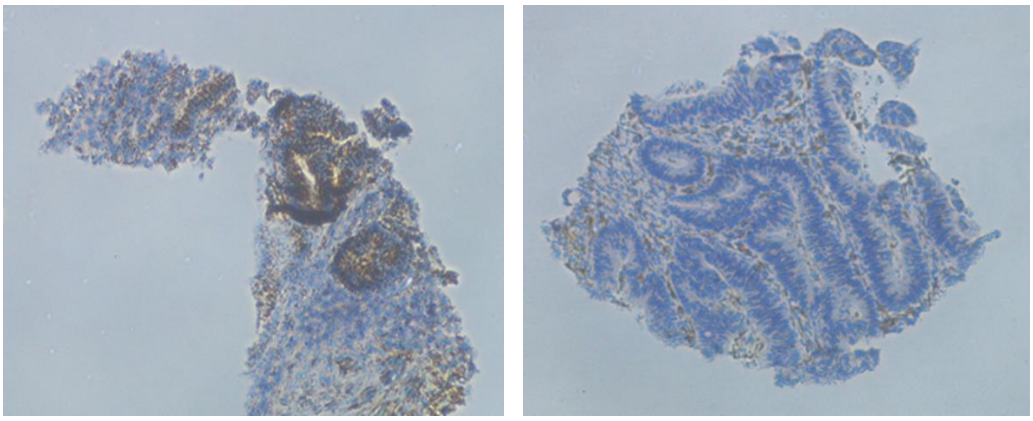

Figure 2.3 – Images of individual cores from one TMA section originating from diagnostic biopsy specimens, taken under light microscopy at x200 magnification – the sections had undergone IHC staining for AC using BD612302 primary antibody at a concentration of 1/500. Differential epithelial staining is observed between the two images. 'Background' staining can also be observed at a comparable intensity and distribution in non-epithelial cells in both images, representing uptake by plasma cells and macrophages and potential stromal cells. Strong staining in the vast majority of epithelial cells in the left-hand image (H score = 5 + 3 = 8) is observed in a case where a poor response to CRT was assigned to the resection specimen (TRG 1). The right-hand image demonstrates no epithelial staining (H score = 0 + 0 = 0) in a case where a subsequent pCR was observed (TRG 4).

An epithelial score and a stromal score was assigned individually for each tissue type where both tissue subsets were present. The scores for each tissue subset and type (i.e. epithelium and stroma in diagnostic biopsy, normal colon, and cancer site) were dichotomised about the median score for that group to determine relatively high versus relatively low expression

of AC for the purposes of statistical analysis. Scoring was undertaken by consultant histopathologist (MW) and I individually, with differences resolved by consensus in order to reduce intra-observer error.

2.2.7 Clinical and Pathological Data

The TMAs were complimented by the collection of a clinical dataset, in order to glean prognostic information that could be analysed against the IHC findings. Data was gathered from computerised patient records at The Countess of Chester NHS Foundation Trust. Information regarding gender, age, radiological staging (pre- and post-neoadjuvant treatment), tumour site (low, mid or high rectum), operation undertaken and timing, histopathological findings (*yp*TNM staging, EMVI, CRM positivity, KRAS status), adjuvant treatment, and stoma rates were collected, as were follow up data to investigate overall- and disease-free survival.

2.2.8 Statistical Analysis

Statistical analysis was undertaken using SPSS® Statistics version 22 (IBM®, New York, USA). Interpretation of the IHC staining of the TMAs was performed by dichotomising the scores for each tissue group about the median value to distinguish between relatively low and relatively high expression. This categorical data was analysed against TRG groupings using the Pearson chi-square test. Correlation of AC expression with the incidence of locally recurrent and metastatic disease, was performed using Fisher's exact test as the expected counts were lower. Kaplan-Meier analysis was used to correlate TRG with survival.

2.3 Results

The median age at diagnosis for the patients in the study was 66 (33-86). There were 82 males (74%) and 29 females (26%). The clinical and pathological data pertaining to these patients is demonstrated in appendix B.

2.3.1 Assessment of Tumour Regression Grading

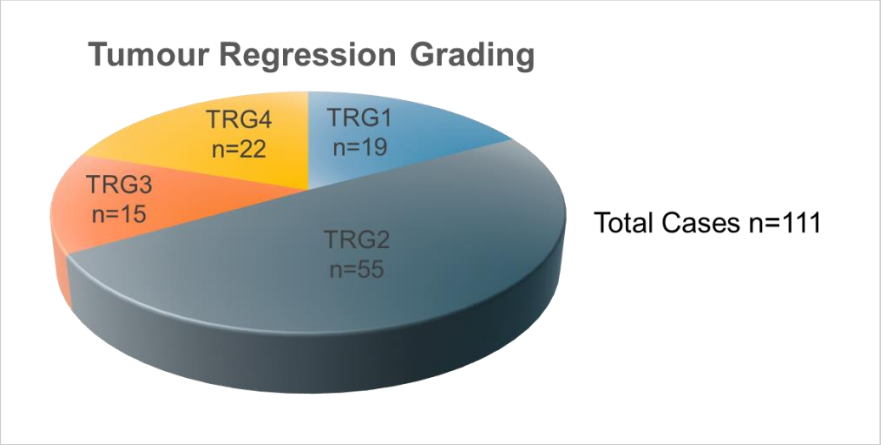

Figure 2.4 – Pie chart demonstrating the groupings of the cases identified, according to the four tier (Ryan) TRG system as recommended by The Royal College of Pathologists.

22/111 (19.9%) of the assessed cases were grouped as TRG 4 (no viable tumour cells, fibrosis or mucus lakes only), and therefore were considered to have achieved a pCR. When combined with the 15 cases (13.5%) that were assessed as TRG 3 (single cells or scattered small groups of cancer cells), 37/111 (33.3%) of cases overall are considered to represent relative responders (TRG 4&3) to neoadjuvant CRT. The greatest number of cases (55/111, representing 49.5%) were assigned as TRG 2 (residual cancer outgrown by fibrosis), with the remaining 19/111 (17.1%) of cases demonstrating TRG 1 (minimal or no regression, extensive residual tumour).

2.3.2 Diagnostic Biopsy Tissue Microarrays

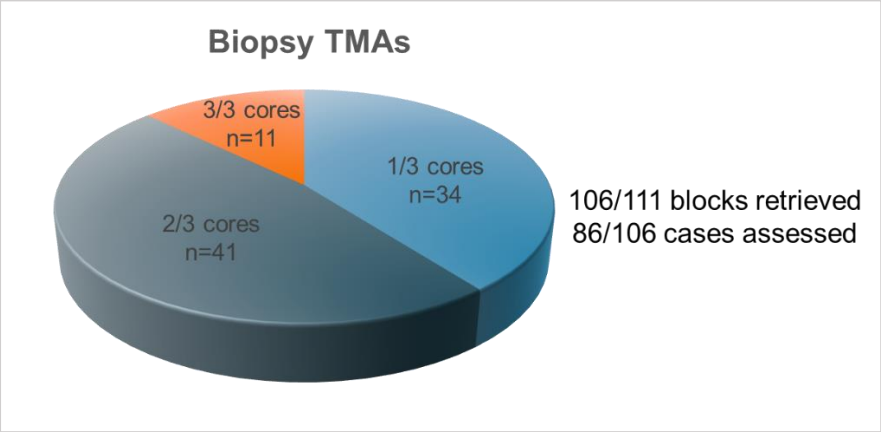

Figure 2.5 – Pie chart demonstrating the number of tissue cores originating from the diagnostic biopsy specimens considered as adequate and scored for AC expression, subsequent to TMA construction, sectioning and IHC staining.

As demonstrated in figure 2.5 106/111 (95.5%) of the tissue blocks for the diagnostic biopsy specimens for the identified cases were retrieved from archived storage and incorporated into the TMAs. Four of the tissue blocks were located in other hospitals, from where it was not possible to retreive them in a timely manner, and the last tissue block was not present in its designated location in storage, and was unable to be found.

Subsequent to TMA construction, sectioning and IHC staining, 86 of the 106 cases (81.1%) demonstrated at least one adequate tissue core that was assessed for AC expression in both epithelium and stroma. Only 11 cases (10.4%) yielded all three cores that were considered adequate for staining assessment, and a total number of 149/318 (46.9%) of the originally transferred cores from the diagnostic biopsy specimens were represented in the final analysis.

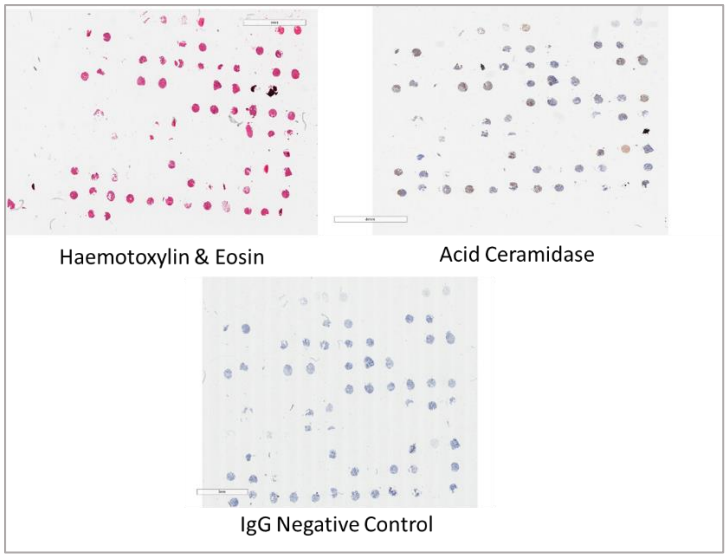

Figure 2.6 - Images of three sections from TMA A (representing cores from diagnostic biopsy specimens) having been stained for H&E, AC (using BD 612302 at a concentration of 1/500), and with mouse IgG as a negative control.

The whole slide sections of TMA A depicted in figure 2.6 are indicative of the coverage achieved with cores from the diagnostic biopsy specimens, both within and between sections, having been stained as described in section 2.2.4. The H&E slide was stained and assessed individually initially to ascertain coverage. Variablility in the brown DAB staining for AC expression can be observed, compared with an absence of staining with the mouse IgG negative control across the whole slide.

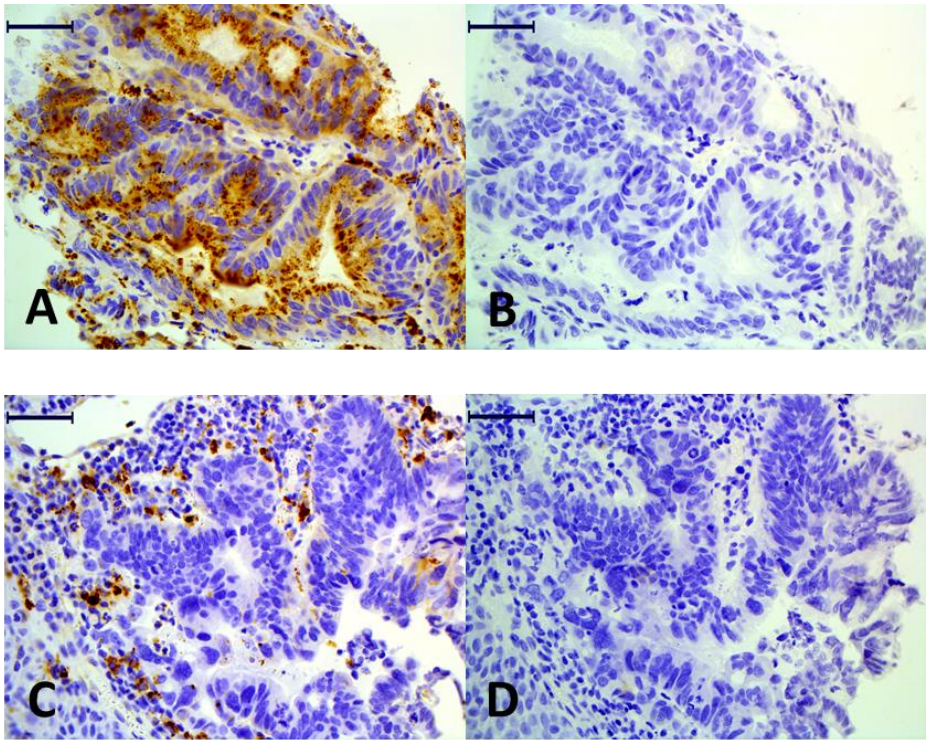

Figure 2.7 - Images of selected diagnostic biopsy TMA cores. The cores were both observed from one section of TMA A, having been stained for AC (A&C), with the corresponding cores (B&D) from another section exposed to a mouse IgG isotype as a negative control. The rectangular bar in each image represents 50μm.

The core marked A in figure 2.7 demonstrates higher epithelial (H-score = 5+3 = 8) and stromal (H-score = 5+2 = 7) expression of AC, in a case where a minimal response to CRT (TRG 2) was assigned to the resection specimen. Lower epithelial (H-score = 1+1 = 2) and stromal expression (H-score = 0+0 = 0) of AC is demonstrated in the core marked C, in a case where a subsequent pCR (TRG 4) was observed. No inappropriate staining is observed in the negative control cores, and the intensity of the background H&E staining is comparable across the cores.

Diagnostic Biopsy TMAs - Epithelial Acid Ceramidase Immunohistochemical Scoring																
Patient	A	B	C		D		Mean	Patient	A	B	C		D		Mean
1	5	6	4				5.0	57		6					6.0
2		8	7				7.5	58	4						4.0
3	5						5.0	59		8	7				7.5
4	0						0.0	60	3		7				5.0
5		7					7.0	61	4		6				5.0
6		3	0				1.5	62		7					7.0
7								63	7		0				3.5
8								64	0		7				3.5
9								65		6					6.0
10	2	3					2.5	66			0				0.0
11	0	0					0.0	67	5	5	5				5.0
12	6	7					6.5	68	7	2					4.5
13								69		2	6				4.0
14								70	4	6					5.0
15	0						0.0	71	0	4					2.0
16								72			6				6.0
17	0	0					0.0	73		8	8				8.0
18								74	0						0.0
19								75	0						0.0
20								76	5		5				5.0
21		8					8.0	77							
22	2	4					3.0	78	5	5	5				5.0
23					0		0.0	79	0						0.0
24								80							
25	0						0.0	81			7				7.0
26								82							
27		0					0.0	83	4						4.0
28	8	7	8				7.7	84				7	6		6.5
29	0	5	6				3.7	85		4					4.0
30	7		4				5.5	86	4						4.0
31		7					7.0	87	2	3	0				1.7
32								88							
33	0		4				2.0	89							
34		0	7				3.5	90	8	8					8.0
35	3						3.0	91							
36	4	5					4.5	92							
37		7					7.0	93	4	3					3.5
38								94	8	6					7.0
39	2		7				4.5	95	7						7.0
40	7	6					6.5	96	3	6					4.5
41		7					7.0	97	4						4.0
42	8	5	7				6.7	98				7	4		5.5
43	3	3	3				3.0	99							
44								100							
45	7	4					5.5	101		6	4				5.0
46	3	7					5.0	102	7	0					3.5
47			7				7.0	103							
48		7					7.0	104		8	7				7.5
49		7	6				6.5	105		5					5.0
50	2	3	4				3.0	106	6	6	7				6.3
51	4		7				5.5	107			7				7.0
52	3		0				1.5	108		0	5				2.5
53	0						0.0	109		5					5.0
54	0	4	7				3.7	110					5		5.0
55								111	3		3				3.0
56				0	2		1.0								

Table 2.2 – H scores observed upon assessment of epithelial AC expression in diagnostic biopsy tissue. The crude H score is presented for each tissue core adequately present on TMAs A, B, C & D, in association with the calculated mean H score for each patient.

Diagnostic Biopsy TMAs - Stromal Acid Ceramidase Immunohistochemical Scoring																
Patient	A	B	C		D		Mean	Patient	A	B	C		D		Mean
1	3	3	0				2.0	57		8					8.0
2		4					4.0	58	4						4.0
3	5						5.0	59			7				7.0
4	3						3.0	60	4		6				5.0
5		2					2.0	61	7		7				7.0
6		2					2.0	62		2					2.0
7								63	5						5.0
8								64	4		6				5.0
9								65		5					5.0
10	0	5					2.5	66			0				0.0
11	5	2					3.5	67	5	6					5.5
12	6	7					6.5	68	5	6					5.5
13								69		7	6				6.5
14								70	6	5					5.5
15	0						0.0	71	5	4					4.5
16								72			4				4.0
17	2	2					2.0	73		7	7				7.0
18								74	5						5.0
19								75	4						4.0
20								76	5		6				5.5
21		3					3.0	77							
22	7	7					7.0	78	4	7	4				5.0
23					0		0.0	79	5						5.0
24								80							
25	3						3.0	81			2				2.0
26								82							
27		7					7.0	83	0						0.0
28	7	5	7				6.3	84				6	6		6.0
29	5	6	6				5.7	85		5					5.0
30	6		4				5.0	86	0						0.0
31		7					7.0	87	0	4	6				3.3
32								88							
33	0		6				3.0	89							
34		5	8				6.5	90	0	7					3.5
35	0						0.0	91							
36	6	6					6.0	92							
37		6					6.0	93	7	6					6.5
38								94	7	6					6.5
39	3						3.0	95	4						4.0
40	5	5					5.0	96	7	7					7.0
41		7					7.0	97	5						5.0
42	8	6	7				7.0	98				7	7		7.0
43	5	4	0				3.0	99							
44								100							
45	5	5					5.0	101		8	7				7.5
46	2	5					3.5	102	7	6					6.5
47			4				4.0	103							
48		7					7.0	104		8	7				7.5
49		7	2				4.5	105		6					6.0
50	4	7	0				3.7	106	2	6	2				3.3
51	5		7				6.0	107			8				8.0
52	4		4				4.0	108		2	3				2.5
53	6						6.0	109		5					5.0
54	4	6	2				4.0	110					7		7.0
55								111	4		5				4.5
56				4	7		5.5								

Table 2.3 – H scores observed upon assessment of stromal AC expression in diagnostic biopsy tissue. The crude H score is presented for each tissue core adequately present on TMAs A, B, C & D, in association with the calculated mean H score for each patient.

The median H-score for AC staining in diagnostic biopsy epithelium was 5.0. There were no statistically significant correlations between a relatively high or low AC expression with either a pCR, a relative response or a poor response to neoadjuvant CRT (p=0.695, p=0.699, and p=0.375 respectively).

The median H-score for AC staining in stromal cells in diagnostic biopsy specimens was also 5.0, and there were again no statistically significant correlations between AC expression with TRG by groupings (p=0.472 and p=0.764 for pCR and relative response respectively). Eleven of the nineteen patients categorised as having a poor response to neoadjuvant CRT (TRG 1) had tissue represented on analysis of the diagnostic biopsy TMAs - 9/11 of these cases demonstrated a relatively high stromal AC expression but this did not quite reach statistical significance (p=0.075).

There were no statistically significant correlations between AC expression in either epithelial or stromal tissue from the diagnostic biopsy and the risk of recurrent disease, metastatic disease or overall survival.

2.3.3 Cancer Site Tissue Microarrays

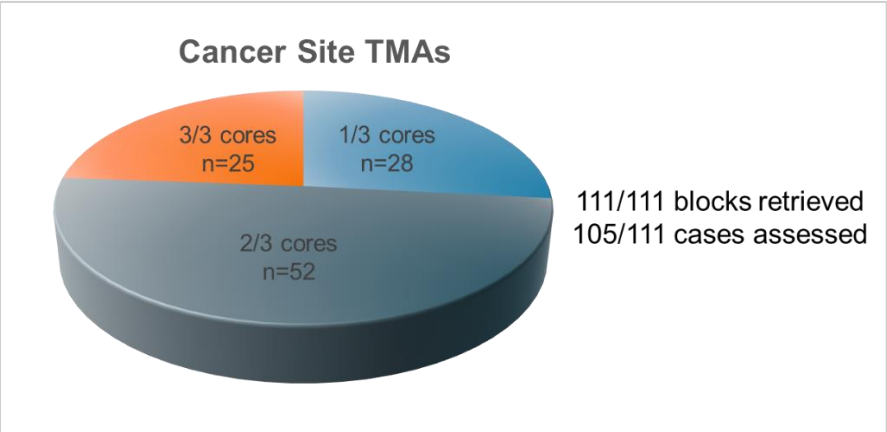

Figure 2.8 – Pie chart demonstrating the number of tissue cores originating from the cancer site specimens considered as adequate and scored for AC expression, subsequent to TMA construction, sectioning and IHC staining.

An appropriate tissue block representing the cancer site was retrieved for all 111/111 of the identified cases (100%), as demonstrated in figure 2.8. After TMA construction, sectioning and IHC staining, 105 of these cases (94.6%) produced at least one core that was considered adequate to assess for AC staining in the stroma. 207/333 (62.2%) of the originally transferred cores were represented in the final analysis. 22 of the resection specimens had been observed to demonstrate a pCR, and therefore were devoid of malignant epithelium – 68 of the 89 potential cases (76.4%) where malignant cancer site epithelium was possible to have been demonstrated in the finally sectioned TMAs, were considered to have yielded at least one adequate core that was analysed.

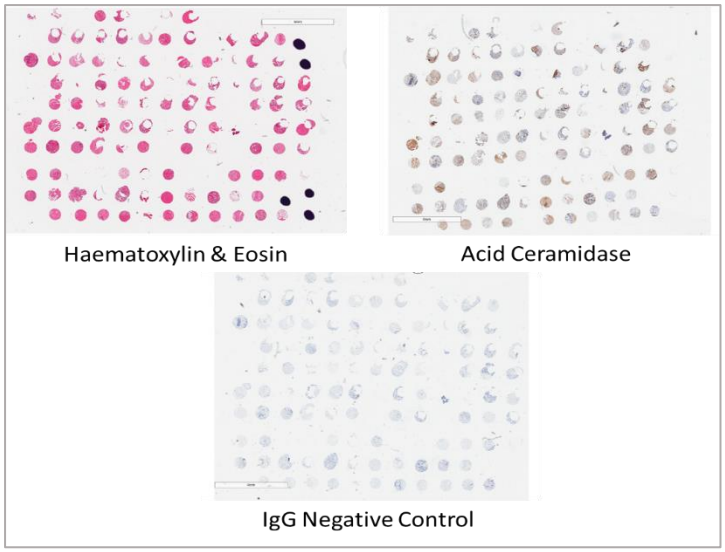

Figure 2.9 - Images of three sections from TMA E (representing cores from the cancer site from resection specimens) having been stained for H&E, AC (using BD 612302 at a concentration of 1/500), and with mouse IgG as a negative control.

The whole slide sections of TMA E depicted in figure 2.9 are indicative of the coverage achieved with the cancer site cores from the resection specimens, both within and between sections, having been stained as described in section 2.2.4. The H&E slide was stained and assessed individually initially to ascertain coverage. Variablility in the brown DAB staining for AC expression can be observed, compared with an absence of staining with the mouse IgG negative control across the whole slide.

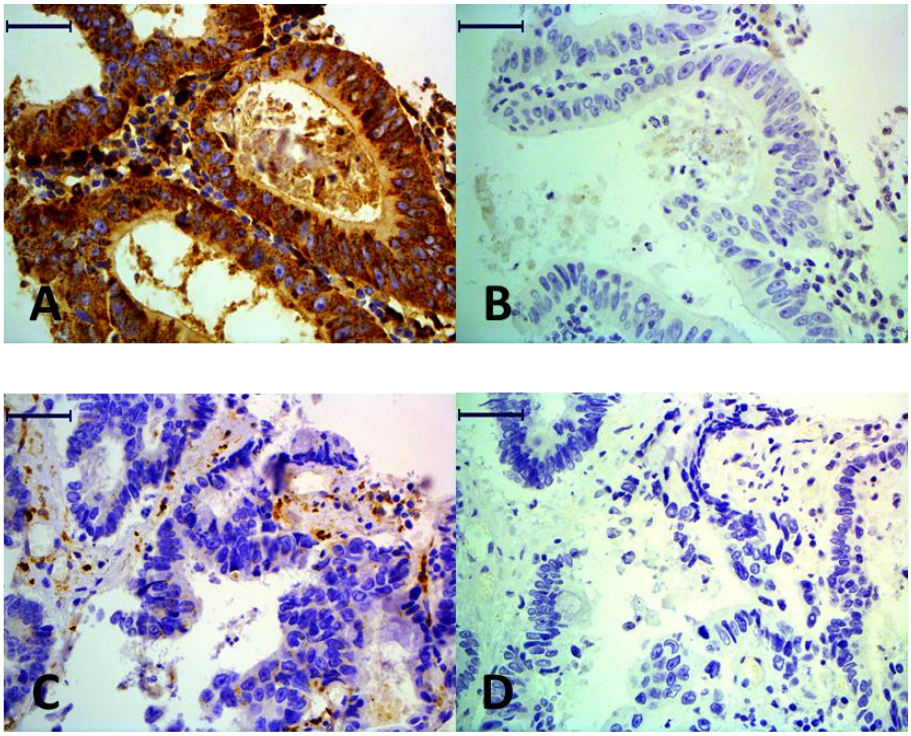

Figure 2.10 - Images of selected cancer site TMA cores from the resection specimens. The cores were both observed from the same section of TMA E, having been stained for AC (A&C), with the corresponding cores (B&D) from another section exposed to a mouse IgG isotype as a negative control. The rectangular bar in each image represents 50µm.

The core marked A in figure 2.10 demonstrates higher epithelial (H-score = 5+3 = 8) and stromal (H-score = 5+2 = 7) expression of AC, in a case where a poor response to CRT (TRG 1) was observed. Lower epithelial (H-score = 0+0 = 0) but higher stromal expression (H-score = 3+2 = 5) of AC is demonstrated in the core marked C in a case with a minimal response to CRT (TRG 2). No inappropriate staining is observed in the negative control cores, and the intensity of the background H&E staining is comparable across the cores.

Cancer Site TMAs - Epithelial Acid Ceramidase Immunohistochemical Scoring												
	Patient	E	F	G	H	Mean	Patient	E	F	G	H	Mean
	1		8			8.0	**57**	4		5		4.5
	2						**58**					
	3						**59**	6	4			5.0
	4	6			6	6.0	**60**					
	5				5	5.0	**61**			5		5.0
	6						**62**					
	7	5	0			2.5	**63**	5		6		5.5
	8				7	7.0	**64**				7	7.0
	9		8	4		6.0	**65**	6		6		6.0
	10						**66**	4		0		2.0
	11	7		2		4.5	**67**			7		7.0
	12						**68**					
	13						**69**	0	0			0.0
	14						**70**	4	3			3.5
	15			6		6.0	**71**					
	16	5		6		5.5	**72**					
	17	8		0	6	4.7	**73**					
	18	5				5.0	**74**					
	19		4			4.0	**75**	5				5.0
	20	5			4	4.5	**76**	5		3		4.0
	21						**77**	4		0	4	2.7
	22				5	5.0	**78**				6	6.0
	23	5		0		2.5	**79**	7	8	6		7.0
	24						**80**					
	25	6		5	6	5.7	**81**					
	26						**82**				6	6.0
	27	7		8		7.5	**83**					
	28						**84**	5	4			4.5
	29			2	6	4.0	**85**					
	30						**86**					
	31		7			7.0	**87**					
	32	7				7.0	**88**	8		7		7.5
	33						**89**	7	6			6.5
	34						**90**					
	35						**91**	7	8	7		7.3
	36						**92**	5		6		5.5
	37						**93**	0				0.0
	38	6				6.0	**94**	8	7			7.5
	39		5	7	7	6.3	**95**	5		7	6	6.0
	40						**96**	5	6	6		5.7
	41			7	8	7.5	**97**	4				4.0
	42						**98**					
	43						**99**	6			2	4.0
	44	6		6		6.0	**100**	4	6			5.0
	45						**101**	6	4	5		5.0
	46		0	2		1.0	**102**	4			5	4.5
	47		7			7.0	**103**					
	48	6		7		6.5	**104**				6	6.0
	49	3				3.0	**105**	6	7			6.5
	50						**106**	0		2		1.0
	51	0		3	0	1.0	**107**	7		6		6.5
	52	5			7	6.0	**108**					
	53						**109**			0		0.0
	54	8				8.0	**110**		5			5.0
	55	0	0	3		1.0	**111**	3		3		3.0
	56	0	3			1.5						

Table 2.4 - H scores observed upon assessment of epithelial AC expression in post-CRT cancer site tissue. The crude H score is presented for each tissue core adequately present on TMAs E, F, G & H, in association with the calculated mean H score for each patient.

Cancer Site TMAs - Stromal Acid Ceramidase Immunohistochemical Scoring												
Patient	E	F	G	H	Mean	Patient	E	F	G	H	Mean
1	6	3			4.5	**57**	5		6		5.5
2	2		0	5	2.3	**58**			0		0.0
3	7	0			3.5	**59**	5	5			5.0
4	2			5	3.5	**60**	2				2.0
5	4	5		6	5.0	**61**		2	6		4.0
6		0			0.0	**62**					
7	4	5			4.5	**63**	4		6		5.0
8	6	6		5	5.7	**64**	7			7	7.0
9	2	4	0	0	1.5	**65**	6		5		5.5
10	0		4		2.0	**66**	6		5		5.5
11	3		6		4.5	**67**			5		5.0
12						**68**			4		4.0
13	6				6.0	**69**	4	7			5.5
14				5	5.0	**70**	6	6			6.0
15			4		4.0	**71**	4		0		2.0
16	2		0		1.0	**72**	5		2		3.5
17	7		2	2	3.7	**73**					
18	3	2	2		2.3	**74**	3				3.0
19		0			0.0	**75**	4				4.0
20	2			3	2.5	**76**	4		0		2.0
21	5				5.0	**77**	6		3	3	4.0
22	3			3	3.0	**78**			2	7	4.5
23	7		7		7.0	**79**		4	4		4.0
24	4			4	4.0	**80**	4	0	4		2.7
25	7		3	7	5.7	**81**	3		4		3.5
26			3		3.0	**82**				2	2.0
27	4		7	7	6.0	**83**	7			6	6.5
28			2	3	2.5	**84**	8	5			6.5
29			2	5	3.5	**85**	0		2		1.0
30	5				5.0	**86**		4			4.0
31	4	0			2.0	**87**	3				3.0
32	4		5		4.5	**88**	7		2		4.5
33	2				2.0	**89**		6			6.0
34						**90**					
35	2			3	2.5	**91**	5	2	6		4.3
36	3				3.0	**92**			6		6.0
37	0				0.0	**93**	6				6.0
38	6		2		4.0	**94**	7	7			7.0
39	4	2	5	6	4.3	**95**	3		3	8	4.7
40	4		5		4.5	**96**	6	3	6		5.0
41	5		6	6	5.7	**97**	2				2.0
42	6	7	0	7	5.0	**98**			4		4.0
43	2		2		2.0	**99**	4		3	5	4.0
44	3				3.0	**100**	6	6			6.0
45	3	0			1.5	**101**		3	4		3.5
46	2	2	4		2.7	**102**	5			4	4.5
47	5	4	6		5.0	**103**	7		3		5.0
48	3		5		4.0	**104**	6		6	7	6.3
49	5				5.0	**105**	4	4			4.0
50	6				6.0	**106**	4		8		6.0
51			6	5	5.5	**107**	6		4		5.0
52	3		0	2	1.7	**108**	8				8.0
53						**109**			0		0.0
54	0				0.0	**110**	5		3		4.0
55	7	3	7		5.7	**111**	2		2		2.0
56	6	2			4.0						

Table 2.5 – H scores observed upon assessment of stromal AC expression in post-CRT cancer site tissue. The crude H score is presented for each tissue core adequately present on TMAs E, F, G & H, in association with the calculated mean H score for each patient.

The median H-score for AC expression in malignant epithelium at the cancer site was 5.5. There was no statistically significant correlation between AC expression with either a relative response or a poor response to neoadjuvant CRT (p=0.506 and p=0.487 respectively).

The median H-score for AC expression in stromal cells at the cancer site was 4.0. 18/22 of the patients where a pCR was observed had a relatively low stromal expression of AC (p=0.003). A relatively low stromal expression was also statistically significantly correlated with relative responders (TRG 4&3) to neoadjuvant CRT (p=0.048). Conversely 13/18 of the assessed tissue samples where a poor response to treatment had been observed (TRG 1), had a relatively high stromal expression of AC (p=0.017).

The incidence of local recurrence varied significantly according to relative expression of AC at the cancer site in both stroma and epithelium. Across all cases where a stromal expression of AC was observed, 6/49 patients with a relatively high expression developed local recurrence, compared to 1/56 with a relatively low expression (p=0.038). In the context of an absence of a pCR, local recurrence occurred in 5/35 patients with a relatively high epithelial expression of AC, compared to 0/33 with a relatively low expression (p=0.031). There was no correlation between cancer site expression of AC in either epithelium or stroma with metastatic disease or survival.

2.3.4 Normal Colon Tissue Microarrays

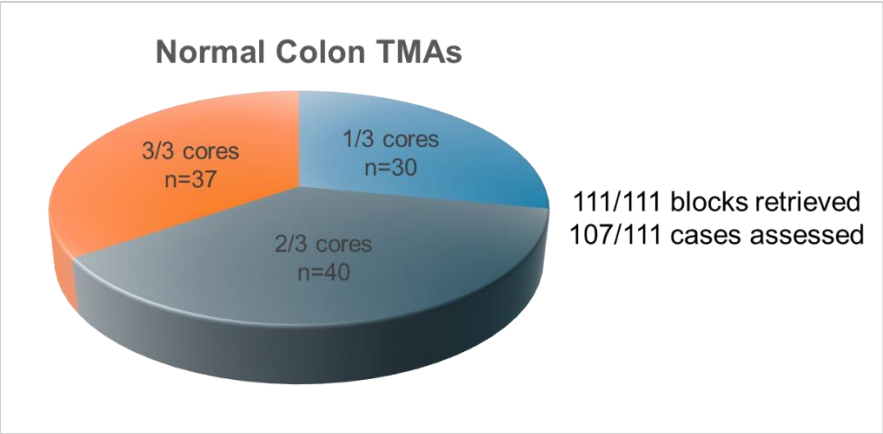

Figure 2.11 - Pie chart demonstrating the number of tissue cores originating from the normal colon specimens considered as adequate and scored for AC expression, subsequent to TMA construction, sectioning and IHC staining.

A tissue block demonstrating normal colonic epithelium was identified and retrieved for all 111/111 cases (100%). The subsequently constructed TMAs yielded the greatest number of adequate cores that were assessed for IHC staining for AC - 221/333 (66.4%), representing 107/111 (96.4%) of the overall cases. It was considered (by MW) that most of these cores were devoid of stromal tissue, and therefore only an epithelial score of AC expression was assigned.

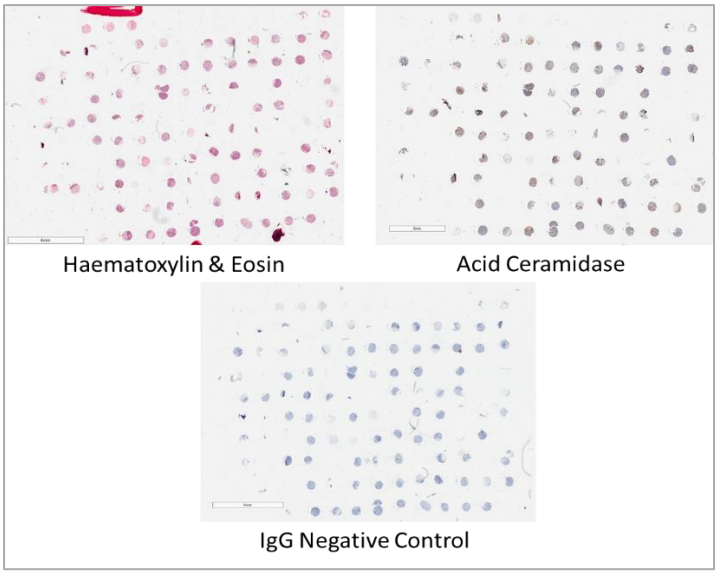

Figure 2.12 - Images of three sections from TMA I (representing cores from normal colon from resection specimens), having been stained for H&E, AC (using BD 612302 at a concentration of 1/500), and with mouse IgG as a negative control.

The whole slide sections of TMA I depicted in figure 2.12 are indicative of the coverage achieved with the cores of normal colon from the resection specimens, both within and between sections, having been stained as described in section 2.2.4. The H&E slide was stained and assessed individually initially to ascertain coverage. Variablility in the brown DAB staining for AC expression can be observed, compared with an absence of staining with the mouse IgG negative control across the whole slide.

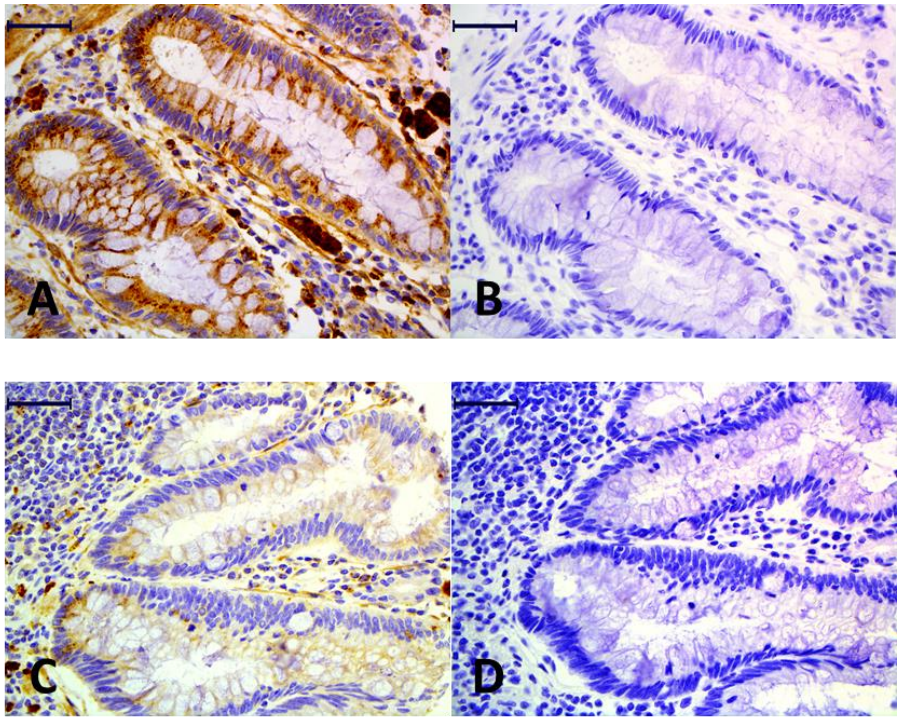

Figure 2.13 - Images of selected TMA cores of normal colon from the resection specimens. The cores were observed from the same section of TMA I, having been stained for AC (A&C), with the corresponding cores (B&D) from another section exposed to a mouse IgG isotype as a negative control. The rectangular bar in each image represents 50µm.

The core marked A in figure 2.13 demonstrates higher epithelial expression of AC (H-score = 5+3 = 8) in a case where a poor response to CRT (TRG 1) was assigned to the resection specimen. Lower epithelial expression of AC is observed in the core marked C (H-score = 2+1 = 3), in a case where a good response to CRT (TRG 3) was assigned to the resection specimen. No inappropriate staining is observed in the negative control cores, and the intensity of the background H&E staining is comparable across the cores.

Normal Colon TMAs - Epithelial Acid Ceramidase Immunhistochemical Scoring																					
Patient	I	J	K	L			M			Mean	Patient	I	J	K	L			M			Mean
1	7									7.0	**57**	7	7								7.0
2	7	6	6							6.3	**58**				7		6				6.5
3	4		7							5.5	**59**	6	7								6.5
4						6				6.0	**60**	7	7								7.0
5		6	6							6.0	**61**		6								6.0
6		7	7	7						7.0	**62**	6			7	7					6.7
7	7	6								6.5	**63**			6							6.0
8	7	6								6.5	**64**	3									3.0
9	5						7	7		6.3	**65**							7			7.0
10		7					6	7	6	6.5	**66**	5	5								5.0
11					8	6				7.0	**67**		7	6							6.5
12	6									6.0	**68**						8				8.0
13	7		7							7.0	**69**	6	5				6				5.7
14	5	6	7							6.0	**70**		7								7.0
15		6								6.0	**71**	7	7	7							7.0
16	6	6	5							5.7	**72**	6	6								6.0
17			6							6.0	**73**	7									7.0
18	7		6							6.5	**74**	8	7	6							7.0
19	6	6	7							6.3	**75**	6	7								6.5
20			6	7	6	7				6.5	**76**	7	7								7.0
21	5									5.0	**77**										
22	5		7							6.0	**78**	7	6	7				7	7		6.8
23	6		6							6.0	**79**	5	6								5.5
24	6									6.0	**80**	7			7		7				7.0
25	7	7	7							7.0	**81**	8									8.0
26	6	6	6							6.0	**82**	7									7.0
27			6							6.0	**83**	7	7								7.0
28			8				8	8		8.0	**84**	5	7	6				7	8		6.6
29		6	6							6.0	**85**	5	6	7							6.0
30	6	7	6			7				6.5	**86**				7		7				7.0
31	5	4								4.5	**87**	5		6							5.5
32											**88**		6	6							6.0
33		7								7.0	**89**			8							8.0
34		6								6.0	**90**		7	8							7.5
35	7	6	4							5.7	**91**	8	7								7.5
36	5		6							5.5	**92**	7		7							7.0
37	7				8	6				7.0	**93**	7		6							6.5
38	7	7	7							7.0	**94**	8			7	7					7.3
39	6									6.0	**95**			7							7.0
40	6									6.0	**96**			7	7	7	7				7.0
41	7	7	6							6.7	**97**	8									8.0
42	6	5	5							5.3	**98**	6									6.0
43	3									3.0	**99**										
44							8	8		8.0	**100**	8	8	7							7.7
45	7	7	7							7.0	**101**	7					7				7.0
46	7		7							7.0	**102**		7			8	7				7.3
47				6						6.0	**103**	7		6							6.5
48	6	5	6							5.7	**104**	8	7	8							7.7
49	7		7							7.0	**105**	7	7	7							7.0
50		6								6.0	**106**	6	8	7							7.0
51	6		6							6.0	**107**										
52	5	7	6							6.0	**108**	6	6	6							6.0
53	6		6							6.0	**109**	8	7	7							7.3
54						7				7.0	**110**						7				7.0
55				7		7				7.0	**111**	7		7							7.0
56		7	7							7.0											

Table 2.6 - H scores observed upon assessment of epithelial AC expression in normal colon tissue. The crude H score is presented for each tissue core adequately present on TMAs I, J, K, L & M, in association with the calculated mean H score for each patient.

The median H-score for AC expression in normal colonic epithelium obtained from the resection specimen was 6.5. There was no correlation between AC expression and either a pCR or a relative response to treatment (p=0.816 and p=0.196 respectively). 14/19 of the assessed tissue cores from patients where a poor response to treatment (TRG 1) had been observed, were found to have a relatively high expression of AC (p=0.012).

There was no correlation between epithelial AC expression in this tissue with the risk of local recurrence or metastatic disease but there was significant correlation between expression and survival. The estimated mean survival in those with a relatively high expression (n=51) was 89.7 months (95% CI 80.7 - 98.8), which was significantly longer (p=0.013, Mantel-Cox) than those with a relatively low expression (n=56), where estimated mean survival was 71.9 months (95% CI 61.5 - 82.3).

2.3.5 Quality Assessment of Tissue Microarray Staining

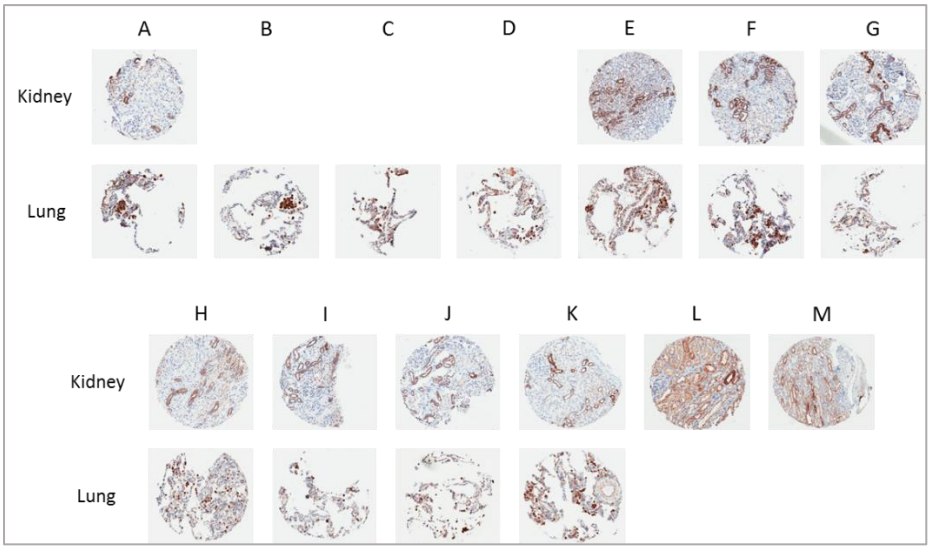

Figure 2.14 - Images of cores of the positive control tissue (kidney and lung) randomised into each TMA constructed (A-M). The cores demonstrate IHC staining for AC and have been observed from the identical sections as those used to score for AC expression in the tissues of interest.

All the present positive control tissue cores as depicted in figure 2.14, achieved the maximal H score of 5+3 = 8 for epithelial staining upon assessment. Cores of kidney tissue were not present for assessment from TMAs B, C & D, and cores of lung tissue were not present for

assessment from TMAs L & M. At least one positive control tissue core was present and assessed for each TMA and represents the best comparison of staining across all TMAs.

2.3.6 Patient Survival Analysis

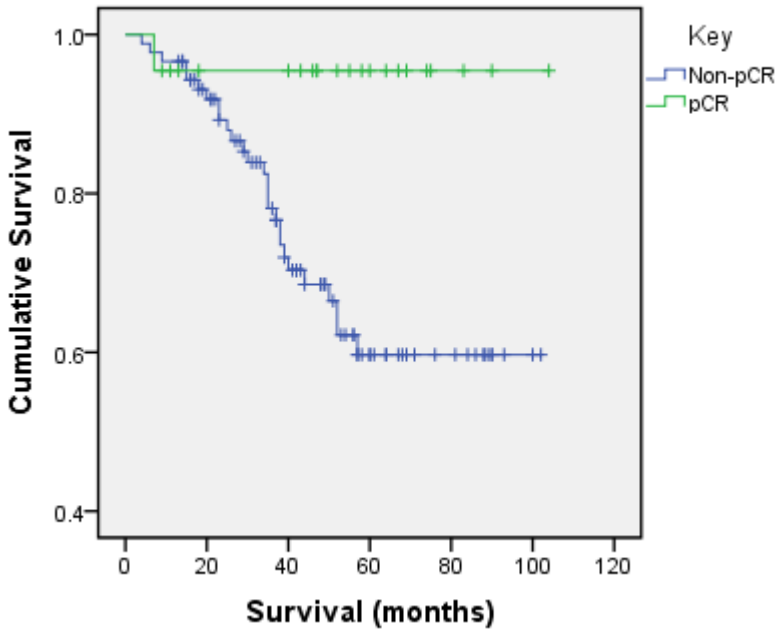

Figure 2.15 - Kaplan-Meier curves demonstrating post-operative survival in months in the patient cohort in this study (n=111), comparing those patients where a pCR (TRG 4, green line n=22) had been observed, against those patients without a pCR (TRG 3/2/1, blue line, n=89).

The estimated mean post-operative survival in this patient cohort where a pCR had been observed (n=22) was 99.6 months (95% CI 91.1 – 108.0), as depicted in figure 2.15. This was significantly better when compared to non-pCR patients (n=89), where the estimated mean survival was 74.5 months (95% CI 66.2 – 82.8, p=0.015, Mantel Cox).

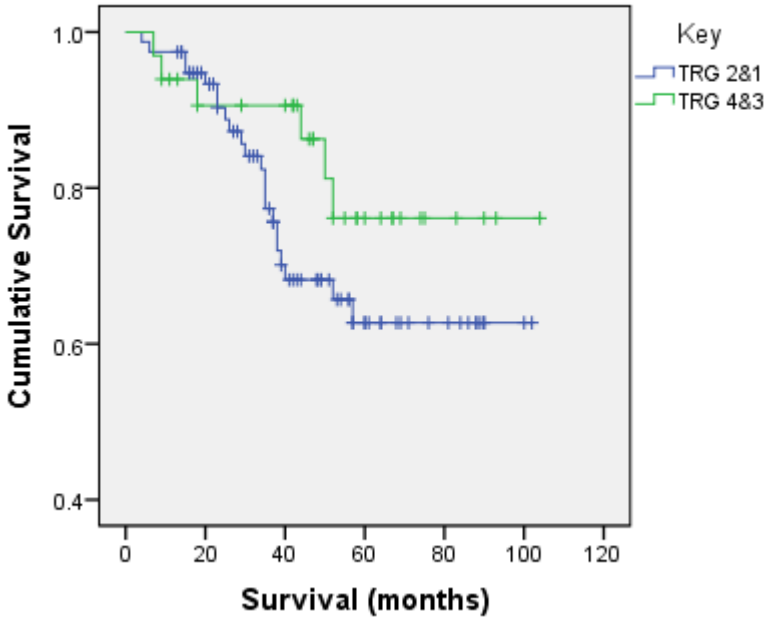

Figure 2.16 - Kaplan-Meier curves demonstrating post-operative survival in months in the patient cohort in this study (n=111), comparing those patients considered to be relative responders to neoadjuvant CRT (TRG 4/3, green line n=37), against those patients considered to be relative non-responders (TRG 2/1, blue line, n=74).

The estimated mean post-operative survival in these patients defined to be relative responders to neoadjuvant CRT (TRG 4/3, n=37) was 87.3 months (95% CI 75.5 – 99.2). This is not statistically significantly better (p=0.182, Mantel Cox) when compared against the group defined to be relative non-responders (TRG 2/1, n=74), where the estimated mean survival was 76.0 months (95% CI 67.2 – 84.9).

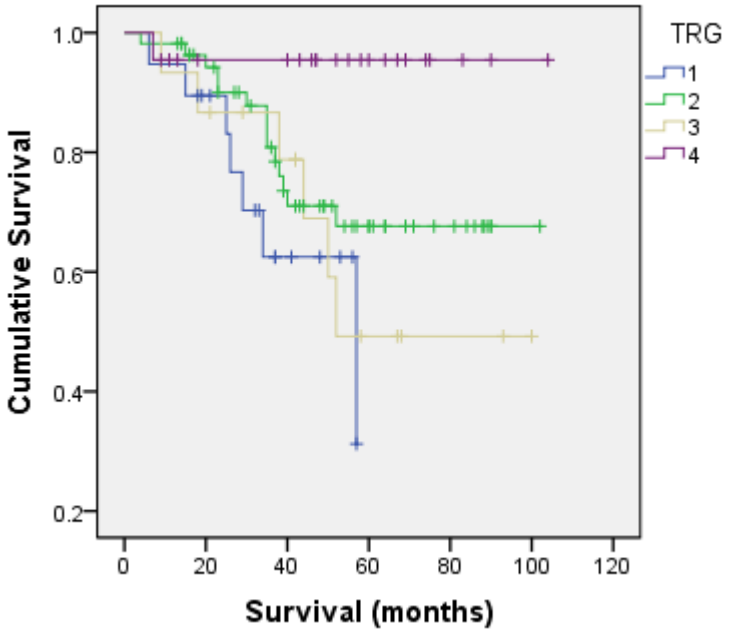

Figure 2.17 - Kaplan-Meier curves demonstrating post-operative survival in months in the patient cohort in this study (n=111), comparing patients between the specific TRG group assigned to their resection specimen. TRG 4 (pCR, n=22) is depicted by the purple curve, TRG 3 (n=15) by beige, TRG 2 (n=55) by green, and TRG 1 (minimal or no regression, n=19) by blue.

The estimated mean post-operative survival in months (with associated 95% CI) for the patients in this study according to their specific TRG was; TRG 4 – 99.6 (91.1 – 108.0), TRG 3 – 68.4 (49.9 – 87.0), TRG 2 79.4 (69.4 – 89.3), TRG 1 – 44.5 (35.6 – 53.4). Complimentary to the comparison in figure 2.15 where survival with a pCR was significantly better than with all other responses combined, it was also demonstrated (as depicted in figure 2.17) to be significantly better when compared to all other responses individually (p=0.010, p=0.040, and p=0.005 for TRG 4 against TRG 3, 2, and 1 respectively). Interestingly the estimated mean post-operative survival for what would be considered a poorer TRG 2 response was longer than for a TRG 3 response (79.4 vs. 68.4 months), although this was not statistically significant (p=0.447), and equally there were no statistically significant differences between any of the non-TRG 4 groups.

2.4 Discussion

2.4.1 Summary of Aims

The aims for the work presented in this chapter were to initially identify rectal cancer resection cases that had completed neoadjuvant CRT, and to assess these cases for histological regression grading. TMAs were to be constructed comprising diagnostic biopsy and resection specimen tissue (including normal colon) from these cases, and subsequently stained for AC expression. Correlation of AC expression with TRG and clinical outcome data was planned in attempt to provide further validation of AC as a predictive and/or prognostic marker in the response of rectal cancer to CRT.

2.4.2 Summary of Results

2.4.2.1 Tissue microarray staining for acid ceramidase

Differential staining of the TMAs for AC was observed across all tissue types (diagnostic biopsy, cancer site, and normal colon) as depicted by the images in figures 2.7, 2.10 and 2.13. 86-107 of the 111 cases were successfully represented in the TMAs (depending on the tissue component).

In stromal tissue at the cancer site from the resection specimen, a relatively low expression of AC was associated with both a pCR (TRG 4, p=0.003) and with relative responders to CRT (TRG 4&3, p=0.048), whereas a relatively high expression of AC was associated with a poor response to CRT (TRG 1) (p=0.017).

Tissue Microarray	Cellular Subset	Cases Represented	Median H Score	TRG Comparison	p Value (χ^2)
Diagnostic Biopsy	Epithelium	86/106	5.0	pCR vs Others	0.695
				Relative Response	0.699
				Others vs Non-response	0.375
	Stroma	86/106	5.0	pCR vs Others	0.472
				Relative Response	0.764
				Others vs Non-response	**0.075**
Cancer Site	Epithelium	68/89	5.5	pCR vs Others	N/A
				Relative Response	0.506
				Others vs Non-response	0.487
	Stroma	105/111	4.0	pCR vs Others	**0.003**
				Relative Response	**0.048**
				Others vs Non-response	**0.017**
Normal Colon	Epithelium	107/111	6.5	pCR vs Others	0.816
				Relative Response	0.196
				Others vs Non-response	**0.012**

Table 2.7 – TMA IHC scoring of AC expression. Each tissue assessed (diagnostic biopsy, resection specimen cancer site or normal colon) and subset (epithelium or stroma) was analysed by correlating lower/higher IHC scoring for AC (dichotomised about the median score) against the respective TRG group (compared as pCR (TRG 4) vs. others (TRG 3-1), relative responders (TRG 4&3) vs. relative non-responders (TRG 2&1), and non-responders (TRG 1) vs. others (TRG 4-2)) using χ^2.

A relatively high epithelial expression of AC in normal colon from the resection specimen was also associated with a poor response to CRT (p=0.012). There were no statistically significant results from the diagnostic biopsy samples, although 9/11 cores representing patients with a poor response to treatment (TRG 1) had a relatively high stromal expression of AC (p=0.075).

The median stromal H score was lower in post-CRT tissue at the cancer site compared with pre-CRT diagnostic biopsy tissue (4.0 vs 5.0). Whilst the median epithelial H score in these 'malignant' tissues subsequent to CRT was higher (5.5 vs 5.0), it is biased by the absence of a score in those with a pCR (and therefore an absence of malignant epithelium). The median H score in normal colon epithelium from the post-CRT resection specimen was higher (6.5) than at the cancer site either pre- or post-treatment.

2.4.2.2 Acid ceramidase expression and outcome

Higher AC expression in both epithelium and stroma from the cancer site post-CRT was associated with local recurrence (p=0.031 and p=0.038 respectively).

A relatively high epithelial expression of AC in normal colon from the resection specimen was independently, and conversely, significantly correlated with improved survival (p=0.001).

Table 2.8 below summarises the correlation of AC expression with the incidence of local recurrence, distant metastases and survival during the follow-up period. The data pertaining to the clinical and pathological data presented in this chapter is included as appendix B.

Tissue	Relative Acid Ceramidase Expression	Local Recurrence		Metastases		Death	
		n=	p value	n=	p value	n=	p value
Diagnostic Biopsy Epithelium	Lower n=42	1	0.518	17	0.061	11	0.263
	Higher n=44	2		10		8	
Diagnostic Biopsy Stroma	Lower n=37	0	0.180	12	0.520	8	0.570
	Higher n=49	3		15		11	
Cancer Site Epithelium	Lower n=33	0	**0.031**	11	0.376	7	0.338
	Higher n=35	5		14		10	
Cancer Site Stroma	Lower n=56	1	**0.038**	17	0.180	11	0.200
	Higher n=49	6		20		14	
Normal Colon Epithelium	Lower n=56	3	0.615	21	0.403	22	**0.001**
	Higher n=51	3		17		6	

Table 2.8 – Correlation of TMA staining for AC with the incidence of local recurrence, metastases and death during the follow-up period in the study, using Fisher's exact test.

2.4.3 Strengths and Limitations

The diagnostic biopsy tissue blocks did not afford sufficient normal epithelial tissue (pre-neoadjuvant CRT) to be assessed for AC expression. The best tissue to be considered as normal was equally from the post-neoadjuvant CRT resection specimen. Although this was targeted to a tissue block of proximal normal colon that would ordinarily be outside the radiotherapy field, irradiation naïve tissue was not guaranteed, and equally this tissue will

have been exposed to systemic chemotherapy. The effect of this is uncertain, although the point at which this tissue is obtained at surgical resection is subsequent to a period of downstaging following cessation of treatment - this is usually at least six weeks, and therefore the tissue may or may not reflect normal pre-CRT tissue. These normal colon samples specifically targeted the epithelium (to mimic an endoscopic biopsy), and were therefore devoid of stromal tissue.

There was clearly no malignant epithelial tissue present at the tumour site in the resection specimens where a pCR had been observed, which makes inter-group comparisons (to assess any change in AC expression with neoadjuvant CRT) in epithelium difficult.

A pragmatic approach was required in performing assessment of the tissue cores. It was technically challenging to obtain cores from the biopsy specimens, given the volume of tissue remaining in the retrieved tissue blocks, and as reflected by the number of cores considered appropriate to score for AC staining on final assessment in this group. Equally achieving malignant epithelium in the TMA sections from the tumour site in the resection specimen blocks was technically difficult in cases of a near complete response – whilst malignant cells were identifiable in the original H&E stained section, localising this area on the tissue block in order to obtain a tissue core was not exact, and equally was not guaranteed to comprise malignant cells at a deeper level after the TMA had been cut-in and further sections obtained. In addition, in cases of mucinous adenocarcinoma, there were scanty epithelial cells present in the cores. This meant that whilst it would have been optimal to only consider a tissue core as appropriate if a minimum number of cells of interest were present, it was not practicable, and an IHC score was assigned at the discretion of the observing consultant histopathologist (MW) and I.

The number of stained TMA cores assessed could be interpreted as low, and a limitation of the study. Triplicate cores for every sample were not present for final analysis, primarily due to the absence of cores from the TMA sections or due to insufficient or non-targeted tissue in the observed cores. The nature of the tissue blocks used in the study contributed to this being an inherent risk but was impacted upon from technical considerations of TMA construction. Whilst this is a recognised limitation, the statistical power of assessment of hundreds of cores overall provides some amelioration of this risk (Parker *et al,* 2002). The desired material may be present in further sections taken from the TMA in some cores but with a risk that other cores would not be present upon deeper sectioning.

Staining of each TMA equally was only performed on a single section due to financial considerations. Despite this, the study has observed significant differences in AC expression with TRG response, and as such has achieved its initial aim of providing some evidence to validate the original proteomic findings. This justifies further investigation of the role of AC in the response to neoadjuvant CRT.

The semi-quantitative scoring system used for analysis of AC expression on the TMAs was a simplified version of an H-score. An alternative version that allows for a slightly more detailed assessment of staining, accounts for the exact percentage of cells staining at the previously described staining intensity (0-3). The score is thus calculated as H = ((% at 0)*0) + ((% at 1+)*1) + ((% at 2+)*2) + ((% at 3+)*3 (McClelland *et al*, 1990), producing a continuous variable that ranges from 0 to 300. For the purposes of our analysis whereby we were seeking to dichotomise the scores about the median for each tissue type analysed (to differentiate between relatively low and high expression for statistical analysis), it was considered that the simplified version was sufficient, along with the consideration of logistical and time constraints in performing a more complex assessment. This is also supported by the literature where simplified scoring systems have correlated highly with the more rigorous H-score (Detre *et al*, 1995) for oestrogen receptor status in breast cancer, although validation of any IHC scoring system for AC has not been undertaken.

A major drawback with TMA construction lies in the approximation of desired tissue spots for transfer into the TMA. The manual alignment of the annotated region from an H&E slide to the donating block is not always exact. Next generation TMA technology based on digital imaging and automated processes would have potentially ameliorated this drawback (Zlobec *et al*, 2013) but was not logistically or financially an option for this study.

Tumour heterogeneity is also a recognised factor with implications for the interpretation of biomarker studies such as this (Rehemtulla, 2012), although the impact of this is potentially lessened by the attempt in this study to obtain triplicate cores from each tissue sample. Validation of triplicate cores correlating with IHC expression of a whole tissue section for p53, MLH1 and MSH2 in CRC has been demonstrated (Jourdan *et al*, 2003). Equally both TMA and whole tissue section expression has been correlated with survival (Nocito *et al,* 2001) in prostate cancer but such studies are limited and may be both tumour and/or protein specific (Khouja *et al,* 2010), and AC in rectal cancer has not previously been validated. It is also established that CRC displays high intra-tumour heterogeneity in comparison with other cancers (Punt *et al,* 2017). The concern with regards to tumour heterogeneity is equally

pertinent for the assessment of post-neoadjuvant CRT specimens, as the surviving tumour cells may not accurately reflect the original tumour. Information gleaned from this tissue is indicative of the response to treatment, and a potential change in the tissue phenotype, as opposed to offering predictive information regarding response to treatment itself.

The original work upon which this thesis is based utilised tissue obtained pre- and post-CRT, and subsequently at the time of surgical resection. No differentiation was possible between epithelium, stroma, muscularis etc. within each sample due to the nature of the processing of the samples. In this study, tissue was targeted for incorporation into TMAs based upon the presence and density of malignant epithelial cells (where appropriate), primarily to guarantee that the tissue being assessed was truly from the cancer site. There is therefore inherent bias between the studies, which makes direct comparison difficult. Further evidence to suggest that AC is implicated in the response to of rectal cancer to neoadjuvant CRT has been demonstrated however.

The correlation of reduced AC expression in epithelial cells with an enhanced response to CRT is potentially straightforward to understand as a mechanism. Whilst the results presented only potentially demonstrate a trend towards this observation, the impact of a low level or down-regulation of AC in tumour cells in response to the cellular insult, may result in a reduction of ceramide cleavage and its subsequent accumulation (Arana *et al,* 2010), with ceramide then exerting its influence in mediating cell cycle arrest and apoptosis (Garcia-Barros *et al*, 2014).

Evaluation of apoptosis as the main predictive mechanism associated with AC activity in the tumours post-CRT could have been undertaken with assessment of IHC staining for the activator caspases -3 and -7, mediated predominantly through mitochondrial dysfunction (Green and Kroemer, 2004). Assessment of active caspase-3 as the main executioner of apoptosis has been evaluated in a variety of FFPE tissues (Gown and Willingham, 2002), although caspase-7 can be activated independent of the mitochondrial pathway (Davidson *et al*, 2005), and could be assessed for IHC expression independently. The cleavage of poly-ADP-ribose-polymerase (PARP), which detects and signals DNA strand breaks, is considered indicative of functional caspase activation (Koh *et al*, 2005), although IHC evaluation whilst possible has been observed to be challenging (Horvath *et al*, 2015). The significance of evaluation of these markers at the point of assessment 6 weeks following cessation of CRT would need to be determined however.

An explanation of the impact of the observed lower AC expression in stromal cells with a significantly improved response to CRT, can potentially be explained by literature evidence for tumour-stromal interaction and signalling between cells.

The stroma (or tumour micro-environment) is considered to play an essential role in both the development of malignancy and in the resistance to treatment. This environment, composed of extracellular matrix, fibroblasts, endothelial cells, and cells of the immune system regulates the behaviour of tumour cells and co-evolves (Werb and Lu, 2015). Cancer cells have been demonstrated to activate and recruit carcinoma-associated fibroblasts, which are able to both stimulate cell growth and invasion, as well as inflammation and angiogenesis but may also be tumour inhibiting (Kalluri and Zeisberg, 2006). This process is considered to be under the regulation of TGFβ signalling, which itself is primarily activated by integrins secreted from both tumour and stromal cells. In normal tissues TGFβ suppresses epithelial cell division but tumour cells can develop escape mechanisms to become resistant to TGFβ growth suppression. In addition, TGFβ drives EMT, increasing the potential for metastasis (Khan and Marshall, 2016).

This signalling process may be mediated through ceramide-based lipid rafts, as micro-domains of regions of the cellular membrane, demonstrated to regulate vesicular traffic, cell polarity, and cell signalling pathways (Bieberich, 2018). They have been found in almost all existing experimental cancer models, including CRC, and play key regulatory roles in cell migration, metastasis, cell survival and tumour progression (Jahn *et al,* 2011). Altered AC expression may therefore have central implications for the regulation of ceramide and key regulatory inter-cellular signalling between stroma and tumour in response to CRT in rectal cancer.

Information as to the exact neoadjuvant CRT treatment protocols for both chemotherapeutic agents used and the radiation doses delivered was not obtained for these patients. It was inferred from the clinical records that a patient had completed the course of treatment by the nature of the request for re-staging imaging, the fact that re-staging imaging had been undertaken, or the request for histopathological assessment citing long course treatment with consistent findings in the resection specimen. 5-FU based therapy, as either intra-venous infusion or oral capecitabine was, and remains, the only chemotherapeutic radio-sensitiser in clinical use in the hospital however.

2.4.4. Conclusion

In relation to the hypotheses set at the outset of the chapter:

- Differential expression of AC is present in rectal cancer, and/or normal colon - **PROVEN**

We have observed differential expression of AC in rectal cancer both pre- and post-CRT in epithelial and stromal tissue, and in epithelial tissue from normal colon.

- Expression of AC in rectal cancer and/or normal colonic tissue can predict response to neoadjuvant CRT, and/or is a biomarker of response to treatment - **PARTIALLY PROVEN**

Significant differences in expression of AC that separate responders and non-responders to neoadjuvant CRT have been observed in stromal tissue from post-treatment resection specimens, and in normal colonic epithelium. These findings validate the original proteomic profiling in implicating AC in the response of rectal cancer to CRT and justifies further investigation.

Statistically significant results were not observed in this study from a potentially predictive diagnostic biopsy but there was a trend towards higher stromal expression from these samples being associated with no response to treatment (TRG 1) - the study may simply be under-powered to detect such an association in this sub-group.

The results in this study overall implicate AC expression in tumour stroma in the response of rectal cancer to neoadjuvant CRT. Whilst lower median H scores were observed in cancer site tumour stroma when compared to pre-treatment diagnostic biopsies, it is not possible to infer if is a lower or decreasing expression that determines response, or if a lower expression is a consequence of response. Higher AC expression in the cancer site post-CRT in both epithelium and stroma was significantly correlated with local disease recurrence ($p=0.031$ and $p=0.038$ respectively). In the context of the epithelial score, this is exclusively in those without pCR. Correlations of AC expression and survival further implicate a role for AC in the response of rectal cancer to CRT and further assessment of AC expression in response to radiotherapy *in vitro* is required.

Chapter 3

Manipulation of Acid Ceramidase Expression and Activity in the HCT116 Colorectal Cancer Cell Line

3.1 Introduction

3.1.1 Background

The effect of variable AC expression upon sensitivity to radiotherapy in rectal cancer, was proposed to be further assessed *in vitro.* It was considered that the sensitivity to irradiation of a CRC cell line should be assessed, both before and following manipulation of AC expression / activity. This manipulation was planned to consist of genetic and pharmacological approaches, in order to both optimise experimental laboratory conditions (with genetic manipulation), and to assess a potentially more immediately translational model of AC dependent radio-sensitivity (with pharmacological inhibition). It was therefore necessary to quantify and optimise the manipulation of AC expression and activity in a CRC cell line.

3.1.1.1 HCT116 colorectal cancer cell line

The HCT116 CRC cell line is commonly utilised for the in vitro modelling of radio-sensitivity in rectal cancer (Schilling *et al*, 2013; Halacli *et al*, 2013; Adeberg *et al*, 2014), owing to both its lineage but also the use of clonogenic assay as an outcome measure and the characteristics of the cells in colonies, which are densely packed and easily visualised. The cell line exists in p53 wild type (p53+/+) and deficient (p53-/-) forms. An original concept was to compare the radio-sensitivity of the two cell lines in an AC dependent model, although in the context of the other work proposed for this thesis, and with the duplication of the required optimisation, it was considered impracticable. Thus, it was determined to perform further experimental modelling with a single cell line - the wild type p53+/+ cell line was available from the Department of Pharmacology, University of Liverpool, and was selected as cell culture protocols were established.

3.1.1.2 Small interfering RNA

Small interfering RNA (siRNA) was first described in 1999 (Hamilton and Baulcombe), since which time its experimental use for simple and rapid gene silencing, including in cell lines, has become widely adopted. It interferes with the expression of specific genes with complimentary nucleotide sequences, and functions by causing mRNA to be broken down after transcription (Agrawal *et al*, 2003). The negatively charged siRNA can be delivered into cells by use of a cationic lipid, forming liposomes which overcome the negative electrostatic repulsion of the cell membrane (Dalby *et al*, 2004).

Whilst the therapeutic potential of siRNA is beginning to be evaluated in gene-therapy in the clinical trial setting, many barriers to its widespread use remain. Intracellular delivery of siRNAs *in vivo* is impeded by their size and negative charge. Whilst they are too large to cross cell membranes, siRNAs are small enough to be filtered by the kidney, and are rapidly excreted unless conjugated to other molecules or incorporated into complexes. Unintended on-target effects in non-redundant functions of the target gene can occur in the targeted tissue, or unwanted effects can occur in non-targeted tissue. Sequence specific off-target effects are rare but innate immune inactivation and toxicity of delivery vehicles are common (Wittrup and Lieberman, 2015).

3.1.1.3 Chemotherapeutic inhibition of acid ceramidase activity

The chemotherapeutic carmofur (as an orally available 5-FU prodrug) was found to be a potent inhibitor of AC activity, whereas 5-FU itself was not (Realini *et al*, 2013). Carmofur is also known to have been used in the clinical setting in the adjuvant treatment of colorectal and breast cancers (Watanabe *et al*, 2006), although neoadjuvant CRT for rectal cancer in the UK currently utilises the mainstream oral 5-FU prodrug capecitabine for radio-sensitisation.

Clearly the finding of carmofur potently inhibiting AC has a potential translational benefit, given the confirmation of differential expression of AC separating responders and non-responders to CRT in rectal cancer. Investigating the response to neoadjuvant CRT in rectal cancer comparing radio-sensitisation with capecitabine against carmofur, could potentially be a logical clinical trial.

It was therefore proposed to assess the effect of inhibition of AC with carmofur *in vitro*, alongside siRNA inhibition. Quantification of mRNA and protein expression would be

determinable using reverse-transcription polymerase chain reaction (RT-PCR) and Western blotting respectively. Assessment of AC activity would provide the key functional significance of any expressional changes.

3.1.1.4 Acid ceramidase activity assay

Historical assessment of AC activity has traditionally been performed using: *i)* enzymatic based activity assays, classically with radiolabelled substrates; *ii)* loading tests, consisting of the addition of exogenous radiolabelled sphingolipids on cultured cells and the study of their metabolism; and *iii)* determination of accumulated ceramide. The main drawbacks of these methods include the lack of commercially available radiolabelled compounds, the laborious processes required in the separation and identification of reaction products, and the need for specific instruments, which has restricted assessment of AC activity to very few expert laboratories (Bedia *et al*, 2010).

The Bedia *et al.* group have developed a fluorometric procedure to determine AC activity using a synthetic ceramide analogue carrying a 2-oxo-2H-chromen-7-yloxy moiety in the CH_3-terminal part of the sphingoid chain (Bedia *et al*, 2007). The structure of this substrate enabled the release of umbelliferone after hydrolysis by AC, periodate oxidation of the resulting aminodiol, and further β-elimination of the aldehyde oxidation product, resulting in a simple assay that could be performed in a 96-well plate format. The specificity of the substrate towards lysosomal AC was further refined by manipulation of the fatty acid chain length, revealing the Rbm14-12 substrate (figure 3.1), possessing a 12-carbon fatty acid chain, as highly specific (Bedia *et al*, 2010).

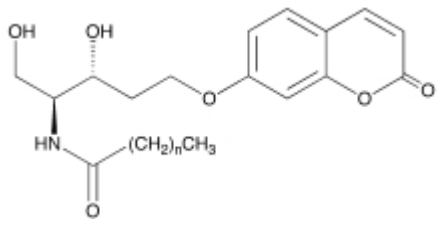

Figure 3.1 – General chemical structure of the Rbm14 compound, where n=10 for Rbm14-12. (Taken from Bedia *et al*, 2010)

The AC activity assay was deemed central to the experimental work in the thesis, to provide the quantifiable functional link between siRNA transfection and small molecule inhibition. It

is equally the functional significance of AC activity, as opposed to expression, that we were seeking to evaluate as the key determinant of potentially translational research.

3.1.2 Hypotheses

- Expression of AC can be inhibited by siRNA transfection in the HCT116 CRC cell line, subsequently inhibiting protein activity
- AC activity +/- expression can be inhibited by the chemotherapeutic carmofur in the HCT116 CRC cell line

3.1.3 Aims and Study Design

- Perform siRNA transfection targeting AC in the HCT116 CRC cell line, assessing subsequent genomic expression, and proteomic expression and activity
- Perform dosing of the HCT116 cells with carmofur, assessing subsequent proteomic expression and activity
- Genomic expression of AC to be quantified by mRNA expression using RT-PCR
- Proteomic expression of AC to be quantified by Western blotting
- AC activity to be quantified by direct activity assay
- Establish the optimal conditions for inhibition of AC in the HCT116 CRC cell line with siRNA and carmofur, establishing maximal activity inhibition whilst minimising off-target effects

3.2 Methods

3.2.1 Culture of the HCT116 Colorectal Cancer Cell Line

The HCT116 cell line is an immortal, epithelial-like CRC derived cell line, originating from a male human colon cancer. The cells are commonly utilised for *in vitro* radiotherapy modelling, and were provided as a kind gift from The Department of Molecular and Clinical Pharmacology at The University of Liverpool.

Cells were maintained in Dulbecco's Modified Eagle's Medium (DMEM, Sigma-Aldrich), 10% foetal bovine serum (Gibco Life Technologies, Cheshire, UK) and 1% penicillin/streptomycin (Sigma-Aldrich), in 75cm^2 Nunc™ (Thermo Fisher Scientific, Cheshire, UK) cell culture flasks, and were incubated at 37°C and 5% CO_2.

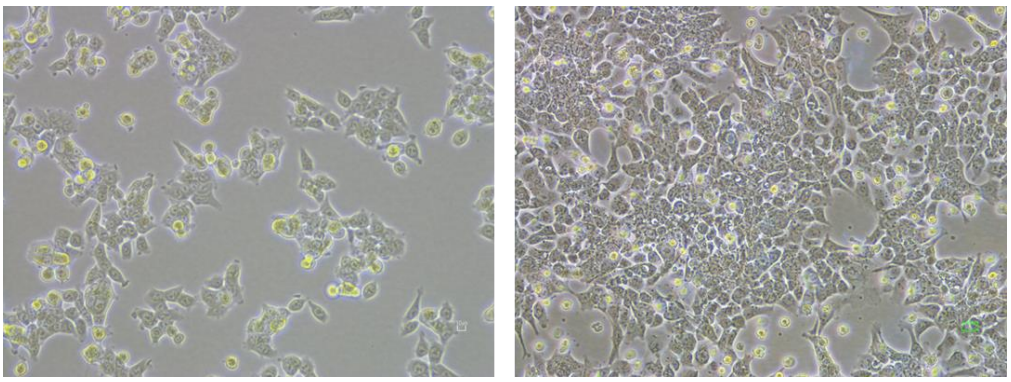

Figure 3.2 – Morphology of the HCT116 CRC cells in culture. Light microscopy images taken at x200 magnification. The image on the left demonstrates adherent cells 1 day after sub-culture, whereas the image on the right demonstrates the cells at 80-90% confluence 3 days after sub-culture.

The morphology and confluence of the cells (figure 3.2) was observed every 1-2 days, and upon establishing 80-90% confluence every 3-4 days, cells were sub-cultured as follows in an Airstream® biological safety cabinet (ESCO, Barnsley, UK). The existing culture medium was removed, and the cells were washed in 5mL DMEM at 37°C to remove all traces of serum containing trypsin inhibitor. 5mL of 0.25% trypsin-EDTA solution at 37°C (Sigma-Aldrich) was applied to the cells and left for one minute. The trypsin-EDTA solution was then removed,

and the cells incubated at 37°C for 5 minutes, before being re-suspended in 5mL DMEM at 37°C and filtered through a sterile needle and syringe. The sub-culture was then established (usually in a 1:5 ratio) in 5mL fresh culture medium at the same temperature.

When re-suspending cells in culture from 6-well plates, 1mL of each solution was applied respectively. Cells in suspension were counted using a haemocytometer to facilitate accurate plate seeding, which is described in greater detail in chapter 4.

3.2.2 Small Interfering RNA Transfection Targeting Acid Ceramidase

A set of four siRNAs targeting different regions of the human ASAH1 gene encoding for AC was purchased (siGENOME human ASAH1 (427) siRNA, MQ-005228-01-0002, Dharmacon, GE Life Sciences, Leicestershire, UK). The siRNAs were re-suspended according to manufacturer's instructions in RNase-free water to create 20µM stock solutions, aliquoted, and stored at -20°C.

Initial assessment of siRNA transfection was performed in 12-well Nunc™ (Thermo Fisher Scientific) cell culture plates, seeded with HCT116 cells at a density of $2x10^5$ in 1mL antibiotic-free culture medium. The cells were allowed to adhere overnight, and a subsequent forward transfection with each of the siRNAs was performed. 2µL of Lipofectamine™ RNAiMAX (Invitrogen Life Technologies, Cheshire, UK) in 100µL Opti-MEM® Reduced Serum Medium (Gibco Life Technologies) was mixed respectively with 1.2µL of each siRNA stock solution in 100µL Opti-MEM®, and incubated at room temperature for 15 minutes, prior to adding to the cells in culture and gentle mixing. A vehicle control for the transfection consisted of the same transfection reagents but with the addition of a non-coding siRNA (siGENOME non-targeting siRNA pool #1, D-001206-13-05, Dharmacon, GE Life Sciences) at the same concentration. The final siRNA concentration for each transfection was 20nM, and the transfected cells were incubated at 37°C for 48 hours prior to assessment of transfection efficiency.

RT-PCR to detect AC mRNA expression, and Western blotting to assess AC protein expression were initially considered in the assessment of siRNA transfection efficiency.

3.2.3 Reverse Transcription Polymerase Chain Reaction Detection of Acid Ceramidase mRNA

Subsequent to siRNA transfection and incubation, the culture medium along with remaining transfection reagents was aspirated, and the cells washed with x1 phosphate buffered saline (Invitrogen). RNA extraction was performed using the miRNeasy Mini Kit (Qiagen, Venlo, Netherlands) in accordance with manufacturer's instruction, prior to RNA quantification and quality control using the Nanodrop™ spectrophotometer (Thermo Fisher Scientific). Complimentary DNA (cDNA) was reverse transcribed using the QuantiTect® Reverse Transcription Kit (Qiagen), again in accordance with manufacturer's instruction.

Specific primers were designed for AC (N-acylsphingosine amidohydrolase, ASAH1 gene), as well as β-actin (ACTB gene) and glyceraldehyde 3-phosphate dehydrogenase (GAPDH gene) for use as housekeeper controls, using the primer designing tool available at http://tools.invitrogen.com/content.cfm?pageid=9716 and Primer Blast available at http://www.ncbi.nlm.nih.gov/tools/primer-blast/index.cgi?LINK_LOC=BlastHome.

The criteria for design of the primers was as follows; a) primer size (bases): minimum 18, optimal 20, maximum 27; b) primer melting temperature (°C): minimum 57, optimal 60, maximum 63; c) primer guanine/cytosine content (%): minimum 40, optimal 50, maximum 60; d) product size (nucleotides): minimum 100, maximum 150; e) salt concentration (mM): 50; f) primer concentration (nM): 50.

The primers designed for AC were specific for all four transcript variants of the gene (NM_001127505.2, NM_004315.5, NM_177924.4, XM_005273504.2) and nothing else. All primers were assessed for self-complementarity, hairpins, and dimerization using http://www.basic.northwestern.edu/biotools/oligocalc.html, and were found to be suitable. Table 3.1 below details the specific sequences generated.

Primer Target	Primer Sequence (5' to 3')
ASAH1	Forward – TGC CCT GAC CCT TGT ATA GG
	Reverse – CCG CGA GTC TTA GTC TTT GG
ACTB	Forward – GAT GAG ATT GGC ATG GCT TT
	Reverse – CAC CTT CAC CGT TCC AGT TT
GAPDH	Forward – GGC CTC CAA GGA GTA AGA CC
	Reverse – AGG GGT CTA CAT GGC AAC TG

Table 3.1 – Forward and reverse primer sequences generated for the gene of interest (ASAH1) and reference genes (ACTB and GAPDH).

The custom primers were synthesized by and purchased from Invitrogen Life Technologies, and were reconstituted according to manufacturer's instruction in Tris-EDTA buffer (10mM Tris-HCl (pH 8.0), 1mM EDTA) to create stock primer solutions of 100µM, which were aliquoted and stored at -20°C.

RT-PCR was performed in 96-well PCR plates (Starlab, Milton Keynes, UK), using SYBR® Green JumpStart™ Taq ReadyMix™ (Sigma-Aldrich) as per the manufacturer's instruction. ASAH1 primer concentrations were optimized prior to undertaking RT-PCR with experimental samples, with optimal concentrations of 250nM in the reaction mix for both forward and reverse primers determined by appropriate product accumulation and melt curve analysis. Template DNA was loaded at the same mass in each well within each RT-PCR run but varied between experimental runs (10-50ng) dependent on the total mass available for the number of reactions to be performed. Relative gene expression was quantified in triplicate samples in each run, and negative control samples consisted of the same reaction mix in the absence of template DNA. Cycle threshold (Ct) values indicating product formation were not observed in negative control samples with any of the primers. RT-PCR was performed using the ABI PRISM® 7000 Sequence Detection System (Applied Biosystems, Waltham, Massachusetts, USA). Thermal cycling was undertaken with an initial denaturation at 94°C for 2 minutes, followed by 40 cycles of denaturation at 94°C for 15 seconds and annealing, extension and read fluorescence at 60°C for 1 minute.

Ct values for the gene of interest (GoI) and housekeeper (HK) genes were observed from the exponential phase of product accumulation, and relative quantification of the GoI calculated using the formula $2^{-\Delta\Delta Ct}$, as published by Livak and Schmittgen (2001). ΔCt can be considered as $Ct_{(GoI)} - Ct_{(HK)}$ (where HK in this instance was the mean of the two housekeeper Ct values) for each treatment group, and ΔΔCt is $\Delta Ct - \Delta Ct_{(Ref)}$ (where Ref = reference sample).

Subsequent to the initial siRNA transfection as detailed in section 3.2.2 and assessment of relative gene expression using RT-PCR, it was determined that siRNA number 3 (out of the set of four siRNAs tested) provided the greatest inhibition of mRNA production. This siRNA (siRNA3) was therefore selected for further optimization of reagent dosing. This was undertaken in an attempt to maximize therapeutic inhibition of AC with consideration of limiting potential off target effects. In brief, this consisted of assessing the response to siRNA transfection across a range of Lipofectamine™ RNAiMAX doses (0.5, 1, 2 and 4µL per well in a 12-well plate respectively), and a range of siRNA3 final concentration per well (1.25, 2.5, 5, 10, 20 and 40nM) over a series of experiments following the same transfection protocol.

3.2.4 Western Blotting for Acid Ceramidase

The functional effect of siRNA transfection to inhibit ASAH1 mRNA production needed to be determined. Equally, the intended small molecule inhibition of AC at the protein level with carmofur, as proposed as part of the experimental plan, would not be assessed by RT-PCR. Western blotting for AC to quantify expression at the protein level was therefore deemed to be appropriate.

3.2.4.1 Sample preparation

Cells in culture were prepared for assessment of protein content on Western blotting by use of Radio-Immunoprecipitation Assay buffer (RIPA buffer, Sigma Aldrich), to enable efficient cell lysis and protein solubilisation, whilst avoiding protein degradation and interference with the proteins' immunoreactivity and biological activity. Following experimental treatment in culture plates, cells were washed with x1 phosphate buffered saline (PBS, Sigma-Aldrich), then RIPA buffer was applied (50µL and 100µL in 12-well and 6-well plates respectively) and incubated at room temperature for 5 minutes. Cells were scraped from the well, and the lysate centrifuged at 15,000rpm at 4°C for 15 minutes. Protein quantification of the resultant supernatant was performed on Bradford assay, and then prepared for use in Western blotting.

Mouse heart tissue (obtained and kindly provided fresh frozen as a by-product from existing work in the department by Mr Philip Roberts, Department of Molecular and Clinical Pharmacology, The University of Liverpool) and a rectal cancer tissue sample known to relatively over-express AC (previously obtained and fresh frozen under continuing research ethics approval (as detailed in chapter 2), and kindly provided by Mr Paul Sutton, Department of Molecular and Clinical Cancer Medicine, The University of Liverpool) were also prepared for use as positive controls for Western blotting. A combination of mechanical and ultrasonic homogenisation of the tissue in PBS was performed, prior to centrifugation as per the cell lysate. The resultant supernatant was used for Western blotting, again after protein quantification on Bradford assay.

An AC protein fragment was purchased (ab114948, Abcam) for use as a positive control and to identify relevant bands in the HCT116 cell samples, subsequent to initial difficulties with antibody specificity as discussed in section 3.3.2 below.

3.2.4.2 Bradford assay (Bradford, 1976)

Standard protein concentrations of bovine serum albumin (BSA, Sigma Aldrich) were prepared at 0, 0.05, 0.1, 0.2, 0.4, 0.6, 0.8 and 1mg/ml in distilled water (dH_2O), and 20µL of each placed in duplicate to the first two columns of a 96-well plate in increasing concentration. Serial dilutions of samples for protein quantification were prepared at concentrations of 1:10, 1:20, 1:50 and 1:100 in dH_20, and 20µL of each concentration placed in duplicate in adjacent paired wells on the plate. Bradford reagent (Bio-Rad, Hemel Hempstead, UK) was diluted in a 1:5 ratio with dH_2O, and 200µL placed in each of the wells and then mixed. Absorbance at 570nm was measured using the Dynex MRX microplate reader (Magellan Biosciences, Chelmsford, UK), and protein concentration of the samples calculated by comparison to the standard curve.

When quantifying protein concentration in samples prepared with RIPA buffer, specifically in the higher concentration sample dilutions of 1:10 and 1:20, the standard protein concentrations of BSA were also prepared to contain the same concentration of RIPA buffer as the samples being investigated.

3.2.4.3 Western blotting

Samples containing 15µg of total protein were prepared for Western blotting by mixing in a 2:1 ratio with Laemmli buffer (Bio-Rad) prepared with β-mercaptoethanol (as a reducing agent) as per the manufacturer's instruction. The samples were then denatured by heating at 85°C for 5 minutes, before loading onto SDS-PAGE (sodium dodecyl sulphate-polyacrylamide gel electrophoresis) gels to undergo electrophoresis in running buffer at 150V for 1 hour. The Precision Plus Protein™ Kaleidoscope (Bio-Rad) molecular weight marker was loaded into one of the wells in the gel to assist with analysis of the molecular weight of the protein samples. 10% SDS-PAGE gels were prepared for proteins anticipated to be detected at 40-50kDa, and 12% gels for proteins of a lower molecular weight.

Subsequent to electrophoresis, the protein in the gel was transferred to a Hybond-ECL nitrocellulose membrane (GE Life Sciences, Buckinghamshire, UK), within a blotting sandwich in a transfer unit containing transfer buffer, at 230A for 1 hour. The membrane was briefly washed in 1xTBST (20mM Tris-Cl pH 7.6, 150mM NaCl, 0.1% Tween 20), and the quality of the transfer assessed with a Ponceau S solution (Sigma Aldrich). The stain was removed with 1xTBST, and the membrane blocked overnight in 10% non-fat dry milk blotting-grade blocker (Bio-Rad) in 1xTBST with constant agitation at 4°C.

Three primary antibodies for AC were ultimately optimised by experimentation for use in Western blotting, as was one for β-actin which was used as a protein loading control. The final conditions used are shown in table 3.2 below. All primary antibodies were diluted in 2% non-fat dry milk blotting grade blocker (Bio-Rad) in 1xTBST, and incubated overnight with constant agitation at 4°C.

Following primary antibody incubation, membranes were washed three times for 10 minutes each in 1xTBST with constant agitation, prior to incubation for one hour with the relevant HRP-conjugated secondary antibody as shown in table 3.2, diluted in 2% non-fat dry milk blotting grade blocker. A further 3 x 10 minute cycles of washes in 1xTBST with constant agitation was undertaken, before applying an enhanced luminol-based chemiluminescent substrate (ECL) (Western Lightning® Plus-ECL, PerkinElmer®, Waltham, Massachusetts, USA) to the membrane, for the detection of HRP conjugates, as per the manufacturer's instruction.

The prepared membrane was then sealed in transparent wallet, and chemiluminescence film (Amersham Hyperfilm™ ECL, GE Healthcare, Buckinghamshire, UK) exposed to the

membrane, the duration of which was dependent on protein band intensity, visualised on development and fixation of the film.

Primary Antibody			Secondary Antibody		
Name	**Manufacturer & Reference**	**Final Dilution**	**Host Species**	**Manufacturer & Reference**	**Final Dilution**
Anti-AC, Rb monoclonal	Abcam ab174828	1:1000	Gt anti-Rb IgG	Sigma A9169	1:10,000
Anti-AC, Rb polyclonal	Abcam ab74469	1:2500	Gt anti-Rb IgG	Sigma A9169	1:10,000
Anti-AC, Ms monoclonal	BD Biosciences BD612302	1:250	Rb anti-Ms IgG	Sigma A9044	1:10,000
Anti-β-actin, Ms monoclonal	Abcam ab8226	1:10,000	Rb anti-Ms IgG	Sigma A9044	1:10,000

Table 3.2 – Antibodies used in Western blotting for the detection and quantification of AC protein expression. Rb = rabbit, Ms = mouse, Gt = goat.

3.2.4.4 Experimental conditions investigated on Western blotting

Subsequent to initial procedural Western blotting optimisation (not described or presented), the samples in the first three blots presented in section 3.3.2 were obtained as described in 3.2.4.

Following the observation of RT-PCR data described in 3.3.1, where siRNA3 at 10nM was selected for future transfection in HCT116 cells, samples for the assessment of protein expression at 12, 24, 36 and 48 following siRNA3 transfection were collected and prepared as previously described, and compared primarily alongside non-coding siRNA transfected cell samples collected at the same time points.

Upon establishing inhibition of AC activity, as described in sections 3.2.5 and 3.3.3, and with developing confidence in determining AC antibody specificity on Western blotting as described in section 3.3.2, it was deemed prudent to assess the effect of a non-toxic dose of carmofur on AC protein expression. A parallel set of plates to those used for incubation of the 2μM samples in the final described experiment in 3.2.5.3 were created for the purpose of sample collection for Western blotting. The effect of dosing with 2μM carmofur in HCT116

cells was therefore assessed at 0.75, 1.5, 3 and 5 hours post incubation, and compared to 0.05% DMSO vehicle control and untreated culture medium only samples.

3.2.4.5 Densitometry

Semi-quantitative analysis of selected Western blots was undertaken by performing densitometry of visualised bands using ImageJ version 1.48 (National Institutes of Health, Bethesda, Maryland, USA). Density measurements of β-actin bands for samples across the blot were normalised to a selected standard, and the measurements from the protein of interest adjusted according to these normalised values. Comparison of the relative expression of the protein of interest was undertaken between experimental samples and their respective controls, and expressed as a percentage of the control value.

3.2.5 Acid Ceramidase Activity Assay

The Rbm14-12 substrate (chemical formula $C_{26}H_{39}NO_6$, molecular weight 461.59g/mol) was purchased from The Research Unit on Bioactive Molecules at The University of Barcelona. 0.5mg of the substrate was dissolved in 270.8µL of ethanol to produce a 4mM solution, which was protected from light and stored at -20°C. The assay was performed as per the Bedia *et al* (2010) paper, and is described below.

To measure AC activity, cultured cells were re-suspended as described in section 3.2.1, and washed with x1 PBS. Cell pellets were re-suspended in 100µL of a 0.2M sucrose solution, and then sonicated. Cell homogenates were centrifuged at 15,000*g* for 3 minutes. The supernatant was collected and used for protein quantification (Bradford assay as described previously, albeit compared against standards containing the same concentration of sucrose solution as the samples in this instance) to work with equal amounts of protein between samples. The enzymatic assay was carried out in 96-well plates.

Each well contained a mixture of 74.5µL of 25mM sodium acetate buffer (pH4.5), 0.5µL of 4mM Rbm14-12 substrate solution in ethanol (substrate final concentration 20µM, ethanol final concentration 0.5%), and a fixed amount of protein in a volume of 25µL of a 0.2M

sucrose solution. Negative control samples consisted in the same incubation mixture in the absence of protein extracts. The plate was incubated at 37°C for 3 hours without agitation.

The enzymatic reaction was stopped by first adding 50µL of methanol, and then 100µL of a fresh 2.5mg/ml sodium periodate solution in 100mM glycine/sodium hydroxide buffer (pH 10.6) to each well. The plate was protected from light for 2 hours and the released fluorescence was subsequently quantified using a microplate fluorescence reader at λex 360nm, λem 446nm (Varioskan Flash, Thermo Fisher Scientific, Massachusetts, USA).

3.2.5.1 Umbelliferone calibration for acid ceramidase activity assay

To validate the fluorescence of umbelliferone, and therefore its use as a marker of activity with the Rbm14-12 substrate, a calibration was performed, as per the protocol received from The University of Barcelona and described below.

A 10mM solution of umbelliferone (molecular weight 162.14g/mol) in ethanol was prepared (8.1mg umbelliferone in 5mL ethanol). 2µL of this 10mM solution was mixed with 198µL of a 25mM sodium acetate buffer (pH 4.5) to give a 100µM umbelliferone solution. 150µL of this 100µM solution was then mixed with a further 850µL of the 25mM sodium acetate buffer, to produce a 15µM umbelliferone solution. Serial 1:2 dilutions of this 15µM solution with the 25mM sodium acetate buffer generated umbelliferone solution concentrations of 15, 7.5, 3.75, 1.88, 0.94, 0.47, 0.23 and 0.12µM respectively. 100µL of each of these solutions were dispensed in triplicate in a 96-well plate, as was the 25mM sodium acetate buffer as an umbelliferone negative control. 50µL of methanol and then 100µL of 100mM glycine/sodium hydroxide buffer (pH 10.6) were added to all wells. Fluorescence was read after 15 minutes using the Varioskan Flash at λex 360nm, λem 446nm.

3.2.5.2 Protein loading validation for acid ceramidase activity assay

The mass of validated protein loading in the Bedia *et al.* (2010) paper for the AC activity assay was 10-25µg but this was derived from two Farber disease fibroblast cell lines that were deficient in and manipulated to overexpress AC respectively. It was therefore imperative to determine appropriate protein loading in the selected HCT116 cell line.

Untreated HCT116 cells in culture and approaching confluence were collected as described previously, and protein extraction and quantification performed as described in section

3.2.4. 0, 5, 10, 15, 20, 25, 30, 35, 40, 45 and 50µg protein samples per 25µL of 0.2M sucrose were prepared in triplicate and the AC activity assay was performed as above.

Mean fluorescence values were adjusted accordingly to account for the background fluorescence from the negative control (0µg) sample, such that 0µg protein = 0 fluorescence.

3.2.5.3 Chemotherapeutic inhibition of acid ceramidase activity

It was necessary to investigate the drug dose response characteristics on AC activity in the HCT116 cell line with carmofur and 5-FU, both in relation to drug concentration applied to the cells and the duration of incubation, in order to establish optimal AC activity inhibition. The work performed by Realini *et al.* (2013) demonstrated significant inhibition of AC activity with carmofur in the human SW403 colonic adenocarcinoma cell line (to approximately 1/3 against vehicle control, $p<0.001$), which approached maximal inhibition at a dose of 3µM, occurring at around 3 hours. Similar results were seen in the human prostate adenocarcinoma cell line LNCaP, albeit with a lower dose of 1µM carmofur.

The main limitation in performing the activity assay was in the cost and availability of the Rbm14-12 substrate. 0.5mg (allowing for ≈540 individual reactions, equivalent to ≈180 samples or ≈5½ 96-well plates) was purchased from The University of Barcelona for €650. Given that each sample required triplicate reaction replicates, allowing for vehicle and negative control samples for each assay run, and in the absence of infinite financial resource, it was necessary to be selective with optimisation experiments.

A test dose of 2.5µM carmofur was determined from MTS proliferation assay data (as detailed in chapter 4) as non-toxic, whilst considering a likely effect on AC activity in view of the data from Realini *et al* (2013). After demonstrating initial inhibition of AC activity with this dose, an experiment to determine the time of peak inhibition was performed. A 5mM solution of carmofur (molecular weight 257.3g/mol, Abcam) was prepared by dissolving 2.4mg of the drug in 1866µL of DMSO. 5µL of this solution was mixed with 10mL of DMEM to give the required experimental concentration of 2.5µM (DMSO final concentration 0.05%). HCT116 cells in exponential growth phase were plated out at $1x10^6$ in 2mL media in 6-well plates, and allowed to adhere overnight. The cells were then incubated with 2.5µM carmofur by replacing the media in the wells with 2mL of media containing the drug in solution. Sample preparation as described above was performed for cell groups collected from individual wells at 0, 0.5, 1, 2, 3.5 and 7 hours respectively. 20µg of total protein (as the

optimal mass of protein for HCT116 cells, determined by the results in section 3.3.3.2) was used in triplicate wells for each sample group for the activity assay. Fluorescence values obtained were adjusted according to the negative control value, then standardised according to the 0 hour time point.

It was subsequently determined to ascertain the maximal AC activity inhibition achievable with carmofur at a single time point following incubation. The effect of drug dosing with a range of concentrations of carmofur (including the highest concentration achievable, whilst allowing for a final non-toxic DMSO concentration of 0.05%) at the 2 hour time point was studied. This time point minimised potential cell toxicity from a longer incubation, whilst likely achieving maximal activity inhibition, and the range of carmofur concentrations allowed for determination of an appropriately therapeutic dose. AC activity with 5-FU drug dosing was also compared at this stage, as this formed a key component of the intended direct comparison of radio-sensitisation with carmofur. An assumption was made that if 5-FU were to inhibit AC, then this would likely occur to some degree by or at the same time as carmofur.

Carmofur is soluble in DMSO to 50mM according to the manufacturer's safety datasheet, therefore the maximal final carmofur concentration achievable in media (with a final 0.05% DMSO concentration) is 25µM. This was applied to the cells in this experiment, alongside concentrations of 10, 1, 0.1, 0.01 and 0.001µM respectively, achieved by serial dilution in DMSO of the 50mM carmofur stock, prior to mixing with media. 5-FU (molecular weight 130.1g/mol, Sigma-Aldrich) is soluble in DMSO to 50mg/mL according to the manufacturer's safety datasheet, allowing for a stock solution of up to 384mM, and a potential maximal final incubation concentration of 192µM (again accounting for a maximal final DMSO concentration of 0.05%). This was considered excessively high in comparison with the maximal 25µM carmofur concentration being applied. Given 5-FU itself had not demonstrated inhibition of AC in SW403 cells at a concentration of 3µM (Realini *et al,* 2013), it was considered that test concentrations higher than this were appropriate, and final 5-FU concentrations applied to the cells were 100, 32 and 8µM. A 200mM stock solution of 5-FU was prepared by dissolving 48mg of the drug in 1845µL DMSO, yielding a 100µM concentration to be added to cells in the well, when 5µL is mixed with 10mL media. Other concentrations were achieved by serial dilution of the 200mM stock with DMSO (final DMSO concentration 0.05% in all treatment groups).

HCT116 cells were cultured and plated in 6-well plates as above, and the drug concentrations applied accordingly and incubated for 2 hours. Cell collection and sample preparation was performed according to the activity assay protocol. 20µg of protein from each sample group was used, with results again adjusted to account for background fluorescence. Fluorescence values were then normalised relative to a vehicle control sample group (0.05% DMSO in media), collected at the same time point to enable direct comparison.

Following this drug dose response analysis, it was considered appropriate to perform longer time-profile responses of AC activity inhibition across a range of potentially therapeutic concentrations of carmofur. 2, 4 and 8µM carmofur (ranging from non-toxic to relatively non-toxic as per the MTS data presented in chapter 4) were studied. HCT116 cells were seeded in 6-well plates as previously described, to enable cell groups exposed to these concentrations of carmofur to be collected at 2, 8 and 24 hours post incubation. Carmofur was dissolved in DMSO comparable with previous descriptions to yield the desired final concentrations in media (with a final DMSO concentration of 0.05%), with 0.05% DMSO vehicle control groups included at the respective time points.

It was also considered pertinent to quantify the effect of combined carmofur and 5-FU dosing on AC activity, given the original proteomic profiling (demonstrating differential AC expression separating responders and non-responders to neoadjuvant CRT) was in a patient group treated with capecitabine (as a 5-FU prodrug). It may be that carmofur (or another small molecule inhibitor of AC) in combination with standard 5-FU therapy enhances radio-sensitivity whereas carmofur (or isolated AC activity inhibition) does not.

A further AC activity assay was undertaken, with treatment groups being exposed to 2µM carmofur and 2µM 5-fluorouracil both individually and combined (maximum DMSO concentration 0.05% in all groups), compared against 0.05% DMSO treated vehicle control groups. These doses were selected as non-toxic concentrations both individually and when combined based on MTS proliferation data as detailed in chapter 4, and with increasing toxicity at higher concentrations. Cells were collected and processed as previously described, following incubation in the respective drug concentrations for 0.75, 1.5, 3 and 6 hours. A 20µg sample of protein from each treatment group was plated in triplicate for the purposes of the activity assay.

3.2.5.4 Small interfering RNA inhibition of acid ceramidase activity

siRNA was utilised to provide a more permanent inhibition of AC activity for the purposes of experimental modelling. The optimisation of siRNA dosing has been described in section 3.3.1 but it was necessary to evaluate the AC activity inhibition profile following application of siRNA, to ascertain the magnitude and timing of activity inhibition.

HCT116 cells in exponential growth phase in culture were collected and plated out in 6-well plates at a density of $5x10^5$ in 2mL of antibiotic-free media. Cells were incubated overnight to adhere prior to forward transfection with siRNA. For each transfected well, 4µL of Lipofectamine™ RNAiMAX in 200µL Opti-MEM® Reduced Serum Medium was mixed with 1.2µL of a 20µM stock of siRNA3 in 200µL Opti-MEM®. This mixture was incubated at room temperature for 15 minutes, before adding to each well and gently mixing (final siRNA concentration 10nM). Vehicle control groups underwent the same transfection process with the non-coding siRNA at the same concentration.

Following transfection, cell groups were collected at 24, 48 and 72 hours to assess for AC activity as previously described, again using 20µg protein per well on the activity assay plate.

3.2.6 Statistical analysis

Statistical analysis was undertaken using SPSS® Statistics version 22 (IBM®, New York, USA), with specific tests used as detailed in the relevant sections.

3.3 Results

3.3.1 Reverse Transcription Polymerase Chain Reaction Assessment of ASAH1 mRNA Expression

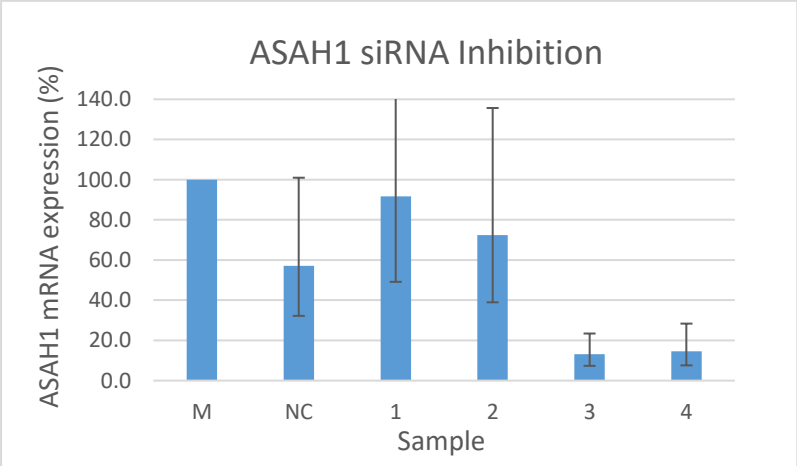

Figure 3.3 – siRNA inhibition of ASAH1 mRNA expression in HCT116 cells with the set of four siRNAs coding for AC (MQ-005228-01-0002, Dharmacon), numbered sequentially as samples 1-4 in the graph. siRNAs were applied at a final concentration of 20nM in the well, including a non-coding siRNA (NC, D-001206-13-05, Dharmacon), and incubated for 48 hours. M represents a non-transfected media only cell sample. Ct data has been obtained in triplicate RT-PCR sample reactions for each mRNA and used to calculate expression of the GoI relative to HK controls. Results are expressed as a percentage normalised to the non-transfected (M) sample, with error bars representing one standard deviation (SD).

Inhibition of AC mRNA expression was observed and considered significant with transfection of two of the four siRNAs targeting ASAH1 (siRNAs 3 and 4) as depicted in figure 3.3; mRNA expression with siRNA3 was calculated to be 13.1% of that of the non-transfected media only control and was selected for to be further validated and optimised.

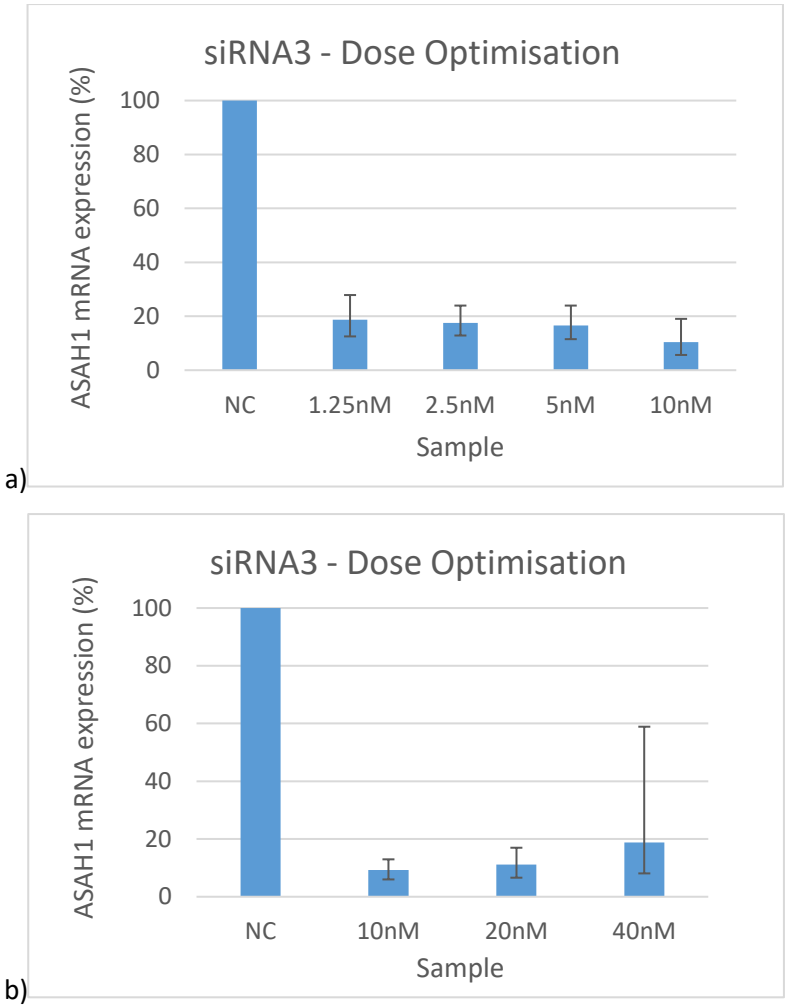

Figure 3.4 – Dose optimisation of siRNA3 transfection in HCT116 cells. ASAH1 mRNA expression was analysed by RT-PCR 48 hours after transfection, using 2µL Lipofectamine™ RNAiMAX per well across a range of siRNA3 concentrations in two experiments. Graph a) demonstrates mRNA expression with final siRNA3 concentrations in the range 1.25-10nM, compared to 10-40nM in graph b). Ct data has been adjusted relative to HK mRNA expression, with results in the charts expressed as a percentage and normalised to the non-coding siRNA vehicle control (NC). Error bars represent one SD of triplicate RT-PCR reactions for each treatment group.

Suppression of ASAH1 mRNA expression was observed with all siRNA3 concentration treatment groups (1.25-40nM) when compared to non-coding siRNA transfected cells as a vehicle control. Greatest suppression was observed with the 10nM concentration in both experiments, as depicted in figure 3.4. Although triplicate experiments were not performed across the range of doses, and therefore not statistically analysed, the 10nM concentration produced ASAH1 mRNA expressions of 10.4% and 9.3% when compared to vehicle control in the two experiments respectively. A lower concentration did not seem to have as great an effect, and interestingly, a higher concentration did not seem to have an increased effect.

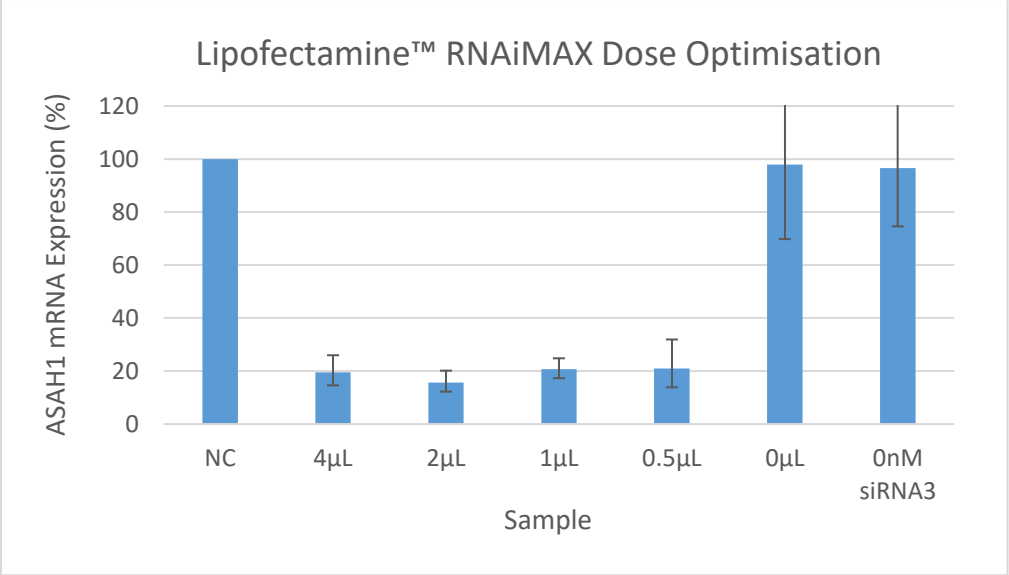

Figure 3.5 – Dose optimisation of Lipofectamine™ RNAiMAX in ASAH1 siRNA transfection in HCT116 cells. ASAH1 mRNA expression was quantified by RT-PCR 48 hours after siRNA transfection across a range of Lipofectamine™ RNAiMAX doses (0.5-4µL per well) in a 12-well plate, with a constant siRNA3 concentration (2nM). mRNA expression was also observed in treatment groups where the same transfection procedure was followed but in the absence of Lipofectamine™ RNAiMAX (0µL) and in the absence of siRNA3 with 2µL Lipofectamine™ RNAiMAX (0nM siRNA3). Ct data has been adjusted relative to HK mRNA expression, with results in the charts expressed as a percentage and normalised to the non-coding siRNA vehicle control (NC). Error bars represent one SD of triplicate RT-PCR reactions for each treatment group.

ASAH1 mRNA expression was universally reduced compared to vehicle control (NC), when the transfection process was undertaken across a range of Lipofectamine™ RNAiMAX doses (0.5-4µL). A 1:600 ratio as the final concentration in the well in subsequent transfections was selected (represented by the 2µL sample in figure 3.5), as this concentration is at the lower limit of the manufacturer's recommendation for use in HCT116 cells (http://tools.thermofisher.com/downloads/HCT116_RNAiMAX.pdf) and produced at least equivalent results. There was no difference in ASAH1 mRNA expression between non-coding siRNA transfected cells, and when the transfection process was followed but in the absence of either Lipofectamine™ RNAiMAX or siRNA (NC, 0µL and 0nM siRNA3 treatments groups respectively as shown in figure 3.5).

		Ct Value				
		ASAH1	**ACTB**	**GAPDH**	**2^-ΔΔCt**	**% Expression**
1	**M**	28.43	25.70	29.01	1.00	**100.0**
	NC	24.24	21.49	19.82	5.70	**17.5**
	siRNA3	29.65	23.19	22.07	61.82	**1.6**
2	**M**	24.92	20.45	20.89	1.00	**100.0**
	NC	23.66	19.26	18.17	1.61	**62.0**
	siRNA3	26.68	19.17	17.75	15.62	**6.4**
3	**M**	21.59	19.77	17.73	1.00	**100.0**
	NC	22.16	18.27	17.85	2.39	**41.8**
	siRNA3	26.66	19.82	18.66	23.92	**4.2**

Table 3.3 – Mean Ct values (of triplicate replicates) for ASAH1, ACTB and GAPDH observed at RT-PCR 48 hours following siRNA transfection targeting ASAH1 in HCT116 cells in triplicate experiments (1, 2 and 3). 10nM of coding (siRNA3), and non-coding (NC) siRNA was present in the final transfection mixtures in each experiment and compared to untreated cells in culture medium only (M) as the reference sample. Relative ASAH1 gene expression is calculated using $2^{-\Delta\Delta Ct}$ and expressed as a percentage of the reference sample for each experiment.

Crude mean Ct values in the ranges demonstrated in table 3.3 (all of which are below 30) are strong positive reactions indicative of abundant target nucleic acid in the samples.

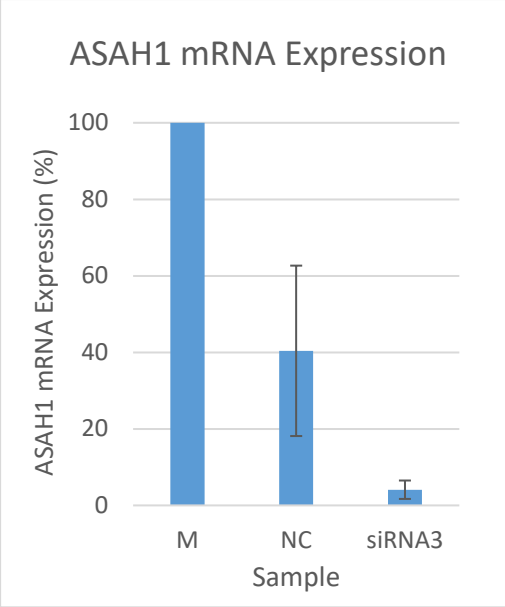

Figure 3.6 – ASAH1 mRNA expression in HCT116 cells 48 hours following siRNA transfection. The depicted results are mean values of the percentage expressions from the triplicated data demonstrated from the experiments in table 3.3, for cells in culture medium only (M, as an untreated control), and those transfected with non-coding (NC, as a vehicle control for the transfection) and the chosen ASAH1 coding (siRNA3) siRNAs at 10nM concentration. Error bars represent one standard deviation of the means.

ASAH1 mRNA expression in HCT116 cells following siRNA transfection with siRNA3 was observed to be significantly lower when compared to both a non-transfected cell population (4.1% vs 100%, $p<0.001$), and to a non-coding siRNA transfected cell population (4.1% vs. 40.4%, $p=0.032$) as depicted in figure 3.6. Interestingly there was a statistically significant difference between the non-coding siRNA transfected and non-transfected cell populations (40.4% vs. 100%, $p=0.003$), implicating the transfection process itself. Statistical analysis has been undertaken using one-way ANOVA followed by Tukey's test.

In spite of a seeming off-target effect with siRNA-NC (or the transfection process), it was considered that in view of significant inhibition of mRNA expression following transfection with siRNA3 when compared with siRNA-NC, further experiments can be interpreted accounting for this effect.

3.3.2 Western Blotting for Acid Ceramidase

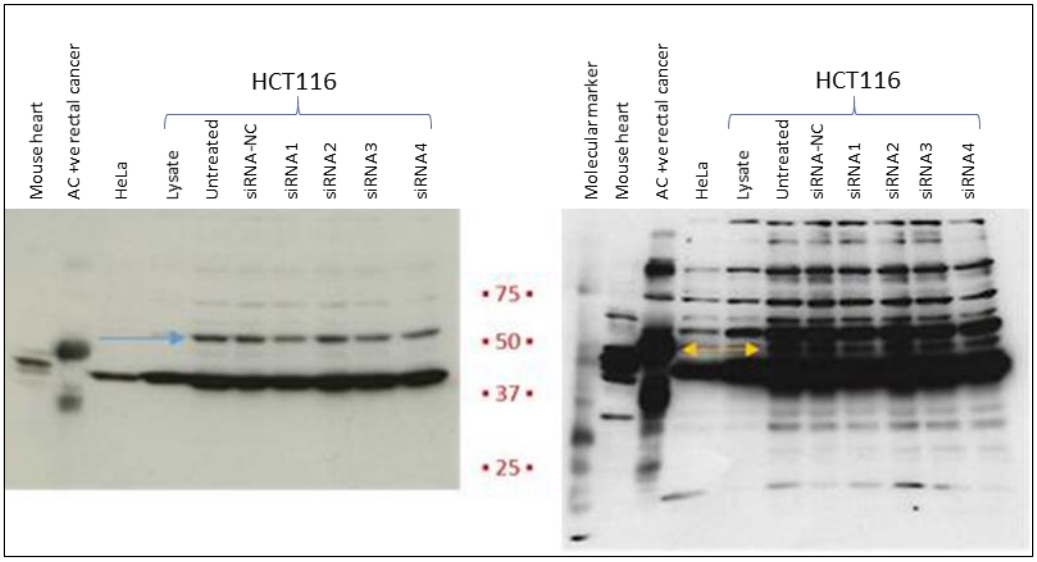

Figure 3.7 – Whole membrane films of a Western blot performed on a 10% SDS-PAGE gel, with ab74469 (Abcam, rabbit polyclonal) anti-AC primary antibody at a concentration of 1:2500, following ASAH1 siRNA transfection in HCT116 cells. Four different siRNAs targeting ASAH1 were incubated at 20nM final concentration for 48 hours. 15µg of extracted protein per sample was prepared and loaded, along with vehicle and positive controls respectively. The images demonstrate film exposures at two time points for the same blot; 2s on the left, and 60s on the right, with band molecular weight (kDa) indicated in red centrally. The blue arrow in the left image highlights a band at around 53kDa, thought to potentially be the precursor AC protein, whereas the orange arrow in the right image demonstrates the band in the HCT116 cells of the same molecular weight as the dominant band originating from the AC positive rectal cancer.

The AC protein originates as a 53kDa precursor molecule, which is cleaved into an active α sub-unit of 13kDa, and a 40kDa β sub-unit (Koch *et al*, 1997). The Western blot in figure 3.7 shows two dominant bands at around the 53 and 40kDa molecular weights in the HCT116 cell samples in the film taken at 2s on the left. Of particular interest in this blot following siRNA transfection, are the bands at ≈53kDa highlighted by the blue arrow representing siRNAs 1, 3 and 4 from the set of four siRNAs targeting ASAH1. It was initially thought that this may represent knockdown of the protein following transfection, albeit with only a partial response as the half-life of AC auto-cleavage into its respective sub-units is 17 hours (Shtraizent *et al*, 2008). Neither of these bands is at the exact molecular weight of the dominant bands demonstrated from the positive controls (mouse heart, which replicates the positive control blot for this antibody as demonstrated on the manufacturer's website http://www.abcam.com/asah1-antibody-ab74469.html, or the AC positive rectal cancer).

The dominant band demonstrated by the AC positive rectal cancer at ≈50kDa, highlighted to the left of the orange arrow in the right image, becomes visible in the HCT116 cell samples to the right of the arrow at this intended prolonged exposure. This band is difficult to interpret however, as the film becomes over-exposed from the two dominant bands seen in the 2s exposure on the left. Furthermore, subsequent Western blots performed with this antibody (Abcam, ab74469) following siRNA3 transfection with optimised conditions as per the RT-PCR data, did not replicate any reduction in band density. Recognition of the AC protein fragment was equally not achieved with this antibody and it was therefore considered too non-specific to pursue further for Western blotting with HCT116 cells.

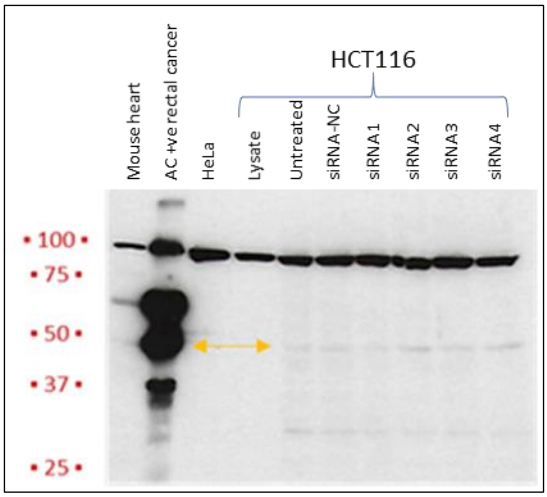

Figure 3.8 – Whole membrane film of a Western blot performed on a 10% SDS-PAGE gel, with ab174828 (Abcam, RabMAb®, rabbit monoclonal) anti-AC primary antibody at a concentration of 1:1000, following ASAH1 siRNA transfection in HCT116 cells. Sample loading in the blot is a replicate of that described in the detail for figure 3.7, for the same samples. The molecular weights of protein bands are indicated in red to the left of the film, which was exposed for 60s. The orange arrow indicates a faint band in the HCT116 cell samples at the same molecular weight as a dominant band in the AC positive rectal cancer just under the 50kDa marker.

The datasheet provided for the antibody used to produce the Western blot in figure 3.8 (Abcam, RabMAb®, ab174828) demonstrates a band at ≈65kDa but states the predicted band size is 45kDa (http://www.abcam.com/asah1-antibody-epr12108-ab174828.html#description_images_1). In the demonstrated blot the most dominant band in the AC positive rectal cancer sample is ≈65kDa but without any bands visible in the HCT116 cell samples. The most dominant band in the cell samples is ≈100kDa, where strong bands are also present in both positive controls but it not possible to conclude that this band

represents AC as it is likely too high molecular weight, and there is equally no evidence of protein knockdown in the siRNA treated HCT116 cell samples. The band highlighted in orange is potentially at the 45kDa molecular weight as stated on the antibody datasheet as being the predicted band weight for AC but again there is no conclusive evidence of protein knockdown in the siRNA treated HCT116 cell samples.

Previous optimisation blots with this antibody had not demonstrated better specificity to ascertain that any band truly represented AC, and recognition of the AC protein fragment was again not achieved. Further optimisation of the antibody for its use in Western blotting with HCT116 cells was not pursued.

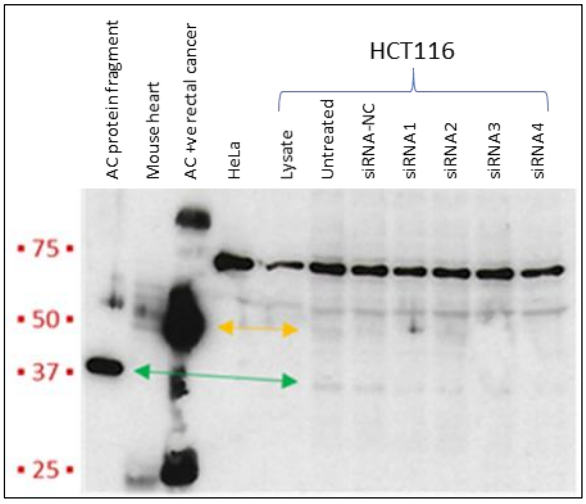

Figure 3.9 – Whole membrane film of a Western blot performed on a 10% SDS-PAGE gel, with BD612302 (BD Transduction Laboratories, mouse monoclonal) anti-AC primary antibody at a concentration of 1:500, following ASAH1 siRNA transfection in HCT116 cells. Sample loading in the blot is a replicate of that described in the detail for figures 3.7 and 3.8, for the same samples, with the addition of the AC protein fragment. The molecular weights in red to the left of the film indicate the position of the standards of the molecular weight marker, and the film was exposed for 60s. The orange arrow indicates bands in the HCT116 cell samples at the same molecular weight as the dominant band in the AC positive rectal cancer, whereas the green arrow does the same but for the AC protein fragment.

The antibody used to produce the Western blot in figure 3.9 was selected from one of the few papers in the literature where use of a specific anti-AC antibody has been detailed (Liu *et al*, 2006), after not establishing specificity for AC in the HCT116 cells with the previously described antibodies. The product datasheet describes the identification a band representing AC at 13kDa, which will represent the α sub-unit of the protein

(http://www.bdbiosciences.com/eu/reagents/research/antibodies-buffers/cell-biology-reagents/cell-biology-antibodies/purified-mouse-anti-acid-ceramidase-23acid-ceramidase/p/612302). The 10% SDS-PAGE gel depicted in figure 3.9 was prepared in parallel with those demonstrated in figures 3.7 and 3.8 and did not facilitate interrogation for AC at the 13kDa molecular weight but does demonstrate some encouraging observations.

Firstly, the AC protein fragment has been identified at ≈37kDa. This is at the predicted molecular weight from the product datasheet (http://www.abcam.com/human-asah1-protein-fragment-ab114948.html), with a corresponding faint band in the HCT116 cell samples at the same molecular weight, as indicated by the green arrow in figure 3.9. In isolation this band does not provide evidence of protein knockdown following siRNA transfection but there is a suspicion of reduced expression in this band representing siRNAs 1, 3 and 4 from the set of four siRNAs targeting ASAH1, as described in section 3.2.2. Complimentary to this is the appearance of similarly reduced protein expression in the faint band ≈50kDa in the same lanes, at the same molecular weight as the most dominant band in the AC positive rectal cancer sample, as indicated by the orange arrow in the image. It was considered that these bands may represent the 53kDa precursor AC protein, and the 40kDa β-subunit. Prolonged film exposure to the membrane did not produce improved development of these bands however.

The most dominant band in the cell samples at ≈70kDa is of uncertain aetiology, and the Western blot was not probed for β-actin to formally validate equivalent protein loading. In spite of this, further optimisation of the antibody was deemed to be justified, and was performed on 12% SDS-PAGE gels to facilitate visualisation of a potential 13kDa band, and in combination with an optimised transfection process with siRNA3, as previously described.

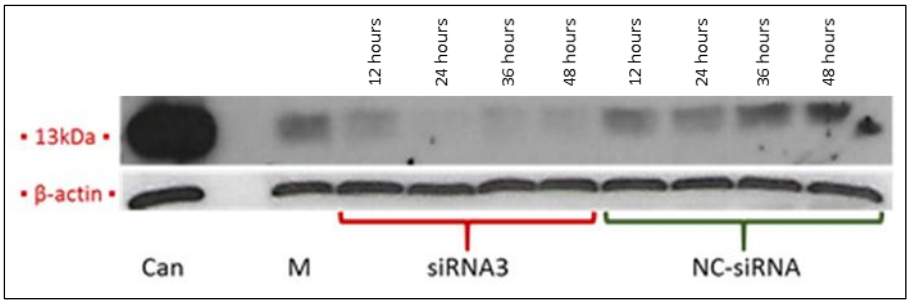

Figure 3.10 – Western blot on a 12% SDS-PAGE gel with BD612302 (BD Transduction Laboratories, mouse monoclonal) anti-AC primary antibody at a concentration of 1:250, following siRNA3 transfection of HCT116 cells. Protein expression was assessed at 12, 24, 36 and 48 hours following transfection with 10nM siRNA3 and a non-coding siRNA, with a sample at each of these time points demonstrated from left to right in the bracketed treatment groups in the image. The membrane was cut to probe for AC specifically at 13kDa, and β-actin was equally assessed as a protein loading control. Untreated cells in culture medium (M), and an AC positive rectal cancer sample (Can), were also utilised as reference and positive controls respectively.

Protein expression in the bracketed siRNA3 treatment samples is reduced at the predicted 13kDa molecular weight in figure 3.10, when compared to non-coding siRNA treated cells at all time points, and the reference control (M). There is equally very strong expression in the AC positive rectal cancer sample at this molecular weight, compared to all cell samples and relative to comparable β-actin expression across all samples. In combination with the appearance of reduced protein expression following ASAH1 siRNA transfection, it is reasonable to conclude that the protein band at 13kDa does indeed represent AC.

On densitometry analysis, the protein expression of this AC band at 13kDa following siRNA3 transfection in HCT116 cells was 57.2, 18.1, 17.3 and 10.8% at 12, 24, 36 and 48 hours respectively, when compared to protein expression in non-coding siRNA treated cells (and following normalisation to β-actin expression).

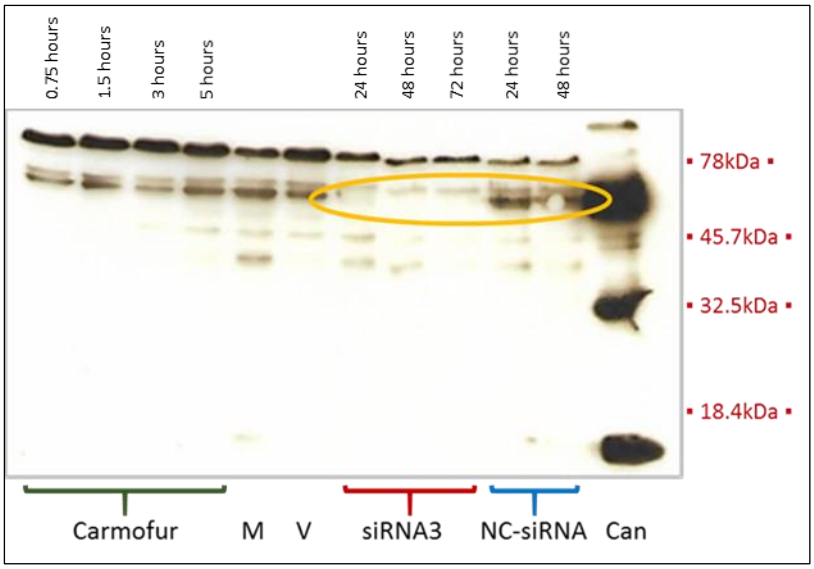

Figure 3.11 – Whole membrane film of a Western blot on a 12% SDS-PAGE gel with BD612302 (BD Transduction Laboratories, mouse monoclonal) anti-AC primary antibody at a concentration of 1:250. The lanes in the blot from left to right depict HCT116 cell samples treated with 2µM carmofur at 0.75, 1.5, 3 and 5 hours (Carmofur), an untreated cell sample in culture medium only (M), 0.05% DMSO drug vehicle control treated cell sample (V), siRNA3 (final concentration 10nM) transfected cell samples at 24, 48 and 72 hours (siRNA3), non-coding transfected cell samples at 24 and 48 hours (NC-siRNA), and an AC positive rectal cancer sample (Can). Molecular weight of the bands is indicated by the figures in red to the right of the image – in this instance the molecular weight marker used was the Kaleidoscope™ Prestained Standards (Bio-Rad). The highlighted bands (ringed in orange) in the image demonstrate a relative absence of protein in siRNA3 transfected cells compared to non-coding transfected cells, at the same molecular weight as a dominant band in the AC positive rectal cancer sample.

It was considered pertinent to assess a whole membrane blot (incorporating the 13kDa band) in order to further validate the specificity of this antibody. This was also an opportunity to perform a parallel assessment of protein expression after dosing the HCT116 cells with carmofur, alongside siRNA3 transfection.

The striking feature in the Western blot depicted in figure 3.11 is the relative absence of three bands pertaining to siRNA3 transfected HCT116 cells, compared to non-coding siRNA transfected cells (as highlighted by the orange ring), at ≈53kDa and of the same molecular weight as a dominant band in the AC positive rectal cancer. This molecular weight band is therefore highly likely to represent the 53kDa AC precursor protein.

The 13kDa band observed in figure 3.9 is not visualised in this blot in the cell samples but the dominant band in the positive control sample (Can) remains strongly visible at this weight. The most dominant band across the cell samples (but that is not visible in the Can positive control) runs at ≈78kDa. Whilst both these observations potentially suggest lower antibody

specificity, with the relative absence of the 53kDa band in siRNA3 transfected samples replicating and complimenting previous results, it remains reasonable to conclude that the antibody is still able to determine reduced AC protein expression.

In relation to the samples from cells dosed with carmofur there may be a reduced protein expression of the 53kDa band at the earlier time points demonstrated, relative to untreated (M) and vehicle (V) control samples. Protein loading for this blot was performed identically and in parallel to the cut membrane demonstrated in figure 3.12, where equivalent β-actin loading (at 42kDa) can be observed.

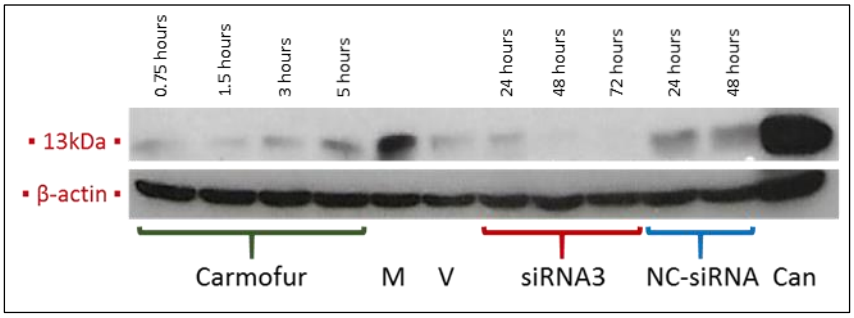

Figure 3.12 – Western blot from a 12% SDS-PAGE gel demonstrating AC protein expression at 13kDa in HCT116 cells following drug inhibition with carmofur and siRNA transfection, and respective vehicle controls. The membrane was incubated with BD612302 (BD Transduction Laboratories, mouse monoclonal) anti-AC primary antibody at a concentration of 1:250. The lanes in the blot from left to right depict HCT116 cell samples treated with 2μM carmofur at 0.75, 1.5, 3 and 5 hours (Carmofur), an untreated cell sample in culture medium only (M), 0.05% DMSO drug vehicle control treated cell sample (V), siRNA3 (final concentration 10nM) transfected cell samples at 24, 48 and 72 hours (siRNA3), non-coding transfected cell samples at 24 and 48 hours (NC-siRNA), and an AC positive rectal cancer sample (Can).

Reduced AC expression at 13kDa was observed in carmofur treated HCT116 cells at 0.75, 1.5 and 3 hours following incubation, when compared to 0.05% DMSO vehicle control. Expression on densitometry (normalised to β-actin) was 53.0, 24.6 and 69.9% of vehicle control expression at these time points respectively and returned to an above baseline 125.3% at 5 hours following incubation. These findings could be artefactual but may suggest carmofur interacts with the α-subunit of the AC protein, and may suggest inhibition with 2μM carmofur to be optimal at some point between 0.75 and 3 hours following incubation.

Reduced AC expression is again demonstrated subsequent to siRNA transfection. A band is not visible for the sample collected 72 hours following transfection although there is no corresponding non-coding siRNA transfected vehicle control sample for comparison. In spite

of this, isolated densitometry analysis of the 24 and 48 hour time points (normalised to β-actin) demonstrate likely significant reduction in AC expression (quantified as 17.5 and 4.3% respectively), relative to control values.

The relative expression on densitometry of the 13kDa AC protein at basal level in HCT116 cells is 28.7%, when compared to the AC positive rectal cancer. This basal level is represented by the untreated cells in culture medium only (M), following normalisation to respective β-actin expression, and combines data from the Western blots depicted in figures 3.10 and 3.12. The M band in figure 3.12 is seemingly disproportionately prominent, when compared to other bands representing controls and in respect to previous blots, and so may even overestimate the basal expression. The strikingly dominant bands from the cancer (Can) sample, the initial difficulty of detecting AC on Western blotting, and considering the band density detected with the BD612302 mouse monoclonal antibody, may indicate a relatively low basal AC expression in HCT116 cells. The functional significance of this potentially low expression remains to be determined.

3.3.3 Acid Ceramidase Activity Assay

3.3.3.1 Umbelliferone calibration for acid ceramidase activity assay

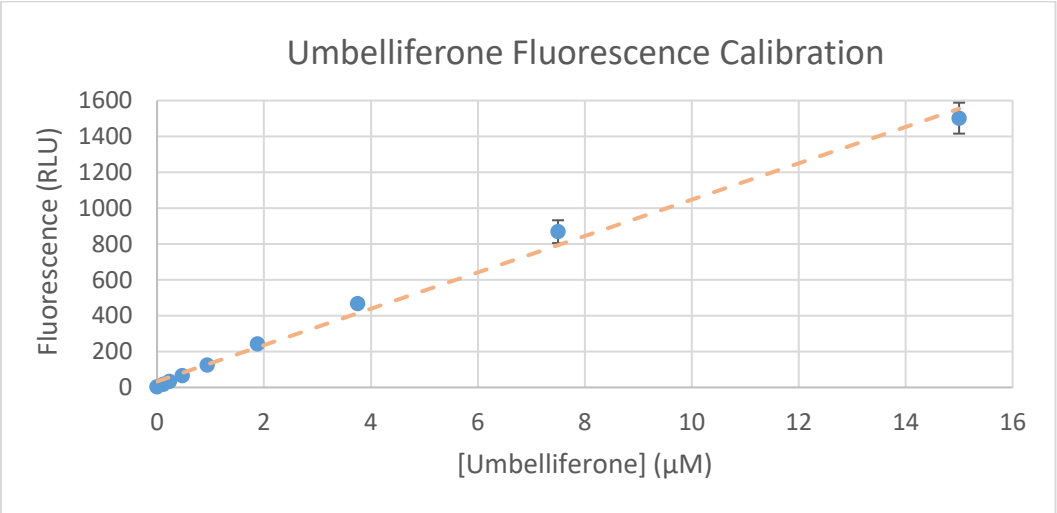

Figure 3.13 – Calibration of umbelliferone fluorescence. Umbelliferone was diluted in ethanol / 25mM sodium acetate buffer (pH 4.5) at a range of concentrations (0-15µM). Fluorescence at these concentrations was measured following the addition of methanol and 100mM glycine/sodium hydroxide buffer (pH 10.6). Mean values are plotted (blue dots), with error bars representing the standard deviation of triplicate experiments. The dashed line represents a line of best fit (linear) across the data points.

Fluorescence was observed to increase with increasing umbelliferone concentration as depicted in figure 3.13, and with very strong linear correlation ($r=0.997$, $p<0.001$, Pearson correlation), thus validating the use of umbelliferone as a fluorescent marker in the assay.

3.3.3.2 Protein loading calibration for acid ceramidase activity assay

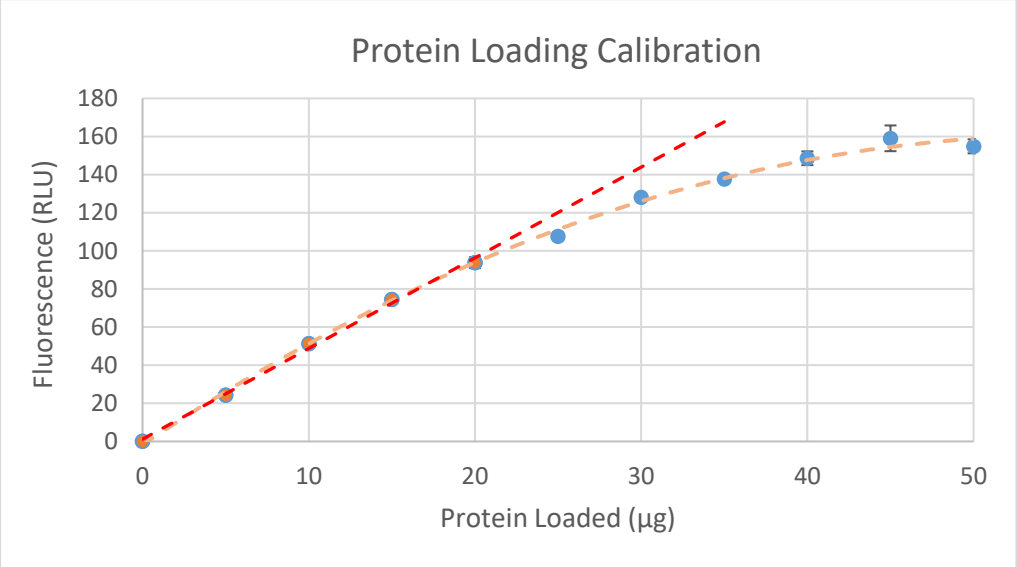

Figure 3.14 – Calibration of protein loading for AC activity in HCT116 cells. Protein samples derived from untreated HCT116 cell lysate were assessed for AC activity across a range of protein masses (0-50µg). Fluorescence was measured and mean values plotted (blue dots), with error bars representing the SD of triplicate samples. Values have been adjusted according to the background negative control sample, so that 0µg protein = 0 fluorescence. The orange dashed line represents a line of best fit across all data points, plotted against a red dashed line of best fit (linear and extrapolated) pertaining to 0-20µg protein loading.

Fluorescence was equally observed to increase with increased protein loading. There was a very strong linear correlation with a protein mass up to 20µg ($r=0.998$, $p<0.001$, Pearson correlation), as depicted by the extrapolated red dashed line in figure 3.14. A further increase in protein load resulted in an increase in fluorescence but this increase started to plateau above 40µg of protein, as visualised with the orange dashed line. The finite mass of substrate (and therefore umbelliferone) used in the activity assay would appear to be a rate limiting step, certainly when the mass of protein sample originating from untreated HCT116 cell lysate is above 30µg. It was therefore determined that protein loading for subsequent activity assay experiments should be 20µg. The crude fluorescence values for this calibration (≤160 relative light units (RLU)), is well within the linear range observed with the umbelliferone calibration (≤1500 RLU), and it is therefore appropriate to conclude that a proportional increase in protein loading (up to 20µg) yields a proportional mass of umbelliferone from the Rbm14-12 substrate due to AC activity, producing a proportional increase in fluorescence.

3.3.3.3 Chemotherapeutic inhibition of acid ceramidase activity

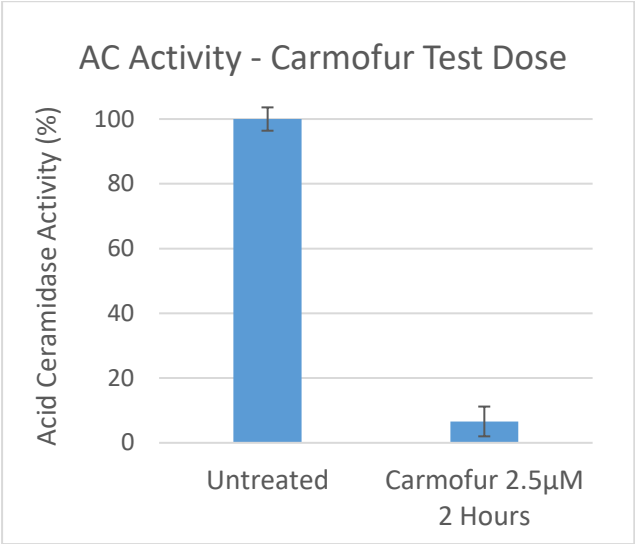

Figure 3.15 – AC activity in HCT116 cells 2 hours after dosing with 2.5µM carmofur, compared to untreated cells. Fluorescence was measured in triplicate samples with values adjusted for background fluorescence and then according to the untreated samples. Mean values are plotted, with error bars representing one SD.

AC activity in HCT116 cells 2 hours after dosing with 2.5µM carmofur was observed to be 6.6% (+/- 4.6%) when compared to untreated cells as depicted in figure 3.15. Statistical analysis was not undertaken as three independent experiments were not performed but the result was considered to represent sufficient evidence of AC activity inhibition in cells dosed with carmofur, to justify further experiments.

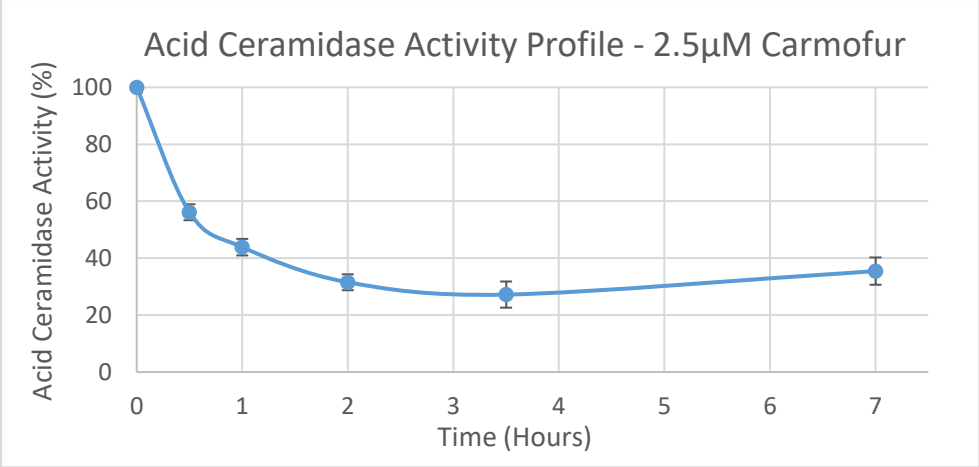

Figure 3.16 – Time profile of AC activity in HCT116 cells in response to dosing with 2.5µM carmofur. Fluorescence was measured in triplicate samples with values adjusted for background fluorescence and then normalised according to the 0-hour time point. Mean values are plotted, with error bars representing one SD.

Inhibition of AC activity was observed in HCT116 cells at the first time point, 30 minutes after incubation in 2.5µM carmofur (figure 3.16). Maximal activity inhibition occurs at and after 2 hours, with activity at 27.2% of baseline observed 3.5 hours after incubation. AC activity seems to increase subsequently, although activity was significantly inhibited at all time points compared to baseline ($p<0.001$, one-way ANOVA followed by Tukey's test).

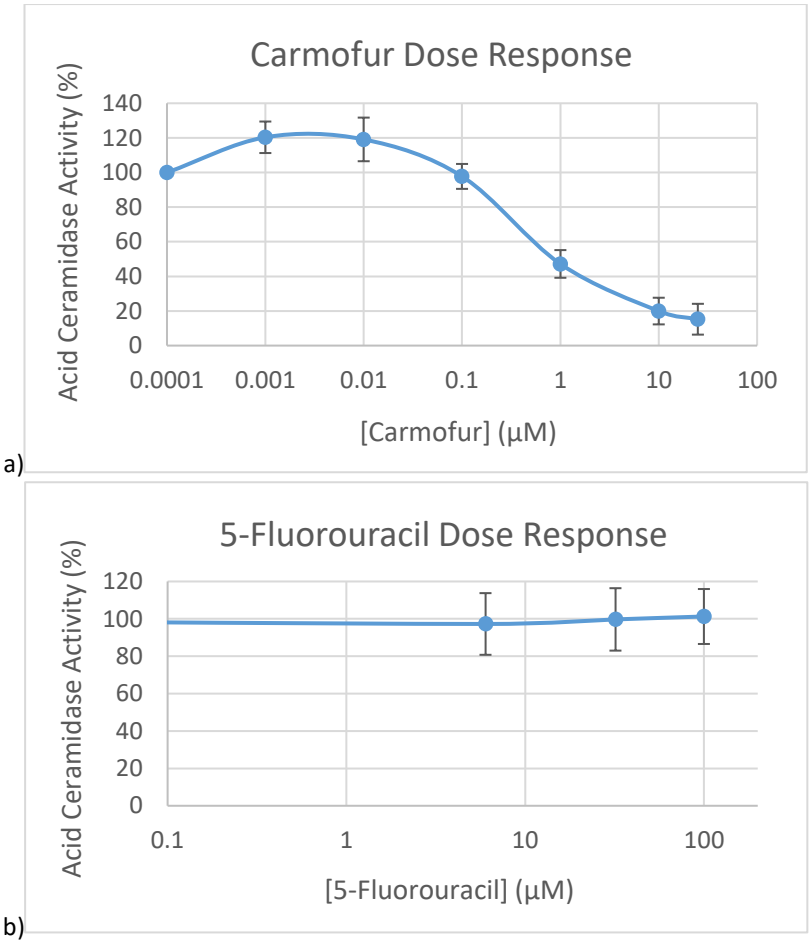

Figure 3.17 – Drug dose responses of AC activity in HCT116 cells in relation to carmofur (a) and 5-FU (b). Fluorescence was measured in triplicate samples at 2 hours, following incubation with the respective drugs at the determined concentrations. Values were adjusted for background fluorescence, and then standardised relative to a vehicle control group (cells treated with 0.05% DMSO). Mean values are plotted, with error bars representing one SD.

The drug dose responses presented in figure 3.17 demonstrate the following observations. There was a significant increase in AC activity observed at very low dose carmofur incubation (0.001 and 0.01µM doses, $p<0.001$), which returned to baseline levels at 0.1µM incubation ($p=0.988$), when compared to the 0.05% DMSO vehicle control groups. Higher carmofur concentrations at and above 1µM resulted in significant AC activity inhibition being observed, when compared to the control samples ($p<0.001$). There was no statistically significant difference in AC activity inhibition between the 10µM and 25µM carmofur treated cell groups ($p=0.724$), therefore treatment above 10µM (which could equally be toxic) was considered excessive. Statistical analysis of carmofur dose response here was performed using one-way ANOVA followed by Tukey's test. Incubation with 5-FU had no effect on AC activity at any of the investigated drug concentrations, with no significant differences between groups ($p=0.738$) on one-way ANOVA.

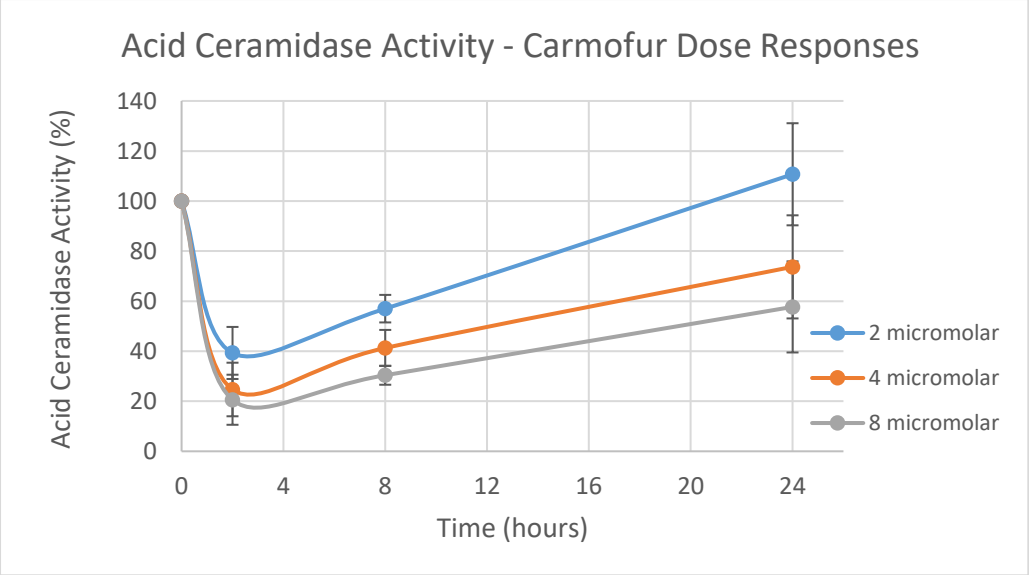

Figure 3.18 – AC activity profiles in relation to potentially therapeutic doses of carmofur. HCT116 cells were exposed to carmofur at doses of 2, 4 and 8µM concentrations respectively, and AC activity was measured at 2, 8 and 24 hours. Fluorescence values obtained from triplicate measurements were adjusted according to the negative control sample, and then normalised to the fluorescence obtained from the 0.05% DMSO vehicle control sample taken at the respective time point. Mean values have been plotted, and error bars represent one SD.

The profiles of AC activity in HCT116 cells in the different carmofur concentration treatment groups follow the same pattern (figure 3.18), albeit with increasing inhibition of AC activity with increasing carmofur concentration. Maximal inhibition of activity occurred at the 2-hour time point in all treatment groups (39.3%, 24.7% and 20.6% with 2, 4 and 8µM carmofur respectively). Subsequent AC activity began to return to that of control sample levels. At 24 hours post incubation with carmofur, AC activity had returned to baseline (0.05% DMSO vehicle control treatment group levels) in the 2µM carmofur treatment group but inhibition of activity persisted with 4 and 8µM treatment groups when compared to controls. The experiment was not replicated, due to the logistical and financial constraints of using the activity assay, and therefore statistical analysis has not been undertaken – the pattern of response is consistent with previous experiments however, and appears to confirm optimal inhibition with carmofur to occur at or soon after 2 hours post incubation.

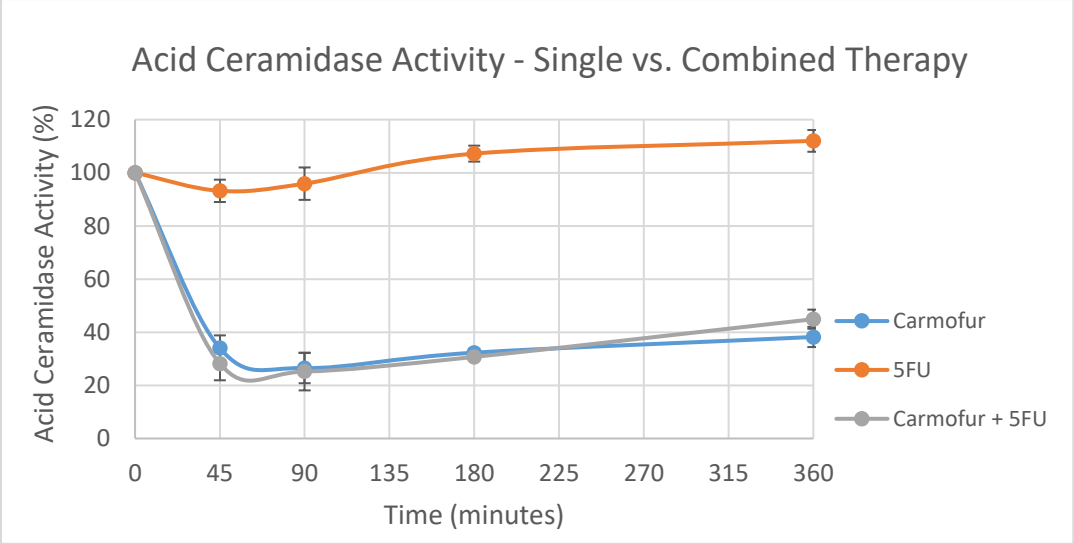

Figure 3.19 – The effect of combined chemotherapeutic dosing on AC activity in HCT116 cells. Carmofur and 5-FU were applied individually and in combination to treatment groups at 2µM concentration. Measured fluorescence values pertaining to AC activity were adjusted to account for background controls and are normalised to the 0.05% DMSO vehicle control measurements obtained at the respective time points. Plotted data points represent the mean of triplicate measurements, with error bars representing one SD.

The profile of AC inhibition in HCT116 cells with carmofur is again comparable to other experiments (figure 3.19). Application of 5-FU in isolation did not appear to significantly alter AC activity, nor did it appear to have a significant synergistic effect when combined with carmofur. Peak inhibition of activity was observed at the 1.5-hour time point, and although activity was comparable to this at 3 hours, it would appear that inhibition of activity is beginning to reduce at this time. The experiment was not replicated as the profiles of AC inhibition with carmofur are consistent with previous results, and for the logistical and financial constraints in using the activity assay, therefore statistical analysis has equally not been undertaken.

There is slight variability in the time of peak inhibition with carmofur (observed by the results depicted in figures 3.16, 3.18 and 3.19) but is considered to overall represent that significant AC inhibition appears to be maximally present at and shortly after 2 hours following incubation.

3.3.3.4 Small interfering RNA inhibition of acid ceramidase activity

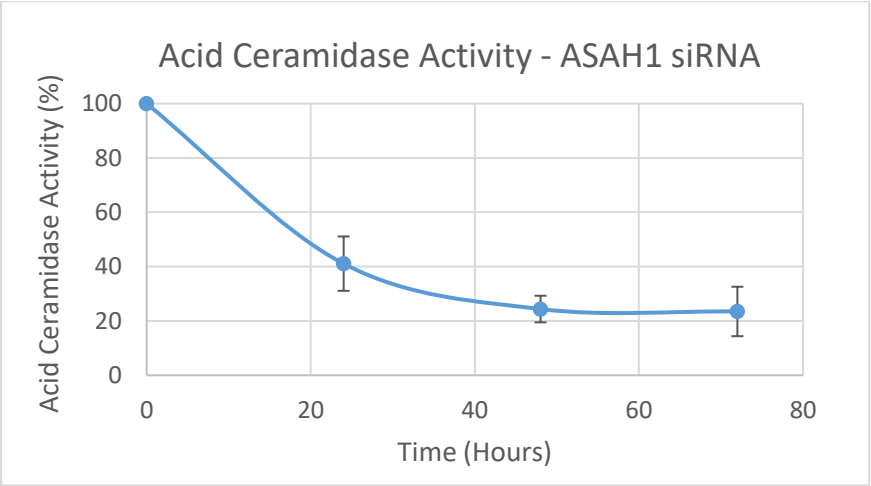

Figure 3.20 – The effect of siRNA3 on AC activity in HCT116 cells. AC activity was quantified at 24, 48 and 72 hours subsequent to forward transfection with siRNA3 at 10nM. Fluorescence values have been adjusted to account for background control results, and then normalised to the non-coding siRNA value for each time point. Data points represent the mean of triplicate samples, with error bars representing one SD.

Application of siRNA3 at 10nM final concentration, inhibits AC activity in HCT116 cells as depicted in figure 3.20. This inhibition is evident at 24 hours but greater inhibition is observed at and after 48 hours (24.4% of the vehicle control activity), subsequent to which the effect appears to plateau. Later time points were not assessed to determine when normalisation of activity inhibition occurs.

Triplicate samples were obtained from different experiments at 72 hours following siRNA3 transfection. Mean AC activity in siRNA3 transfected groups was 15.5% of that observed in non-coding siRNA transfected groups (95% CI, 8.1-22.9%) at this time point, which is statistically significantly reduced ($p<0.001$). There was no difference in AC activity between the non-coding siRNA transfected groups and untreated cells at this time point (100% vs 88.6% respectively, $p=0.18$). Statistical analysis has again been performed using one-way ANOVA followed by Tukey's test.

3.4 Discussion

3.4.1 Summary of Aims

The aims of the experimental work presented were to establish inhibition of AC in the HCT116 CRC cell line, and to provide quantitative evidence of this inhibition. siRNA transfection and pharmacological inhibition with carmofur were performed. ASAH1 mRNA expression following siRNA transfection was quantified using RT-PCR, AC protein expression following transfection and drug dosing was assessed by Western blotting, and the functional effects of treatments were quantified using a direct AC activity assay. Dosing parameters in terms of reagent concentrations and timing of application were profiled using the activity assay to determine optimal and maximal inhibition of AC in order to facilitate the further development of radio-sensitivity modelling in the cell line.

3.4.2 Summary of Results

ASAH1 mRNA expression on RT-PCR was initially used to determine that siRNA3 produced the greatest effect of the set of four siRNAs obtained. Subsequent experiments produced consistent suppression of mRNA expression with use of siRNA3, and dosing parameters for the siRNA and Lipofectamine™ RNAiMAX were optimised. A 10nM concentration of the siRNA in the final transfection mix was optimised, producing suppression of mRNA to 4.1% of that of an untreated cell population ($p<0.001$) 48 hours after transfection.

The non-coding siRNA transfected cells also displayed reduced ASAH1 mRNA expression to 40.4% of that of the untreated cell population ($p=0.003$) at 48 hours. This was demonstrated to likely be due to the presence of Opti-MEM® Reduced Serum Medium, and not the other transfection reagents, and suggests this product is activating alternative pathways that are then affecting AC expression, for example apoptosis, growth arrest or senescence as discussed.

The effect of ASAH1 siRNA transfection was ultimately used to determine the specific bands that represent AC on Western blotting, in combination with appropriate positive control samples. Reduced band expression was observed at ≈53kDa and ≈13kDa across the blots with the mouse monoclonal antibody from BD Biosciences (BD612302), representing the molecular weights of the precursor AC protein, and the α-subunit. The protein expression of AC following siRNA transfection was assessed semi-quantitatively with densitometry but not replicated sufficiently to allow for statistical analysis. Interpretation of the densitometry analysis from the Western blots depicted in figures 3.10 and 3.12 however may suggest protein expression of AC 24 and 48 hours after transfection with siRNA3 to be 17.8% and 7.6% respectively.

Protein expression of AC subsequent to dosing with carmofur was also able to be assessed on Western blotting when relevant bands had been determined. Alterations in band densities were potentially observed at ≈53 and ≈13kDa. Densitometry expression of the 13kDa subunit was 53.0%, 24.6%, 69.9% and 125.3% at 0.75, 1.5, 3 and 5 hours following 2μM carmofur dosing in the HCT116 cells. These data were not replicated sufficiently for statistical analysis but may represent carmofur interaction with the α-subunit of AC, and are consistent with the AC activity assay data.

The functional effect of siRNA3 transfection and pharmacological inhibition of AC was quantified by direct activity assay. The assay was validated for its use of umbelliferone as a fluorescent marker, and optimised in the HCT116 cells for protein loading. A very strong linear correlation was observed between umbelliferone concentration and fluorescence on calibration ($r=0.997$, $p<0.001$), and between protein loading up to 20μg and fluorescence in assay optimisation ($r=0.998$, $p<0.001$).

Maximal AC activity inhibition on assay was quantified at 15.5% of the vehicle control value 72 hours following siRNA3 transfection ($p<0.001$). Dosing the HCT116 cells with carmofur equally produced a significant AC activity inhibition of 15.2% albeit with a potentially toxic 25μM concentration. Activity inhibition with carmofur occurred maximally at or soon after 2 hours following drug incubation dependent on the experimental run performed. Significant activity inhibition persisted 8 hours following drug incubation but had normalised by 24 hours with a 2μM carmofur dose. 5-FU produced no discernible inhibition of AC activity, and there was no additive effect of combined therapy.

3.4.3 Strengths and Limitations

The data presented to demonstrate expression and activity of AC encompass genomic mRNA expression, protein expression and protein activity, i.e. from post-transcriptional to functional level. There are consistencies both within and between the two treatment modalities applied to the HCT116 cells (siRNA transfection and pharmacological inhibition) from RT-PCR mRNA expression, protein expression on Western blotting, and protein activity on direct assay, thus providing cross-validation of the detection techniques as well as the methods of AC inhibition.

RT-PCR produced reproducible data, and indicated significantly reduced ASAH1 mRNA expression with siRNA transfection. Observed Ct values were consistent with abundant target nucleic acid in the samples, and the primers were specific without any product formation observed in negative control reactions, indicating reliability. ASAH1 mRNA expression was not anticipated to change after pharmacological manipulation but was not assessed.

The results observed are comparable to the limited literature evidence of siRNA inhibition of AC. Morales *et al* (2007) demonstrated siRNA inhibition to reduce ASAH1 mRNA expression to 18% of control at 36 hours post-transfection in the Hep-G2 hepatoma cell line, and Bedia *et al* (2011) demonstrated ASAH1 mRNA expression reduced to 15% of control at 72 hours in the A375 melanoma cell line, compared to 4% at 48 hours in this study. Roh *et al* (2016) used short hairpin RNA instead of siRNA, and Elojeimy *et al* (2007) and Mahdy *et al* (2009) simply demonstrated reduced (non-quantified) AC expression on Western blotting without assessing mRNA expression.

ASAH1 mRNA suppression was also observed significantly with non-coding siRNA transfection, although was significantly further suppressed in ASAH1 coding transfection. Given the data presented in figure 3.5, where comparable results were observed in transfection processes in the absence of either Lipofectamine™ RNAiMAX or siRNA, when compared to non-coding siRNA transfection, this would seem to be explained by the transfection process and in particular, the presence of Opti-MEM® Reduced Serum Medium. This is not reported in the Morales *et al* (2007) or Bedia *et al* (2011) studies where results are presented against a scrambled siRNA control in isolation. One hypothesis to explain this finding may be due to the implicated involvement of ceramide in apoptosis, cell growth

arrest and senescence (Kolesnick and Fuks, 2003). Reduced ASAH1 mRNA (and subsequent protein) expression would lead to intra-cellular ceramide accumulation, indicating a potential stress response to incubation with the reduced serum medium.

Antibody specificity was an initial problem in identifying AC on Western blotting but was ultimately overcome with observation of reduced band density at the expected molecular weights with siRNA transfection, alongside positive control samples, and with the third antibody used. Consequently, Western blotting was not performed in sufficient replicates to enable formal statistical analysis but qualitatively provided data consistent with RT-PCR and the activity assay.

Reduced AC band density following inhibition with siRNA transfection can be explained by loss of translation due to reduced mRNA expression. The reduced band density observed at 13kDa and potentially 53kDa may be as a consequence of interaction of carmofur with the 13kDa α-subunit in its precursor or active form. This interaction may alter the molecular weight of a potential carmofur-AC molecule, or may competitively inhibit antibody binding and subsequent detection. In a recent study (Dementiev *et al*, 2019), have characterised carmofur to contain an electrophilic carbonyl group that targets the catalytic cysteine residue on AC, forming a covalent complex.

The approach to the AC activity assay was limited to some degree by the financial and logistical constraints in obtaining the Rbm14-12 substrate, and the experimental approach was therefore focussed to determine the timing of maximal inhibition following carmofur dosing, alongside refining a non-toxic but therapeutic dose. Umbelliferone and protein loading calibrations were undertaken to internally validate the assay, which in itself is not a commercially available product, and has not been widely validated but produced consistent and seemingly specific results within and between experimental runs, and significant inhibition of AC activity was observed. In the optimisation of the assay, Bedia *et al* (2011) demonstrate a linear response with up to 25µg of protein obtained from the FD1 fibroblast cell line over-expressing AC, consistent with my optimisation in the HCT116 cells, where a linear response was observed to 20µg.

The inhibitory profile of carmofur on AC activity is also comparable to the results presented by Bedia *et al* (2011) in the SW403 colon and LNCaP prostate cancer cell lines, with significant activity inhibition between 45 minutes and 3 hours, reversal of activity inhibition by 12 hours, and maximal AC activity inhibition with a 3µM dose of carmofur at 30-40% of control activity.

There was equally no effect on AC activity with 5-FU in the cell lines in this study, consistent with the results observed in the HCT116 cells.

3.4.4 Conclusion

In relation to the hypotheses set at the origin of the chapter:

- Expression of AC can be inhibited by siRNA transfection in the HCT116 CRC cell line, subsequently inhibiting protein activity – **PROVEN**

Data has been observed to demonstrate significantly reduced; mRNA expression on RT-PCR, protein expression on Western blotting, and protein activity on direct assay. The optimal concentration for transfection with siRNA3 is 10nM, with maximal inhibition of AC activity occurring from 48 following transfections.

- AC activity +/- expression can be inhibited by the chemotherapeutic carmofur in the HCT116 CRC cell line – **PROVEN**

Data has been observed to demonstrate significantly reduced; protein expression on Western blotting, and protein activity on direct assay. Whilst maximal inhibition of AC activity was achieved with a 25µM dose, a non-toxic 2µM dose produced inhibition to ≈25% of baseline activity.

Chapter 4

Development of an *in vitro* Model of Acid Ceramidase Dependent Sensitivity to Chemoradiotherapy in Rectal Cancer

4.1 Introduction

4.1.1 Background

4.1.1.1 Cell survival assays

A colony forming (or clonogenic) cell survival assay is a technique that evaluates the ability of single cells to survive and reproduce, and is quantified by how many of a predetermined number of seeded cells in a plate go on to form colonies after 7-12 days. The assay is considered as a gold standard for assessment of cell survival after exposure to cytotoxic agents, as it measures the sum of all modes of cell death, and accounts for delayed growth arrest (Mirzayans *et al*, 2007) due to the longer incubation period involved. One limitation of the assay though is that it cannot measure the impact of cell-cell interaction on proliferation, as cells are plated at low density.

Acute cytotoxicity can be measured with a number of non-clonogenic assays. Enzyme release assays assess the activity of soluble, cytosolic enzymes in culture supernatant, released proportionally to loss of cell membrane integrity due to direct damage or cell death. The GAPDH release assay is considered amongst the most sensitive due to the coupled luminescent signal-amplification system yielding a strong signal for even small amounts of released enzyme (Corey *et al*, 1997), although no enzyme release assay provides insight into the mechanism underlying the observed cytotoxicity.

Cell viability can be simply measured by the Trypan Blue exclusion method, as a direct measure of early cytotoxicity. The stain permeates the membrane of dead cells but is excluded by living cells. The traditional manual cell counting using a haemocytometer has been developed to allow for automated processes (Louis *et al*, 2011), although assessing this viability does not assess for reduced cell proliferation or survival.

The major assays to quantify cell survival primarily use colourimetric methods to assess a single intracellular end point. The ease, sensitivity, rapidity and low cost have made MTT (3-(4,5-dimethylthiazol-2-yl)-2,5-diphenyltetrazolium bromide) or MTS (3-(4,5-dimethylthiazol-2-yl)-5-(3-carboxymethoxyphenyl)-2-(4-sulfophenyl)-2H-tetrazolium) assays amongst the most widely used for quantifying cytotoxicity in short-term cell cultures over a 24 to 96-hour

period (Sumantran, 2011). MTT is a yellow tetrazole that is reduced to purple formazan in living cells (Mosmann, 1983). MTS in the presence of phenazine methosulphate, produces a coloured formazan product which has an absorbance maximum at 490-500 nm, with measured absorbance of the formazan product being proportional to cell viability. The solubility of the product reduces the need for detergents, and the rapid colour change and ease of storage make it desirable for this use (Buttke *et al,* 1993).

Tetrazolium dye reduction is dependent on reduced nicotinamide adenine dinucleotide (NAD(P)H)-dependent oxidoreductase enzymes, largely in the cytosolic compartment of the cell, and is a measure of mitochondrial function. Reduction of MTT or MTS therefore depends on cellular metabolic activity due to NAD(P)H flux (Berridge *et al*, 2005). As well as reflecting the number of viable cells present, tetrazolium dye assays can also be used to quantify cytotoxicity or cytostatic activity. The MTS assay is described as a 'one-step' MTT assay, offering the convenience of adding the reagent straight to cells in culture without the intermediate steps required in an MTT assay. This convenience can be limited by colourimetric interference from traces of coloured compounds normally removed by the stages of the MTT assay but can be overcome by correlation with qualitative assessment using light microscopy (Cory *et al*, 1991).

Cell death occurs either via apoptosis, as an energy-dependent and programmed process involving the activation of caspases, or by necrosis, as an energy-independent process often involving direct damage to the cell membrane. Morphological and biochemical features of the two processes can overlap but cell death assays to detect both early and late features of apoptosis can determine that cell death is occurring via apoptosis (Elmore, 2007). Early apoptosis can be assessed by detection of caspase activation, quantified sensitively and definitively by action on fluorescent or luciferin labelled substrates (Gurtu *et al,* 1997). Later hallmarks of apoptosis are commonly assessed using flow and image cytometry, including assessment of mitochondrial transmembrane potential, DNA fragmentation, and plasma membrane alterations (Wlodkowic *et al,* 2011).

The MTS assay was selected for convenience to be trialled in assessment of short-term cytotoxicity in chemotherapeutic dosing optimisation, and could potentially be employed alongside the gold-standard clonogenic assay to compliment assessment of survivability / reproducibility after cell irradiation.

4.1.1.2 Chemotherapeutic selection

The original mass spectrometry data upon which this thesis is based, determining differential expression of AC to separate relative responders and non-responders to CRT, was undertaken in a group of patients that had all received 5-FU based chemotherapy with capecitabine as a radio-sensitiser. It was therefore pertinent to assess *in vitro* whether any changes in response to irradiation, based upon genetic or pharmacological inhibition of AC, were equally dependent upon the presence of 5-FU.

The work presented in chapter 3 details the optimisation of inhibition of AC in the HCT116 CRC cell line, both genetically with siRNA, and pharmacologically with carmofur. Carmofur was selected for this purpose as a known 5-FU prodrug, in addition to its observed potent inhibition of AC. 5-FU itself does not inhibit AC, therefore carmofur offers a potentially translational model of AC dependent sensitivity to CRT in rectal cancer.

4.1.2 Hypotheses

- HCT116 cell radio-sensitivity can be increased by the pharmacological inhibition of AC activity using the chemotherapeutic carmofur
- HCT116 cell radio-sensitivity can be increased by the genetic suppression of AC expression (and subsequent activity) using siRNA transfection
- Any increase in cell radio-sensitivity based on inhibition of AC is independent of the presence of 5-FU

4.1.3 Aims and Study Design

- Perform dose-response analysis in the HCT116 cells subsequent to exposure to 5-FU, capecitabine and carmofur, both individually and in combination
    - MTS assay to assess cell viability / survivability subsequent to chemotherapeutic exposure

- Establish the effect on TS in the HCT116 cells as the primary target for 5-FU based therapy, subsequent to exposure to 5-FU, capecitabine and carmofur
    - Western blotting for TS subsequent to chemotherapeutic exposure
- Establish a dosing strategy that facilitates optimal inhibition of AC in the HCT116 cells at the point of irradiation, with consideration for chemotherapeutic radio-sensitisation
- Clonogenic assay and MTS assay to assess cell reproducibility and viability subsequent to exposure to irradiation

4.2 Methods

4.2.1 MTS Assay

Cell proliferation and viability in response to chemotherapeutic dosing was assessed using MTS assay. 20µL of MTS reagent (Promega) was applied to each experimental well on the 96-well plates, to cells in culture 72 hours after exposure to treatment. Plates were then incubated for two hours before absorbance at 490nm was measured using the Varioskan Flash. Absorbance values were adjusted according to background control wells on each plate (culture medium without cells, at the same 200µL volume as added when seeding cells), and then normalised to absorbance from cell wells treated with 0.05% DMSO in culture medium as a vehicle control, to facilitate direct comparison.

The dose-response on the basis of MTS assay in the HCT116 cells to capecitabine, 5-FU and carmofur was assessed primarily. Optimisation experiments to define an appropriate range of concentrations for accurate determination of the IC_{50} was undertaken. 2,500 HCT116 cells in 200µL DMEM were seeded per well of a 96-well Nunc™ plate (Thermo Fisher Scientific) and incubated overnight to adhere. The chemotherapeutics were dissolved in DMSO and mixed with DMEM, and this mixture was then exchanged for the existing culture medium in the wells of the plate thus dosing the adherent cells.

Initial concentrations of 5-FU and carmofur resulted in the observation that the IC_{50} was likely to lie in the 2-8µM range, and therefore further experiments assessing the response to 1, 2, 4, 8, and 16µM concentrations of these drugs was performed in triplicate wells in three independent experiments to establish an accurate IC_{50}. Capecitabine (molecular weight 359.35g/mol, Sigma Aldrich) was applied to the HCT116 cells at a range of concentrations from 1-400µM but demonstrated no toxicity (see section 4.3.1 below) in three independent experiments and was therefore not considered further for use as a 5-FU based control in the experimental design.

32mM stock concentrations of 5-FU (molecular weight 130.1g/mol, Sigma Aldrich) and carmofur (molecular weight 257.3g/mol, Sigma Aldrich) were prepared by dissolving 8.2mg of 5-FU in 1,970µL DMSO, and 10.5mg of carmofur in 638µL DMSO. The 32mM stock

solutions were serially dilute 1:1 with DMSO to generate further concentrations of 16, 8, 4, and 2mM. 5µL of each of these solutions mixed with 5mL of DMEM produced 16, 8, 4, 2 and 1µM concentrations of the drugs (final DMSO concentration 0.05%) which were applied to adherent cells in the 96 well plates in triplicate wells in three independent experiments.

Combined application of carmofur and 5-FU was also assessed, in parallel to designing the clonogenic model. This was in attempt to establish an equivalent control effect of 5-FU, under the assumption that the 5-FU based effect of carmofur and 5-FU itself are not necessarily equivalent. 2.5µL of the same concentration drug solution (i.e. 2.5µL of 32mM 5-FU and 2.5µL of 32mM carmofur) was combined in 5mL DMEM for the 32, 16, 8 and 4mM stock solutions, generating combined 8, 4, 2 and 1µM solutions with a final 0.05% DMSO concentration. 5µL of each 32mM stock in 5mL culture medium produced a combined 16µM concentration but with a final 0.1% DMSO concentration. Adherent cells in triplicate wells were again dosed with these concentrations in three independent experiments.

4.2.2 Clonogenic Model Development

The fundamental basis for the development of the clonogenic model surrounds AC inhibition. It was considered that for the treatment groups in the model, exposing cells to irradiation at the point of maximal inhibition of AC was a reasonable starting point. Pharmacological inhibition of AC activity has been observed in chapter 3 to return to baseline 24 hours after dosing. Although the clonogenic assay was planned to run for 7-12 days, and that ongoing pharmacological AC activity inhibition would therefore not be maintained, it was considered that re-dosing cells at seeding in the clonogenic plates, or that re-dosing the seeded cells over the course of the clonogenic assay risked affecting the outcome significantly, either by altering the ability of the cells to adhere in the clonogenic plate, or by washing cells or colonies away. Equally cells should enter apoptosis within this 24 hour period, and re-dosing should not be necessary. The effect of siRNA inhibition of AC on activity was observed in chapter 3 to persist maximally 72 hours subsequent to transfection, and therefore ongoing significant AC inhibition in these treatment groups, which may potentially affect sensitivity to irradiation, would be likely. The application of pharmacological manipulation could be further optimised if needed, dependent on these results.

Given the original proteomic data separating relative responders and non-responders to CRT was in the context of radio-sensitisation with 5-FU based capecitabine, it was considered that it would be prudent to incorporate 5-FU treatment into the modelling. Genetic inhibition of AC with siRNA, and pharmacological inhibition of AC with carmofur was planned to be compared both against and in combination with standard 5-FU radio-sensitisation. This design allows potentially for any AC inhibition specific radio-sensitivity differences to be observed over and above any benefit from the modelled standard 5-FU control treatment. The resultant 11 experimental treatment groups, including vehicle controls for both transfection and pharmacological manipulation, are detailed in table 4.1 below.

Genetic Manipulation (siRNA)		Pharmacological Manipulation	
ASAH1 siRNA	Non-coding siRNA	Chemotherapeutic	Control
+ Media (3,M)	+ Media (NC,M)	Carmofur (C)	Media (M)
+ DMSO (3,D)	+ DMSO (NC,D)	5-fluorouracil (5)	DMSO (D)
+ 5-fluorouracil (3,5)	+ 5-fluorouracil (NC,5)	Carmofur + 5-fluorouracil (C,5)	

Table 4.1 – Experimental treatment groups to compare genetic and pharmacological manipulation of AC as radio-sensitisation in an *in vitro* clonogenic based model, incorporating 5-FU as a standard treatment control, and vehicle controls for transfection and chemotherapeutic application.

The concentration / volume of transfection reagents was optimised as described in section 3.3. The concentrations for pharmacological treatment required determination and potential further optimisation but a 2µM concentration of carmofur and 5-FU was selected initially in the clonogenic model for the following reasons.

Administration of this concentration of the drugs either individually or in combination demonstrated no significant variation in proliferation/viability of the HCT116 cells on MTS assay compared to vehicle control (as demonstrated later in figure 4.8), whereas higher individual concentrations decreased cell proliferation, and increasingly so when combined. 3µM 5-FU is considered to be a biologically equivalent concentration to that observed in plasma in the clinical setting in patients receiving 5-FU in CRT (Spitzner *et al*, 2010) - 2µM is a reasonably similar concentration, and the intention is for a 5-FU based effect in this model

to be that of radio-sensitisation, and not for it to directly affect viability. Carmofur was equally observed to significantly decrease AC activity in the HCT116 cells at a concentration of 2μM (as described in section 3.3.3.3).

The experimental plan, as depicted in figure 4.1 below, was therefore designed. Cells would be originally seeded at $2x10^5$ in 2mL culture medium in individual 35mm CellBIND® cell culture dishes (Corning®, New York, USA), and incubated overnight to adhere. Transfection would be undertaken in pertinent groups, with irradiation planned two days later to facilitate maximal inhibition of AC at that point. Cell groups not undergoing transfection would remain incubated in culture for this time. The media in all groups would be changed two hours prior to irradiation to deliver the desired pharmacological treatment, to optimise inhibition of AC activity with carmofur at the point of irradiation, and to establish an equivalent volume of culture medium in each plate at irradiation.

Cell irradiation was undertaken in a different laboratory. To facilitate this process the cells in their individual lidded dishes were placed on ice, covered, and transported (walked) to the irradiator. The individual dishes were removed from ice briefly to undertake the desired irradiation, and placed back on ice before being transported back to the parent laboratory for cell resuspension, counting and re-seeding into the clonogenic plates.

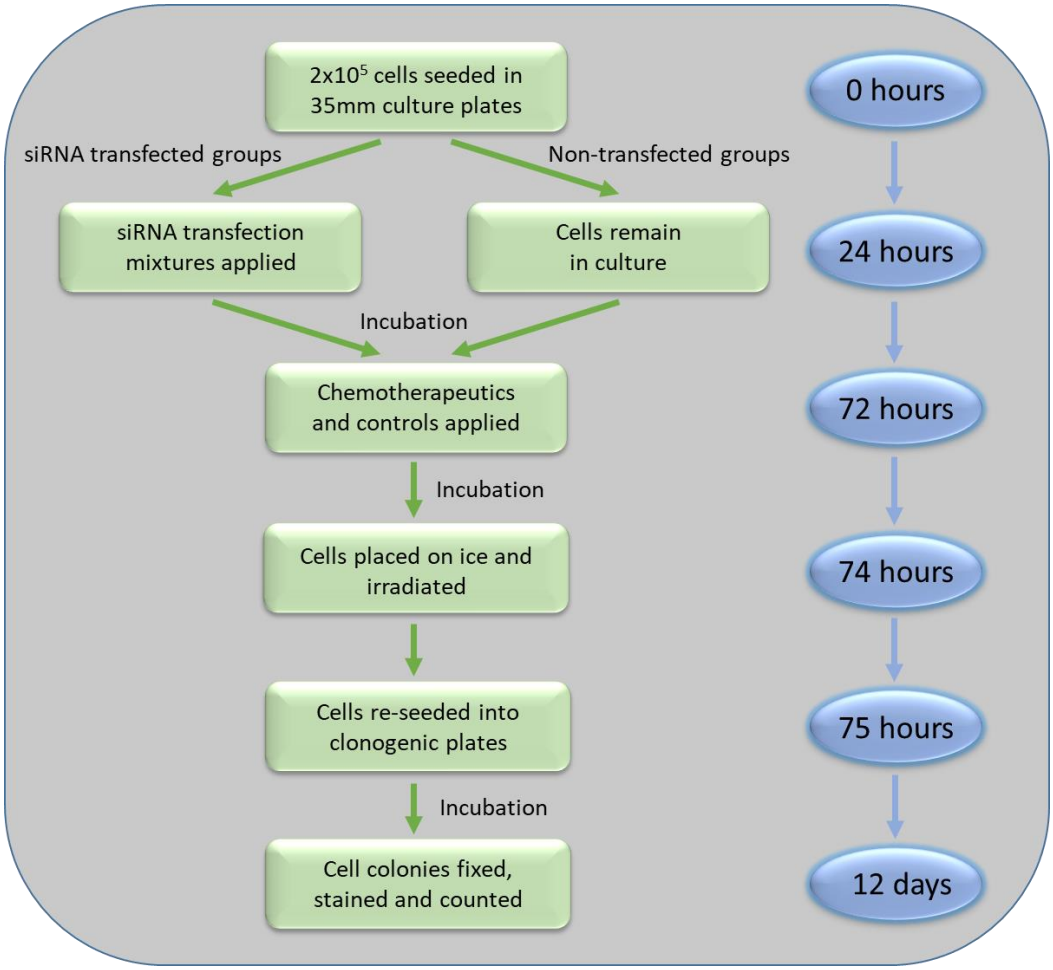

Figure 4.1 – A schematic demonstrating the experimental process undertaken to assess irradiation response in the HCT116 cells across all treatment groups. The process was designed to facilitate irradiation delivery at the point of maximal AC activity inhibition. Cells were initially seeded in individual 35mm cell culture dishes and incubated overnight to adhere. siRNA (final concentration 10nM) transfection was undertaken (siRNA3 and non-coding control) after 24 hours in relevant cell groups by adding the transfection mix to the dishes, whereas pharmacologically-only treated groups (not undergoing transfection) remained in culture. At 72 hours the respective pharmacological treatments (including 0.05% DMSO vehicle controls) were applied to the cells in both groups, undertaken by exchanging the existing culture medium for dosed DMEM. In those groups where a pharmacological treatment was not applied, the culture medium was equally exchanged at this point. Following incubation with the pharmacological treatments for two hours, the cells in the dishes were placed on ice and irradiated across the range of experimental doses, then re-seeded into 6-well cell culture plates for the clonogenic assay. Formed cell colonies were fixed and stained in the plates after incubation for 9 days, and subsequently counted.

4.2.3 Cell Counting and Plate Seeding

It was crucial that seeding of the clonogenic plates particularly was performed as accurately as possible. The specific procedure undertaken for cell counting and plate seeding is therefore described.

The range of treatments to be assessed on clonogenic and MTS proliferation assays were applied to adherent cells in 35mm cell culture dishes. Subsequent to irradiation, the cells in each dish were collected and re-suspended as described in section 3.2.1 but using 1mL of each respective reagent, and taking care to re-suspend all possible cells. The resultant 1mL of DMEM containing the re-suspended cells was added to a further 4mL of DMEM and appropriately mixed. A 100µL aliquot of this 5mL cell suspension was then mixed with 100µL of 0.4% trypan-blue (Sigma-Aldrich), and a further aliquot of this resultant mixture applied to a haemocytometer under a cover slip as depicted in figure 4.2.

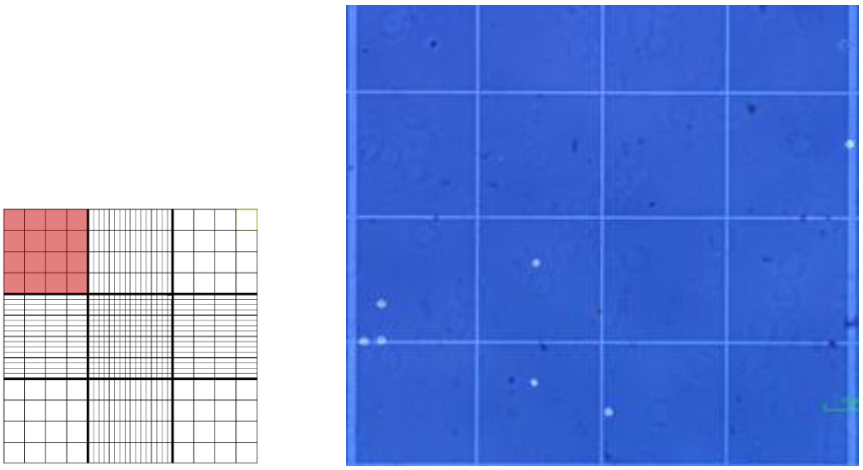

Figure 4.2 – Haemocytometer cell counting performed for the determination of accurate plate seeding. The left side of the figure depicts the haemocytometer grid (adapted from https://en.wikipedia.org/wiki/File:Haemocytometer_grid.svg), with a corner square representing 1x1mm (and containing a further 4x4 grid) highlighted in red. The right side of the figure demonstrates a near-complete image of this 1x1mm square taken from a performed cell count. An aliquot of cells in suspension and appropriately mixed, is mixed 1:1 with 0.4% trypan-blue and applied to the haemocytometer under a cover slip at 0.1mm depth. Cells are counted in each of the four corner 1x1mm squares, the total count divided by 4, and this number (representing the number of cells in 100nL) multiplied by 20,000 (as the original cell solution was diluted 50:50 with trypan-blue) to give the cell count per mL of the original suspension. In the demonstrated image, 7 live cells (seen as white dots, where trypan-blue has not permeated the cell membrane) can be observed.

A manual cell count was performed by counting observed live cells in each of the four 1x1mm corner squares on the haemocytometer. The total live cell count was divided by 4 to represent the number of live cells in 100nL of the cell/trypan-blue mixture, and this number was multiplied by 20,000 to give the live cell count per mL of the 5mL cell suspension.

Once the live cell count of the 5mL cell suspension had been calculated, further calculations were performed to ascertain the required volumes of this suspension to be diluted for seeding the 6-well Nunc plates for the clonogenic assay, and the 96-well Nunc plates for the MTS proliferation assay.

Seeding for the clonogenic assay was optimised by irradiation of untreated HCT116 cells (as described in section 4.2.6), and related to the radiation dose administered as demonstrated in table 4.2 below, to account for reduced plating efficiencies with higher doses.

Irradiation Dose (Gy)	Clonogenic Plate Seeding (cells/well on a 6-well plate)
0	200 (x3) & 400 (x3)
0.5	200 (x3) & 400 (x3)
1	400 (x3) & 800 (x3)
2	400 (x3) & 800 (x3)
4	800 (x3) & 1,600 (x3)

Table 4.2 – Seeding of the clonogenic assay plate. A 6-well cell culture plate was seeded at two densities (each in triplicate) for each treatment group at each irradiation dose. The seeding was determined from the colony count (surviving fraction) observed with untreated HCT116 cells irradiated at that dose.

The 5mL cell suspension was mixed again prior to diluting the required volume (to account for the lower of each paired seeding number for that irradiation dose to be present per mL) in a final volume of 20mL DMEM. After further mixing, 1mL of this final volume was added with 1mL of DMEM in triplicate to a 6-well cell culture plate, and 2mL of this final volume was added in triplicate to the remaining wells. This allowed for the required seeding numbers to be present in triplicate in a volume of 2mL culture medium per well on each

plate. The plate was gently swirled to distribute the cells in the culture medium prior to undisturbed incubation at 37°C and 5% CO_2 for nine days.

The 96-well MTS proliferation assay plate was seeded in triplicate at 2,500 cells per well, irrespective of irradiation dose for each treatment group. The 5mL cell suspension was again mixed, prior to diluting a volume calculated to contain 62,500 cells in a final 5mL volume of culture medium. This final volume was mixed before pipetting 200µL (containing 2,500 cells) in triplicate on the 96-well plate, which was subsequently incubated under the same conditions as above for three days.

4.2.4 Colony Staining

The duration of incubation for the clonogenic assay was optimised in non-irradiated and untreated HCT116 cells, and was determined to be nine days. After this time colonies were observed to become increasingly confluent, and accurate interpretation of the clonogenic assay would not have been possible.

To stain the clonogenic plates, the culture medium in each well was aspirated, and the wells gently washed individually with 1mL of cold PBS. The wash was aspirated, prior to the addition of 1mL of cold methanol to fix the colonies, which was left for 15 minutes. This was then aspirated, before 1mL of a 0.5% crystal violet solution was added as a stain. After a further 15 minutes, the excess stain solution was aspirated before the plate was washed in a water bath, and then left to air dry. Each aspiration was performed by the careful introduction of a pipette tip at the 6 o'clock position of the well whilst tipping the plate towards that point, and the careful addition of each reagent was performed at the same point, again whilst tipping the plate. It was observed that this technique did not result in cell colonies being washed away.

4.2.5 Colony Counting

Colony counting was undertaken using the GelCount™ (Oxford-Optronix, Abingdon, UK) automated colony counter, which facilitates consistent analysis and counting across multiple plates. The system acquires a digital image of the clonogenic plate, which is then analysed. Colony detection parameters (predominantly colony size, density and shape) were optimised and integrated into the Compact Hough and Radial Map (CHARM™) processing algorithm at the outset, to detect colonies of more than 50 cells that had been characterised initially under light microscopy.

The areas of the 6-well plates analysed was also defined at the outset by a designated 'mask', based on the specification of the loaded plate, such that the entire area of each well on the plate is encompassed. This was visually checked for each analysed plate, and corrected if minor adjustments were required based on slight variation of the position of the plate in the GelCount™ scanner at the point of image acquisition. Figure 4.3 demonstrates these processes in one of the experimental clonogenic plates.

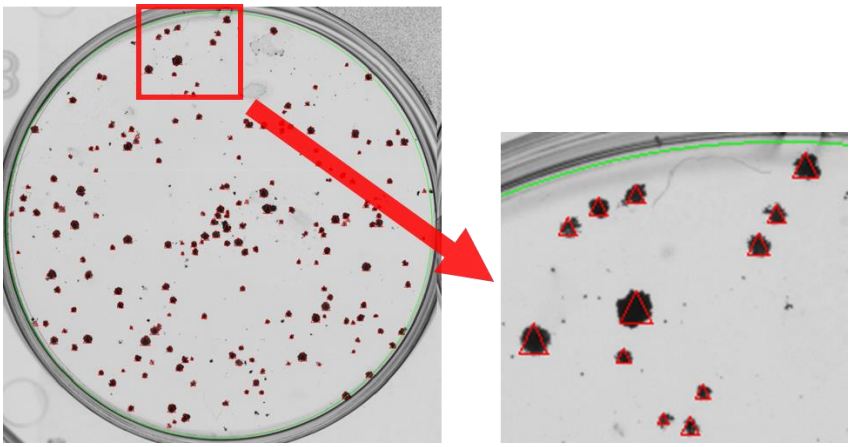

Figure 4.3 – Colony detection using the GelCount™ automated colony counter. The image on the left depicts the digitally acquired image obtained by the system and demonstrates a single well from one of the 6-well experimental plates used. The section of the area highlighted by the red box (as magnified in the right side of the figure) demonstrates the automated analysis of the digital image. A 'mask' is applied to the image (as demonstrated by the circumferential green line) to determine the areas for analysis in relation to the specification of the plate loaded, encompassing the area of each well individually. CHARM™ settings are then optimised based primarily on cell colony density and for the size of colonies for detection, and the system identifies the colonies (as demonstrated by the red triangles, with each triangle counting as one colony) within the designated 'mask' for each experimental well.

As can be observed in the right-sided image in figure 4.3, insignificant debris within the well is not identifed. The pre-determined settings allow for consistent analysis across multiple plates.

4.2.6 Cell Irradiation Delivery

Cells in culture were subjected to radiation using the CellRad (Faxitron, Tucson, Arizona, USA) benchtop irradiator. The irradiator delivers a consistent beam of x-rays across a 30cm diameter field, although all cells in our experiments were irradiated in 35mm tissue culture dishes placed in the same position at the centre of the field. Equivalent irradiation doses are achieved with the irradiator between experimental runs due to the internal calibration of the system, and the ability to programme delivery of a desired dose. A dose rate of 3 Gy/min was used throughout.

Optimisation of irradiation dosing was performed at 0, 0.5, 1, 2, 4 and 8Gy in HCT116 cells in culture (results not presented), with negligible colony formation following 8Gy irradiation, and minimal reduction in surviving fraction at 0.5Gy. Experimental treatment groups were therefore exposed to 0, 1, 2 and 4Gy irradiation, although the model was later refined to include a 0.5Gy irradiation dose in selected groups, when it became apparent that radiation specific differences were more likely to be observed at this dose in the experimental groups.

4.2.7 Western Blotting for Thymidylate Synthetase

Western blotting was performed as described in section 3.2.4, albeit with the use of an HRP-conjugated anti-TS primary antibody (ab198599, rabbit monoclonal, Abcam) at a final concentration of 1:5000 as per the manufacturer's instruction (http://www.abcam.com/thymidylate-synthase-antibody-epr4545-hrp-ab198599.html), and obviating the need for incubation with a HRP-conjugated secondary antibody.

4.2.7.1 Experimental conditions investigated on Western blotting

The MTS proliferation data assessing drug dose response to 5-FU and carmofur (as described in section 4.3.1) was observed to demonstrate that a 2μM incubation with each drug did not result in significant toxicity in HCT116 cells. Significant AC activity inhibition occurred in the cells with carmofur (as described in section 3.3.3.3) at this concentration, and therefore it was considered that 2μM was the optimal dose of the drugs to take forward for the modelling of AC dependent sensitivity to CRT. It was considered prudent to assess the effect of the drugs at this concentration on their primary target (TS) in attempt to demonstrate an approximation of their 5-FU based effect, and therefore isolate any AC specific effect.

HCT116 cells were seeded in 6-well Nunc plates at a density of $1x10^6$ and allowed to adhere overnight. The cells were then incubated with a 2μM concentration of carmofur or 5-FU in DMEM, alongside untreated cells and 0.05% DMSO vehicle control groups, with samples at 1, 2, 4, 8, 16, and 24 hours following incubation, collected and processed as described in section 3.2.4.

4.2.8 Post-Clonogenic Evaluation of Treatment Group Characteristics

Subsequent to performing clonogenic assay across all treatment groups and over the range of irradiation doses, it was observed on the basis of the baseline (0Gy) surviving fraction that there were likely fundamental differences between pre-irradiation treatment groups; ASAH1 siRNA transfected vs. non-coding siRNA transfected vs. non-transfected (see section 4.3.4 below). The original hypotheses did not encompass this eventuality but it was considered that further investigation of these differences was valid. It was further hypothesised that the differences observed could relate to cell proliferation rate, the ability to adhere as individual cells in the clonogenic plate on re-seeding, apoptotic predisposition, or to a combination of these factors.

4.2.8.1 Evaluation of cell proliferation

Data concerning cell proliferation to the point immediately after delivery of irradiation had already been collected in a surrogate capacity, when the cells were re-suspended and counted upon re-seeding into the clonogenic plates. $2x10^5$ cells had been plated at the outset in all groups, with the only significant variability between treatment groups being the application of the transfection reagents 48 hours prior. The observed cell counts at this point therefore reflected the effect of application of siRNA3 transfection vs. siRNA-NC transfection vs. no transfection.

It was considered that evaluation of proliferation subsequent to re-seeding after transfection was more pertinent. This data had also been collected in a surrogate capacity on MTS assay in the non-irradiated cell groups, with the crude absorbance values obtained at 72 hours being directly comparable between groups.

In attempt to validate this surrogate data, a further post-transfection assessment of proliferation was undertaken in a HCT116 cell population that had undergone plasmid transfection to stably express luciferase under the influence of Zeocin™. This cell line had been validated to exhibit luminescence proportional to cell viability in the presence of luciferin (data not provided) and was generously provided by Mr Jonathan Evans, Department of Molecular and Clinical Cancer Medicine, The University of Liverpool. Quantification of luminescence (to reflect viability) in this cell population over time, both with and without transfection, would assess proliferation in the different treatment groups.

$2x10^5$ luciferase expressing HCT116 cells were seeded into 6-well Nunc cell culture plates in 2mL DMEM and incubated overnight to adhere. ASAH1 siRNA transfection and non-coding siRNA transfection (as previously described) was undertaken in two wells respectively, with a third non-transfected well remaining. 48 hours subsequent to transfection, the cells in all experimental groups were individually re-suspended and re-seeded at 2,500 cells per well into white-bottomed 96-well cell culture plates (Sigma-Aldrich) in 200µL culture medium in triplicate.

A stock solution of VivoGlo™ firefly luciferin (Promega, Southampton, UK) was created by diluting the purchased powder to 15mg/ml in 1x PBS. This stock solution was further diluted 100-fold to 150µg/ml in DMEM and 100µl added to the cells in culture on parallel plates at 0, 27, 53 and 72 hours subsequent to re-seeding. Plates were incubated at 37°C for 2 hours before luminescence was quantified using the Varioskan Flash. Results were adjusted for

background luminescence from negative control wells (culture medium without cells), and three independent experiments were performed.

4.2.8.2 Evaluation of caspase 3/7 activity

The execution phase of apoptosis is characterized by the activation of effector caspases, such as caspase-3 and caspase-7, which cleave key regulatory or structural proteins and in particular activate apoptotic nucleases (Vaughan *et al*, 2002). The Caspase-Glo® 3/7 assay (Promega) provides a luminogenic caspase 3/7 substrate, which when added to adherent cells or those in suspension results in cell lysis, followed by caspase cleavage of the substrate, and generation of luminescent signal produced by luciferase. The assay substrate is specific for caspase 3/7, and luminescence observed is proportional to caspase activity (Bayascas *et al*, 2002). Caspase 3/7 activity in ASAH1 siRNA transfected, non-coding siRNA transfected and non-transfected cell populations could therefore indicate apoptotic predisposition.

$2x10^5$ HCT116 cells were seeded into 6-well cell culture plates in 2mL culture medium, and incubated overnight to adhere. ASAH1 siRNA transfection and non-coding siRNA transfection (as previously described) was undertaken in two wells respectively, with a third non-transfected well remaining. 48 hours subsequent to transfection, the cells in all experimental groups were individually re-suspended and re-seeded at 10,000 cells per well into white-bottomed 96-well cell culture plates in 100µL culture medium in triplicate. 100µL of Caspase-Glo® 3/7 reagent (reconstituted as per manufacturer's instruction) was added to each well on parallel plates at 0, 2.5, 7 and 24 hours subsequent to re-seeding. Plates were incubated at 37°C for 2 hours before luminescence was quantified using the Varioskan Flash. Results were adjusted for background luminescence from negative control wells (culture medium without cells), and three independent experiments were performed.

4.2.9 Statistical Analysis

IC_{50} values were calculated with GraphPad Prism version 5 (GraphPad Software Inc., La Jolla, California, USA), using nonlinear regression modelling of 'log(inhibitor) vs. response'.

Other statistical analysis was undertaken using SPSS® Statistics version 22 (IBM®, New York, USA), with specific tests used as detailed in the relevant sections.

4.3 Results

4.3.1 MTS Assay – Chemotherapeutic Dose-Response

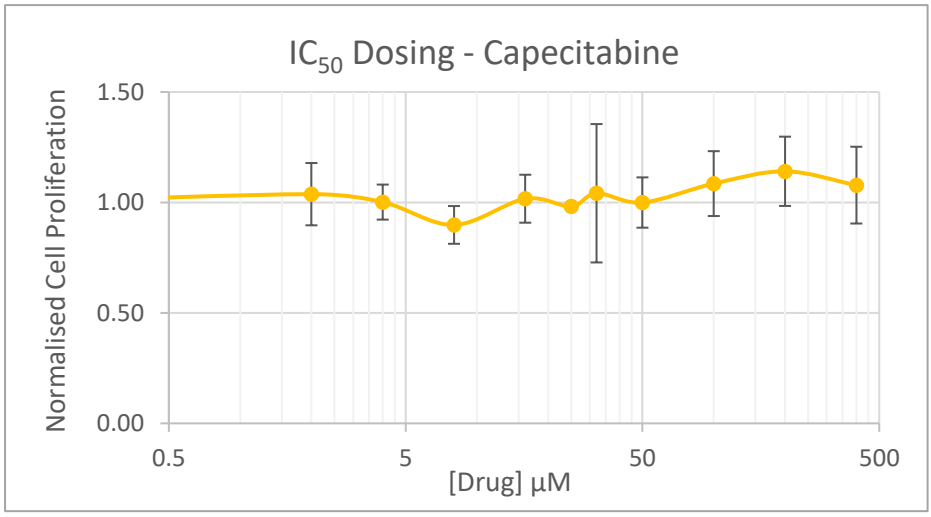

Figure 4.4 – Dose-response to capecitabine in HCT116 cells, evaluated on MTS proliferation assay. Absorbance at 490nm was quantified from triplicate samples in three independent experiments, 72 hours after dosing with the demonstrated range of concentrations of the drug. Data was adjusted to account for background absorbance and has been normalised to absorbance of vehicle control samples (0.05% DMSO). Mean values are plotted with error bars representing one SD.

No toxicity was observed subsequent to dosing with capecitabine in the HCT116 cells, even at a maximal concentration of 400µM. An IC_{50} value is therefore not presented.

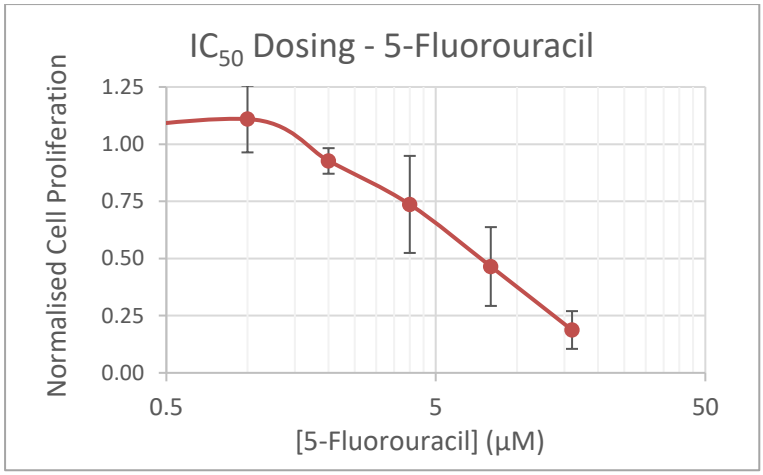

Figure 4.5 – Dose-response to 5-FU in HCT116 cells, evaluated on MTS proliferation assay. Absorbance at 490nm was quantified from triplicate samples in five independent experiments, 72 hours after dosing with the demonstrated range of concentrations of the drug. Data was adjusted to account for background absorbance and has been normalised to absorbance of vehicle control samples (0.05% DMSO). Mean values are plotted with error bars representing one SD.

Toxicity was observed in the HCT116 cells subsequent to dosing with 5-FU at concentrations above 2µM. The IC_{50} for the drug is calculated to be 5.48µM (95%CI 4.11-7.31, R^2=0.875).

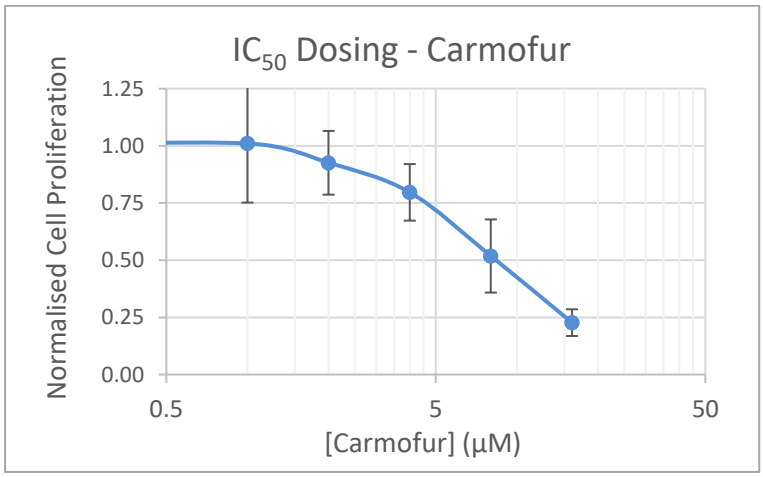

Figure 4.6 – Dose-response to carmofur in HCT116 cells, evaluated on MTS proliferation assay. Absorbance at 490nm was quantified from triplicate samples in five independent experiments, 72 hours after dosing with the demonstrated range of concentrations of the drug. Data was adjusted to account for background absorbance and has been normalised to absorbance of vehicle control samples (0.05% DMSO). Mean values are plotted with error bars representing one SD.

Toxicity was observed in the HCT116 cells subsequent to dosing with carmofur at concentrations above 2µM. The IC_{50} for the drug is calculated to be 7.48µM (95%CI 5.96-9.38, R^2=0.843).

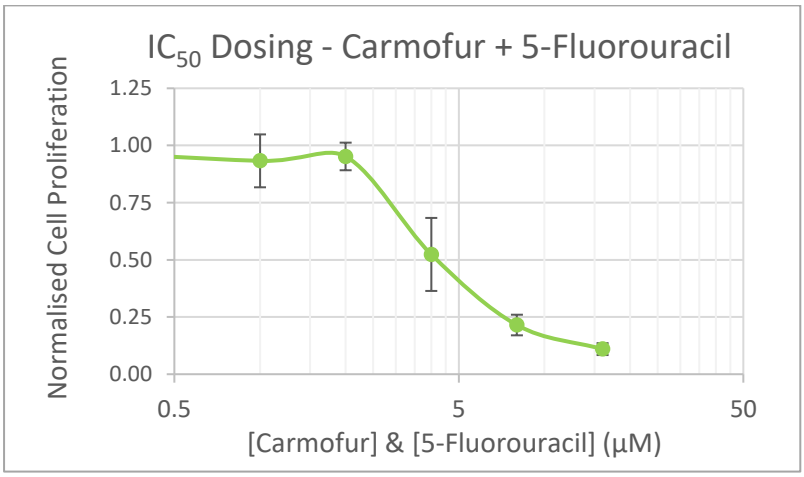

Figure 4.7 – Dose-response to combining carmofur and 5-FU in HCT116 cells, evaluated on MTS proliferation assay. Absorbance at 490nm was quantified from triplicate samples in five independent experiments, 72 hours after dosing with the demonstrated range of concentrations of the drugs in combination. Data was adjusted to account for background absorbance and has been normalised to absorbance of vehicle control samples (0.05% DMSO). Mean values are plotted with error bars representing one SD.

Toxicity was observed in the HCT116 cells, subsequent to dosing with combination carmofur and 5-FU, at concentrations of each drug above 2µM. The IC_{50} when combining the drugs is calculated to be 3.95µM for each drug (95%CI 3.64-4.29, R^2=0.930).

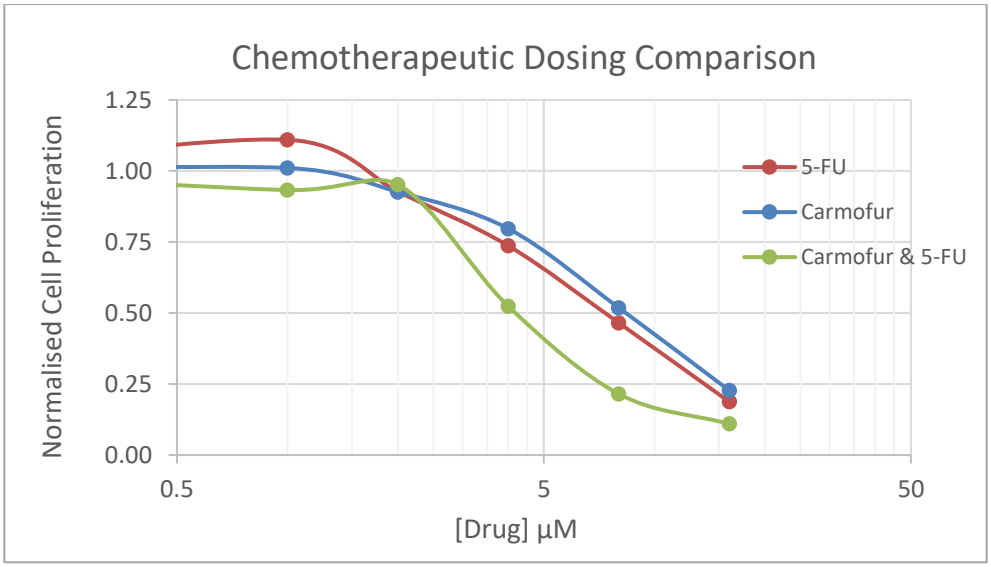

Figure 4.8 – Dose-response profiles of 5-FU, carmofur, and carmofur & 5-FU, evaluated on MTS proliferation assay. The graph depicts the data presented in figures 4.5, 4.6 and 4.7 to facilitate direct comparison.

The dose-reponse to application of 5-FU and carmofur to HCT116 cells individually is observed to be comparable, both graphically as demonstrated in figure 4.8 and on the basis of overlapping 95% CI for their IC_{50} values (4.11-7.31µM and 5.96-9.38µM respectively). The IC_{50} value for combined application of the drugs is lower (3.95µM), although a comparable effect is observed between the drugs individually and in combination at a concentration of 2µM. The effect of treatment at this 2µM concentration is not statistically significantly different between any groups or in relation to baseline (p=0.465, one-way ANOVA).

4.3.2 Western Blotting for Thymidylate Synthetase

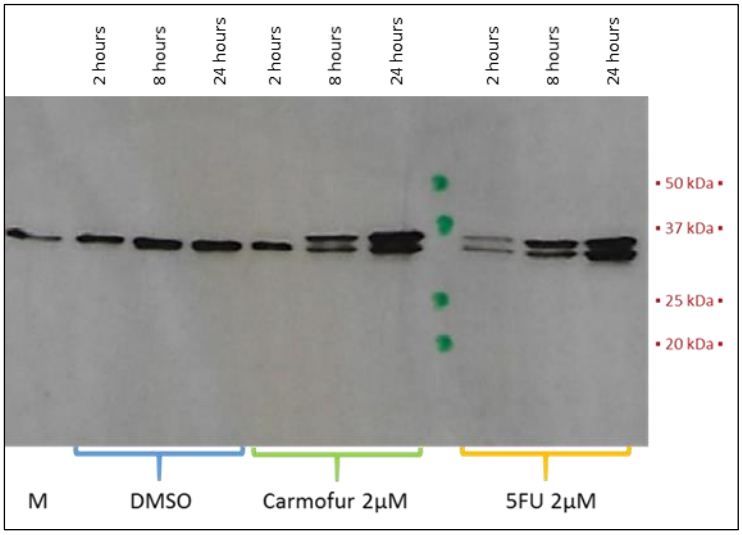

Figure 4.9 – Whole membrane film of a Western blot performed on a 10% SDS-PAGE gel, with ab198599 (Abcam, RabMAb®, rabbit monoclonal) anti-TS primary antibody at a concentration of 1:5000. The green dots represent the position of the bands from the molecular weight marker, as per the weights depicted to the right of the film. The grouped bands from 0.05% DMSO vehicle control samples, 2µM carmofur treated samples, and 2µM 5-FU treated samples, were obtained at 2, 8 and 24 hours following incubation in each group from left to right respectively in HCT116 cells. M represents untreated cells incubated in culture medium only.

The film imaged in figure 4.9 demonstrates excellent specificity for a band at ≈36kDa at the predicted molecular weight for TS. A single band is observed in untreated and vehicle control treated samples, whereas the band is duplicated in HCT116 cells treated with carmofur collected 8 and 24 hours after incubation with the drug, and equally in samples treated with 5-FU collected 2, 8 and 24 hours after incubation with the drug. This duplication indicates some effect with drug treatment, presumably due to binding of the drug metabolite to TS with a shift in its mobility and subsequent increase in protein stability. The fact this alteration is observed only in 5-FU and carmofur treated samples would further validate the observed band to be TS.

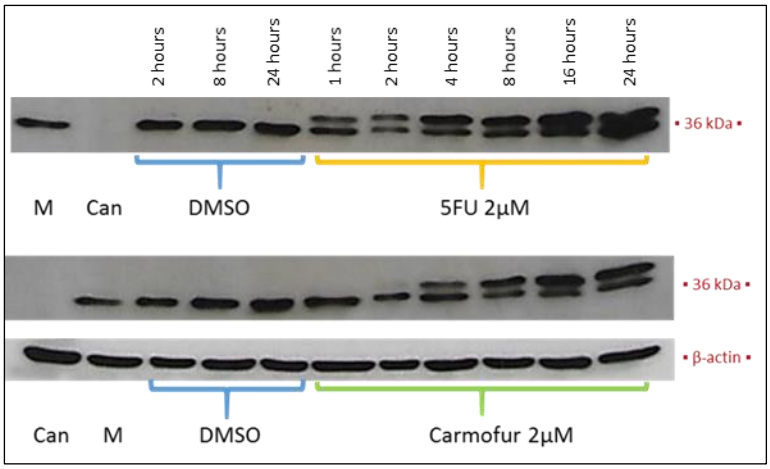

Figure 4.10 – Band specific films of Western blots performed on a 10% SDS-PAGE gel, with ab198599 (Abcam, RabMAb®, rabbit monoclonal) anti-TS primary antibody at a concentration of 1:5000. The top film represents TS expression (at 36kDa) in HCT116 cells at 1, 2, 4, 8, 16, and 24 hours (from left to right respectively in the yellow bracketed bands) subsequent to incubation with 2µM 5-FU, compared to expression subsequent to incubation with 2µM carmofur at the same time points (from left to right respectively in the green bracketed bands) in the middle film. The 0.05% DMSO vehicle control treated cell samples and untreated culture medium only cell sample (M) are those as described in figure 4.9. Can represents a rectal cancer sample obtained from the original proteomic profiling known to have relatively high AC expression. A β-actin reference band was obtained for the carmofur treated samples blot.

Quantitative assessment of the expression of the bands in either figure 4.9 or 4.10 has not been undertaken, as a β-actin reference band to normalise protein loading is not universally present. Qualitative assessment of the β-actin band in figure 4.10 would suggest equivalent protein loading however. The functional effect of carmofur and 5-FU on TS expression can be observed by the duplication of the bands in the experimental cell samples. This is observed to occur in the 5-FU treated cells 1 hour after incubation and persists to 24 hours. Duplication of the band is only faintly observed in the cell sample collected 2 hours after incubation with carmofur but again persists thereafter to 24 hours. The effect on TS of the two drugs therefore seems to occur earlier in treatment with 5-FU. Any potential observed increase in radio-sensitivity on clonogenic assay in AC inhibited cells irradiated 2 hours after application of a non-toxic dose of carmofur with or without 5-FU, could be argued to be independent of the effect on TS.

4.3.3 Clonogenic Assay – Post-Irradiation / Acid Ceramidase Inhibition

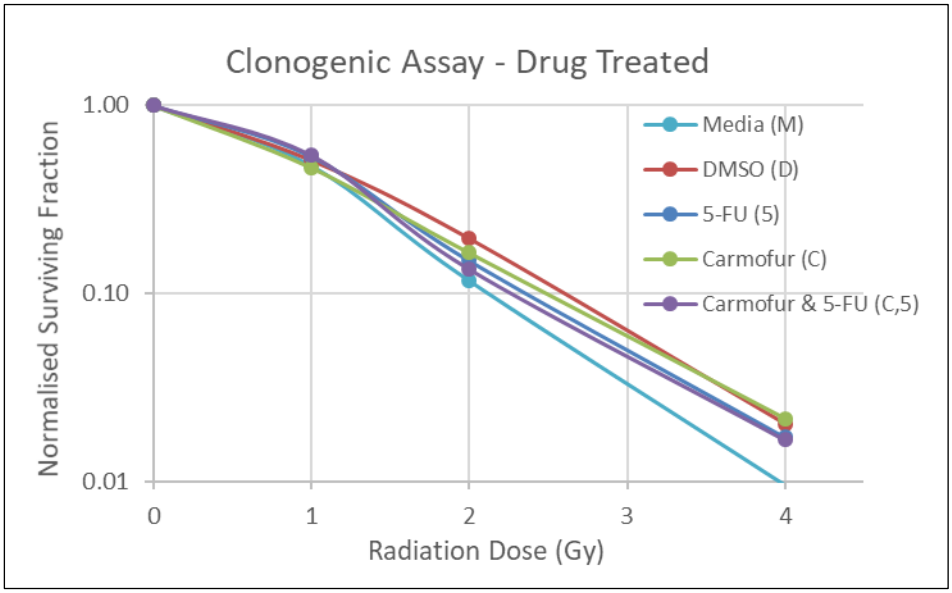

Figure 4.11 – HCT116 cell colonies observed after irradiation (0-4Gy) in the pharmacological manipulation arm of the AC dependent model of sensitivity to CRT. Colony formation was assessed 9 days after plate seeding, subsequent to irradiation and prior pre-irradiation manipulation of AC activity with carmofur. The treatment groups are those as defined in table 4.1. The surviving fraction for each irradiation dose has been normalised to the non-irradiated (0Gy) control for the respective pre-irradiation treatment, to facilitate direct comparison of any radiation specific effect. Results are the means of three independent experiments.

The surviving fraction (colonies formed / cells seeded) in all pharmacological treatment groups is observed to reduce with increasing radiation dose. The surviving fraction at 4Gy irradiation (normalised to the non-irradiated control for the respective pre-irradiated treatment) ranges from 0.010 (M) to 0.022 (C), and as such represents an insignificant number of surviving cells to detect a meaningful variation between pre-irradiation treatment. A similar effect is observed at 2Gy irradiation, where the normalised surviving fraction ranges from 11.7% (M) to 19.6% (D), and representing crude surviving fractions ≈5-10%. At 1Gy irradiation the range of normalised surviving fractions is observed to be even closer between pre-irradiation treatment groups (46.7% (C) to 54.4% (C,5)). Error bars are not presented in figure 4.11 as there were no statistically significant differences between groups, and to facilitate ease of interpretation.

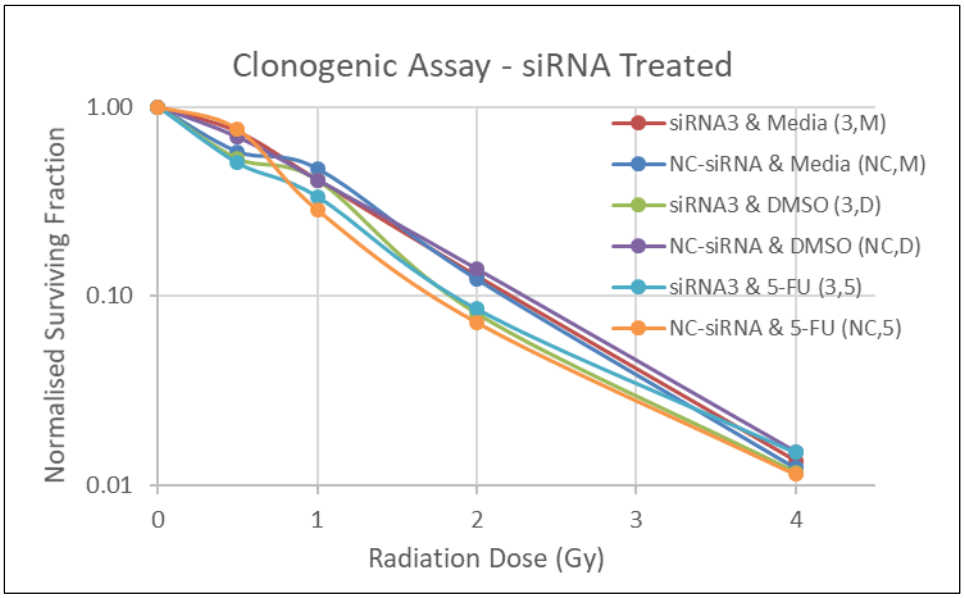

Figure 4.12 – HCT116 cell colonies observed after irradiation (0-4Gy) in the genetic manipulation arm of the AC dependent model of sensitivity to CRT. Colony formation was assessed 9 days after plate seeding, subsequent to irradiation and prior pre-irradiation manipulation of AC activity with siRNA3. The treatment groups are those as defined in table 4.1. The surviving fraction for each irradiation dose has been normalised to the non-irradiated (0Gy) control for the respective pre-irradiation treatment, to facilitate direct comparison of any radiation specific effect. Results are the means of three independent experiments.

The surviving fraction in the genetic manipulation arm of the clonogenic assay is observed to reduce in all treatment groups with increasing radiation dose. An insignificant normalised surviving fraction is observed at 4Gy irradiation, with a range from 0.011 (NC,5) to 0.015 (3,5), and also at 2Gy irradiation, where the range of normalised surviving fractions is observed to be 0.073 (NC,5) to 0.139 (NC,D). A wider range of surviving fraction from 0.285 (NC,5) to 0.471 (NC,M) at 1Gy is observed when compared with the corresponding results from the pharmacological pre-irradiation treatments presented in figure 4.11. It was for this reason that further investigation utilising 0.5Gy was undertaken - the range of normalised surviving fraction observed at this radiation dose was 0.505 (3,5) to 0.759 (NC,5). Error bars are not presented in figure 4.12 to facilitate ease of interpretation but a more detailed analysis of surviving fractions at 1Gy and 0.5Gy irradiation doses is presented in figures 4.13 and 4.14 below.

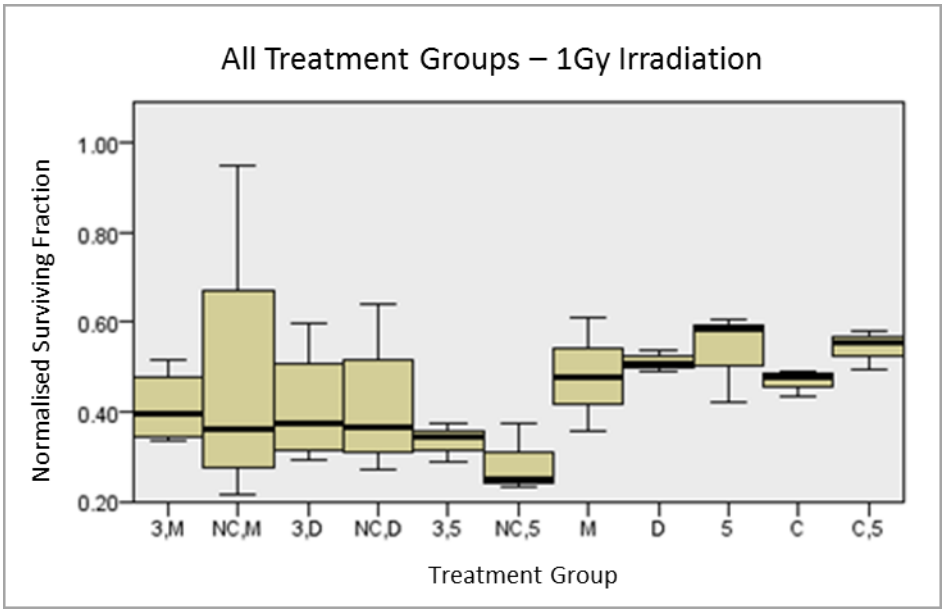

Figure 4.13 – Box-and-whisker plots demonstrating the surviving fraction at 1Gy irradiation, across all experimental treatment groups investigated on clonogenic assay. Results have been normalised to the non-irradiated (0Gy) control for the respective pre-irradiation treatment to facilitate direct comparison of any radiation specific effect. The treatment groups are those as defined in table 4.1.

The graph in figure 4.13 represents a direct comparison of the outcome of all experimental treatment groups at 1Gy irradiation assessed by clonogenic assay. The lowest normalised surviving fraction is 0.285 in the NC,5 treatment group, with the highest being 0.544 in the C,5 treatment group. On Kruskal-Wallis analysis there was no statistically significant difference across all treatment groups (p=0.167).

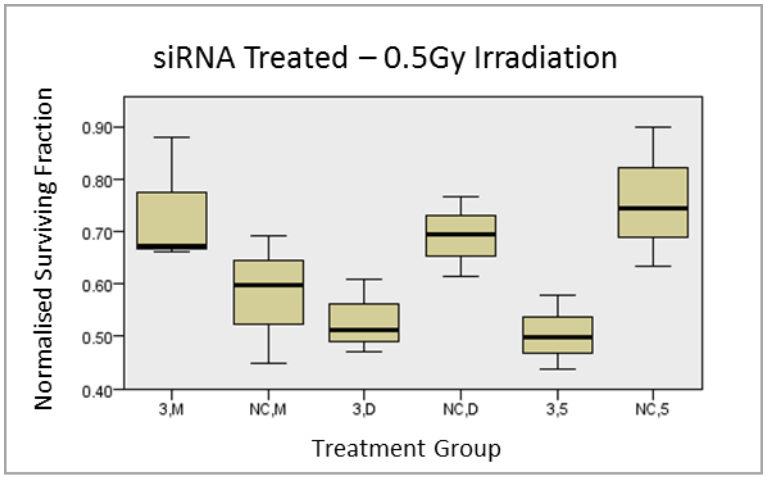

Figure 4.14 – Box-and-whisker plots demonstrating the surviving fraction at 0.5Gy irradiation, across all transfected treatment groups investigated on clonogenic assay. Results have been normalised to the non-irradiated (0Gy) control for the respective pre-irradiation treatment to facilitate direct comparison of any radiation specific effect. The treatment groups are those as defined in table 4.1.

The graph in figure 4.14 represents the observed normalised surviving fractions for the transfected treatment groups, where further investigation at 0.5Gy irradiation was undertaken. The lowest observed normalised surviving fraction is 0.505 in the 3,5 group, and a statistically significant difference between all groups was identified on Kruskal-Wallis analysis (p=0.048). On pairwise comparison 3,5 was significantly lower than 3,M (0.737, p=0.027), NC,D (0.692, p=0.032) and NC,5 (0.759, p=0.014), as was 3,D (0.530) against NC,5 (p=0.039). There was no difference between the normalised surviving fraction of the control treatment group NC,M (0.579) with either 3,D (p=0.646) or 3,5 (p=0.400) however, indicating no AC inhibition specific effect.

4.3.4 Baseline Surviving Fraction

Throughout the course of performing the clonogenic assays, it was observed that the crude surviving fractions in the baseline non-irradiated (0Gy) control samples was apparently different between cell populations that had been transfected with siRNA coding for AC, and both those transfected with a non-coding siRNA and non-transfected cell populations. This apparent difference is as depicted in figure 4.15 below.

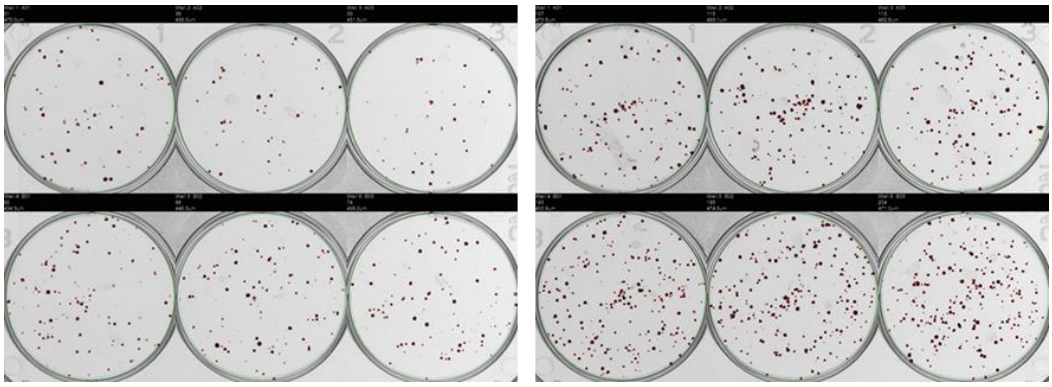

Figure 4.15 – Images acquired by the GelCount™ automated colony counter of two of the 6-well experimental clonogenic assay plates. The comparison demonstrated is to illustrate a representative outcome following transfection with siRNA3 (left side) against non-coding siRNA (right side). The cells on both plates were incubated with media only following the respective transfection and are the non-irradiated (0Gy) control group for their pre-irradiation treatment. Cell seeding densities were identical between the plates, with each well in the top rows seeded with 200 cells, and 400 cells seeded into each well in the bottom rows.

Fewer colonies are observed in the image of the 6-well plate on the left side of figure 4.15 on clonogenic assay where the cells had prior been transfected with siRNA coding for AC, compared to a greater number of colonies observed in the image of the 6-well plate on the right side where the cells had prior been transfected with a non-coding siRNA. Cell seeding into both plates had been identical, and it was considered that further investigation of this apparent difference was justified.

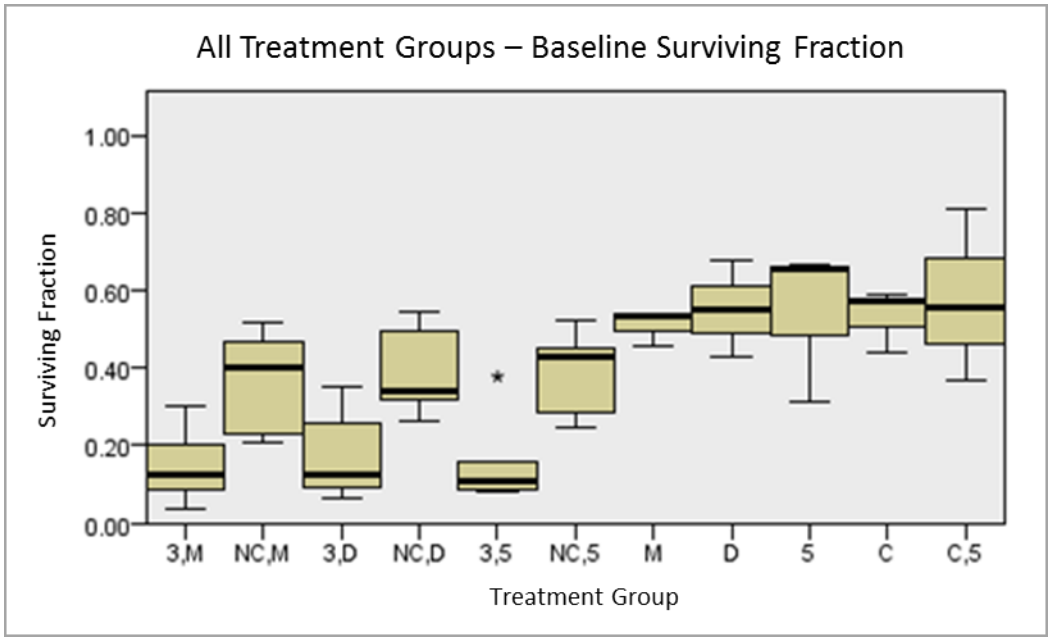

Figure 4.16 – Box-and-whisker plots demonstrating the observed surviving fraction across all experimental treatment groups investigated on clonogenic assay, for the non-irradiated (0Gy) control group of the respective pre-irradiation treatment. The treatment groups are those as defined in table 4.1.

Figure 4.16 demonstrates the crude surviving fractions on clonogenic assay of all investigated treatment groups in the baseline non-irradiated (0Gy) cell populations. On Kruskal-Wallis analysis there was significant difference across all categories of group ($p<0.001$), although on pairwise comparison there was no difference between cell populations that had been transfected with siRNA coding for AC (3,M, 3,D and 3,5), between cell populations transfected with a non-coding siRNA (NC,M, NC,D and NC,5), or between non-transfected cell populations (M, D, C, 5 and C,5). It was considered that this represented the pharmacological manipulation undertaken prior to re-seeding in the clonogenic plate had not affected the inherent viability in these non-irradiated cells, and that any differences were due to the siRNA transfection for AC or the transfection process itself.

A statistical analysis of the baseline surviving fraction in non-irradiated cells was further undertaken according to grouping based on transfection, and is presented in figure 4.17 below.

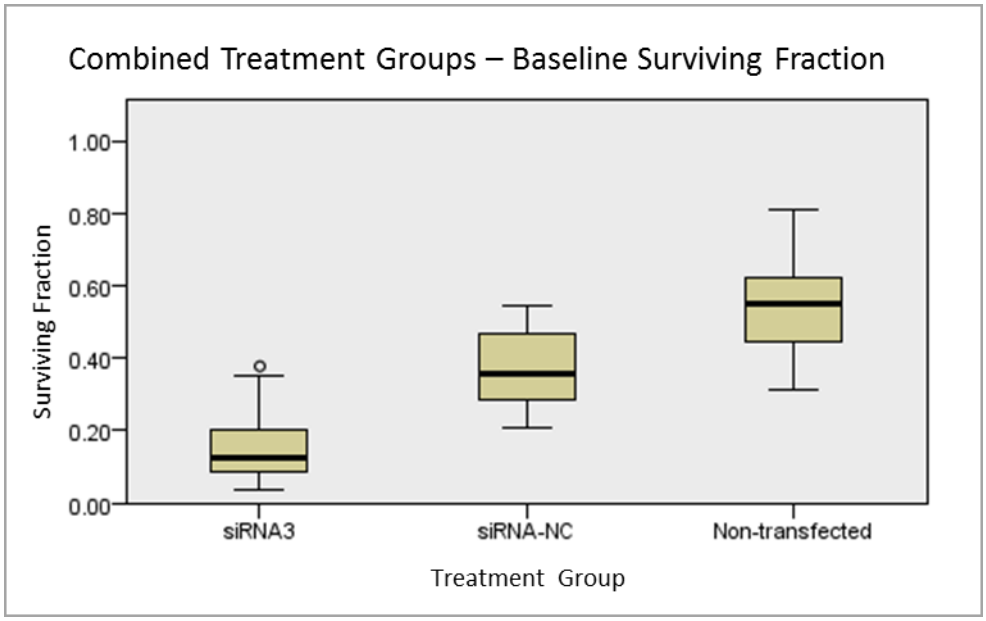

Figure 4.17 – Box-and-whisker plots demonstrating the grouped observed surviving fraction at baseline (non-irradiated, 0Gy controls) on clonogenic assay between cell populations that had undergone ASAH1 siRNA transfection (siRNA3), non-coding siRNA transfection (siRNA-NC) and non-transfected cells. The grouped results originate from the data presented in figure 4.16; siRNA3 combines 3,M, 3,D and 3,5; siRNA-NC combines NC,M, NC,D and NC,5; non-transfected combines M, D, 5, C and C,5.

The median baseline surviving fraction on clonogenic assay in non-irradiated cell populations subjected to siRNA transfection (siRNA3, n=17) is 0.123 with an interquartile range (IQR) of 0.141. This is significantly lower on pairwise comparison following Kruskal-Wallis analysis, than both cell populations subjected to transfection with a non-coding siRNA (siRNA-NC, n=17) where the median surviving fraction is 0.359 IQR 0.206 ($p=0.002$), and non-transfected cell populations (n=15) where the median surviving fraction is 0.548 IQR 0.211 ($p<0.001$). There was no statistically significant difference between cell populations transfected with a non-coding siRNA and non-transfected cell populations ($p=0.057$).

4.3.5 MTS Assay – Post-Irradiation / Acid Ceramidase Inhibition

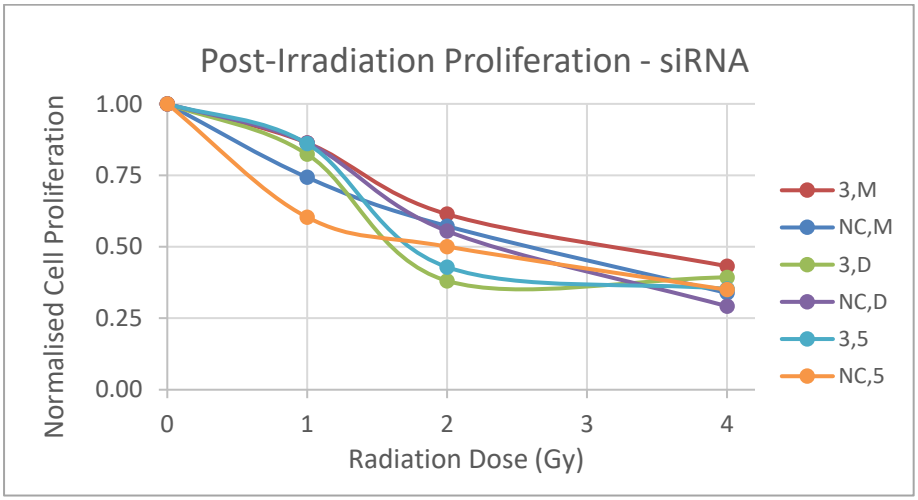

Figure 4.18 – HCT116 cell proliferation after irradiation (0-4Gy) as observed on MTS assay in siRNA transfected populations. Cell populations had undergone pre-irradiation ASAH1 siRNA transfection (or non-coding siRNA transfection as control) +/- 5-FU dosing (or respective control). MTS assay was performed 72 hours following the seeding of 2,500 cells from each population in triplicate in 96-well plates, with three independent experimental replicates performed. Absorbance at 490nm was measured, data adjusted according to background control samples, then normalised to the 0Gy value for each treatment group to facilitate direct comparison. The treatment groups are those as defined in table 4.1.

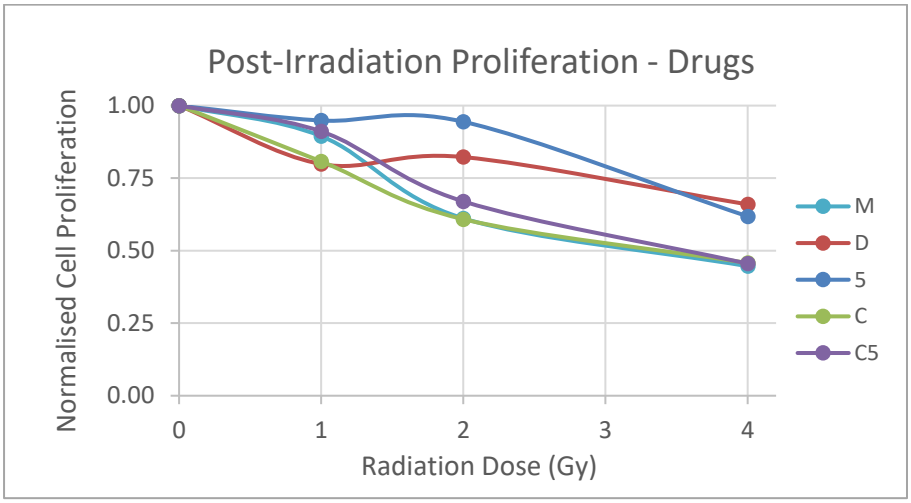

Figure 4.19 – HCT116 cell proliferation after irradiation (0-4Gy) as observed on MTS assay in pharmacologically treated populations. Cell populations had undergone pre-irradiation treatment with 5-FU, carmofur, combined treatment or vehicle control. MTS assay was performed 72 hours following the seeding of 2,500 cells from each population in triplicate in 96-well plates, with three independent experimental replicates performed. Absorbance at 490nm was measured, data adjusted according to background control samples, then normalised to the 0Gy value for each treatment group to facilitate direct comparison. The treatment groups are those as defined in table 4.1.

The results of the MTS proliferation assay subsequent to irradiation have been split between cell populations undergoing transfection prior to irradiation (figure 4.18) and pharmacologically-only treated (non-transfected) populations (figure 4.19), to allow for relative ease of interpretation but can be directly compared. HCT116 cell proliferation is observed to generally decrease with increasing radiation dose in all treatment groups but there is no statistically significant difference (Kruskal Wallis analysis) between any of the treatment groups at 1 (p=0.542), 2 (p=0.214) or 4Gy (p=0.515) irradiation respectively. Equally, there does not appear to be a consistent trend between treatment groups across the range of radiation doses. Error bars are not presented in figures 4.18 and 4.19 for this reason and to facilitate ease of interpretation.

4.3.6 Post-Transfection Proliferation

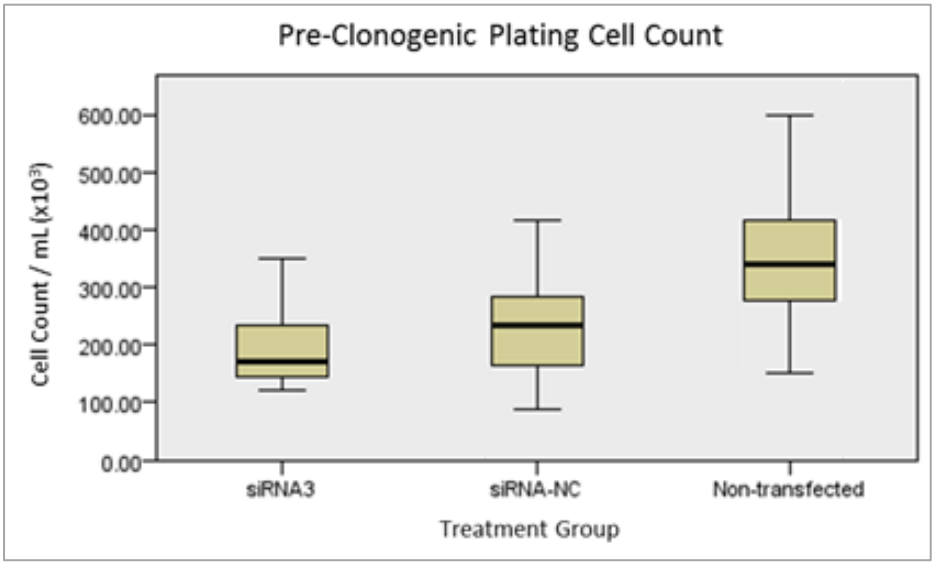

Figure 4.20 – Box-and-whisker plots representing the live cell counts observed prior to seeding in the clonogenic plates, according to respective grouped treatment. $2x10^5$ cells in 2mL culture medium were seeded in each 35mm cell culture dish at the outset, prior to transfection of coding (siRNA3) and non-coding (siRNA-NC) siRNA. Some cell groups were exposed to pharmacological treatment only (non-transfected), and control groups were incorporated across the range of treatments as described in table 4.1. All cell groups underwent a change of culture medium (to facilitate pharmacological treatment) 2 hours prior to exposure to 0-4Gy irradiation. The cell counts were observed immediately subsequent to irradiation (74 hours following initial seeding) upon re-seeding into the clonogenic plates.

The cell counts observed prior to seeding into the clonogenic plates, grouped according to pre-irradiation treatment (non-transfected n=63, ASAH1 siRNA transfected n=56, and non-coding siRNA transfected n=56) as demonstrated in figure 4.20, were 347.9 +/- 101.7 $x10^3$ per mL, 192.6 +/- 56.9 $x10^3$ per mL, and 228.0 +/- 85.1 $x10^3$ per mL respectively. There was a significant difference in the observed cell count between groups on Kruskal-Wallis analysis ($p<0.001$), which was specifically between non-transfected cells and both ASAH1 siRNA transfected cells ($p<0.001$) and non-coding transfected cells ($p<0.001$) on pairwise comparison. There was no difference in cell count between the two transfected cell groups ($p=0.105$).

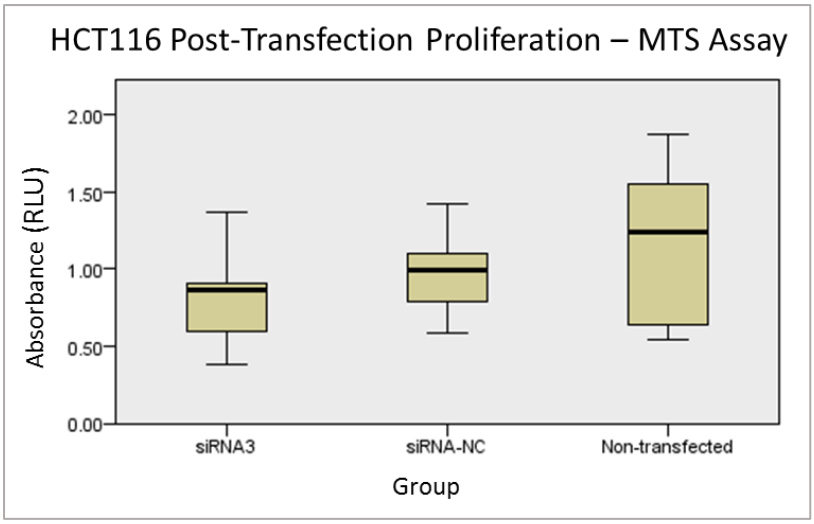

Figure 4.21 - Box-and-whisker plots representing the crude absorbance values observed on MTS assay from non-irradiated cell populations exposed to; siRNA transfection coding for AC (siRNA3), non-coding siRNA transfection (siRNA-NC), and non-transfected cells. Transfection or control treatment was undertaken prior to re-seeding the cells in 96-well plates at 2,500 cells per well, and MTS was applied after incubation for 72 hours. The values have been adjusted according the background absorbance observed from an equivalent volume of media in wells on the plates and represent triplicate values from three independent experiments.

An observation of post-transfection proliferation 72 hours after re-seeding can be obtained from the non-irradiated control groups from the MTS assay data, as presented in figures 4.18 and 4.19. The crude absorbance values obtained from these experiments are presented in figure 4.21, where no statistically significant difference is observed between all groups on Kruskal-Wallis analysis ($p=0.216$).

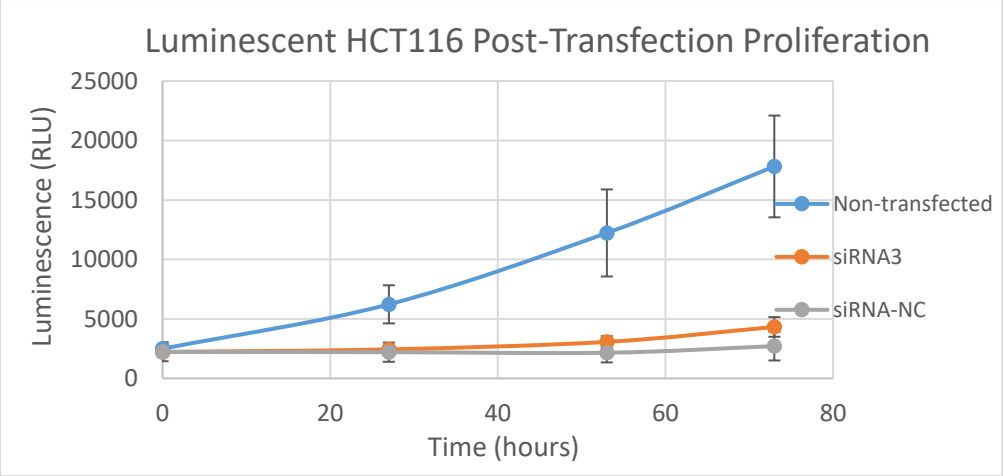

Figure 4.22 – Luminescence observed in luciferase-expressing HCT116 cells comparing ASAH1 siRNA transfected (siRNA3), non-coding siRNA transfected (siRNA-NC) and non-transfected (Media) cell populations, using VivoGlo™ Luciferin assay (Promega). Transfection or control treatment was undertaken prior to re-seeding the cells in white-bottomed 96-well plates at 2,500 cells per well. Luminescence (as a surrogate for cell proliferation) was observed at time points over the subsequent 72 hours following the application of VivoGlo™ Luciferin. Triplicate wells were seeded for each time point for each population, with three independent experiments performed. Mean fluorescence values observed are plotted with error bars representing one SD.

Cell proliferation, as represented by luminescence in figure 4.22, was observed to be comparable at baseline between groups upon re-seeding into the 96-well plate. This was confirmed on Kruskal-Wallis analysis ($p=0.463$). The non-transfected group (cells pre-incubated in culture medium only) began to demonstrate proliferation by 27 hours, at which point there was significant variance between treatment groups ($p<0.001$), which persisted to 72 hours ($p<0.001$). There was no difference on pairwise comparison between siRNA transfected groups (ASAH1 and non-coding) at 27 hours however ($p=1.000$), which remained the case at 72 hours ($p=0.105$). Proliferation in these transfected cell groups is observed to begin to increase by and after 53 hours but the rate of proliferation is observed to be slower than non-transfected cells. This may be due to an off-target effect of transfection in the luminescent population.

4.3.7 Post-Transfection Caspase 3/7 Activity

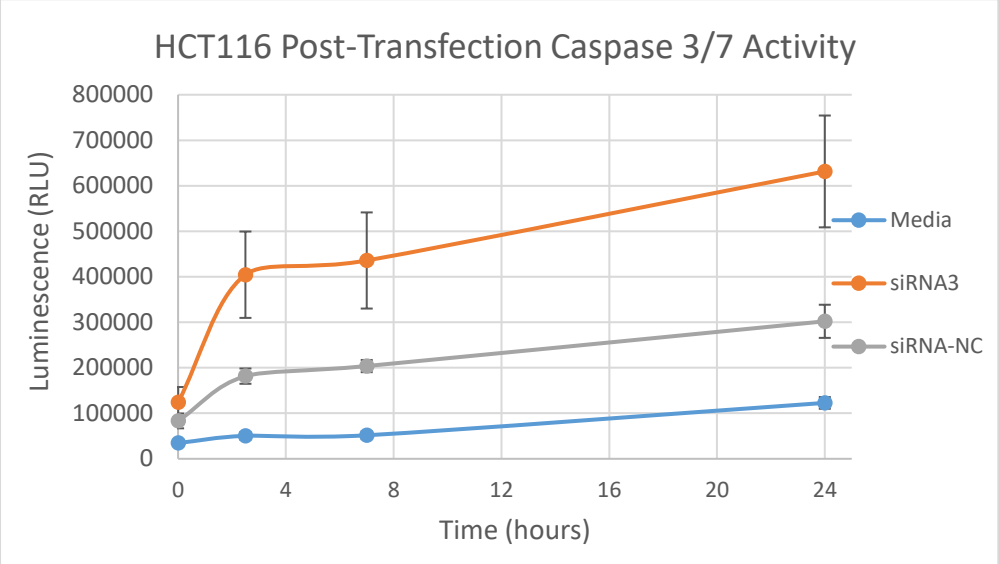

Figure 4.23 – Luminescence observed in HCT116 cells subsequent to undertaking the Caspase-Glo® 3/7 assay (Promega) in ASAH1 siRNA transfected (siRNA3), non-coding siRNA transfected (siRNA-NC) and non-transfected (Media) cell populations. Transfection or control treatment was undertaken prior to re-seeding the cells in white-bottomed 96-well plates at 10,000 cells per well. Luminescence (as a marker of caspase 3/7 activity) was observed at 0, 2.5, 7 and 24 hours following the application of Caspase-Glo® reagent. Triplicate wells were seeded for each time point for each population, with three independent experiments performed. Mean fluorescence values observed are plotted, with error bars representing one SD.

Caspase 3/7 activity, as represented by luminescence in figure 4.23, was observed to increase in all treatment groups over the time points represented, although the rate of increase of activity was observed to be greatest initially, particularly in transfected cell populations. Highest caspase 3/7 activity was observed in ASAH1 siRNA transfected cells, whereas lowest activity was observed in non-transfected cells. Whilst there was significant variance between all treatment groups on Kruskal-Wallis analysis ($p<0.001$) at all time points, there was no difference particularly in caspase 3/7 activity on pairwise comparison between ASAH1 siRNA transfected and non-coding siRNA transfected cells at the 0-hour time point ($p=0.184$) upon re-seeding into the 96-well plate, although significant variance had developed by the 2.5-hour time point ($p=0.048$), which persisted through to 24 hours ($p=0.048$).

4.4 Discussion

4.4.1 Summary of Aims

The overall aim of the work in this chapter was to assess the effect of genetic and pharmacological manipulation of AC on the *in vitro* radio-sensitivity of a CRC cell line. This effect would be assessed using primarily clonogenic assay and MTS viability assay. To facilitate an optimal dosing strategy in the model, it was necessary to perform preliminary dose-response analysis with the 5-FU-based potential pharmacological radio-sensitisers, and to establish the specific 5-FU based effect of these chemotherapeutics in the cell line, to isolate any potential effect based upon AC inhibition.

Whilst performing the clonogenic assays, it was observed there was a fundamental difference in baseline surviving fraction between cell populations subjected to transfection with siRNA coding for ASAH1, and both those subjected to non-coding siRNA transfection and non-transfected cell populations. A further aim was developed to assess whether this difference could be explained by an alteration in cell proliferation both prior and subsequent to re-seeding following transfection, or by apoptotic predisposition, and whether any difference was specific to this genetic inhibition of AC expression.

4.4.2 Summary of Results

Dose-response analysis with the chemotherapeutics capecitabine, 5-FU and carmofur was performed in the HCT116 cell line using MTS assay. Capecitabine demonstrated no toxicity and was not pursued further in the development of the clonogenic model. The IC_{50} values for 5-FU and carmofur were observed to be 5.48µM (95%CI 4.11-7.31, R^2=0.875) and 7.48µM (95%CI 5.96-9.38, R^2=0.843) respectively, and 3.95µM for each drug (95%CI 3.64-4.29, R^2=0.930) when in combination. No significant toxicity was observed at a 2µM concentration of these drugs either individually or in combination in the cell line (p=0.465).

2μM concentrations of carmofur and 5-FU were assessed for their effect upon TS in the HCT116 cells on Western blotting. Qualitative assessment revealed an earlier effect on TS with 5-FU but with some effect on TS following a 2-hour incubation with carmofur.

These results, combined with the timing for inhibition of AC activity with carmofur as detailed in chapter 3, led to the development of the pharmacological dosing strategy in the clonogenic model.

HCT116 cell radio-sensitivity was not demonstrated to be significantly different in either the genetic (with or without 5-FU) or pharmacological arms of AC inhibition modelling, either on clonogenic or MTS assay. An insignificant surviving fraction was observed on clonogenic assay at both 2Gy and 4Gy irradiation, which did not correlate with MTS assay.

A significant difference in surviving fraction was observed at baseline between non-irradiated cell groups on clonogenic assay. Following siRNA transfection coding for ASAH1, a low median baseline surviving fraction of 12.3% was observed. This was significantly lower than in cells transfected with a non-coding siRNA (35.9%, $p=0.002$) or non-transfected cells (54.8%, $p<0.001$), whereas there was no difference between these latter two groups ($p=0.057$).

This low baseline surviving fraction was therefore attributable to an AC specific effect, and further assessment was undertaken. There was no difference in the cell count observed prior to re-seeding into the clonogenic plates between cell populations subjected to siRNA transfection coding for ASAH1 or non-coding siRNA transfection ($p=0.105$) although both groups were lower than for non-transfected cells ($p<0.001$). Proliferation after re-seeding was assessed using MTS assay data already obtained, where no difference was identified between either transfection groups or non-transfected cells ($p=0.216$), and based on fluorescence observed in a stably-transfected luciferin-expressing HCT116 cell line on luciferase assay. Whilst a significantly higher fluorescence was observed in non-transfected cells ($p<0.001$), there was again no difference between cells transfected with siRNA coding for ASAH1 or non-coding siRNA transfected cells ($p=0.105$).

Caspase 3/7 assay was undertaken in these groups to assess for a potential apoptotic predisposition. At the point of re-seeding subsequent to transfection, there was no difference between cells subjected to siRNA transfection coding for ASAH1 and non-coding siRNA transfected cells ($p=0.184$). Caspase 3/7 activity increased in all groups over the 24-hour duration of the assay. Significantly higher caspase 3/7 activity was observed in the cell

population subjected to siRNA transfection coding for ASAH1 at the 2.5-hour time point, when compared to non-coding siRNA transfected cells and non-transfected cells, and this significant difference persisted to 24 hours (p=0.048).

4.4.3 Strengths and Limitations

The HCT116 cell line used for investigation of AC dependent radiotherapy modelling in this thesis is p53+/+ (wild type). The HCT116 p53-/- (deficient) cell line is known to be radio-resistant (Huerta *et al*, 2013), therefore it is plausible that the wild type cells used are inherently radio-sensitive, and that it is not easily possible to demonstrate significant further radio-sensitivity. p53 was equally not identified as significantly differentially expressed in the original proteomic profiling, and as such may not be relevant to our investigation of AC.

Basal AC expression in the HCT116 cell line was observed to be relatively low (by a factor of over 3 - 28.7%) on densitometry when compared to a rectal cancer sample known from the work performed in the original proteomic profiling to relatively overexpress AC. In the original proteomic profiling, the relative difference in expression was considered significant above a factor of 1.5. It may therefore be the case that the HCT116 p53+/+ is inherently radio-sensitive based on a low expression of AC. A logical further investigation would be to profile basal expression of AC in the HCT116 p53-/- cell line, and to potentially perform the same range of experiments as in this thesis, particularly if the basal expression was observed to be higher. Alternatively, it could be possible to upregulate AC in the HCT116 p53+/+ cell line using a plasmid vector.

If the basal expression of AC in the HCT116 p53+/+ cell line is low, then despite the results presented in chapter 3 in the cell line demonstrating statistically significant inhibition of AC expression and activity, it may be that further inhibition of AC from a potential low expression and activity baseline, does not produce any changes in functional effect, and does not further alter radio-sensitivity.

The dosing of carmofur and 5-FU in the clonogenic assay model was performed to facilitate an optimal inhibition of AC from carmofur at the point of irradiation delivery, and to approximate the 5-FU based effect of both drugs. It is plausible that their mode of action in

facilitating radio-sensitivity occurs later than a therapeutically effective concentration of the drug persisted in the cells. It was considered that either plating the cells out in dosed media after irradiation (due to an unquantified potential differential 5-FU based effect between 5-FU and carmofur) or performing re-dosing of the cells after seeding in the clonogenic plate (i.e. daily for the duration of incubation for the clonogenic assay) would introduce a greater bias than the risk of the drug not being therapeutic for long enough. The risk of concern in re-dosing the clonogenic plate is that cells or colonies are washed away, and that this would occur in an inconsistent manner between wells.

5-FU was also observed to effect TS protein levels on Western blotting earlier than carmofur. This may be explained by the required intra-cellular conversion of carmofur to 5-FU prior to its inhibition of TS, which may occur through CYP2A6 comparable to tegafur (El Sayed and Sadée, 1983) but is not known. In one study it has been observed that carmofur-induced inhibition of TS activity didn't alter cellular proliferation in comparison to 5-FU (Nishiyama *et al*, 1988), suggesting a more complex mechanism for its action that potentially involves AC (Realini *et al*, 2013), again potentially explaining the observed later or reduced effect on TS.

The effect of siRNA inhibition of AC was anticipated to outlast the pharmacological inhibition but despite this, it is possible that the AC dependent radio-sensitivity being investigated still remains dependent on the presence of 5-FU (all the patients in the original proteomic profiling were treated with capecitabine as a radio-sensitiser). Whilst it may be that the effective 5-FU concentration did not last for a sufficient time alongside AC inhibition with siRNA to effect radio-sensitivity, the baseline surviving fraction in non-irradiated cells subsequent to ASAH1 siRNA transfection was significantly reduced (12.3%) - a further significant reduction in surviving fraction based on increased radio-sensitivity may not be appreciable.

Further evaluation of the duration of AC expression and activity inhibition following re-plating in normal culture medium after siRNA transfection and pharmacological dosing could be performed.

Capecitabine was considered to be used as the standard treatment against which carmofur should be compared but capecitabine demonstrated no toxicity in the HCT116 cells even at the highest achievable concentration of 400μM – this may reflect that the purchased product was not appropriate, or that the HCT116 cells do not express the CES proteins at the levels required for the conversion of capecitabine into 5-dFCR, or that another of the required proteins upstream of final conversion to 5-FU is not expressed sufficiently. This was not

investigated but offers a potential alternative explanation as to why the HCT116 cells in the clonogenic experiments did not display any significantly altered radio-sensitivity, if it is treatment in the clinical setting with capecitabine in the presence of a low expression of AC that confers radio-sensitivity.

Another explanation for a lack of alteration in radio-sensitivity but under the assumption of appropriate inhibition of AC in the clonogenic model, is that the behaviour of the HCT116 cell line in culture does not mimic the complex environment of a tumour *in situ*. The function of AC in the two contexts may be very different, and the importance of AC in the *in vitro* survival or function of the HCT116 cells in either a monolayer in culture or when seeded in individual cells to form colonies may be negligible. Alternative potential routes of investigation in an AC dependent model of sensitivity to CRT could be to use primary cell culture (particularly in a tumour where AC was overexpressed), 3D cell culture in the HCT116 p53+/+ cell line to represent a more physiologically accurate environment (Ludwig *et al*, 2013), or consideration of the development of a mouse model.

The data presented to represent cell outcome following irradiation was obtained using both MTS viability assay and clonogenic assay. There would appear to be a disparity in the outcomes with these assays, in that the normalised data would seem to under-represent the effect of irradiation when using the MTS assay. At 4Gy irradiation, the normalised surviving fraction was only 1-2% of seeded cells on clonogenic assay, whereas viability 3 days after seeding on MTS assay was in the range 29-66%. Combined with the inconsistent and wide-ranging data observed on MTS assay, it would seem that the irradiation effect at 3 days is not complete, and that cells remain viable at this time even though they are ultimately unable to proliferate. This is consistent with the description of these techniques at the outset of the chapter (Mirzayans *et al*, 2007), and MTS assay at this time would seemingly not be the optimal modality to determine outcome following irradiation.

Logistical limitations may have existed in undertaking the clonogenic assay, with irradiation being undertaken in a different laboratory and with the requirement to place cells on ice whilst transporting them to and from these locations, undertaking irradiation and re-plating. The time taken to undertake this process was not specifically recorded but it is likely that cell groups were on ice for 1-2 hours. This may have resulted in the activation of survival mechanisms which negated the effect of AC inhibition and irradiation, with evidence to suggest that cells, tissues and organs have differing survival strategies to overcome environmental extremes (Brockbank *et al,* 2011).

Another potential concern is with regard the validity of the controls used for siRNA transfection. This is in the context of non-significant irradiation-specific results with AC inhibition, and with reduced ASAH1 mRNA expression following the transfection process, both with the presence and absence of non-coding siRNA. My conclusion from the data presented in chapter 3 is that this wasn't specific to the non-coding siRNA but there was clearly a significant off-target effect which may have impacted on the clonogenic results. Alternative non-coding sequences could be examined. The mechanism of siRNA-mediated reduction in cellular proliferation has been considered to be due to either innate immunity mechanisms responding to the presence of exogenous RNA molecules (Fedorov *et al*, 2006), or to competitive interactions of the siRNA molecules with endogenous RNAs Liang *et al*, 2013).

The use of luciferase-expressing HCT116 cells was an attempt to provide cross-validation for the MTS assay data relating to post-siRNA transfection proliferation, which did not separate ASAH1 siRNA transfected, non-coding siRNA transfected and non-transfected cells. The non-transfected cells demonstrated significantly greater luminescence (as a surrogate for viability / proliferation) with this assay compared to the transfected cell groups, which is contrary to the MTS assay proliferation data presented. There were no statistically significant differences between the transfected cell groups over the course of the assay, although luminescence was only observed to begin to increase marginally and much later than in non-transfected cells. This may be due to on off-target effect of transfection in the HCT116-luc population.

4.4.4. Conclusion

- HCT116 cell radio-sensitivity can be increased by the pharmacological inhibition of AC activity using the chemotherapeutic carmofur - **NOT PROVEN**

No difference in HCT116 cell radio-sensitivity was observed in this study subsequent to pharmacological inhibition of AC with carmofur. Significant limitations may exist with the dosing strategy undertaken, or with a low baseline expression of AC in the cell line, which could have impacted upon these results.

- HCT116 cell radio-sensitivity can be increased by the genetic suppression of AC expression (and subsequent activity) using siRNA transfection - **NOT PROVEN**

No difference in HCT116 cell radio-sensitivity was observed in this study subsequent to genetic manipulation of AC expression with siRNA transfection. A significantly lower baseline surviving fraction was observed on clonogenic assay in non-irradiated cell populations subjected to siRNA transfection coding for ASAH1, when compared to non-coding siRNA transfected and non-transfected cell populations - a finding which is therefore specific to AC inhibition. This baseline surviving fraction of 12.3% of those cells seeded into the clonogenic plates, compared to 54.8% in non-transfected cell populations, represents a significantly reduced baseline. A further irradiation specific effect was not observed relative to genetic and/or pharmacological manipulation but this significantly reduced baseline surviving fraction with siRNA inhibition of AC, may not have afforded sufficient sensitivity.

- Any increase in cell radio-sensitivity based on inhibition of AC is independent of the presence of 5-FU - **NOT PROVEN**

It has been demonstrated that carmofur and 5-FU independently produce an effect on TS within the dosing window employed in the clonogenic assay. No increase in cell radio-sensitivity was observed in the presence of 5-FU, with or without pharmacological inhibition of AC with carmofur. This again may relate to the limitations with the pharmacological dosing strategy, or to a low baseline expression of AC in the cell line.

In the context of genetic manipulation of AC expression with siRNA transfection, increased radio-sensitivity was not observed with the presence of 5-FU. This could relate to the pharmacological dosing strategy but may be more likely to be related to the significantly reduced baseline surviving fraction following ASAH1 siRNA transfection, as previously described.

4.4.4.1 Assessment of reduced baseline surviving fraction post-transfection

The significantly reduced surviving fraction observed on clonogenic assay in HCT116 cells subjected to ASAH1 siRNA transfection was not anticipated but implicates AC in their inherent survivability. This may relate to cell adhesion and/or colony formation and growth, or apoptosis. Whilst cell growth during transfection was reduced in both coding and non-coding groups compared to non-transfected cells based on cell counts observed upon re-

seeding into the clonogenic plates, there was no difference between coding and non-coding siRNA transfected cell populations. Equally there was no difference in proliferation between these two transfection groups subsequent to re-seeding, observed with MTS and luciferin assays.

Caspase 3/7 activity was higher in both transfection groups compared to non-transfected cells at the point of re-seeding but subsequent observations of increased caspase 3/7 activity were significantly higher in cells transfected with siRNA coding for ASAH1. Increased caspase 3/7 activity suggests apoptotic predisposition, and this significantly higher caspase activity with inhibition of AC potentially explains the reduced surviving fraction observed on clonogenic assay. This observation of caspase activity also separates the cell group from the non-coding control consistent with the clonogenic data. It is not possible to determine from the work presented if this presumed apoptotic predisposition is; a) a direct consequence of siRNA inhibition of AC, or b) related to re-seeding and an inability to adhere to the plate subsequent to inhibition of AC, which then triggers apoptosis.

AC inhibition is therefore implicated *in vitro* in the survivability of HCT116 CRC cells, and may predispose to apoptosis.

Chapter 5

Concluding Discussion

5.1 Background Summary

The response to CRT in rectal cancer varies from pCR, with associated survival benefit, to disease progression. Predicting response is not currently possible but identifying biomarkers which may do this has been highlighted as a priority for research from national association strategy. The ability to predict response would facilitate personalised treatment, and minimise morbidity from CRT and prevent delays in the systemic and local management of the disease in non-responders. Therapeutic targets may also be revealed with the aim of improving the efficacy of CRT, and further facilitate non-operative or rectal-preservation strategies. An initial novel temporal proteomic profiling of rectal cancer has revealed differential expression of AC between relative responders and non-responders to CRT, and AC is proposed for further evaluation as a potential predictive and/or prognostic biomarker of response.

5.2 Original Aim

The original aim of this thesis was to attempt to provide further validation of AC as a biomarker of response to CRT in rectal cancer with assessment in a wider clinical dataset, and to perform an *in vitro* evaluation of the effect of AC inhibition on radio-sensitivity in a CRC cell line.

5.3 Initial Research Questions and Study Design

The research questions to be answered by this thesis were:

- Does AC expression predict response to CRT in clinical rectal cancer samples in a larger patient cohort?
- Does the inhibition of AC in a CRC derived cell line increase radio-sensitivity?
- Does inhibition of AC increase radio-sensitivity when compared to standard 5-FU radio-sensitisation?

It was initially determined to answer these questions with the following study plan:

- Identify ≥100 rectal cancer cases, whereby surgical resection of the primary tumour had been performed following completion of neoadjuvant CRT, and assess TRG in these cases
- Construct TMAs comprising; tissue from the diagnostic biopsy specimen, and normal epithelium and cancer site tissue from the resection specimen
- Assess TMA IHC expression of AC, and correlate with TRG and clinical and pathological data
- Perform genetic inhibition of AC with siRNA in the HCT116 CRC cell line, assessing mRNA expression, and protein expression and activity
- Assess the effect of pharmacological inhibition of AC with carmofur in the HCT116 CRC cell line on protein expression and activity
- Establish the effect of carmofur, capecitabine and 5-FU dosing on toxicity and TS expression in the HCT116 CRC cell line
- Assess the effect of AC inhibition on radio-sensitivity in the HCT116 CRC cell line

This study plan was executed in entirety other than for complete evaluation of capecitabine, including its effect on radio-sensitivity, upon determining it to be non-toxic in the HCT 116 cells. A further experimental plan evolved with closer evaluation of the clonogenic assay (when no radiation-specific effects were apparent) where ASAH1 siRNA transfected cells were observed to have an inherent reduced survivability:

- Assess the effect of ASAH1 siRNA transfection in the HCT 116 cells on proliferation during and after transfection, and apoptotic predisposition, to potentially explain their inherent reduced survivability

5.4 Summary of Results

5.4.1 Chapter 2

111 consecutive rectal cancer resection cases post-CRT were identified and incorporated into TMAs for analysis. There were 22 patients with pCR (19.8%), which was associated with improved estimated mean overall survival against non-pCR regression grades (99.6 vs 74.5 months, p=0.015). AC expression in diagnostic biopsy tissue, and in cancer site and normal colon epithelium from resection specimens was evaluated in the TMAs, discriminating between epithelial and stromal expression. 86-107 of the 111 cases were represented in the final analysis, dependent upon the tissue component. A trend towards higher stromal AC expression in the diagnostic biopsies was observed in non-responders (TRG 1) to CRT (p=0.075). Stromal expression at the cancer site post-CRT was significantly associated with response, with a lower expression in pCR (p=0.003) and higher expression in non-responders (TRG 1, p=0.017). A higher expression in normal colon epithelium from the resection specimen post-CRT was also observed in non-responders (p=0.012). The incidence of local disease recurrence was associated with a higher expression of AC at the cancer site post-CRT on both epithelial and stromal assessment (p=0.031 and p=0.038 respectively). The epithelial score here is exclusively in those not achieving pCR.

5.4.2 Chapter 3

Inhibition of AC by genetic (siRNA) and pharmacological (carmofur) manipulation was optimised in the HCT116 CRC cell line. ASAH1 mRNA expression was significantly inhibited to 4.1% ($p<0.001$) against control at 48 hours following siRNA transfection, with confirmatory qualitative assessment of reduced AC expression on Western blotting. ASAH1 mRNA expression was also observed to be significantly inhibited by a non-coding siRNA transfection to 40.4% (p=0.003) against control at 48 hours. AC activity was quantified by direct activity assay. siRNA targeting ASAH1 resulted in maximal AC activity inhibition of 15.5% 72 hours following transfection. Dose-dependent inhibition of AC activity was observed with carmofur – maximal inhibition to 15.2% was achieved with a 25µM concentration but statistically significant inhibition to 47.2% ($p<0.001$) was achieved with a 1µM concentration. Activity

inhibition of AC was maximal 2 hours after cell dosing but had normalised by 24 hours. 5-FU was observed not to inhibit AC activity in the cell line.

5.4.3 Chapter 4

Dose-response analysis with the chemotherapeutics capecitabine, 5-FU and carmofur was performed in the HCT116 cell line using MTS assay. Capecitabine demonstrated no toxicity and was not pursued further in the development of the clonogenic model. The IC50 values for 5-FU and carmofur were observed to be 5.48μM (95%CI 4.11-7.31, R^2=0.875) and 7.48μM (95%CI 5.96-9.38, R^2=0.843) respectively, and 3.95μM for each drug (95%CI 3.64-4.29, R^2=0.930) when in combination. No significant toxicity was observed at a 2μM concentration of these drugs either individually or in combination in the cell line (p=0.465). A comparable effect on TS expression was observed on Western blotting with 2μM concentrations of 5-FU and carmofur. No radiation-dependent differences were observed with genetic or pharmacological inhibition of AC in HCT 116 cells, either on clonogenic or MTS assay. Cells transfected with ASAH1 siRNA demonstrated a reduced baseline surviving fraction (12.3%), compared to non-coding siRNA cells (35.9%, p=0.002) or non-transfected cells (54.8%, p<0.001), with no statistical difference between these latter two groups (p=0.057). The only difference observed in the ASAH1 siRNA transfected cells was a potential predisposition to apoptosis with significantly higher caspase 3/7 activity observed over both non-coding siRNA transfected and non-transfected cells (p=0.048).

5.5 Study Limitations and Further Work

A detailed evaluation of the potential limitations with the *in vitro* experimentation performed, which may have impacted on the lack of observed radiation-dependent sensitivity with AC inhibition in the HCT 116 (p53+/+) cells has been discussed. Whilst further modifications to dosing strategy and repeated experimentation could be considered, the finding of higher caspase 3/7 activity in ASAH1 siRNA transfected cells suggests that AC inhibition in these cells predisposes to apoptosis, or further implicates AC in apoptotic pathways.

This conclusion is consistent with the literature presented in the introduction relating to the potential for ceramide to predispose to apoptosis, considered to involve activation of extrinsic apoptotic pathways through enhanced signalling of pro-apoptotic membrane molecules, or via intrinsic pathways by the formation of trans-membrane mitochondrial channels which allows the release of apoptosis inducing proteins such as caspase-3 and cytochrome c (Siskind *et al*, 2002). AC activity removes ceramide or limits its accumulation by de-acetylation towards S1P (Garcia-Barros *et al*, 2014). S1P has equally been demonstrated to initiate the pro-survival PIK3/AKT signalling pathway (Bonnaud *et al*, 2012), which has also been implicated independently in resistance to CRT in rectal cancer (Peng *et al*, 2018). AC is therefore centrally placed in potentially determining cellular fate in regulating the balance between ceramide and S1P.

These conclusions are also consistent with the literature evidence of over-expression of AC in particular in head and neck (Roh *et al*, 2016) and prostate (Cheng *et al*, 2013) cancers, both of which are commonly treated with radiotherapy. Its over-expression is also associated with melanoma (Realini *et al*, 2016) and myeloid leukaemia (Tan *et al* 2016), with *in vitro* data demonstrating AC over-expression conferring resistance to treatment in all these malignancies, and with clinical corroboration of this in particular with radiotherapy in prostate cancer (Cheng *et al,* 2013). Inhibition of AC *in vitro* in cell lines in head and neck cancer (Korbelik *et al*, 2016), melanoma (Bedia *et al*, 2011), myeloid leukaemia (Hu *et al,* 2011), non-small cell lung cancer (Ramírez de Molina *et al*, 2012), breast cancer (Flowers *et al*, 2011), hepatoma (Morales *et al*, 2007) and prostate cancer (Mahdy *et al*, 2009) is demonstrated to improve sensitivity to both irradiation and chemotherapeutic treatments, with most studies also demonstrating AC inhibition to result in increased ceramide levels,

reduced S1P levels and increased apoptosis. These pathways could be further investigated in the HCT116 cells with a view to evaluating for irradiation-specific effects and mechanisms.

The reduced ASAH1 mRNA expression observed with non-coding siRNA transfection and/or the transfection process is also potentially a product of a stress response on the cell. A mechanism to reduce AC expression and activity, that may increase intra-cellular ceramide and activate apoptotic pathways could be a protective response. This potential mechanism should also be investigated to evaluate for other biomolecules that may represent therapeutic targets, or to further validate AC.

An alternative further *in vitro* evaluation of AC dependent radio-sensitivity could be performed in the radio-resistant HCT 116 p53-/- cell line, or other cell lines with inherent differential expression of AC. To this end, a collaboration has been sought with Dr Ultan McDermott at the Sanger Institute (Cambridge, UK), who has provided data regarding AC protein expression from 10K proteome in 49 colorectal cancer cell lines (data presented in appendix C, with values normalised to an internal control line). Evaluation of radio-sensitivity with and without inhibition of AC can be performed using clonogenic assay as the outcome measure in a selection of these cell lines. This may be most relevant in cells which over-express AC but may also be relevant in cells with a low expression which are dependent on the protein.

The main limitation in this study relates to the implication of tumour heterogeneity, and in the tissue targeted for incorporation into the TMAs. Most tumours are considered to arise from a monoclonal cell population but with growth and the accumulation of mutations at different rates in different areas, tumours are well known to have diverse cell populations with different biological characteristics (Rehemtulla, 2012). This clearly has implications for the targeted tissue from which the TMAs in this study were created. The diagnostic biopsy cores were from a few endoscopic biopsy bites of what will have been superficial tumour. Prospectively collected tissue with more extensive mapping of the tumour would likely provide the most clinically available and robust mechanism from which to derive information regarding the expression and predictive value of any potential protein biomarker, alongside standardisation and validation of tissue collection, preservation, storage, processing and quantification (Stewart *et al,* 2017). The finding of near statistical significance in this study for higher stromal AC expression correlating with a poor response to CRT does not validate its use as a predictive marker but should be evaluated in a larger prospective study.

The correlation of reduced AC expression in epithelial cells with an enhanced response to CRT is potentially straightforward to understand as a mechanism. Whilst the results presented only potentially demonstrate a trend towards this observation, the impact of a low level or down-regulation of AC in tumour cells in response to the cellular insult, may result in a reduction of ceramide cleavage and its subsequent accumulation (Arana *et al,* 2010), with ceramide then exerting its influence in mediating cell cycle arrest and apoptosis (Garcia-Barros *et al*, 2014).

The targeting of residual malignant epithelium at the cancer site is equally inherently biased, as by definition this tissue has been resistant to CRT. Whilst optimal tissue cores were obtained from these tissue blocks, triplicate samples remain unlikely to overcome the limitations with tumour heterogeneity but were practicably the most viable option. Lower stromal expression of AC in this tissue though was significantly correlated with pCR, and higher expression with non-response. It is not possible to determine if this represents cause or effect but demonstrates the likelihood of stromal interaction with AC expression as a determinant of response to CRT, with AC representing a potential therapeutic target.

Correlation of AC expression with outcome data has additionally demonstrated association between relatively high epithelial and stromal expression in post-CRT cancer site tissue and local recurrence, and poorer survival with relatively low epithelial expression in normal colon. The finding of higher epithelial expression of AC in residual malignancy post-CRT correlating with local disease recurrence is consistent with the findings of AC expression, treatment resistance (including to radiotherapy), and poorer outcome associated with other malignancies as outlined in the introduction in 1.4.4. This epithelial score from the cancer site is exclusively from non-pCR patients and is therefore considered to further validate and implicate AC as a likely therapeutic target to improve response to CRT in rectal cancer. The latter finding of relatively low AC expression in normal colon epithelium correlating with poorer survival seems contrary to higher expression also correlating with no response to CRT. This may be a statistical anomaly or may represent activation of alternative pathways based on response to CRT (this tissue was from post-CRT samples) but requires further analysis in a prospective dataset obtained from pre-CRT samples.

The stroma (or tumour micro-environment) is considered to play an essential role in both the development of malignancy and in the resistance to treatment. This environment, composed of extracellular matrix, fibroblasts, endothelial cells, and cells of the immune system regulates the behaviour of tumour cells and co-evolves (Werb and Lu, 2015). Cancer

cells have been demonstrated to activate and recruit carcinoma-associated fibroblasts, which are able to both stimulate cell growth and invasion, as well as inflammation and angiogenesis but may also be tumour inhibiting (Kalluri and Zeisberg, 2006). This process is considered to be under the regulation of TGFβ signalling, which itself is primarily activated by integrins secreted from both tumour and stromal cells. In normal tissues TGFβ suppresses epithelial cell division but tumour cells can develop escape mechanisms to become resistant to TGFβ growth suppression. In addition, TGFβ drives EMT, increasing the potential for metastasis (Khan and Marshall, 2016).

The host response, through natural killer cells, has also been recently observed as a determinant of response to CRT (Alderdice *et al*, 2017), and gene expression profiles derived from the (non-malignant) stroma have been demonstrated to influence the classification of CRC molecular subtype (Dunne *et al*, 2016). Particularly given the association of higher expression of AC in normal colon epithelium (post-CRT) with a poor response to CRT, and differential stromal cancer site expression post-CRT correlating with response, it may be AC is implicated in mediating radio-resistance through tumour-stroma interaction or host response.

This signalling process may be mediated through ceramide-based lipid rafts, as micro-domains of regions of the cellular membrane, demonstrated to regulate vesicular traffic, cell polarity, and cell signalling pathways (Bieberich, 2018). They have been found in almost all existing experimental cancer models, including CRC, and play key regulatory roles in cell migration, metastasis, cell survival and tumour progression (Jahn *et al,* 2011). Altered AC expression may therefore have central implications for the regulation of ceramide and key regulatory inter-cellular signalling between stroma and tumour in response to CRT in rectal cancer.

AC was one of eight proteins identified from the original proteomic profiling as differentially expressed between relative responders and non-responders to CRT (appendix A). It was selected individually for further assessment on the basis of the evidence for its implication in prostate cancer response to radiotherapy specifically, and the availability of a commercially available chemotherapeutic inhibitor. The proteomic profiling also revealed myoferlin as another protein that may be implicated in response to CRT. Myoferlin is a muscle specific protein that has been identified in cancer cells and has been shown to confer a poor prognosis in oropharyngeal cancers (Kumar *et al*, 2016), another tumour group often

treated with radiotherapy. Further work is also needed to assess the role of this protein in rectal cancer, which can be undertaken initially using the established TMAs.

On the basis of the literature review undertaken in 1.3.3, it would also seem reasonable to assess TMA protein expression of EGFR, TS, and β-catenin.

5.6 Review of Hypotheses

The determined hypotheses at the outset of this thesis have been evaluated by the work presented:

- Differential expression of AC is present in rectal cancer and/or normal colon – **PROVEN**

Differential expression of AC in rectal cancer has been observed both pre- and post-CRT in epithelial and stromal tissue, and in epithelial tissue from normal colon.

- Expression of AC in rectal cancer and/or normal colonic tissue can predict response to neoadjuvant CRT, and/or is a biomarker of response to treatment – **PARTIALLY PROVEN**

There is a trend towards significance to correlate a high stromal diagnostic biopsy expression of AC with non-response to CRT. Low AC expression post-CRT in cancer site stroma correlates with pCR and high expression with non-response to CRT. High epithelial cancer site expression of AC post-CRT also correlates with local disease recurrence. AC therefore at least represents a potential biomarker of response to CRT and may represent a therapeutic target.

- Expression of AC can be inhibited by siRNA transfection in the HCT116 CRC cell line, subsequently inhibiting protein activity – **PROVEN**

Significant ASAH1 mRNA inhibition, and AC protein expression and activity have been demonstrated following siRNA transfection in the cell line.

- AC activity +/- expression can be inhibited by the chemotherapeutic carmofur in the HCT116 CRC cell line – **PROVEN**

Reduced AC protein expression and significantly reduced AC activity have been demonstrated following carmofur dosing of the cell line.

- HCT116 cell radio-sensitivity can be increased by the pharmacological inhibition of AC activity using the chemotherapeutic carmofur – **NOT PROVEN**

No difference in cell radio-sensitivity was observed with pharmacological inhibition of AC with carmofur in this study.

- HCT116 cell radio-sensitivity can be increased by the genetic suppression of AC expression (and subsequent activity) using siRNA transfection – **NOT PROVEN**

No difference in cell radio-sensitivity was observed following genetic inhibition of AC by siRNA transfection in this study. These cells did demonstrate an inherently reduced survivability.

- Any increase in cell radio-sensitivity based on inhibition of AC is independent of the presence of 5-FU – **NOT PROVEN**

Similar to previous, no difference in cell radio-sensitivity was observed in this study, irrespective of the presence of 5-FU.

The inherently reduced survivability of HCT 116 cells following ASAH1 siRNA transfection was further demonstrated to likely be induced by a predisposition to apoptosis on the basis of significantly raised caspase 3/7 activity.

5.7 Conclusion

AC remains a novel potential biomarker of response to CRT in rectal cancer. It does not in isolation represent a predictive biomarker, particularly given the complexity of tumour biology and tumour heterogeneity, although further investigation of its implicated role in mediating radio-resistance is required. *In vitro* genetic inhibition of expression seemingly predisposes to apoptosis, consistent with literature evidence for its action. Given this and its expression in radio-sensitive and radio-resistant tumours, it would seem reasonable to further consider AC as a potential therapeutic target. Further evaluation of AC expression in rectal cancer in a larger prospective dataset is required for wider validation, as is further *in vitro* evaluation of its mechanism of action, most specifically in a radio-resistant cell line.

A proposed mechanism for the action of AC is in its regulation of ceramide, both with low expression (or reduced in response to CRT) facilitating ceramide accumulation and subsequently promoting apoptosis directly within cells, or mediating changes in inter-cellular signalling (stromal-tumour interaction) through an effect upon ceramide-based lipid rafts.

Carmofur has been demonstrated to directly interact with AC and results in significant inhibition of activity. Its effect on TS as the effector of 5-FU-based therapy in comparison to 5-FU itself does not appear equivalent, and therefore is proposed to mediate its effects through combined AC and TS inhibition. Whilst 5-FU does not have an effect on AC inhibition, its role in improving response to radiotherapy in the clinical setting suggests that TS inhibition is also important, and therefore optimisation of combined TS and AC with carmofur or other novel small molecule inhibitors may improve CRT response further.

Bibliography

Aaltonen L, Peltomäki P, Leach F, Sistonen P, Pylkkanen L, Mecklin J, Jarvinen H, Powell S, Jen J, Hamilton S, *et al*. Clues to the pathogenesis of familial colorectal cancer. Science 1993; 260(1509): 812-6.

Abraham N, Young J, Solomon M. Meta-analysis of short-term outcomes after laparoscopic resection for colorectal cancer. British Journal of Surgery 2004; 91(9): 1111–24.

Adams RB, Aloia TA, Loyer E, Pawlik TM, Taouli B, Vauthey JN. Selection for hepatic resection of colorectal liver metastases: expert consensus statement. HPB (Oxford) 2013; 15: 91–103.

Adeberg S, Baris D, Habermehl D, Rieken S, Brons S, Weber KJ, Roth W, Debus J, Combs SE. Evaluation of chemoradiotherapy with carbon ions and the influence of p53 mutational status in the colorectal carcinoma cell line HCT 116. Tumori 2014 Nov-Dec; 100(6): 675-84.

Agrawal N, Dasaradhi PVN, Mohmmed A, Malhotra P, Bhatnagar RK, Mukherjee SK. RNA interference: biology, mechanism, and applications. Microbiol Mol Biol Rev 2003 Dec; 67(4): 657-85.

Aklilu M, Eng C. The current landscape of locally advanced rectal cancer. Nat Rev Clin Oncol. 2011 Aug 9; 8(11): 649-59.

Alberici P, Fodde R. The role of the APC tumor suppressor in chromosomal instability. Genome Dynamics 2006; 1: 149-70.

Alderdice M, Dunne PD, Cole AJ, O'Reilly PG, McArt DG, Bingham V, Fuchs MA, McQuaid S, Loughrey MB, Murray GI, Samuel LM, Lawler M, Wilson RH, Salto-Tellez M, Coyle VM. Natural killer-like signature observed post therapy in locally advanced rectal cancer is a determinant of pathological response and improved survival. Mod Pathol. 2017 Sep; 30(9): 1287-1298.

American Joint Committee on Cancer – Cancer Staging References, Colon and Rectum 8th Edition 2017. https://pathologyoutlines.com/topic/colontumourstaging8ed.html. [Accessed 24 May 2018]

Appelt AL, Pløen J, Vogelius IR, Bentzen SM, Jakobsen A. Radiation dose-response model for locally advanced rectal cancer after preoperative chemoradiation therapy. Int J Radiat Oncol Biol Phys. 2013 Jan 1; 85(1): 74-80.

Appelt AL, Pløen J, Harling H, Jensen FS, Jensen LH, Jørgensen JC, Lindebjerg J, Rafaelsen SR, Jakobsen A. High-dose chemoradiotherapy and watchful waiting for distal rectal cancer: a prospective observational study. Lancet Oncol. 2015 Aug; 16(8): 919-27.

Arana L, Gangoiti P, Ouro A, Trueba M, Gómez-Muñoz A. Ceramide and ceramide 1-phosphate in health and disease. Lipids Health Dis. 2010 Feb; 9: 15.

Arulampalam T, Francis D, Visvikis D, Taylor I, Ell P. FDG-PET for the preoperative evaluation of colorectal liver metastases. European Journal of Surgical Oncology 2004; 30(3): 286-91.

Ashraf S, Hompes R, Slater A, Lindsey I, Bach S, Mortensen NJ, Cunningham C, and on behalf of the Association of Coloproctology of Great Britain and Ireland Transanal Endoscopic

Microsurgery (TEM) Collaboration. A critical appraisal of endorectal ultrasound and transanal endoscopic microsurgery and decision-making in early rectal cancer. Colorectal Disease 2012; 14: 821-826.

Atallah S, Albert R. Transanal minimally invasive surgery (TAMIS) versus transanal endoscopic microsurgery (TEM): Is one better than the other? Surgical Endoscopy 2013; 27(12): 4750-1.

Atkin WS, Edwards R, Kralj-Hans I, Wooldrage K, Hart AR, Northover JM, Parkin DM, Wardle J, Duffy SW, Cuzick J. Once-only flexible sigmoidoscopy screening in prevention of colorectal cancer: a multicentre randomised controlled trial. Lancet 2010; 375: 1624–33.

Atkin W, Dadswell E, Wooldrage K, Kralj-Hans I, von Wagner C, Edwards R, Yao G, Kay C, Burling D, Faiz O, Teare J, Lilford RJ, Morton D, Wardle J, Halligan S. Computed tomographic colonography versus colonoscopy for investigation of patients with symptoms suggestive of colorectal cancer (SIGGAR): a multicentre randomised trial. Lancet 2013; 381: 1194–202.

Aune D, Chan DS, Lau R, Vieira R, Greenwood DC, Kampman E, Norat T. Dietary fibre, whole grains, and risk of colorectal cancer: systematic review and dose-response meta-analysis of prospective studies. BMJ. 2011 Nov 10; 343: d6617.

Bach SP, Hill J, Monson JR, Simson JN, Lane L, Merrie A, Warren B, Mortensen NJ. A predictive model for local recurrence after transanal endoscopic microsurgery for rectal cancer. Br J Surg 2009; 96: 280–90.

Bagnardi V, Rota M, Botteri E, Tramacere I, Islami F, Fedirko V, Scotti L, Jenab M, Turati F, Pasquali E, Pelucchi C, Galeone C, Bellocco R, Negri E, Corrao G, Boffetta P, La Vecchia C. Alcohol consumption and site-specific cancer risk: a comprehensive dose-response meta-analysis. Br J Cancer. 2015 Feb 3; 112(3): 580-93.

Baker S, Preisinger A, Jessup J, Paraskeva C, Markowitz S, Wilson J, Hamilton S, Vogelstein B. p53 gene mutations occur in combination with 17p allelic deletions as late events in colorectal tumorigenesis. Cancer Research 1990; 50(23): 7717-22.

Barber T, McManus K, Yuen K, Reis M, Parmigiani G, Shen D, Barrett I, Nouhi Y, Spencer F, Markowitz S, Velculescu V, Kinzler K, Vogelstein B, Lengauer C, Hieter P. Chromatid cohesion defects may underlie chromosome instability in human colorectal cancers. Proceedings of the National Academy of Sciences of the United States of America 2008; 105(9): 3443-8.

Battersby NJ, Moran B, Yu S, Tekkis P, Brown G. MR imaging for rectal cancer: the role in staging the primary and response to neoadjuvant therapy. Expert Rev Gastroenterol Hepatol. 2014 Aug; 8(6): 703-19.

Battersby NJ, Juul T, Christensen P, Janjua AZ, Branagan G, Emmertsen KJ, Norton C, Hughes R, Laurberg S, Moran BJ; United Kingdom Low Anterior Resection Syndrome Study Group. Predicting the Risk of Bowel-Related Quality-of-Life Impairment After Restorative Resection for Rectal Cancer: A Multicenter Cross-Sectional Study. Dis Colon Rectum. 2016 Apr; 59(4): 270-80.

Battersby NJ, Dattani M, Rao S, Cunningham D, Tait D, Adams R, Moran BJ, Khakoo S, Tekkis P, Rasheed S, Mirnezami A, Quirke P, West NP, Nagtegaal I, Chong I, Sadanandam A, Valeri N, Thomas K, Frost M, Brown G. A rectal cancer feasibility study with an embedded phase III trial design assessing magnetic resonance tumour regression grade (mrTRG) as a novel

biomarker to stratify management by good and poor response to chemoradiotherapy (TRIGGER): study protocol for a randomised controlled trial. Trials. 2017 Aug 29; 18(1): 394.

Bauer NC, Anita H. Corbett AH, Doetsch PW. The current state of eukaryotic DNA base damage and repair. Nucleic Acids Res. 2015 Dec; 43(21): 10083-101.

Bayascas JR, Yuste VJ, Benito E, Garcia-Fernàndez J, Comella JX. Isolation of AmphiCASP-3/7, an ancestral caspase from amphioxus (Branchiostoma floridae). Evolutionary considerations for vertebrate caspases. Cell Death Differ 2002 Oct; 9(10): 1078-89.

Bedia C, Casas J, Garcia V, Levade T, Fabrias G. Synthesis of a novel ceramide analogue and its use in a high-throughput fluorogenic assay for ceramidases. Chembiochem 2007; 8: 642-8.

Bedia C, Camacho L, Abad JL, Fabrias G, Levade T. A simple fluorogenic method for determination of acid ceramidase activity and diagnosis of Farber disease. J Lipid Res 2010 Dec; 51(12): 3542-7.

Bedia C, Casas J, Andrieu-Abadie N, Fabriàs G, Levade T. Acid ceramidase expression modulates the sensitivity of A375 melanoma cells to dacarbazine. J Biol Chem. 2011 Aug; 286(32): 28200-9.

Ben Q, Wang L, Liu J, Qian A, Wang Q, Yuan Y. Alcohol drinking and the risk of colorectal adenoma: a dose-response meta-analysis. Eur J Cancer Prev. 2015 Jul; 24(4): 286-95.

Bernardo K, Hurwitz R, Zenk T, Desnick RJ, Ferlinz K, Schuchman EH, Sandhoff K. Purification, characterization, and biosynthesis of human acid ceramidase. J Biol Chem. 1995 May; 270(19): 11098-102.

Berndt N, Patel R, Yang H, Balasis ME, Sebti SM. Akt2 and acid ceramidase cooperate to induce cell invasion and resistance to apoptosis. Cell Cycle. 2013 Jul; 12(13): 2024-32.

Berridge MV, Herst PM, Tan AS. Tetrazolium dyes as tools in cell biology: new insights into their cellular reduction. Biotechnol Annu Rev 2005; 11: 127-52.

Bhangu A, Wood G, Brown G, Darzi A, Tekkis P, Goldin R. The role of epithelial mesenchymal transition and resistance to neoadjuvant therapy in locally advanced rectal cancer. Colorectal Dis. 2014 Apr; 16(4): O133-43.

Bieberich E. Sphingolipids and lipid rafts: Novel concepts and methods of analysis. Chem Phys Lipids. 2018 Nov; 216: 114-131.

Blazic IM, Lilic GB, Gajic MM. Quantitative Assessment of Rectal Cancer Response to Neoadjuvant Combined Chemotherapy and Radiation Therapy: Comparison of Three Methods of Positioning Region of Interest for ADC Measurements at Diffusion-weighted MR Imaging. Radiology. 2017 Feb; 282(2): 418-28.

Boland C, Thibodeau S, Hamilton S, Sidransky D, Eshleman J, Burt R, Meltzer S, Rodriguez-Bigas M, Fodde R, Ranzani G, Srivastava S. A National Cancer Institute Workshop on Microsatellite Instability for cancer detection and familial predisposition: development of international criteria for the determination of microsatellite instability in colorectal cancer. Cancer Research 1998; 58(22): 5248-57.

Bonnaud S, Niaudet C, Legoux F, Corre I, Delpon G, Saulquin X, Fuks Z, Gaugler MH, Kolesnick R, Paris F. Sphingosine-1-phosphate activates the AKT pathway to protect small intestines from radiation-induced endothelial apoptosis. Cancer Res. 2010 Dec; 70(23): 9905-15.

Bosset JF, Collette L, Calais G, Mineur L, Maingon P, Radosevic-Jelic L, Daban A, Bardet E, Beny A, Ollier JC; EORTC Radiotherapy Group Trial 22921. Chemotherapy with preoperative radiotherapy in rectal cancer. N Engl J Med. 2006 Sep 14; 355(11): 1114-23.

Botteri E, Iodice S, Raimondi S, Maisonneuve P, Lowenfels AB. Cigarette smoking and adenomatous polyps: a meta-analysis. Gastroenterology. 2008 Feb; 134(2): 388-95.

Bradford M. A rapid and sensitive method for the quantification of microgram quantities of protein utilizing the principle of protein-dye binding. Analytical Biochemistry 1976; 7(72): 248-54.

Brettingham-Moore KH, Duong CP, Greenawalt DM, Heriot AG, Ellul J, Dow CA, Murray WK, Hicks RJ, Tjandra J, Chao M, Bui A, Joon DL, Thomas RJ, Phillips WA. Pretreatment transcriptional profiling for predicting response to neoadjuvant chemoradiotherapy in rectal adenocarcinoma. Clin Cancer Res. 2011 May 1; 17(9): 3039-47.

Brockbank KG, Campbell LH, Greene ED, Brockbank MC, Duman JG. Lessons from nature for preservation of mammalian cells, tissues, and organs. In Vitro Cell Dev Biol Anim. 2011 Mar; 47(3): 210-7.

Buecher B, Cacheux W, Rouleau E, Dieumegard B, Mitry E, Lièvre A. Role of microsatellite instability in the management of colorectal cancers. Digestive Liver Disease 2013; 45(6): 441-9.

Bujko K, Nowacki MP, Nasierowska-Guttmejer A, Michalski W, Bebenek M, Pudelko M, Kryj M, Oledzki J, Szmeja J, Sluszniak J, Serkies K, Kladny J, Pamucka M, Kukolowicz P. Sphincter preservation following preoperative radiotherapy for rectal cancer: report of a randomised trial comparing short-term radiotherapy vs. conventionally fractionated radiochemotherapy. Radiother Oncol 2004; 72: 15–24.

Bujko K, Nowacki M, Nasierowska-Guttmejer A, Michalski W, Bebenek M, Kryj M. Long-term results of a randomized trial comparing preoperative short-course radiotherapy with preoperative conventionally fractionated chemoradiation for rectal cancer. British Journal of Surgery 2006; 93(10): 1215-23.

Bujko K, Kepka L, Michalski W, Nowacki MP. Does rectal cancer shrinkage induced by preoperative radio(chemo)therapy increase the likelihood of anterior resection? A systematic review of randomised trials. Radiother Oncol. 2006a Jul; 80(1): 4-12.

Bujko K, Kolodziejczyk M, Nasierowska-Guttmejer A, Michalski W, Kepka L, Chmielik E, Wojnar A, Chwalinski M; Polish Colorectal Cancer Group. Tumour regression grading in patients with residual rectal cancer after preoperative chemoradiation. Radiother Oncol. 2010 Jun; 95(3): 298-302.

Butterworth AS, Higgins JP, Pharoah P. Relative and absolute risk of colorectal cancer for individuals with a family history: a meta-analysis. Eur J Cancer. 2006 Jan; 42(2): 216-27.

Buttke T, McCubrey J, Owen T. Use of an aqueous soluble tetrazolium/formazan assay to measure viability and proliferation of lymphokine-dependent cell lines. Journal of Immunological Methods 1993; 157(1-2): 233-40.

Calin GA, Croce CM. MicroRNA signatures in human cancers. Nat Rev Cancer. 2006 Nov; 6(11): 857-66.

Camacho L, Meca-Cortés O, Abad JL, García S, Rubio N, Díaz A, Celià-Terrassa T, Cingolani F, Bermudo R, Fernández PL, Blanco J, Delgado A, Casas J, Fabriàs G, Thomson TM. Acid ceramidase as a therapeutic target in metastatic prostate cancer. J Lipid Res. 2013 May; 54(5): 1207-20.

Cancer Research UK. Bowel Cancer Statistics (online). http://www.cancerresearchuk.org/health-professional/cancer-statistics/statistics-by-cancer-type/bowel-cancer. [Accessed 7 June 2015]

Carragher L, Snell K, Giblett S, Aldridge V, Patel B, Cook S. V600EBraf induces gastrointestinal crypt senescence and promotes tumour progression through enhanced CpG methylation of p16INK4a. EMBO Molecular Medicine 2010; 2(11): 458-71.

Carrato A. Adjuvant treatment of colorectal cancer. Gastrointestinal Cancer Research 2008: 2(4): S42-6.

Carter RJ, Parsons JL. Base Excision Repair, a Pathway Regulated by Posttranslational Modifications. Mol Cell Biol. 2016 May; 36(10): 1426-37.

Caudle KE, Thorn CF, Klein TE, Swen JJ, McLeod HL, Diasio RB, Schwab M. Clinical Pharmacogenetics Implementation Consortium guidelines for dihydropyrimidine dehydrogenase genotype and fluoropyrimidine dosing. Clin Pharmacol Ther. 2013 Dec; 94(6): 640-5.

Chau I, Brown G, Cunningham D, Tait D, Wotherspoon A, Norman AR, Tebbutt N, Hill M, Ross PJ, Massey A, Oates J. Neoadjuvant capecitabine and oxaliplatin followed by synchronous chemoradiation and total mesorectal excision in magnetic resonance imaging-defined poor-risk rectal cancer. J Clin Oncol. 2006 Feb; 24(4): 668-74.

Cheng JC, Bai A, Beckham TH, Marrison ST, Yount CL, Young K, Lu P, Bartlett AM, Wu BX, Keane BJ, Armeson KE, Marshall DT, Keane TE, Smith MT, Jones EE, Drake RR Jr, Bielawska A, Norris JS, Liu X. Radiation-induced acid ceramidase confers prostate cancer resistance and tumor relapse. J Clin Invest. 2013 Oct; 123(10): 4344-58.

Chionh F, Lau D, Yeung Y, Price T, Tebbutt N. Oral versus intravenous fluoropyrimidines for colorectal cancer. Cochrane Database Syst Rev. 2017 Jul; 7: CD008398.

Colorectal Cancer Collaborative Group. Adjuvant radiotherapy for rectal cancer: a systematic overview of 8,507 patients from 22 randomised trials. Lancet 2001; 358: 1291–304.

Cong YJ, Gan Y, Sun HL, Deng J, Cao SY, Xu X, Lu ZX. Association of sedentary behaviour with colon and rectal cancer: a meta-analysis of observational studies. Br J Cancer. 2014 Feb; 110(3): 817-26.

Corey MJ, Kinders RJ, Brown LG, Vessella RL. A very sensitive coupled luminescent assay for cytotoxicity and complement-mediated lysis. J Immunol Methods 1997 Aug; 207(1): 43-51.

Cory AH, Owen TC, Barltrop JA, Cory JG. Use of an aqueous soluble tetrazolium/formazan assay for cell growth assays in culture. Cancer Commun 1991 Jul; 3(7): 207-12.

Creavin B, Ryan E, Martin ST, Hanly A, O'Connell PR, Sheahan K, Winter DC. Organ preservation with local excision or active surveillance following chemoradiotherapy for rectal cancer. Br J Cancer. 2017 Jan 17; 116(2): 169-174.

Cunningham C, Leong K, Clark S, Plumb A, Taylor S, Geh I, Karandikar S, Moran B. Association of Coloproctology of Great Britain & Ireland (ACPGBI): Guidelines for the Management of Cancer of the Colon, Rectum and Anus (2017) - Diagnosis, Investigations and Screening. Colorectal Dis. 2017 Jul; 19 Suppl 1: 9-17.

Dalby B, Cates S, Harris A, Ohki EC, Tilkins ML, Price PJ, Ciccarone VC. Advanced transfection with Lipofectamine 2000 reagent: primary neurons, siRNA, and high-throughput applications. Methods 2004 Jun; 33(2): 95-103.

Davidson DJ, Haskell C, Majest S, Kherzai A, Egan DA, Walter KA, Schneider A, Gubbins EF, Solomon L, Chen Z, Lesniewski R, Henkin J. Kringle 5 of human plasminogen induces apoptosis of endothelial and tumor cells through surface-expressed glucose-regulated protein 78. Cancer Res. 2005 Jun 1; 65(11): 4663-72.

De Angelis R, Sant M, Coleman MP, Francisci S, Baili P, Pierannunzio D, Trama A, Visser O, Brenner H, Ardanaz E, Bielska-Lasota M, Engholm G, Nennecke A, Siesling S, Berrino F, Capocaccia R, and the EUROCARE-5 Working Group. Cancer survival in Europe 1999–2007 by country and age: results of EUROCARE-5 - a population-based study. Lancet Oncology 2014; 15: 931-42.

De Graaf EJ, Doornebosch PG, Tollenaar RA, Meershoek-Klein Kranenbarg E, de Boer AC, Bekkering FC, van de Velde CJ. Transanal endoscopic microsurgery versus total mesorectal excision of T1 rectal adenocarcinomas with curative intention. Eur J Surg Oncol 2009; 35: 1280–5.

Della Vittoria Scarpati G, Falcetta F, Carlomagno C, Ubezio P, Marchini S, De Stefano A, Singh VK, D'Incalci M, De Placido S, Pepe S. A specific miRNA signature correlates with complete pathological response to neoadjuvant chemoradiotherapy in locally advanced rectal cancer. Int J Radiat Oncol Biol Phys. 2012 Jul 15; 83(4): 1113-9.

Dementiev A, Joachimiak A, Nguyen H, Gorelik A, Illes K, Shabani S, Gelsomino M, Ahn EE, Nagar B, Doan N. Molecular Mechanism of Inhibition of Acid Ceramidase by Carmofur. J Med Chem. 2019 Jan 24; 62(2): 987-992.

Denoix P. *Enquete permanent dans les centres anticancereaux. Bulletin de l'Institut National d'Hygiene* 1946; 1: 70-5.

Detre S, Saclani Jotti G, Dowsett M. A "quickscore" method for immunohistochemical semiquantitation: validation for oestrogen receptor in breast carcinomas. J Clin Pathol. 1995 Sep; 48(9): 876–878.

Diasio R, Harris B. Clinical pharmacology of 5-fluorouracil. Clinical Pharmacokinetics 1989; 16(4): 215-37.

Dighe S, Purkayastha S, Swift I, Tekkis PP, Darzi A, A'Hern R, Brown G. Diagnostic precision of CT in local staging of colon cancers: a meta-analysis. Clin Radiol 2010; 65: 708–19.

Downward J. Targeting RAS signalling pathways in cancer therapy. Nature Reviews Cancer 2003; 3(1): 11-22.

Drebber U, Lay M, Wedemeyer I, Vallböhmer D, Bollschweiler E, Brabender J, Mönig SP, Hölscher AH, Dienes HP, Odenthal M. Altered levels of the onco-microRNA 21 and the tumor-supressor microRNAs 143 and 145 in advanced rectal cancer indicate successful neoadjuvant chemoradiotherapy. Int J Oncol. 2011 Aug; 39(2): 409-15.

Dukes C. The classification of cancer of the rectum. The Journal of Pathology and Bacteriology 1932; 35(3): 323-32.

Dukes C, Bussey H. The spread of rectal cancer and its effect on prognosis. British Journal of Cancer 1958; 12(3): 309-20.

Dunne PD, McArt DG, Bradley CA, O'Reilly PG, Barrett HL, Cummins R, O'Grady T, Arthur K, Loughrey MB, Allen WL, McDade SS, Waugh DJ, Hamilton PW, Longley DB, Kay EW, Johnston PG, Lawler M, Salto-Tellez M, Van Schaeybroeck S. Challenging the Cancer Molecular Stratification Dogma: Intratumoral Heterogeneity Undermines Consensus Molecular Subtypes and Potential Diagnostic Value in Colorectal Cancer. Clin Cancer Res. 2016 Aug; 22(16): 4095-104.

Dworak O, Keilholz L, Hoffmann A. Pathological features of rectal cancer after preoperative radiochemotherapy. Int J Colorectal Dis. 1997; 12(1): 19-23.

Eisenhauer E, Therasse P, Bogaerts J, Schwartz L, Sargent D, Ford R, Dancey J, Arbuck S, Gwyther S, Mooney M, Rubinstein L, Shankar L, Dodd L, Kaplan R, Lacombe D, Verweil J. New response evaluation criteria in solid tumours: Revised RECIST guideline (version 1.1). European Journal of Cancer 2009; 45(2): 228-47.

Elmore S. Apoptosis: a review of programmed cell death. Toxicol Pathol 2007 Jun; 35(4): 495-516.

Elojeimy S, Liu X, McKillop JC, El-Zawahry AM, Holman DH, Cheng JY, Meacham WD, Mahdy AE, Saad AF, Turner LS, Cheng J, A Day T, Dong JY, Bielawska A, Hannun YA, Norris JS. Role of acid ceramidase in resistance to FasL: therapeutic approaches based on acid ceramidase inhibitors and FasL gene therapy. Mol Ther. 2007 Jul; 15(7): 1259-63.

El Sayed YM, Sadée W. Metabolic activation of R,S-1-(tetrahydro-2-furanyl)-5-fluorouracil (ftorafur) to 5-fluorouracil by soluble enzymes. Cancer Res. 1983 Sep; 43(9): 4039-44.

Farber S. A lipid metabolic disorder: disseminated lipogranulomatosis; a syndrome with similarity to, and important difference from, Niemann-Pick and Hand-Schüller-Christian disease. AMA American Journal of Diseases of Children 1952: 84(4): 499-500.

Fearnhead NS, Wilding JL, Bodmer WF. Genetics of colorectal cancer: hereditary aspects and overview of colorectal tumorigenesis. Br Med Bull. 2002; 64: 27-43.

Fearon E, Vogelstein B. A genetic model for colorectal tumorigenesis. Cell 1990; 61(5): 759-67.

Fearon E. Molecular genetics of colorectal cancer. Annual Review of Pathology 2011; 6: 479-507.

Fedorov Y, Anderson EM, Birmingham A, Reynolds A, Karpilow J, Robinson K, Leake D, Marshall WS, Khvorova A. Off-target effects by siRNA can induce toxic phenotype. RNA. 2006 Jul; 12(7): 1188-96

Fernández-Martos C, Pericay C, Aparicio J, Salud A, Safont M, Massuti B, Vera R, Escudero P, Maurel J, Marcuello E, Mengual JL, Saigi E, Estevan R, Mira M, Polo S, Hernandez A, Gallen M, Arias F, Serra J, Alonso V. Phase II, randomized study of concomitant chemoradiotherapy followed by surgery and adjuvant capecitabine plus oxaliplatin (CAPOX) compared with induction CAPOX followed by concomitant chemoradiotherapy and surgery in magnetic resonance imaging-defined, locally advanced rectal cancer: Grupo cancer de recto 3 study. J Clin Oncol. 2010 Feb; 28(5): 859-65.

Flowers M, Fabriás G, Delgado A, Casas J, Abad JL, Cabot MC. C6-ceramide and targeted inhibition of acid ceramidase induce synergistic decreases in breast cancer cell growth. Breast Cancer Res Treat. 2012 Jun; 133(2): 447-58.

Foxtrot Collaborative Group. Feasibility of preoperative chemotherapy for locally advanced, operable colon cancer: the pilot phase of a randomised controlled trial. Lancet Oncol 2012; 13: 1152–60.

Francois Y, Nemoz CJ, Baulieux J, Vignal J, Grandjean JP, Partensky C, Souquet JC, Adeleine P, Gerard JP. Influence of the interval between preoperative radiation therapy and surgery on downstaging and on the rate of sphincter-sparing surgery for rectal cancer: the Lyon R90-01 randomized trial. J Clin Oncol. 1999 Aug; 17(8): 2396.

Fucini C, Messerini L, Saieva C, Orzalesi L, Carroni V, Bartolini N. Apoptotic proteins as prognostic markers and indicators of radiochemosensitivity in stage II/III rectal cancers. Colorectal Dis. 2012 Feb; 14(2): e64-71.

Gantt GA, Chen Y, Dejulius K, Mace AG, Barnholtz-Sloan J, Kalady MF. Gene expression profile is associated with chemoradiation resistance in rectal cancer. Colorectal Dis. 2014 Jan; 16(1): 57-66.

García-Barros M, Coant N, Truman JP, Snider AJ, Hannun YA. Sphingolipids in colon cancer. Biochim Biophys Acta. 2014 May; 1841(5): 773-82.

Gérard J, Conroy T, Bonnetain F, Bouché O, Chapet O, Closon-Dejardin M, Untereiner M, Leduc B, Francois E, Maurel J, Seitz J, Buecher B, Mackiewicz R, Ducreux M, Bedenne L. Preoperative radiotherapy with or without concurrent fluorouracil and leucovorin in T3-4 rectal cancers: Results of FFCD 9203. Journal of Clinical Oncology 2006; 24(28): 4620-5.

Gerard JP, Azria D, Gourgou-Bourgade S, Martel-Lafay I, Hennequin C, Etienne PL, Vendrely V, Francois E, de La Roche G, Bouche O, Mirabel X, Denis B, Mineur L, Berdah JF, Mahe MA, Becouarn Y, Dupuis O, Lledo G, Seitz JF, Bedenne L, Juzyna B, Conroy T. Clinical outcome of the ACCORD 12/0405 PRODIGE 2 randomized trial in rectal cancer. J Clin Oncol 2012; 30: 4558-65.

Ghadimi BM, Grade M, Difilippantonio MJ, Varma S, Simon R, Montagna C, Füzesi L, Langer C, Becker H, Liersch T, Ried T. Effectiveness of gene expression profiling for response prediction of rectal adenocarcinomas to preoperative chemoradiotherapy. J Clin Oncol. 2005 Mar 20; 23(9): 1826-38.

Gilbert A, Ziegler L, Martland M, Davidson S, Efficace F, Sebag-Montefiore D, Velikova G. Systematic review of radiation therapy toxicity reporting in randomized controlled trials of rectal cancer: a comparison of patient-reported outcomes and clinician toxicity reporting. Int J Radiat Oncol Biol Phys 2015; 92: 555–67.

Glynne-Jones R, Hughes R. Critical appraisal of the 'wait and see' approach in rectal cancer for clinical complete responders after chemoradiation. Br J Surg 2012; 99: 897-909.

Gollins S, Sun Myint A, Haylock B, Wise M, Saunders M, Neupane R, Essapen S, Samuel L, Dougal M, Lloyd A, Morris J, Topham C, Susnerwala S. Preoperative chemoradiotherapy using concurrent capecitabine and irinotecan in magnetic resonance imaging-defined locally advanced rectal cancer: impact on long-term clinical outcomes. J Clin Oncol 2011; 29: 1042-9.

Gollins S, Moran B, Adams R, Cunningham C, Bach S, Myint AS, Renehan A, Karandikar S, Goh V, Prezzi D, Langman G, Ahmedzai S, Geh I. Association of Coloproctology of Great Britain & Ireland (ACPGBI): Guidelines for the Management of Cancer of the Colon, Rectum and Anus (2017) - Multidisciplinary Management. Colorectal Dis. 2017 Jul; 19 Suppl 1: 37-66.

Gollub MJ, Gultekin DH, Akin O, Do RK, Fuqua JL 3rd, Gonen M, Kuk D, Weiser M, Saltz L, Schrag D, Goodman K, Paty P, Guillem J, Nash GM, Temple L, Shia J, Schwartz LH. Dynamic contrast enhanced-MRI for the detection of pathological complete response to neoadjuvant chemotherapy for locally advanced rectal cancer. Eur Radiol. 2012 Apr; 22(4): 821-31.

Gouazé-Andersson V, Flowers M, Karimi R, Fabriás G, Delgado A, Casas J, Cabot MC. Inhibition of acid ceramidase by a 2-substituted aminoethanol amide synergistically sensitizes prostate cancer cells to N-(4-hydroxyphenyl) retinamide. Prostate. 2011 Jul; 71(10): 1064-73.

Gown AM, Willingham MC. Improved detection of apoptotic cells in archival paraffin sections: immunohistochemistry using antibodies to cleaved caspase 3. J Histochem Cytochem. 2002 Apr; 50(4): 449-54.

Grade M, Wolff HA, Gaedcke J, Ghadimi BM. The molecular basis of chemoradiosensitivity in rectal cancer: implications for personalized therapies. Langenbecks Arch Surg. 2012 Apr; 397(4): 543-55.

Grady W. Genomic instability and colon cancer. Cancer Metastasis Review 2004; 23(1-2): 11-27.

Grady W, Carethers J. Genomic and epigenetic instability in colorectal cancer pathogenesis. Gastroenterology 2008; 135(4): 1079-99.

Green BL, Marshall HC, Collinson F, Quirke P, Guillou P, Jayne DG, Brown JM. Long-term follow-up of the Medical Research Council CLASSIC trial of conventional *versus* laparoscopically assisted resection in colorectal cancer. British Journal of Surgery 2013; 100: 75-82.

Green DR, Kroemer G. The pathophysiology of mitochondrial cell death. Science. 2004 Jul 30; 305(5684): 626-9.

Guinney J, Dienstmann R, Wang X, de Reyniès A, Schlicker A, Soneson C, Marisa L, Roepman P, Nyamundanda G, Angelino P, Bot BM, Morris JS, Simon IM, Gerster S, Fessler E, De Sousa

E Melo F, Missiaglia E, Ramay H, Barras D, Homicsko K, Maru D, Manyam GC, Broom B, Boige V, Perez-Villamil B, Laderas T, Salazar R, Gray JW, Hanahan D, Tabernero J, Bernards R, Friend SH, Laurent-Puig P, Medema JP, Sadanandam A, Wessels L, Delorenzi M, Kopetz S, Vermeulen L, Tejpar S. The consensus molecular subtypes of colorectal cancer. Nat Med. 2015 Nov; 21(11): 1350-6.

Gurtu V, Kain SR, Zhang G. Fluorometric and colorimetric detection of caspase activity associated with apoptosis. Anal Biochem 1997 Aug; 251(1): 98-102.

Habr-Gama A, de Souza PM, Ribeiro U Jr, Nadalin W, Gansl R, Sousa AH Jr, Campos FG, Gama-Rodrigues J. Low rectal cancer: impact of radiation and chemotherapy on surgical treatment. Dis Colon Rectum. 1998 Sep; 41(9): 1087-96.

Habr-Gama A, Perez RO, Nadalin W, Sabbaga J, Ribeiro U Jr, Silva e Sousa AH Jr, Campos FG, Kiss DR, Gama-Rodrigues J. Operative versus nonoperative treatment for stage 0 distal rectal cancer following chemoradiation therapy: long-term results. Ann Surg. 2004 Oct; 240(4): 711-7.

Habr-Gama A, Perez RO, Wynn G, Marks J, Kessler H, Gama-Rodrigues J. Complete clinical response after neoadjuvant chemoradiation therapy for distal rectal cancer: characterization of clinical and endoscopic findings for standardization. Dis Colon Rectum. 2010 Dec; 53(12): 1692-8.

Habr-Gama A, Sabbaga J, Gama-Rodrigues J, Sao Juliao GP, Proscurshim I, Bailao Aguilar P, Nadalin W, Perez RO. Watch and wait approach following extended neoadjuvant chemoradiation for distal rectal cancer: are we getting closer to anal cancer management? Dis Colon Rectum 2013; 56: 1109-17.

Haimovitz-Friedman A, Kan CC, Ehleiter D, Persaud RS, McLoughlin M, Fuks Z, Kolesnick RN. Ionizing radiation acts on cellular membranes to generate ceramide and initiate apoptosis. J Exp Med. 1994 Aug; 180(2): 525-35.

Halacli SO, Canpinar H, Cimen E, Sunguroglu A. Effects of gamma irradiation on cell cycle, apoptosis and telomerase activity in p53 wild-type and deficient HCT116 colon cancer cell lines. Oncol Lett 2013 Sep; 6(3): 807-10.

Halligan S, Wooldrage K, Dadswell E, Kralj-Hans I, von Wagner C, Edwards R, Yao G, Kay C, Burling D, Faiz O, Teare J, Lilford RJ, Morton D, Wardle J, Atkin W. Computed tomographic colonography versus barium enema for diagnosis of colorectal cancer or large polyps in symptomatic patients (SIGGAR): a multicentre randomised trial. Lancet 2013; 381: 1185–93.

Hamilton A, Baulcombe D. A species of small antisense RNA in posttranscriptional gene silencing in plants. Science 1999; 286(5441): 950-2.

Hamilton SR, Bosman FT, Boffetta P, Ilyas M, Morreau H, Nakamura SI et al. Carcinoma of the colon and rectum. In: Bosman FT, Carniero F, Hruban RH, Theise ND, editors. WHO Classification of Tumours of the Digestive System (4th ed). Lyon: IARC Press, 2010.

Hanker LC, Karn T, Holtrich U, Gätje R, Rody A, Heinrich T, Ruckhäberle E, Engels K. Acid ceramidase (AC)--a key enzyme of sphingolipid metabolism--correlates with better prognosis in epithelial ovarian cancer. Int J Gynecol Pathol. 2013 May; 32(3): 249-57.

Hartley A, Ho KF, McConkey C, Geh JI. Pathological complete response following pre-operative chemoradiotherapy in rectal cancer: analysis of phase II/III trials. Br J Radiol 2005; 78: 934-8.

He X, Okino N, Dhami R, Dagan A, Gatt S, Schulze H, Sandhoff K, Schuchman EH. Purification and characterization of recombinant, human acid ceramidase. Catalytic reactions and interactions with acid sphingomyelinase. J Biol Chem. 2003 Aug; 278(35): 32978-86.

Heald R, Husband E, Ryall R. The mesorectum in rectal cancer surgery - the clue to pelvic recurrence? British Journal of Surgery 1982; 69(10): 613-6.

Heald R. The 'Holy Plane' of rectal surgery. Journal of the Royal Society of Medicine 1988; 81(9): 503-8.

Heald R, Moran B, Ryall R, Sexton R, MacFarlane J. Rectal cancer: The Basingstoke experience of total mesorectal excision, 1978-1997. Archives of Surgery 1998; 133(8): 894-9.

Hehlgans S, Petraki C, Reichert S, Cordes N, Rödel C, Rödel F. Double targeting of surviving and XIAP radiosensitizes 3D grown human colorectal tumour cells and decreases migration. Radiother Oncol. 2013 Jul; 108(1): 32-9.

Heijnen LA, Lambregts DM, Mondal D, Martens MH, Riedl RG, Beets GL, Beets-Tan RG. Diffusion-weighted MR imaging in primary rectal cancer staging demonstrates but does not characterise lymph nodes. Eur Radiol 2013; 23: 3354-60.

Hermanek P, Merkel S, Hohenberger W. Prognosis of rectal carcinoma after multimodal treatment: ypTNM classification and tumor regression grading are essential. Anticancer Res 2013 Feb; 33(2): 559-66.

Hewitson P, Glasziou P, Watson E, Towler B, Irwig L. Cochrane systematic review of colorectal cancer screening using the fecal occult blood test (hemoccult): an update. Am J Gastroenterol 2008; 103: 1541-9.

Hoffman RM. In vitro sensitivity assays in cancer: a review, analysis, and prognosis. Journal of Clinical Laboratory Analysis 1991; 5(2): 133-43.

Hofheinz RD, Wenz F, Post S, Matzdorff A, Laechelt S, Hartmann JT, Müller L, Link H, Moehler M, Kettner E, Fritz E, Hieber U, Lindemann HW, Grunewald M, Kremers S, Constantin C, Hipp M, Hartung G, Gencer D, Kienle P, Burkholder I, Hochhaus A. Chemoradiotherapy with capecitabine versus fluorouracil for locally advanced rectal cancer: a randomised, multicentre, non-inferiority, phase 3 trial. Lancet Oncol. 2012 Jun; 13(6): 579-88.

Hollstein M, Sidransky D, Vogelstein B, Harris C. p53 mutations in human cancers. Science 1991; 253(5015): 49-53.

Holm T. Controversies in abdominoperineal excision. Surg Oncol Clin N Am. 2014 Jan; 23(1): 93-111.

Holman DH, Turner LS, El-Zawahry A, Elojeimy S, Liu X, Bielawski J, Szulc ZM, Norris K, Zeidan YH, Hannun YA, Bielawska A, Norris JS. Lysosomotropic acid ceramidase inhibitor induces apoptosis in prostate cancer cells. Cancer Chemother Pharmacol. 2008 Feb; 61(2): 231-42.

Horvath EM, Zsengellér ZK, Szabo C. Quantification of PARP activity in human tissues: ex vivo assays in blood cells, and immunohistochemistry in human biopsies. Methods Mol Biol. 2011; 780: 267–275.

Horvath L, Henshall S. The application of tissue microarrays to cancer research. Pathology 2001 May; 33(2): 125-9.

How P, Stelzner S, Branagan G, Bundy K, Chandrakumaran K, Heald RJ, Moran B. Comparative quality of life in patients following abdominoperineal excision and low anterior resection for low rectal cancer. Dis Colon Rectum. 2012 Apr; 55(4): 400-6.

Hu X, Yang D, Zimmerman M, Liu F, Yang J, Kannan S, Burchert A, Szulc Z, Bielawska A, Ozato K, Bhalla K, Liu K. IRF8 regulates acid ceramidase expression to mediate apoptosis and suppresses myelogeneous leukemia. Cancer Res. 2011 Apr; 71(8): 2882-91.

Huarte M, Guttman M, Feldser D, Garber M, Koziol MJ, Kenzelmann-Broz D, Khalil AM, Zuk O, Amit I, Rabani M, Attardi LD, Regev A, Lander ES, Jacks T, Rinn JL. A large intergenic noncoding RNA induced by p53 mediates global gene repression in the p53 response. Cell. 2010 Aug; 142(3): 409-19.

Huebner R, Park K, Shepherd J, Schwimmer J, Czernin J, Phelps M, Gambhir S. A meta-analysis of the literature for whole-body FDG PET detection of recurrent colorectal cancer. Journal of Nuclear Medicine 2000; 41(7): 1177-89.

Huebner M, Wolff BG, Smyrk TC, Aakre J, Larson DW. Partial pathologic response and nodal status as most significant prognostic factors for advanced rectal cancer treated with preoperative chemoradiotherapy. World J Surg. 2012 Mar; 36(3): 675-83.

Huerta S, Gao X, Livingston E, Kapur P, Sun H, Anthony T. In vitro and in vivo radiosensitization of colorectal cancer HT-29 cells by the smac mimetic JP-1201. Surgery. 2010 Aug; 148(2): 346-53.

Huerta S, Goa X, Dineen S, Kapur P, Saha D, Meyer J. Role of p53, Bax, p21, and DNA-PKcs in radiation sensitivity of HCT-116 cells and xenografts. Surgery. 2013 Aug; 154(2): 143-51.

Hughes R, Glynne-Jones R, Grainger J, Richman P, Makris A, Harrison M, Ashford R, Harrison RA, Livingstone JI, McDonald PJ, Meyrick Thomas J, Mitchell IC, Northover JM, Phillips R, Wallace M, Windsor A, Novell JR. Can pathological complete response in the primary tumour following pre-operative pelvic chemoradiotherapy for T3-T4 rectal cancer predict for sterilisation of pelvic lymph nodes, a low risk of local recurrence and the appropriateness of local excision? Int J Colorectal Dis. 2006 Jan; 21(1): 11-7.

Huxley R, Ansary-Moghaddam A, Clifton P, Czernichow S, Parr C, Woodward M. The impact of dietary and lifestyle risk factors on risk of colorectal cancer: A quantitative overview of the epidemiological evidence. International Journal of Cancer 2009; 125(1): 171-80.

Issa J. CpG island methylator phenotype in cancer. National Review of Cancer 2004; 4(12): 988-93.

Jahn KA, Su Y, Braet F. Multifaceted nature of membrane microdomains in colorectal cancer. World J Gastroenterol. 2011 Feb 14; 17(6): 681-90.

Jass J. Classification of colorectal cancer based on correlation of clinical, morphological and molecular features. Histopathology 2007; 50(1): 113-30.

Jo WS, Carethers JM. Chemotherapeutic implications in microsatellite unstable colorectal cancer. Cancer Biomark. 2006; 2(1-2): 51-60.

Johnston DF, Lawrence KM, Sizer BF, Arulampalam TH, Motson RW, Dove E, Lacey N. Locally advanced rectal cancer: histopathological correlation and predictive accuracy of serial MRI after neoadjuvant chemotherapy. Br J Radiol. 2009 Apr; 82(976): 332-6.

Johnston P, Kaye S. Capecitabine: A novel agent for the treatment of solid tumors. Anticancer Drugs 2001; 12(8): 639-46.

Jourdan F, Sebbagh N, Comperat E, Mourra N, Flahault A, Olschwang S, Duval A, Hamelin R, Flejou JF. Tissue microarray technology: validation in colorectal carcinoma and analysis of p53, hMLH1, and hMSH2 immunohistochemical expression. Virchows Arch. 2003 Aug; 443(2): 115-21.

Kallioniemi OP, Wagner U, Kononen J, Sauter G. Tissue microarray technology for high-throughput molecular profiling of cancer. Hum Mol Genet 2001; 10: 657.

Kalluri R, Zeisberg M. Fibroblasts in cancer. Nat Rev Cancer. 2006 May; 6(5): 392-401.

Kalluri R, Weinberg RA. The basics of epithelial-mesenchymal transition. J Clin Invest. 2009 Jun; 119(6): 1420-8.

Kamel I, Bluemke D. MR imaging of liver tumors. Radiologic Clinics of North America 2003; 41(1): 51-65.

Kapiteijn E, Marijnen C, Nagtegaal I, Putter H, Steup W, Wiggers T, Rutten H, Pahlman L, Glimelius B, van Krieken J, Leer J, van de Velde C, The Dutch Colorectal Cancer Group. Preoperative radiotherapy combined with total mesorectal excision for resectable rectal cancer. New England Journal of Medicine 2001; 345(9): 638-46.

Kapur P. Tailoring treatment of rectal adenocarcinoma: immunohistochemistry for predictive biomarkers. Anticancer Drugs. 2011 Apr; 22(4): 362-70.

Khan Z, Marshall JF. The role of integrins in TGFβ activation in the tumour stroma. Cell Tissue Res. 2016 Sep; 365(3): 657-73.

Kheirelseid EA, Miller N, Chang KH, Curran C, Hennessey E, Sheehan M, Newell J, Lemetre C, Balls G, Kerin MJ. miRNA expressions in rectal cancer as predictors of response to neoadjuvant chemoradiation therapy. Int J Colorectal Dis. 2013 Feb; 28(2): 247-60.

Khouja MH, Baekelandt M, Sarab A, Nesland JM, Holm R. Limitations of tissue microarrays compared with whole tissue sections in survival analysis. Oncol Lett. 2010 Sep; 1(5): 827-831.

Kim IJ, Lim SB, Kang HC, Chang HJ, Ahn SA, Park HW, Jang SG, Park JH, Kim DY, Jung KH, Choi HS, Jeong SY, Sohn DK, Kim DW, Park JG. Microarray gene expression profiling for predicting complete response to preoperative chemoradiotherapy in patients with advanced rectal cancer. Dis Colon Rectum. 2007 Sep; 50(9): 1342-53.

Kinzler K, Vogelstein B. Lessons from hereditary colorectal cancer. Cell 1990; 87(2): 159-70.

Kobunai T, Watanabe T, Fukusato T. REG4, NEIL2, and BIRC5 gene expression correlates with gamma-radiation sensitivity in patients with rectal cancer receiving radiotherapy. Anticancer Res. 2011 Dec; 31(12): 4147-53.

Koch J, Gartner S, Li CM, Quintern LE, Bernardo K, Levran O, Schnabel D, Desnick RJ, Schchman EH, Sandhoff K. Molecular cloning and characterization of a full-length complementary DNA encoding human acid ceramidase. Identification of the first molecular lesion causing Farber disease. J Biol Chem 1997 Jan; 271(51): 33110-5.

Koh DW, Dawson TM, Dawson VL. Mediation of cell death by poly(ADP-ribose) polymerase-1. Pharmacol Res. 2005 Jul; 52(1): 5-14.

Kolesnick R, Fuks Z. Radiation and ceramide-induced apoptosis. Oncogene 2003 Sep 1; 22(37): 5897-906.

Kononen J, Bubendorf L, Kallioniemi A, Barlund M, Schraml P, Leighton S, Torhorst J, Mihatsch MJ, Sauter G, Kallioniemi OP. Tissue microarrays for high-throughput molecular profiling of tumor specimens. Nat Med 1998; 4: 844-47.

Korbelik M, Banáth J, Zhang W, Saw KM, Szulc ZM, Bielawska A, Separovic D. Interaction of acid ceramidase inhibitor LCL521 with tumor response to photodynamic therapy and photodynamic therapy-generated vaccine. Int J Cancer. 2016 Sep 15; 139(6): 1372-8.

Kulkarni T, Gollins S, Maw A, Hobson P, Byrne R, Widdowson D. Magnetic resonance imaging in rectal cancer downstaged using neoadjuvant chemoradiation: accuracy of prediction of tumour stage and circumferential resection margin status. Colorectal Dis. 2008 Jun; 10(5): 479-89.

Kumar B, Brown NV, Swanson BJ, Schmitt AC, Old M, Ozer E, Agrawal A, Schuller DE, Teknos TN, Kumar P. High expression of myoferlin is associated with poor outcome in oropharyngeal squamous cell carcinoma patients and is inversely associated with HPV-status. Oncotarget. 2016 Apr; 7(14): 18665-77.

Kuremsky JG, Tepper JE, McLeod HL. Biomarkers for response to neoadjuvant chemoradiation for rectal cancer. Int J Radiat Oncol Biol Phys. 2009 Jul 1; 74(3): 673-88.

Lambregts DM, Vandecaveye V, Barbaro B, Bakers FC, Lambrecht M, Maas M, Haustermans K, Valentini V, Beets GL, Beets-Tan RG. Diffusion-weighted MRI for selection of complete responders after chemoradiation for locally advanced rectal cancer: a multicenter study. Ann Surg Oncol. 2011 Aug; 18(8): 2224-31.

Langevin J, Nivatvongs S. The true incidence of synchronous cancer of the large bowel. A prospective study. American Journal of Surgery 1984; 47(3): 330-3.

Larsson SC, Wolk A. Meat consumption and risk of colorectal cancer: a meta-analysis of prospective studies. Int J Cancer. 2006 Dec 1; 119(11): 2657-64.

Lefevre JH, Mineur L, Kotti S, Rullier E, Rouanet P, de Chaisemartin C, Meunier B, Mehrdad J, Cotte E, Desrame J, Karoui M, Benoist S, Kirzin S, Berger A, Panis Y, Piessen G, Saudemont A, Prudhomme M, Peschaud F, Dubois A, Loriau J, Tuech JJ, Meurette G, Lupinacci R, Goasgen N, Parc Y, Simon T, Tiret E. Effect of Interval (7 or 11 weeks) Between Neoadjuvant Radiochemotherapy and Surgery on Complete Pathologic Response in Rectal Cancer: A

Multicenter, Randomized, Controlled Trial (GRECCAR-6). J Clin Oncol. 2016 Nov 1; 34(31): 3773-80.

Le Guen T, Ragu S, Guirouilh-Barbat J, Lopez BS. Role of the double-strand break repair pathway in the maintenance of genomic stability. Mol Cell Oncol. 2014 Oct; 2(1): e968020.

Lengauer C, Kinzler K, Vogelstein B. Genetic instability in colorectal cancers. Nature 1997; 386(6625): 623-7.

Li CM, Park JH, He X, Levy B, Chen F, Arai K, Adler DA, Disteche CM, Koch J, Sandhoff K, Schuchman EH. The human acid ceramidase gene (ASAH): structure, chromosomal location, mutation analysis, and expression. Genomics. 1999 Dec; 62(2): 223-31.

Liang XH, Hart CE, Crooke ST. Transfection of siRNAs can alter miRNA levels and trigger non-specific protein degradation in mammalian cells. Biochim Biophys Acta. 2013 May; 1829(5): 455-68.

Liu X, Elojeimy S, El-Zawahry AM, Holman DH, Bielawska A, Bielawska J, Rubinchik S, Guo GW, Dong JY, Keane T, Hannun YA, Tavassoli M, Norris JS. Modulation of ceramide metabolism enhances viral protein apoptin's cytotoxicity in prostate cancer. Mol Ther 2006 Nov; 14(5): 637-46.

Liu Y, Prasad R, Beard WA, Kedar PS, Hou EW, Shock DD, Wilson SH. Coordination of steps in single-nucleotide base excision repair mediated by apurinic/apyrimidinic endonuclease 1 and DNA polymerase beta. J Biol Chem. 2007 May 4; 282(18): 13532-41.

Livak KJ, Schmittgen TD. Analysis of relative gene expression data using real time quantitative PCR and the 2-ΔΔCt method. Methods 2001; 25: 402-8.

Longley DB, Harkin DP, Johnston PG. 5-fluorouracil: mechanisms of action and clinical strategies. Nat Rev Cancer 2003; 3(5): 330-8.

Lopes-Ramos CM, Habr-Gama A, Quevedo Bde S, Felício NM, Bettoni F, Koyama FC, Asprino PF, Galante PA, Gama-Rodrigues J, Camargo AA, Perez RO, Parmigiani RB. Overexpression of miR-21-5p as a predictive marker for complete tumor regression to neoadjuvant chemoradiotherapy in rectal cancer patients. BMC Med Genomics. 2014 Dec 11; 7: 68.

Losi L, Luppi G, Gavioli M, Iachetta F, Bertolini F, D'Amico R, Jovic G, Bertoni F, Falchi AM, Conte PF. Prognostic value of Dworak grade of regression (GR) in patients with rectal carcinoma treated with preoperative radiochemotherapy. Int J Colorectal Dis. 2006 Oct; 21(7): 645-51.

Louis KS, Siegel AC. Cell viability analysis using trypan blue: manual and automated methods. Methods Mol Biol 2011; 740: 7-12.

Ludwig K, Tse ES, Wang JY. Colon cancer cells adopt an invasive phenotype without mesenchymal transition in 3-D but not 2-D culture upon combined stimulation with EGF and crypt growth factors. BMC Cancer 2013 May 2; 13: 221 doi:10.1186/1471-2407-13-221.

Luo W, Cao Y, Liao C, Gao F. Diabetes mellitus and the incidence and mortality of colorectal cancer: a meta-analysis of 24 cohort studies. Colorectal Dis 2012 Nov; 14(11): 1307-12.

Lutgens MW, van Oijen MG, van der Heijden GJ, Vleggaar FP, Siersema PD, Oldenburg B. Declining risk of colorectal cancer in inflammatory bowel disease: an updated meta-analysis of population-based cohort studies. Inflamm Bowel Dis. 2013 Mar-Apr; 19(4): 789-99.

Lynch H, de la Chapelle A. Hereditary colorectal cancer. The New England Journal of Medicine 2003; 348(10): 919-32.

Maas M, Lambregts DM, Nelemans PJ, Heijnen LA, Martens MH, Leijtens JW, Sosef M, Hulsewe KW, Hoff C, Breukink SO, Stassen L, Beets-Tan RG, Beets GL. Assessment of clinical complete response after chemoradiation for rectal cancer with digital rectal examination, endoscopy, and MRI: selection for organ-saving treatment. Ann Surg Oncol 2015; 22: 3873-80.

Mahdy AE, Cheng JC, Li J, Elojeimy S, Meacham WD, Turner LS, Bai A, Gault CR, McPherson AS, Garcia N, Beckham TH, Saad A, Bielawska A, Bielawski J, Hannun YA, Keane TE, Taha MI, Hammouda HM, Norris JS, Liu X. Acid ceramidase upregulation in prostate cancer cells confers resistance to radiation: AC inhibition, a potential radiosensitizer. Mol Ther. 2009 Mar; 17(3): 430-8.

Majumdar S, Fletcher R, Evans A. How does colorectal cancer present? Symptoms, duration, and clues to location. American Journal of Gastroenterology 1999; 94(10): 3039-45.

Mandard AM, Dalibard F, Mandard JC, Marnay J, Henry-Amar M, Petiot JF, Roussel A, Jacob JH, Segol P, Samama G, et al. Pathologic assessment of tumor regression after preoperative chemoradiotherapy of esophageal carcinoma. Clinicopathologic correlations. Cancer. 1994 Jun; 73(11): 2680-6.

Mander B, Carney L, Scott H, Donaldson D. Jass staging is a predictor of outcome following "curative" resection of Dukes' B colorectal carcinoma. The Surgeon 2006; 4(4): 227-30.

Marijnen CA, Kapiteijn E, van de Velde CJ, Martijn H, Steup WH, Wiggers T, Kranenbarg EK, Leer JW. Acute side effects and complications after short-term preoperative radiotherapy combined with total mesorectal excision in primary rectal cancer: report of a multicenter randomized trial. J Clin Oncol 2002; 20: 817–25.

Marijnen CA, van de Velde CJ, Putter H, van den Brink M, Maas CP, Martijn H, Rutten HJ, Wiggers T, Kranenbarg EK, Leer JW, Stiggelbout AM. Impact of short-term preoperative radiotherapy on health-related quality of life and sexual functioning in primary rectal cancer: report of a multicenter randomized trial. J Clin Oncol 2005; 23: 1847-58.

Marsh PJ, James RD, Schofield PF. Adjuvant preoperative radiotherapy for locally advanced rectal carcinoma. Results of a prospective, randomized trial. Dis Colon Rectum 1994 Dec; 37(12): 1205-14.

Martin ST, Heneghan HM, Winter DC. Systematic review and meta-analysis of outcomes following pathological complete response to neoadjuvant chemoradiotherapy for rectal cancer. Br J Surg. 2012 Jul; 99(7): 918-28.

McClelland RA, Finlay P, Walker KJ, Nicholson D, Robertson JF, Blamey RW, Nicholson RI. Automated quantitation of immunocytochemically localized estrogen receptors in human breast cancer. Cancer Res. 1990 Jun 15; 50(12): 3545-50.

Medical Research Council Rectal Cancer Working Party. Randomised trial of surgery alone versus radiotherapy followed by surgery for potentially operable locally advanced rectal cancer. Lancet. 1996 Dec 14; 348(9042): 1605-10.

Meng WJ, Yan H, Zhou B, Zhang W, Kong XH, Wang R, Zhan L, Li Y, Zhou ZG, Sun XF. Correlation of SATB1 overexpression with the progression of human rectal cancer. Int J Colorectal Dis. 2012 Feb; 27(2): 143-50.

MERCURY Study Group. Diagnostic accuracy of preoperative magnetic resonance imaging in predicting curative resection of rectal cancer: Prospective observational study. British Medical Journal 2006; 333(7572): 779.

Mirzayans R, Andrais B, Scott A, Tessier A, Murray D. A sensitivity assay for the evaluation of cytotoxicity and its pharmacological modulation in human solid tumour-derived cell lines exposed to cancer-therapeutic agents. J Pharm Pharm Sci 2007; 10(2): 298s-311s.

Miyaji M, Jin ZX, Yamaoka S, Amakawa R, Fukuhara S, Sato SB, Kobayashi T, Domae N, Mimori T, Bloom ET, Okazaki T, Umehara H. Role of membrane sphingomyelin and ceramide in platform formation for Fas-mediated apoptosis. J Exp Med. 2005 Jul; 202(2): 249-59.

Mohsin SK, Weiss H, Havighurst T, Clark GM, Berardo M, Roanh le D, To TV, Qian Z, Love RR, Allred DC. Progesterone receptor by immunohistochemistry and clinical outcome in breast cancer: a validation study. Mod Pathol 2004 Dec; 17(12): 1545-54.

Morales A, París R, Villanueva A, Llacuna L, García-Ruiz C, Fernández-Checa JC. Pharmacological inhibition or small interfering RNA targeting acid ceramidase sensitizes hepatoma cells to chemotherapy and reduces tumor growth in vivo. Oncogene. 2007 Feb; 26(6): 905-16.

Moran BJ, Holm T, Brannagan G, Chave H, Quirke P, West N, Brown G, Glynne-Jones R, Sebag-Montefiore D, Cunningham C, Janjua AZ, Battersby NJ, Crane S, McMeeking A. The English national low rectal cancer development programme: key messages and future perspectives. Colorectal Dis. 2014 Mar; 16(3): 173-8.

Mosmann T. Rapid colorimetric assay for cellular growth and survival: application to proliferation and cytotoxicity assays. J Immunol Methods 1983 Dec; 65(1-2): 55-63.

Moss S, Mathews C, Day TJ, Smith S, Seaman HE, Snowball J, Halloran SP. Increased uptake and improved outcomes of bowel cancer screening with a faecal immunochemical test: results from a pilot study within the national screening programme in England. Gut 2017 Sep; 66(9): 1631-44.

Moussata D, Amara S, Sideek B, Decaussin M, Hehlgans S, Paul-Bellon R, Mornex F, Gerard JP, Romestaing P, Rödel F, Flourie B, Benahmed M, Mauduit C. XIAP as a radioresistance factor and prognostic marker for radiotherapy in human rectal adenocarcinoma. Am J Pathol. 2012 Oct; 181(4): 1271-8.

Nagtegaal ID, van de Velde CJ, Marijnen CA, van Krieken JH, Quirke P; Dutch Colorectal Cancer Group; Pathology Review Committee. Low rectal cancer: a call for a change of approach in abdominoperineal resection. J Clin Oncol. 2005 Dec 20; 23(36): 9257-64.

Nagtegaal I, Quirke P. What is the role for the circumferential margin in the modern treatment of rectal cancer? Journal of Clinical Oncology 2008; 2: 303-12.

National Cancer Intelligence Network – Colorectal Cancer Survival by Stage (online). http://www.ncin.org.uk/cancer_type_and_topic_specific_work/cancer_type_specific_work/colorectal_cancer. [Accessed 7 June 2015]

National Institute for Health and Clinical Excellence. Suspected cancer: recognition and referral. NICE guideline [NG12], 2015. https://www.nice.org.uk/guidance/NG12 [Accessed 24 February 2018]

National Institute for Health and Care Excellence. Colorectal cancer: diagnosis and management. Clinical guideline (CG131), 2011. https://www.nice.org.uk/guidance/CG131 [Accessed 25 February 2018]

National Institute for Health and Care Excellence. Suspected cancer: recognition and referral. NICE guideline [NG12] published: June 2015, updated: July 2017. https://www.nice.org.uk/guidance/ng12 [Accessed 25 February 2018]

Neri E, Halligan S, Hellstrom M, Lefere P, Mang T, Regge D, Stoker J, Taylor S, Laghi A. The second ESGAR consensus statement on CT colonography. Eur Radiol 2013; 23: 720–9.

Ngan SY, Burmeister B, Fisher RJ, Solomon M, Goldstein D, Joseph D, Ackland SP, Schache D, McClure B, McLachlan SA, McKendrick J, Leong T, Hartopeanu C, Zalcberg J, Mackay J. Randomized trial of short-course radiotherapy versus long-course chemoradiation comparing rates of local recurrence in patients with T3 rectal cancer: Trans-Tasman Radiation Oncology Group trial 01.04. J Clin Oncol. 2012 Nov; 30(31): 3827-33.

Ngan SY, Fisher R, Burmeister B, Mackay J, McLachlan S, Beresford J, McClure B, Goldstein D, Joseph D, Solomon M. Long-term quality of life in patients treated in TROG 01.04: a randomized trial comparing short course and long course preoperative radiation therapy for rectal cancer. Int J Radiat Oncol Biol Phys 2012a; 84: S143-4.

Nishioka M, Shimada M, Kurita N, Iwata T, Morimoto S, Yoshikawa K, Higashijima J, Miyatani T. Gene expression profile can predict pathological response to preoperative chemoradiotherapy in rectal cancer. Cancer Genomics Proteomics. 2011 Mar-Apr; 8(2): 87-92.

Nishiyama M, Takagami S, Kim R, Kirihara Y, Saeki T, Jinushi K, Niimoto M, Hattori T. [Inhibition of thymidylate synthetase and antiproliferative effect by 1-hexylcarbamoyl-5-fluorouracil]. Gan To Kagaku Ryoho. 1988 Nov; 15(11): 3109-13.

Nocito A, Bubendorf L, Tinner EM, Süess K, Wagner U, Forster T, Kononen J, Fijan A, Bruderer J, Schmid U, Ackermann D, Maurer R, Alund G, Knönagel H, Rist M, Anabitarte M, Hering F, Hardmeier T, Schoenenberger AJ, Flury R, Jäger P, Fehr JL, Schraml P, Moch H, Mihatsch MJ, Gasser T, Sauter G. Microarrays of bladder cancer tissue are highly representative of proliferation index and histological grade. J Pathol. 2001 Jul; 194(3): 349-57.

Ogretmen B, Schady D, Usta J, Wood R, Kraveka JM, Luberto C, Birbes H, Hannun YA, Obeid LM. Role of ceramide in mediating the inhibition of telomerase activity in A549 human lung adenocarcinoma cells. J Biol Chem. 2001 Jul; 276(27): 24901-10.

Omata F, Deshpande GA, Ohde S, Mine T, Fukui T. The association between obesity and colorectal adenoma: systematic review and meta-analysis. Scand J Gastroenterol. 2013 Feb; 48(2): 136-46.

Ong K, Leen E. Radiological staging of colorectal liver metastases. Surgical Oncology 2007; 16(1): 7-14.

Parker RL, Huntsman DG, Lesack DW, Cupples JB, Grant DR, Akbari M, Gilks CB. Assessment of interlaboratory variation in the immunohistochemical determination of estrogen receptor status using a breast cancer tissue microarray. Am J Clin Pathol. 2002 May; 117(5): 723-8.

Parkin DM, Boyd L, Walker LC. The fraction of cancer attributable to lifestyle and environmental factors in the UK in 2010. British Journal of Cancer 2011; 105(S2): S77-81.

Patel UB, Taylor F, Blomqvist L, George C, Evans H, Tekkis P, Quirke P, Sebag-Montefiore D, Moran B, Heald R, Guthrie A, Bees N, Swift I, Pennert K, Brown G. Magnetic resonance imaging-detected tumor response for locally advanced rectal cancer predicts survival outcomes: MERCURY experience. J Clin Oncol. 2011 Oct; 29(28): 3753-60.

Peng J, Ma W, Zhou Z, Gu Y, Lu Z, Zhang R, Pan Z. Genetic variations in the PI3K/PTEN/AKT/mTOR pathway predict tumor response and disease-free survival in locally advanced rectal cancer patients receiving preoperative chemoradiotherapy and radical surgery. J Cancer. 2018 Feb 28; 9(6): 1067-1077.

Perez K, Safran H, Sikov W, Vrees M, Klipfel A, Shah N, Schechter S, Oldenburg N, Pricolo V, Rosati K, Dipetrillo T. Complete Neoadjuvant Treatment for Rectal Cancer: The Brown University Oncology Group CONTRE Study. Am J Clin Oncol. 2017 Jun; 40(3): 283-287.

Pietrzak L, Bujko K, Nowacki MP, Kepka L, Oledzki J, Rutkowski A, Szmeja J, Kladny J, Dymecki D, Wieczorek A, Pawlak M, Lesniak T, Kowalska T, Richter P. Quality of life, anorectal and sexual functions after preoperative radiotherapy for rectal cancer: report of a randomised trial. Radiother Oncol 2007; 84: 217-25.

Polakis P. The many ways of Wnt in cancer. Current Opinion in Genetics and Development 2007; 17(1): 45-51.

Popat S, Matakidou A, Houlston RS. Thymidylate synthase expression and prognosis in colorectal cancer: a systematic review and meta-analysis. J Clin Oncol. 2004 Feb; 22(3): 529-36.

Pretlow TP, Pretlow TG. Mutant KRAS in aberrant crypt foci (ACF): Initiation of colorectal cancer? *Biochimica et Biophysica Acta* 2005; 1756(2): 83-96.

Punt CJ, Koopman M, Vermeulen L. From tumour heterogeneity to advances in precision treatment of colorectal cancer. Nat Rev Clin Oncol. 2017 Apr; 14(4): 235-246.

Rajagopalan H, Bardelli A, Lengauer C, Kinzler K, Vogelstein B, Velculescu V. Tumorigenesis: RAF/RAS oncogenes and mismatch-repair status. Nature 2002; 418(6901): 934.

Ramírez de Molina A, de la Cueva A, Machado-Pinilla R, Rodriguez-Fanjul V, Gomez del Pulgar T, Cebrian A, Perona R, Lacal JC. Acid ceramidase as a chemotherapeutic target to overcome resistance to the antitumoral effect of choline kinase α inhibition. Curr Cancer Drug Targets. 2012 Jul; 12(6): 617-24.

Realini N, Solorzano C, Pagliuca C, Pizzirani D, Armirotti A, Luciani R, Costi MP, Bandiera T, Piomelli D. Discovery of highly potent acid ceramidase inhibitors with in vitro tumor chemosensitizing activity. Sci Rep 2013; 3: 1035.

Realini N, Palese F, Pizzirani D, Pontis S, Basit A, Bach A, Ganesan A, Piomelli D. Acid Ceramidase in Melanoma: EXPRESSION, LOCALIZATION, AND EFFECTS OF PHARMACOLOGICAL INHIBITION. J Biol Chem. 2016 Jan; 291(5): 2422-34.

Rehemtulla A. Overcoming intratumor heterogeneity of polygenic cancer drug resistance with improved biomarker integration. Neoplasia 2012 Dec; 14(12): 1278-89.

Renehan AG, Malcomson L, Emsley R, Gollins S, Maw A, Myint AS, Rooney PS, Susnerwala S, Blower A, Saunders MP, Wilson MS, Scott N, O'Dwyer ST. Watch-and-wait approach versus surgical resection after chemoradiotherapy for patients with rectal cancer (the OnCoRe project): a propensity-score matched cohort analysis. Lancet Oncol 2015; 17: 174-83.

Rex D, Lehman G, Ulbright T, Smith J, Pound D, Hawes R, Helper D, Wiersema M, Langefeld C, Li W. Colonic neoplasia in asymptomatic persons with negative fecal occult blood tests: Influence of age, gender, and family history. American Journal of Gastroenterology 1993; 88(6): 825-31.

Ribic C, Sargent D, Moore M, Thibodeau S, French A, Goldberg R, Hamilton S, Laurent-Puig P, Gryfe R, Shepherd L, Tu D, Redston M, Gallinger S. Tumor microsatellite-instability status as a predictor of benefit from fluorouracil-based adjuvant chemotherapy for colon cancer. New England Journal of Medicine 2003; 349(3): 247-57.

Rimkus C, Friederichs J, Boulesteix AL, Theisen J, Mages J, Becker K, Nekarda H, Rosenberg R, Janssen KP, Siewert JR. Microarray-based prediction of tumor response to neoadjuvant radiochemotherapy of patients with locally advanced rectal cancer. Clin Gastroenterol Hepatol. 2008 Jan; 6(1): 53-61.

Rödel F, Hoffman J, Distel L, Herrmann M, Noisternig T, Papadopoulos T, Sauer R, Rödel C. Survivin as a radioresistance factor, and prognostic and therapeutic target for radiotherapy in rectal cancer. Cancer Res. 2005 Jun 1; 65(11): 4881-7.

Roh JL, Park JY, Kim EH, Jang HJ. Targeting acid ceramidase sensitises head and neck cancer to cisplatin. Eur J Cancer. 2016 Jan; 52: 163-72.

Rombouts AJM, Al-Najami I, Abbott NL, Appelt A, Baatrup G, Bach S, Bhangu A, Garm Spindler KL, Gray R, Handley K, Kaur M, Kerkhof E, Kronborg CJ, Magill L, Marijnen CAM, Nagtegaal ID, Nyvang L, Peters FP, Pfeiffer P, Punt C, Quirke P, Sebag-Montefiore D, Teo M, West N, de Wilt JHW; for STAR-TREC Collaborative Group. Can we Save the rectum by watchful waiting or TransAnal microsurgery following (chemo) Radiotherapy versus Total mesorectal excision for early REctal Cancer (STAR-TREC study)?: protocol for a multicentre, randomised feasibility study. BMJ Open. 2017 Dec 28; 7(12): e019474.

Rose C, Wu H. Morphologic criteria of invasive colonic adenocarcinoma on biopsy specimens. The Internet Journal of Pathology 2010; 12(1): 1.

Rullier E, Rouanet P, Tuech JJ, Valverde A, Lelong B, Rivoire M, Faucheron JL, Jafari M, Portier G, Meunier B, Sileznieff I, Prudhomme M, Marchal F, Pocard M, Pezet D, Rullier A, Vendrely V, Denost Q, Asselineau J, Doussau A. Organ preservation for rectal cancer (GRECCAR 2): a prospective, randomised, open-label, multicentre, phase 3 trial. Lancet. 2017 Jul; 390(10093): 469-79.

Rustgi AK. The genetics of hereditary colon cancer. Genes and Development 2007; 21(20): 2525-38.

Ryan JE, Warrier SK, Lynch AC, Ramsay RG, Phillips WA, Heriot AG. Predicting pathological complete response to neoadjuvant chemoradiotherapy in locally advanced rectal cancer: a systematic review. Colorectal Dis. 2016 Mar; 18(3): 234-46.

Ryan R, Gibbons D, Hyland JM, Treanor D, White A, Mulcahy HE, O'Donoghue DP, Moriarty M, Fennelly D, Sheahan K. Pathological response following long-course neoadjuvant chemoradiotherapy for locally advanced rectal cancer. Histopathology 2005 Aug; 47(2): 141-6.

Salendo J, Spitzner M, Kramer F, Zhang X, Jo P, Wolff HA, Kitz J, Kaulfuß S, Beißbarth T, Dobbelstein M, Ghadimi M, Grade M, Gaedcke J. Identification of a microRNA expression signature for chemoradiosensitivity of colorectal cancer cells, involving miRNAs-320a, -224, -132 and let7g. Radiother Oncol. 2013 Sep; 108(3): 451-7.

Sänger N, Ruckhäberle E, Györffy B, Engels K, Heinrich T, Fehm T, Graf A, Holtrich U, Becker S, Karn T. Acid ceramidase is associated with an improved prognosis in both DCIS and invasive breast cancer. Mol Oncol. 2015 Jan; 9(1): 58-67.

Santos MD, Silva C, Rocha A, Matos E, Nogueira C, Lopes C. Prognostic value of mandard and dworak tumor regression grading in rectal cancer: study of a single tertiary center. ISRN Surg. 2014 Mar; 2014: 310542.

Sauer R, Fietkau R, Wittekind C, Rödel C, Martus P, Hohenberger W, Tschmelitsch J, Sabitzer H, Karstens J, Becker H, Hess C, Raab R, The German Rectal Cancer Group. Adjuvant vs. neoadjuvant radiochemotherapy for locally advanced rectal cancer: The German trial CAO/ARO/AIO-94. Colorectal Disease 2003; 5(5): 406-15.

Sauer R, Becker H, Hohenberger W, Rodel C, Wittekind C, Fietkau R, Martus P, Tschmelitsch J, Hager E, Hess CF, Karstens JH, Liersch T, Schmidberger H, Raab R. Preoperative versus postoperative chemoradiotherapy for rectal cancer. N Engl J Med 2004; 351: 1731–40.

Sauer R, Liersch T, Merkel S, Fietkau R, Hohenberger W, Hess C, Becker H, Raab HR, Villanueva MT, Witzigmann H, Wittekind C, Beissbarth T, Rödel C. Preoperative versus postoperative chemoradiotherapy for locally advanced rectal cancer: results of the German CAO/ARO/AIO-94 randomized phase III trial after a median follow-up of 11 years. J Clin Oncol. 2012 Jun; 30(16): 1926-33.

Schilling D, Düwel M, Molls M, Multhoff G. Radiosensitization of wildtype p53 cancer cells by the MDM2-inhibitor PXN727 is associated with altered heat shock protein 70 (Hsp70) levels. Cell Stress Chaperones 2013 Mar; 18(2): 183-91.

Schüller J, Cassidy J, Dumont E, Roos B, Durston S, Banken L, Utoh M, Mori K, Weidekamm E, Reigner B. Preferential activation of capecitabine in tumor following oral administration to colorectal cancer patients. Cancer Chemotherapy and Pharmacology 2000; 45(4): 291-7.

Scott D, Guthrie J, Arnold P, Ward J, Atchley J, Wilson D, Robinson P. Dual phase helical CT versus portal venous phase CT for the detection of colorectal liver metastases: Correlation with intra-operative sonography, surgical and pathological findings. Clinical Radiology 2001; 56(3): 235-42.

Sebag-Montefiore D, Stephens R, Steele R, Monson J, Grieve R, Khanna S, Quirke P, Couture J, de Metz C, Myint A, Bessell E, Griffiths G, Thompson L, Parmar M. Preoperative radiotherapy versus selective postoperative chemoradiotherapy in patients with rectal

cancer (MRC CR07 and NCIC-CTG C016): A multicentre, randomised trial. Lancet 2009; 373(9666): 811-20.

Sebio A, Salazar J, Páez D, Berenguer-Llergo A, Del Río E, Tobeña M, Martín-Richard M, Sullivan I, Targarona E, Balart J, Baiget M, Barnadas A. EGFR ligands and DNA repair genes: genomic predictors of complete response after capecitabine-based chemoradiotherapy in locally advanced rectal cancer. Pharmacogenomics J. 2015 Feb; 15(1): 77-83.

Separovic D, Breen P, Boppana NB, Van Buren E, Joseph N, Kraveka JM, Rahmaniyan M, Li L, Gudz TI, Bielawska A, Bai A, Bielawski J, Pierce JS, Korbelik M. Increased killing of SCCVII squamous cell carcinoma cells after the combination of Pc 4 photodynamic therapy and dasatinib is associated with enhanced caspase-3 activity and ceramide synthase 1 upregulation. Int J Oncol. 2013 Dec; 43(6): 2064-72.

Shihab OC, Quirke P, Heald RJ, Moran BJ, Brown G. Magnetic resonance imaging-detected lymph nodes close to the mesorectal fascia are rarely a cause of margin involvement after total mesorectal excision. Br J Surg 2010; 97: 1431-6.

Shiovitz S, Bertagnolli M, Renfro L, Nam E, Foster N, Dzieciatkowski S, Luo Y, Lao V, Monnat Jr R, Emond M, Maizels N, Niedzwiecki D, Goldberg R, Saltz L, Venook A, Warren R, Grady W, The Alliance for Clinical Trials in Oncology. CpG island methylator phenotype is associated with response to adjuvant irinotecan-based therapy for stage III colon cancer. Gastroenterology 2014; 147(3): 637-45.

Shirasawa S, Furuse M, Yokoyama N, Sasazuki T. Altered growth of human colon cancer cell lines disrupted at activated Ki-ras. Science 1993; 260(5104): 85-8.

Shtraizent N, Eliyahu E, Park JH, He X, Shalgi R, Schuchman EH. Autoproteolytic cleavage and activation of human acid ceramidase. J Biol Chem 2008 Apr 25; 283(17): 11253-9.

Siskind LJ, Kolesnick RN, Colombini M. Ceramide channels increase the permeability of the mitochondrial outer membrane to small proteins. J Biol Chem. 2002 Jul; 277(30): 26796-803.

Slaby O, Svoboda M, Fabian P, Smerdova T, Knoflickova D, Bednarikova M, Nenutil R, Vyzula R. Altered expression of miR-21, miR-31, miR-143 and miR-145 is related to clinicopathologic features of colorectal cancer. Oncology. 2007; 72(5-6): 397-402.

Smart CJ, Korsgen S, Hill J, Speake D, Levy B, Steward M, Geh JI, Robinson J, Sebag-Montefiore D, Bach SP. Multicentre study of short-course radiotherapy and transanal endoscopic microsurgery for early rectal cancer. Br J Surg 2016; 103: 1069–75.

Smith NJ, Bees N, Barbachano Y, Norman AR, Swift RI, Brown G. Preoperative computed tomography staging of nonmetastatic colon cancer predicts outcome: implications for clinical trials. Br J Cancer 2007; 96: 1030–6.

Smith NJ, Barbachano Y, Norman AR, Swift RI, Abulafi AM, Brown G. Prognostic significance of magnetic resonance imaging-detected extramural vascular invasion in rectal cancer. Br J Surg 2008; 95: 229-36.

Smith FM, Wiland H, Mace A, Pai RK, Kalady MF. Clinical criteria underestimate complete pathological response in rectal cancer treated with neoadjuvant chemoradiotherapy. Dis Colon Rectum. 2014 Mar; 57(3): 311-5.

Spitzner M, Emons G, Kramer F, Gaedcke J, Rave-Fränk M, Scharf JG, Burfeind P, Becker H, Beissbarth T, Ghadimi BM, Ried T, Grade M. A gene expression signature for chemoradiosensitivity of colorectal cancer cells. Int J Radiat Oncol Biol Phys. 2010 Nov 15; 78(4): 1184-92.

Stephens RJ, Thompson LC, Quirke P, Steele R, Grieve R, Couture J, Griffiths GO, Sebag-Montefiore D. Impact of short-course preoperative radiotherapy for rectal cancer on patients' quality of life: data from the Medical Research Council CR07/National Cancer Institute of Canada Clinical Trials Group C016 randomized clinical trial. J Clin Oncol 2010; 28: 4233-9.

Stewart JP, Richman S, Maughan T, Lawler M, Dunne PD, Salto-Tellez M. Standardising RNA profiling based biomarker application in cancer-The need for robust control of technical variables. Biochim Biophys Acta Rev Cancer. 2017 Aug; 1868(1): 258-272.

Stryker S, Wolff B, Culp C, Libbe S, Ilstrup D, MacCarthy R. Natural history of untreated colonic polyps. Gastroenterology 1987; 93(5): 1009-13.

Sumantran VN. Cellular chemosensitivity assays: an overview. Methods Mol Biol 2011; 731: 219-36.

Sun Z, Adam MA, Kim J, Czito B, Mantyh C, Migaly J. Intensity-Modulated Radiation Therapy Is Not Associated with Perioperative or Survival Benefit over 3D-Conformal Radiotherapy for Rectal Cancer. J Gastrointest Surg. 2017 Jan; 21(1): 106-11.

Svoboda M, Sana J, Fabian P, Kocakova I, Gombosova J, Nekvindova J, Radova L, Vyzula R, Slaby O. MicroRNA expression profile associated with response to neoadjuvant chemoradiotherapy in locally advanced rectal cancer patients. Radiat Oncol. 2012 Nov 20; 7: 195.

Swedish Rectal Cancer Trial. Improved survival with preoperative radiotherapy in resectable rectal cancer. N Engl J Med. 1997 Apr 3; 336(14): 980-7.

Tan SF, Liu X, Fox TE, Barth BM, Sharma A, Turner SD, Awwad A, Dewey A, Doi K, Spitzer B, Shah MV, Morad SA, Desai D, Amin S, Zhu J, Liao J, Yun J, Kester M, Claxton DF, Wang HG, Cabot MC, Schuchman EH, Levine RL, Feith DJ, Loughran TP Jr. Acid ceramidase is upregulated in AML and represents a novel therapeutic target. Oncotarget. 2016 Dec; 7(50): 83208-22.

Taylor F, Quirke P, Heald R, Moran B, Blomqvist L, Swift I, Sebag-Montefiore D, Tekkis P, Brown G, MERCURY study group. Preoperative high resolution magnetic resonance imaging can identify good prognosis stage I, II, and III rectal cancer best managed by surgery alone: A prospective, multicenter, European study. Annals of Surgery 2011; 253(4): 711-9.

Tey J, Leong CN, Cheong WK, Sze TG, Yong WP, Tham IWK, Lee KM. A phase II trial of preoperative concurrent chemotherapy and dose escalated intensity modulated radiotherapy (IMRT) for locally advanced rectal cancer. J Cancer. 2017 Sep 6; 8(16): 3114-21.

Therasse P, Arbuck S, Eisenhauer E, Wanders J, Kaplan R, Rubinstein L, Verweij J, Van Glabbeke M, van Oosterom A, Christian M, Gwyther S. New guidelines to evaluate the response to treatment in solid tumors. European Organization for Research and Treatment

of Cancer, National Cancer Institute of the United States, National Cancer Institute of Canada. Journal of the National Cancer Institute 2000; 92(3): 205-16.

Tiernan J, Cook A, Geh I, George B, Magill L, Northover J, Verjee A, Wheeler J, Fearnhead N. Use of a modified Delphi approach to develop research priorities for the association of coloproctology of Great Britain and Ireland. Colorectal Dis. 2014 Dec; 16(12): 965-70.

Torino F, Sarmiento R, Gasparini G. The contribution of targeted therapy to the neoadjuvant chemoradiation of rectal cancer. Crit Rev Oncol Hematol. 2013 Sep; 87(3): 283-305.

Truman JP, García-Barros M, Obeid LM, Hannun YA. Evolving concepts in cancer therapy through targeting sphingolipid metabolism. Biochim Biophys Acta. 2014 Aug; 1841(8): 1174-88.

Turnbull Jr R, Kyle K, Watson F, Spratt J. Cancer of the colon: The influence of the no-touch isolation technic on survival rates. Annals of Surgery 1967; 166(3): 420-7.

Turner LS, Cheng JC, Beckham TH, Keane TE, Norris JS, Liu X. Autophagy is increased in prostate cancer cells overexpressing acid ceramidase and enhances resistance to C6 ceramide. Prostate Cancer Prostatic Dis. 2011 Mar; 14(1): 30-7.

Tytherleigh MG, Warren BF, Mortensen NJ. Management of early rectal cancer. Br J Surg 2008; 95: 409–23.

UKCCCR (1989) Handbook for the clinicopathological assessment and staging of colorectal cancer.

Ullio C, Casas J, Brunk UT, Sala G, Fabriàs G, Ghidoni R, Bonelli G, Baccino FM, Autelli R. Sphingosine mediates TNFα-induced lysosomal membrane permeabilization and ensuing programmed cell death in hepatoma cells. J Lipid Res. 2012 Jun; 53(6): 1134-43.

van den Broek CB, Vermeer TA, Bastiaannet E, Rutten HJ, van de Velde CJ, Marijnen CA. Impact of the interval between short-course radiotherapy and surgery on outcomes of rectal cancer patients. Eur J Cancer 2013; 49: 3131–9.

Vaughan AT, Betti CJ, Villalobos MJ. Surviving apoptosis. Apoptosis 2002 Apr; 7(2): 173-7.

Veldkamp R, Kuhry E, Hop W, Jeekel J, Kazemier G, Bonjer H, Haglind E, Påhlman L, Cuesta M, Msika S, Morino M, Lacy A. Laparoscopic surgery versus open surgery for colon cancer: Short-term outcomes of a randomised trial. Colon cancer Laparoscopic or Open Resection Study Group (COLOR). Lancet Oncology 2005; 6(7): 477-84.

Vens C, Begg A. Targeting base excision repair as a sensitization strategy in radiotherapy. Seminars in Radiation Oncology 2010; 20(4): 241-9.

Verseveld M, de Graaf EJ, Verhoef C, van Meerten E, Punt CJ, de Hingh IH, Nagtegaal ID, Nuyttens JJ, Marijnen CA, de Wilt JH. Chemoradiation therapy for rectal cancer in the distal rectum followed by organ-sparing transanal endoscopic microsurgery (CARTS study). Br J Surg 2015; 102: 853–60.

Vizcaíno JA, Csordas A, del-Toro N, Dianes JA, Griss J, Lavidas I, Mayer G, Perez-Riverol Y, Reisinger F, Ternent T, Xu QW, Wang R, Hermjakob H. 2016 update of the PRIDE database and its related tools. Nucleic Acids Res. 2016 Jan;44(D1): D447-56.

Voduc D, Kenney C, Nielsen TO. Tissue microarrays in clinical oncology. Semin Radiat Oncol 2008; 18: 89.

Vousden K, Prives C. Blinded by the Light: The Growing Complexity of p53. Cell 2009; 137(3): 413-31.

Walther A, Johnstone E, Swanton C, Midgley R, Tomlinson I, Kerr D. Genetic prognostic and predictive markers in colorectal cancer. Nat Rev Cancer. 2009 Jul; 9(7): 489-99.

Wang G, Li Z, Zhao Q, Zhu Y, Zhao C, Li X, Ma Z, Li X, Zhang Y. LincRNA-p21 enhances the sensitivity of radiotherapy for human colorectal cancer by targeting the Wnt/β-catenin signaling pathway. Oncol Rep. 2014 Apr; 31(4): 1839-45.

Wang L, Zhang XM, Li Z, Liu XJ, Chai J, Zhang GY, Cheng YF. Overexpression of nuclear β-catenin in rectal adenocarcinoma is associated with radioresistance. World J Gastroenterol. 2013 Oct 28; 19(40): 6876-82.

Watanabe M, Kodaira S, Takahashi T, Tominaga T, Hojo K, Kato T, Kunitomo K, Isomoto H, Ohashi Y, Yasutomi M. Randomized trial of the efficacy of adjuvant chemotherapy for colon cancer with combination therapy incorporating the oral pyrimidine 1-hexylcarbamoyl-5-fluorouracil. Langenbecks Arch Surg 2006 Aug; 391(4): 330-7.

Watanabe T, Komuro Y, Kiyomatsu T, Kanazawa T, Kazama Y, Tanaka J, Tanaka T, Yamamoto Y, Shirane M, Muto T, Nagawa H. Prediction of sensitivity of rectal cancer cells in response to preoperative radiotherapy by DNA microarray analysis of gene expression profiles. Cancer Res. 2006 Apr 1; 66(7): 3370-4.

Watanabe T, Kobunai T, Akiyoshi T, Matsuda K, Ishihara S, Nozawa K. Prediction of response to preoperative chemoradiotherapy in rectal cancer by using reverse transcriptase polymerase chain reaction analysis of four genes. Dis Colon Rectum. 2014 Jan; 57(1): 23-31.

Werb Z, Lu P. The role of stroma in tumor development. Cancer J. 2015 Jul-Aug; 21(4): 250-3.

Williams JG, Pullan RD, Hill J, Horgan PG, Salmo E, Buchanan GN, Rasheed S, McGee SG, Haboubi N. Management of the malignant colorectal polyp: ACPGBI position statement. Colorectal Dis 2013; 15(Suppl 2): 1–38.

Wittrup A, Lieberman J. Knocking down disease: a progress report on siRNA therapeutics. Nat Rev Genet 2015 Sep; 16(9): 543-52.

Wlodkowic D, Telford W, Skommer J, Darzynkiewicz Z. Apoptosis and beyond: cytometry in studies of programmed cell death. Methods Cell Biol 2011; 103: 55-98.

Wood L, Parsons D, Jones S, Lin J, Sjöblom T, Leary R, Shen D, Boca S, Barber T, Ptak J, Silliman N, Szabo S, Dezso Z, Ustyanksky V, Nikolskaya T, Nikolsky Y, Karchin R, Wilson P, Kaminker J, Zhang Z, Croshaw R, Willis J, Dawson D, Shipitsin M, Willson J, Sukumar S, Polyak K, Park B, Pethiyagoda C, Pant P, Ballinger D, Sparks A, Hartigan J, Smith D, Suh E, Papadopoulos N, Buckhaults P, Markowitz S, Parmigiani G, Kinzler K, Velculescu V, Vogelstein B. The genomic landscapes of human breast and colorectal cancers. Science 2007; 318(5853): 1108-13.

Wright J, Dreyfuss A, el-Magharbel I, Trites D, Jones S, Holden S, Rosowsky A, Frei E. Selective expansion of 5,10-methylenetetrahydrofolate pools and modulation of 5-fluorouracil antitumor activity by leucovorin in vivo. Cancer Research 1989; 49(10): 2592-6.

Xue K, Li FF, Chen YW, Zhou YH, He J. Body mass index and the risk of cancer in women compared with men: a meta-analysis of prospective cohort studies. Eur J Cancer Prev. 2017 Jan; 26(1): 94-105.

Yoder J, Soman N, Verdine G, Bestor T. DNA (cytosine-5)-methyltransferases in mouse cells and tissues. Studies with a mechanism-based probe. Journal of Molecular Biology 1997; 270(3): 385-95.

Yoshioka A, Tanaka S, Hiraoka O, Koyama Y, Hirota Y, Ayusawa D, Seno T, Garrett C, Wataya Y. Deoxyribonucleoside triphosphate imbalance. 5Fluorodeoxyuridine-induced DNA double strand breaks in mouse FM3A cells and the mechanism of cell death. Journal of Biological Chemistry 1987; 262(17): 8235-41.

Young N, Pearl DK, Van Brocklyn JR. Sphingosine-1-phosphate regulates glioblastoma cell invasiveness through the urokinase plasminogen activator system and CCN1/Cyr61. Mol Cancer Res. 2009 Jan; 7(1): 23-32.

Zhou J, Tawk M, Tiziano FD, Veillet J, Bayes M, Nolent F, Garcia V, Servidei S, Bertini E, Castro-Giner F, Renda Y, Carpentier S, Andrieu-Abadie N, Gut I, Levade T, Topaloglu H, Melki J. Spinal muscular atrophy associated with progressive myoclonic epilepsy is caused by mutations in ASAH1. Am J Hum Genet. 2012 Jul; 91(1): 5-14.

Zlobec I, Koelzer VH, Dawson H, Perren A, Lugli A. Next-generation tissue microarray (ngTMA) increases the quality of biomarker studies: an example using CD3, CD8, and CD45RO in the tumor microenvironment of six different solid tumor types. J Transl Med 2013 Apr 30; 11: 104.

Zöller B, Li X, Sundquist J, Sundquist K. Familial transmission of prostate, breast and colorectal cancer in adoptees is related to cancer in biological but not in adoptive parents: a nationwide family study. Eur J Cancer. 2014 Sep; 50(13): 2319-27.

Appendix A – Differentially Expressed Proteins Identified at Original Proteomic Profiling

Accession Number	Name	p Value	Log2 Fold-Change
Q9NZM1	Myoferlin	4.35E-02	-1.633
Q13510	Acid ceramidase	1.17E-02	-1.526
P09525	Annexin A4	1.93E-02	-1.524
P41219	Peripherin	2.13E-02	1.583
P12109	Collagen alpha-1(VI) chain	3.61E-02	1.800
P80748	Ig lambda chain V-III region LOI	4.82E-02	1.866
P07602	Proactivator polypeptide	5.90E-04	1.943
P01860	Ig gamma-3 chain C region	2.74E-02	2.549

Table A1 – Those proteins differentially expressed between relative responders and non-responders to chemoradiotherapy on diagnostic samples. 8 proteins were identified, 3 of which were downregulated in responders (negative values for fold change) and 5 upregulated (positive values for fold change).

Accession Number	Name	p Value	Log2 Fold-Change
P12109	Collagen alpha-1(VI) chain	1.34E-02	-1.953
P12429	Annexin A3	9.71E-03	-1.757
Q1KMD3	Heterogeneous nuclear ribonucleoprotein U-like protein 2	3.76E-02	1.521
P51648	Fatty aldehyde dehydrogenase	1.11E-02	1.525
Q13162	Peroxiredoxin-4	1.84E-02	1.572
Q96PD5	N-acetylmuramoyl-L-alanine amidase	3.04E-02	1.686
P02652	Apolipoprotein A-II	1.02E-02	1.758
Q9BY50	Signal peptidase complex catalytic subunit SEC11C	1.69E-02	1.760
Q9Y6R7	IgGFc-binding protein	3.22E-03	1.761
P01023	Alpha-2-macroglobulin	1.54E-02	1.783
P01859	Ig gamma-2 chain C region	2.67E-02	1.801
Q8NBS9	Thioredoxin domain-containing protein 5	1.17E-02	1.823
P01591	Immunoglobulin J chain	2.57E-02	1.861
O75795	UDP-glucuronosyltransferase 2B17	3.03E-02	1.946
P02765	Alpha-2-HS-glycoprotein	2.18E-02	2.105
P01275	Glucagon	2.77E-04	2.381
P04114	Apolipoprotein B-100	1.75E-02	2.429
P10645	Chromogranin-A	6.10E-03	3.357

Table A2 – Those proteins differentially expressed between rectal tumours post chemoradiotherapy and diagnostic samples. 18 proteins were identified, 2 of which were downregulated (negative values for fold change) and 16 upregulated (positive values for fold change).

Accession Number	Name	p Value	Log2 Fold-Change
P10645	Chromogranin-A	1.12E-02	-3.430
P04114	Apolipoprotein B-100	2.22E-02	-2.630
P01275	Glucagon	4.03E-04	-2.562
P12532	Creatine kinase U-type, mitochondrial	3.62E-02	-2.427
O75795	UDP-glucuronosyltransferase 2B17	2.21E-02	-2.293
Q9Y5M8	Signal recognition particle receptor subunit beta	3.61E-02	-2.226
Q9Y6R7	IgGFc-binding protein	1.62E-03	-2.095
P01833	Polymeric immunoglobulin receptor	3.21E-02	-2.078
P01591	Immunoglobulin J chain	2.99E-02	-1.992
Q07654	Trefoil factor 3	9.92E-03	-1.952
P21397	Amine oxidase [flavin-containing] A	4.66E-02	-1.882
P17931	Galectin-3	3.48E-02	-1.830
Q16836	Hydroxyacyl-coenzyme A dehydrogenase, mitochondrial	1.91E-02	-1.787
P00966	Argininosuccinate synthase	2.71E-02	-1.757
Q96EY8	Cob(I)yrinic acid a,c-diamide adenosyltransferase, mitochondrial	9.12E-03	-1.726
Q8NBS9	Thioredoxin domain-containing protein 5	3.23E-02	-1.725
P31930	Cytochrome b-c1 complex subunit 1, mitochondrial	3.25E-02	-1.714
P38117	Electron transfer flavoprotein subunit beta	2.28E-02	-1.691
P19075	Tetraspanin-8	3.31E-02	-1.686
O75874	Isocitrate dehydrogenase [NADP] cytoplasmic	3.49E-02	-1.682
P80303	Nucleobindin-2	4.17E-02	-1.661
Q96FQ6	Protein S100-A16	1.44E-02	-1.648
Q9HAT2	Sialate O-acetylesterase	9.52E-03	-1.626
P17980	26S protease regulatory subunit 6A	2.19E-02	-1.624
Q1KMD3	Heterogeneous nuclear ribonucleoprotein U-like protein 2	3.93E-02	-1.614
P51648	Fatty aldehyde dehydrogenase	1.33E-02	-1.596
P15880	40S ribosomal protein S2	4.52E-02	-1.583
Q13510	Acid ceramidase	1.35E-02	-1.568
O96000	NADH dehydrogenase [ubiquinone] 1 beta subcomplex subunit 10	2.29E-03	-1.538
P30049	ATP synthase subunit delta, mitochondrial	1.15E-03	-1.537
Q16658	Fascin	7.94E-03	1.628
P61106	Ras-related protein Rab-14	2.03E-02	1.706
Q9H4M9	EH domain-containing protein 1	2.25E-02	1.769
P08572	Collagen alpha-2(IV) chain	4.48E-02	2.006
P12429	Annexin A3	6.90E-03	2.009

P98160	Basement membrane-specific heparan sulfate proteoglycan core protein	2.73E-02	2.021
P12109	Collagen alpha-1(VI) chain	1.45E-02	2.136
P13674	Prolyl 4-hydroxylase subunit alpha-1	9.64E-03	2.569
P24821	Tenascin	3.63E-02	3.329

Table A3 – Those proteins differentially expressed between rectal tumours at resection and immediately following completion of chemoradiotherapy. 39 proteins were identified, 30 of which were downregulated (negative values for fold change) and 9 upregulated (positive values for fold change).

Accession Number	Name	p Value	Log2 Fold-Change
O95881	Thioredoxin domain-containing protein 12	3.98E-02	-2.779
P16444	Dipeptidase 1	3.35E-02	-2.740
Q13228	Selenium-binding protein 1	2.03E-02	-2.013
P05783	Keratin, type I cytoskeletal 18	3.44E-02	-1.835
Q9BY42	UPF0549 protein C20orf43	2.97E-02	-1.732
P09874	Poly [ADP-ribose] polymerase 1	5.82E-03	-1.599
O96008	Mitochondrial import receptor subunit TOM40 homolog	8.41E-03	-1.566
Q9NX63	Coiled-coil-helix-coiled-coil-helix domain-containing protein 3, mitochondrial	4.29E-02	-1.548
P11940	Polyadenylate-binding protein 1	4.44E-02	-1.530
P05455	Lupus La protein	3.78E-02	-1.525
P07099	Epoxide hydrolase 1	4.17E-02	1.504
O14773	Tripeptidyl-peptidase 1	1.17E-02	1.590
Q99536	Synaptic vesicle membrane protein VAT-1 homolog	2.76E-02	1.644
Q92930	Ras-related protein Rab-8B	1.03E-02	1.690
Q9H4M9	EH domain-containing protein 1	1.24E-02	1.714
Q9UJ70	N-acetyl-D-glucosamine kinase	1.59E-02	1.737
P08758	Annexin A5	2.30E-02	1.770
P53004	Biliverdin reductase A	1.61E-02	1.842
P04271	Protein S100-B	4.74E-02	1.882
P02765	Alpha-2-HS-glycoprotein	3.26E-02	1.896
Q9BUF5	Tubulin beta-6 chain	4.44E-02	2.002
P01824	Ig heavy chain V-II region WAH	1.80E-02	2.073
P13674	Prolyl 4-hydroxylase subunit alpha-1	1.06E-02	2.141
B9A064	Immunoglobulin lambda-like polypeptide 5	2.80E-02	2.249
P01860	Ig gamma-3 chain C region	4.99E-02	2.271
P08603	Complement factor H	4.15E-02	2.310
P01008	Antithrombin-III	2.61E-02	2.317
P01834	Ig kappa chain C region	4.25E-02	2.731
P10909	Clusterin	4.97E-02	4.945

Table A4 – Those proteins differentially expressed between rectal tumours at resection and at diagnosis. 29 proteins were identified, 10 of which were downregulated (negative values for fold change) and 19 upregulated (positive values for fold change).

Appendix B – Clinical and Pathological Patient Data for Tissue Microarray Analysis

Patient	Age	Gender	Pre-CRT Staging (MRI + CT)			Procedure	Histopathology				Regression	Adjuvant	Follow Up	Outcome		
			T	N	M		T	N	CRM	EMVI	(Ryan)	Therapy	(months)	Recurrence	Metastases	Death
1	72	M	3	0	0	APR	3	0	0	Yes	2	Yes	102	No	No	No
2	57	F	3	1	0	Hartmann's	0	0	0	No	4	No	7	No	Yes	Yes
3	80	M	3	0	0	AR	0	0	0	No	4	No	104	No	No	No
4	74	F	3	2	1	AR	4	1	1	No	2	Yes	35	No	Yes	Yes
5	63	M	3	2	0	AR	2	0	0	No	3	Yes	100	No	No	No
6	62	M	3	0	0	AR	3	0	0	No	3	Yes	52	No	Yes	Yes
7	59	F	3	2	0	Exenteration	3	2	2	No	1	Yes	15	No	Yes	Yes
8	69	M				APR	3	0	2	No	2	No	4	No	No	Yes
9	46	F	3	2	0	AR	3	1	0	No	3	Yes	93	No	No	No
10	57	M	2	0	0	APR	0	0	0	No	4	No	83	No	No	No
11	61	M	3	1	0	AR	3	1	0	Yes	2	Yes	90	No	Yes	No
12	74	M	3	1	0	APR	3	1	0	No	2	Yes	23	No	Yes	Yes
13	70	M	3	1	0	Hartmann's	3	2	1	Yes	2	Yes	15	Yes	Yes	Yes
14	60	F	3	1	0	AR	2	1	0	No	2	Yes	88	No	No	No
15	69	M	3	1	0	APR	2	0	0	No	2	No	52	No	Yes	Yes
16	58	M				APR	3	0	0	No	1		57	No	Yes	Yes
17	64	F	3	2	0	AR	2	0	0	No	2	Yes	90	No	No	No
18	65	M	3	1	0	AR	3	2	1	No	2	Yes	30	No	Yes	Yes
19	72	M	3	1	0	APR	3	0	0	No	2	Yes	89	No	No	No
20	43	M	4	2	0	AR	3	0	2	No	1	Yes	6	No	No	Yes
21	46	F	4	2	0	APR	0	0	0	No	4	Yes	90	No	No	No
22	63	M	3	0	0	APR	1	0	0	No	2	No	28	No	No	No
23	65	M	2	0	0	APR	2	0	0	No	2	Yes	88	No	No	No
24	70	M	3	0	1	AR	2	0	0	No	3	No	44	No	Yes	Yes
25	39	M				APR	3	0	0	No	2		27	No	No	No
26	76	F	3	0	0	APR	2	0	0	No	2	No	81	No	No	No
27	76	M	3	0	0	Hartmann's	3	0	0	No	3	Yes	38	Yes	Yes	Yes
28	63	M	3	0	0	APR	0	0	0	No	4	No	69	No	No	No
29	51	M	2	0	0	APR	2	0	0	No	2		86	No	No	No
30	56	F	2	0	0	AR	0	0	0	No	4	Yes	75	No	No	No
31	46	F	3	1	0	AR	3	1	0	No	2	Yes	40	Yes	Yes	Yes
32	52	M	3	2	0	APR	2	0	0	No	2	Yes	84	Yes	Yes	No
33	54	F	2	0	0	AR	2	1	0	No	2	Yes	38	No	Yes	Yes
34	77	M	2	0	0	AR	3	1	0	No	2	Yes	39	No	No	Yes
35	66	M	3	2	0	AR	2	0	0	No	2	Yes	71	No	No	No
36	55	F	4	2	0	AR	0	0	0	No	4	Yes	74	No	Yes	No
37	68	F	3	0	0	AR	0	0	0	No	4	Yes	64	No	No	No
38	67	M	3	0	0	AR	3	0	0	No	2	No	76	No	No	No
39	67	F	3	2	0	AR	4	2	2	Yes	1	Yes	25	No	Yes	Yes
40	54	M	3	1	0	AR	3	0	0	No	2	Yes	35	Yes	No	Yes
41	63	M	1	0	0	AR	3	0	0	No	2	Yes	69	No	No	No
42	73	F	3	2	0	AR	2	0	0	No	3	Yes	68	No	No	No
43	64	F				APR	0	0	0	No	4		43	No	No	No
44	27	F	4	2	0	AR	4	0	0	No	3	Yes	67	No	No	No
45	76	M	2	0	0	AR	0	0	0	No	4	Yes	67	No	No	No
46	69	M	3	2	0	AR	3	0	0	No	2	Yes	64	No	No	No
47	62	M	3	2	0	APR	2	0	0	No	2	Yes	64	No	No	No
48	55	M	3	2	0	AR	3	0	0	No	2	Yes	61	No	No	No
49	64	M	3	1	1	APR	2	0	1	No	2	Yes	20	No	Yes	Yes
50	61	M	3	0	0	APR	2	0	0	No	3	Yes	50	No	Yes	Yes
51	74	M	3	0	0	Hartmann's	3	1	0	No	2	Yes	23	No	Yes	Yes
52	74	M				APR	3	1	0	Yes	2	Yes	60	No	No	No
53	72	F	3	2	0	AR	3	0	0	Yes	3	No	9	No	Yes	Yes
54	47	M	3	1	0	APR	3	0	0	No	2	Yes	60	No	No	No
55	45	M	3	2	1	AR	3	2	0	No	1	Yes	29	No	Yes	Yes
56	67	M	2	0	0	Hartmann's	1	0	0	No	1	Yes	57	No	No	No
57	45	M	3	1	0	APR	2	0	0	No	2	Yes	42	No	No	No
58	71	M	3	0	0	Hartmann's	0	0	0	No	4	Yes	58	No	No	No
59	63	M	3	0	0	AR	3	0	0	No	2	Yes	36	No	No	No
60	70	F	3	2	0	AR	0	0	0	No	4	No	60	No	No	No
61	86	F	3	0	0	Hartmann's	2	0	0	No	2	No	57	No	No	No
62	72	M	3	1	0	AR	3	0	0	Yes	2	No	49	No	No	No
63	57	M	4	0	0	AR	3	2	0	Yes	2	Yes	35	No	Yes	Yes
64	69	F	3	2	0	Hartmann's	3	1	0	No	3	Yes	58	No	Yes	No
65	72	M	3	1	0	APR	3	0	0	No	1	Yes	56	No	No	No
66	55	M	3	1	0	AR	4	2	0	No	2	Yes	54	No	Yes	No
67	26	M	3	1	0	APR	3	2	0	Yes	1	Yes	26	No	No	Yes
68	77	M	3	1	0	AR	2	0	0	No	2	No	56	No	Yes	No
69	51	M	3	1	0	AR	4	2	0	Yes	2	Yes	37	No	Yes	Yes
70	59	M	3	1	0	AR	3	1	0	No	1	Yes	53	No	Yes	No
71	56	M	2	0	0	APR	0	0	0	No	4	No	55	No	No	No
72	68	F	3	0	0	AR	0	0	0	No	4	Yes	52	No	No	No
73	66	M	3	2	0	APR	3	2	0	No	2	Yes	44	No	No	No
74	71	M	3	0	0	AR	0	0	0	No	4	Yes	47	No	No	No
75	75	M	2	0	0	APR	2	0	0	No	2	No	51	No	No	No
76	76	M	4	0	0	Hartmann's	3	0	0	No	1	No	48	No	No	No
77	74	M	4	1	0	AR	3	0	0	Yes	2	Yes	49	No	No	No
78	58	M	3	1	0	AR	1	0	0	No	3	Yes	42	No	No	No

Patient	Age	Gender	Pre-CRT Staging (MRI + CT)			Procedure	Histopathology				Regression	Adjuvant	Follow Up	Outcome		
			T	N	M		T	N	CRM	EMVI	(Ryan)	Therapy	(months)	Recurrence	Metastases	Death
79	61	F	3	2	0	AR	3	1	0	Yes	2	Yes	48	No	No	No
80	81	F	4	1	0	Hartmann's	0	0	0	No	4	No	47	No	Yes	No
81	56	M	3	1	1	Hartmann's	0	0	0	No	4	No	46	No	Yes	No
82	27	M	3	2	0	proctocolectc	3	2	0	Yes	2	Yes	43	No	Yes	No
83	76	M	4	1	0	AR	2	1	0	Yes	3	Yes	42	No	No	No
84	60	M	3	2	0	AR	3	2	0	Yes	1	Yes	41	No	No	No
85	53	M	3	0	0	AR	0	0	0	No	4	Yes	40	No	No	No
86	74	M	3	2	0	AR	2	0	0	No	2	Yes	31	No	No	No
87	48	M	2	0	0	APR	4	0	2	No	2	Yes	39	No	Yes	No
88	75	M	3	0	0	Hartmann's	3	0	0	No	2	No	37	No	No	No
89	57	F	3	2	0	AR	4	2	1	Yes	1	No	34	Yes	Yes	Yes
90	72	M	3	0	0	AR	2	0	0	No	1		37	No	No	No
91	49	M	4	1	0	APR	4	2	2	No	1	Yes	37	Yes	Yes	No
92	56	M	3	0	0	AR	2	0	0	No	1	No	33	No	Yes	No
93	76	M	3	0	0	APR	2	0	0	No	3	Yes	29	No	No	No
94	73	M	3	2	1	APR	4	1	0	Yes	1	Yes	32	No	Yes	No
95	77	F	4	2	0	Hartmann's	2	1	0	No	2	No	23	No	No	No
96	66	M	3	1	0	AR	2	0	0	No	2	Yes	22	No	No	No
97	33	F	3	0	0	AR	3	2	0	No	1	Yes	21	No	No	No
98	64	M	4	1	1	APR	2	0	0	No	3	Yes	18	No	Yes	Yes
99	79	M	3	1	1	APR	3	0	0	No	3	No	21	No	No	No
100	69	M	3	1	0	APR	3	2	0	Yes	1	Yes	19	No	No	No
101	70	M	3	1	0	Hartmann's	3	0	0	Yes	2	Yes	16	No	Yes	No
102	55	M	3	2	1	AR	3	1	1	No	1	Yes	18	No	Yes	No
103	79	F	3	0	0	APR	0	0	0	No	4	No	18	No	No	No
104	60	M	2	0	0	APR	2	0	0	No	2	No	17	No	No	No
105	76	M	4	2	0	APR	3	0	0	No	2	Yes	13	No	No	No
106	77	F	3	2	0	AR	3	1	0	Yes	2	Yes	16	No	No	No
107	71	M	4	2	0	Hartmann's	2	0	0	No	2	No	14	No	No	No
108	66	M	3	2	0	APR	0	0	0	No	4	Yes	13	No	No	No
109	66	M	3	2	0	APR	2	0	0	No	2	Yes	14	No	No	No
110	67	M	3	1	0	AR	0	0	0	No	4	Yes	11	No	No	No
111	67	M	3	0	0	APR	0	0	0	No	4	No	9	No	No	No

Appendix C – Acid Ceramidase Expression from 10K Proteome in 49 Colorectal Cancer Cell Lines

Cell Line	Relative AC Expression
NCI-H716	-2.060838
GEO	-1.451349
HT-29	-1.254239
SNU-61	-1.210463
LoVo	-0.959903
COLO-320-HSR	-0.920947
SW1116	-0.792969
HCC-56	-0.715943
HT-115	-0.712558
SW620	-0.649576
SW837	-0.649537
HCT-116	-0.633228
HT55	-0.60389
RKO	-0.59612
LS-411N	-0.5289
T84	-0.472482
HCT-15	-0.471081
SNU-175	-0.470129
LS-1034	-0.350895
SNU-C1	-0.342144
SNU-C2B	-0.332953
CL-11	-0.24496
KM12	-0.200412
SW1463	-0.149981
GP5d	-0.141356
SW948	-0.090236
SNU-C5	-0.038223
SK-CO-1	-0.00629
NCI-H630	0.172662
HCC2998	0.305689
SNU-407	0.375464
LS-180	0.382029
SNU-1040	0.471951
COLO-205	0.505021
CW-2	0.571851
CCK-81	0.595101
LS-513	0.627615
CL-40	0.666811
LS-123	0.667567
SNU-81	0.67398
DIFI	0.849557
CaR-1	0.988862
COLO-678	1.051976
RCM-1	1.181756
C2BBe1	1.279105
NCI-H747	1.41401
MDST8	1.419318
LIM1215	1.554641
NCI-H508	1.602017

Appendix D – Supporting Publications, Presentations and Grants

Publications

Proteomic profiling of rectal cancer reveals acid ceramidase is implicated in radiation response

D Bowden, P Sutton, M Wall, P Jithesh, D Palmer, C Goldring, J Parsons, N Kitteringham, D Vimalachandran

J Proteomics. 2018 May 15; 179: 53-60. doi: 10.1016/j.jprot.2018.02.030.

PMID: 29518574

Sphingolipids and acid ceramidase as therapeutic targets in cancer therapy

N Govindarajah, R Clifford, D Bowden, P Sutton, J Parsons, D Vimalachandran

Crit Rev Oncol Hematol. 2019 Apr 13; 138: 104-111. doi: 10.1016/j.critrevonc.2019.03.018.

PMID: 31092365

Presentations

Investigating the role of acid ceramidase (AC) on the radiotherapy response of colorectal cancer cells

Govindarajah, Sutton, Bowden, Vimalachandran, Parsons

Poster presentation at NCRI Cancer Conference – November 2017

Investigating the role of acid ceramidase in the radiotherapy response of an *in vitro* model of colorectal cancer

Govindarajah, Vimalachandran, Sutton, Bowden, Parsons

Poster presentation at ACPGBI – July 2017

Evaluation of acid ceramidase as response predictor and therapeutic target in neoadjuvant chemoradiotherapy for rectal cancer.

Bowden, Sutton, Wall, Parsons, Kitteringham, Vimalachandran

Poster presentation at ACPGBI – July 2016

Evaluation of Acid Ceramidase as Response Predictor and Therapeutic Target in the Neoadjuvant Treatment of Rectal Cancer

Bowden, Sutton, Wall, Parsons, Kitteringham, Vimalachandran

Oral presentation at The Liverpool & North West Society of Surgeons Annual Meeting – December 2015

High Expression of acid ceramidase confers radio-resistance in rectal cancer

Sutton, Bowden, Hamid, Abbott, Goldring, Palmer, Kitteringham, Vimalachandran

Poster presentations at NCRI Cancer Conference - November 2014, ESSO 34 / BASO 2014 - October 2014

Temporal phenotypic profiling of rectal cancer to predict response to neoadjuvant chemoradiotherapy

Sutton, Jithesh, Bowden, Abbott, Hamid, Jenkins, Palmer, Goldring, Kitteringham, Vimalachandran

Oral presentation at Tripartite Colorectal Meeting – July 2014

Grants

Arising from and for the continuation of the work presented in the thesis:

NHS Health Education North West Madel Research Fellowship (2014) £80,000

Awarded to facilitate me undertaking this research

Bowel Disease Research Foundation (2015) £12,400

Awarded to fund consumables for this research

Bowel Disease Research Foundation (2016) £10,000

Awarded to our rectal cancer radiotherapy research response group to fund a pilot project to facilitate and standardise prospective national tissue collection